UiT The Arctic University of Norway

Faculty of Biosciences, Fisheries and Economics

Department of Arctic and Marine Biology

Evolution of seasonal adaptations in voles

A physiological and genetic approach

Mattis Jayme van Dalum

A dissertation for the degree of Philosophiae Doctor (PhD) January 2022

Evolution of seasonal adaptations in voles

A physiological and genetic approach

Mattis Jayme van Dalum

A dissertation for the degree of Philosophiae Doctor – January 2022

UiT- The Arctic University of Norway

Faculty of Biosciences, Fisheries and Economics

Department of Arctic and Marine Biology

Arctic Chronobiology and Physiology Research Group

Cover art: M.J.van Dalum, December 2021

“It is not the strongest of the species that survives, nor the most intelligent that survives. It is the one that is the most adaptable to change”

Charles Darwin

Table of contents

I. Acknowledgements

This was a long journey with many scientific- and personal hurdles to take. Yet it is a journey completed and many people have inspired and motivated me on the way.

First, thanks to my main supervisor David Hazlerigg, who made it possible to start with this fascinating project in a fantastic place. Thanks for the inspiring academic guidance and admirable insight. Maybe even more important, thanks for the understanding and invaluable support on the personal level. You have also given me the opportunity to move to Tromsø, where I feel home, where I can indulge in outdoor activities and where I can experience the most extreme of the beautiful seasons.

I also want to thank Gabi Wagner who was one of the first people here whom I trusted with personal issues and thanks for still expressing interest in non-science related things such as my artwork and stories. Also, thanks to my family and my friends all over the world for all the support and love through tough, but also good times. This also counts for my feline company. Here I also include my friends and colleagues in Tromsø: Alex West, Daniel Appenroth, Gabriele Grenier, Chiara Ciccone , Marianne Iversen, Frank Meissner and Raphael & Ulrike Grote for the inspiring conversations and many ski-, hike-, kayak tours and/or game evenings. Not to forget my office mates and other nice colleagues, who have been good company and sources of fun.

Without my collaborator Laura van Rosmalen and co-supervisor Roelof Hut, I wouldn't have had such an interesting dataset to work with. Thanks for the interesting collaboration and the experiences in Groningen. The same goes for Patrik R. Mörch who has showed me how to perform these complex genomic data analyses and who has always been ready to help with the weirdest of errors. Also thanks to Jakob Högland for saving us 'out of the fire' when the computer cluster at UiT got closed down and for providing me the opportunity to come to Uppsala together with Daniel. Never have I had so much beer in a two weeks' time! Also thanks to Simen R. Sandve for doing your R-magic when I was stuck and for being our sequencing- and bioinformatics guru.

I should also thank our research group, now called Arctic Chronobiology and Physiology, established by Arnoldus S. Blix and currently led by Lars Folkow. Also thanks to Elina Halttunen, leader of the Arctic and Marine Biology institute. You have been of great support, also on the personal level. Last but certainly not least, I should mention and respect the many, many voles whose lives have been sacrificed for this research.

II. Thesis abstract

This thesis addressed phenotypic and genetic variation in seasonal time keeping mechanisms of the tundra vole (*Microtus oeconomus*) and the common vole (*Microtus arvalis*). Voles (*Microtus*) are short-lived, non-hibernating and seasonally breeding rodents. The genus has rapidly evolved (< 2 million years) into one of the most speciose mammalian genera (Sitnikova et al. 2007; Triant and DeWoody 2006) and occupies a wide range of latitudes (14-78°N) with the tundra vole being the most wide spread species.

Seasonality is strong at high latitudes with lower and more seasonally fluctuating ambient temperatures (Hut et al. 2013). Therefore, animals have evolved mechanisms to time their life cycles with the strongly cyclical environment. The annual day length cycle is the most reliable cue to predict upcoming changes and prepare accordingly. This information is integrated by the photoneuroendocrine system (PNES) that coordinates phenotypic changes such as seasonal molt and reproduction (Hazlerigg and Simonneaux 2015). **In paper I**, we showed that under laboratory conditions, short winter photoperiods alone reduced somatic growth (body mass) in tundra voles and gonadal growth (reproduction) in common voles. Since both vole species were caught at the same location (the Netherlands, 53°N), the different response can be ascribed to genetic variation between the species. This was possibly shaped by different selection pressures occurring during the more northern (tundra vole) and southern (common vole) paleogeographic history of the two species.

Within and among vole species, the timing of breeding shows great year-to-year variation (Tast 1966; T. Ergon et al. 2001), which is apparently influenced by environmental conditions such as ambient temperature (Kriegsfeld, Trasy, and Nelson 2000). The breeding season starts in spring with the overwintering individuals producing the first spring-born cohort of pups. The short gestation and development times allow these spring-born cohorts to reproduce during the same breeding season as their parents and produce several subsequent cohorts until the end of the breeding season in autumn (Horton 1984a; Gliwicz 1996). In **papers II** and **III,** we investigated the critical photoperiod thresholds for initiation of accelerated reproductive maturation in voles on a spring developmental program and for the deceleration of development in voles on an autumn program. Further, we assessed the influence of ambient temperature (10°C or 21°C) on the response parameters. Seasonal gene expression, hormone levels, downstream body-mass and gonadal mass had different species-specific response thresholds to photoperiod and temperature. This indicates that the system has a hierarchical organization that allowed for

independent modulation at various levels. The results of these experiments also emphasise the importance of the direction of day length change in setting maturation trajectories.

In **Paper IV** we searched for signatures of selection across the genomes of tundra voles from a northern (70°N) and southern (53°N) population. A signature of selection is a reduction in population diversity at a certain genomic position because of positive selection on a favoured allele. We found selection on a paralogue of the *Aldh1a1* gene located between the *Aldh1a1* and *Aldh1a7* genes. We found two additional *Aldh1a1*-like paralogues on the same locus. Other voles investigated also had two or three paralogues, which are not present in mouse and rat genomes. ALDH1A1 has a central role in photoperiodic retinoic acid signaling in the rodent hypothalamus, which may be involved in seasonal body mass regulation (Helfer, Barrett, and Morgan 2019; Shearer, Stoney, Nanescu, et al. 2012). ALDH1A7 is also considered as a paralogue of ALDH1A1 (90% amino acid sequence homology in the mouse) but it is not involved in retinoic acid signaling (Hsu et al. 1999). The paralogues found in the vole had the highest sequence homology with ALDH1A7. Future research has to clarify the function of this gene and whether this selection pressure is associated with latitude.

Taken together we found various levels of flexibility within the vole PNES where ambient temperature and photoperiodic history can modulate the seasonal response which is possibly affected by evolution at different latitudes. Reproductive opportunism and an ability to override photoperiodic information may be favoured in voles living at higher latitudes which may lead to genetic differences between and within species.

III. List of papers

Review

Maternal Photoperiodic Programming: Melatonin and Seasonal Synchronization Before Birth

Mattis Jayme van Dalum*, Vebjørn J. Melum*, Shona H. Wood, David G. Hazlerigg
Arctic Chronobiology and Physiology, Arctic and Marine Biology, UiT – the Arctic University of Norway, 9019 Tromsø, Norway
*These authors contributed equally
Frontiers in Endocrinology, 2020, 10 (901).
Doi: 10.3389/fendo.2019.00901

Paper I

Gonads or body? Differences in gonadal and somatic photoperiodic growth response in two vole species

Laura van Rosmalen[1], Mattis Jayme van Dalum[2], David G. Hazlerigg[2], Roelof A. Hut[1]
[1]Chronobiology Unit, Groningen Institute for Evolutionary Life Sciences, University of Groningen, 9747 AG Groningen, the Netherlands
[2]Arctic Chronobiology and Physiology, Arctic and Marine Biology, UiT – the Arctic University of Norway, 9019 Tromsø, Norway

Journal of Experimental Biology 2020, 223 (20), jeb230987.
Doi:10.1242/jeb230987

Paper II

Mechanisms of temperature modulation in mammalian seasonal timing

Laura van Rosmalen[1], Mattis Jayme van Dalum[2], Daniel Appenroth[2], Renzo T.M. Roodenrijs[1], Lauren de Wit[1], David G. Hazlerigg[2], Roelof A. Hut[1]
[1]Chronobiology Unit, Groningen Institute for Evolutionary Life Sciences, University of Groningen, 9747 AG Groningen, the Netherlands
[2]Arctic Chronobiology and Physiology, Arctic and Marine Biology, UiT – the Arctic University of Norway, 9019 Tromsø, Norway

The FASEB Journal. 2021; 35 (5):e21605.
https://doi.org/10.1096/fj.202100162R

Paper III

Differential effects of ambient temperature on the photoperiod-regulated spring and autumn growth programme in *Microtus oeconomus* and their relationship to the primary photoneuroendocrine response pathway

Mattis Jayme van Dalum[1]*, Laura van Rosmalen[2]*, Daniel Appenroth[1], Renzo T.M. Roodenrijs[2], Lauren de Wit[2], Roelof A. Hut[2], David G.Hazlerigg[1]

Manuscript

[1]Arctic Chronobiology and Physiology, Arctic and Marine Biology, UiT – the Arctic University of Norway, 9019 Tromsø, Norway
[2]Chronobiology Unit, Groningen Institute for Evolutionary Life Sciences, University of Groningen, 9747 AG Groningen, the Netherlands
*These authors contributed equally

Manuscript

Paper IV

Evidence for repeated local gene duplication at the *Aldh1a1* locus in an herbivorous rodent (*Microtus oeconomus*).

Mattis Jayme van Dalum[1], Simen R. Sandve[2], Patrik R. Mörch[3], Roelof A. Hut[4], David G. Hazlerigg[1]
[1]Arctic Chronobiology and Physiology, Arctic and Marine Biology, UiT – the Arctic University of Norway, 9019 Tromsø, Norway
[2]Centre of Integrative Genetics, Department of Animal and Aquaculture Sciences, Norwegian University of Life Sciences, Ås NO-1432
[3]Evolutionsbiologisk centrum (EBC), Department of Ecology and Genetics, Animal Ecology. Uppsala University, 752 36 Uppsala, Sweden.
[4]Chronobiology Unit, Groningen Institute for Evolutionary Life Sciences, University of Groningen, 9747 AG Groningen, the Netherlands

Manuscript

IV. Abbreviations

α-GSU	Pituitary glycoprotein α-subunit
Aldh1a1/Aldh1a2/ Aldh1a7	Aldehyde dehydrogenase 1 Family member A1, A2 or A7 genes.
ALDH1A1/ALDH1A2/ ALDH1A7	Aldehyde dehydrogenase 1 Family member A1, A2, or A7 enzymes
bp	Base pairs, nucleotides (A,C,T,G) within the DNA
BLAST	Basic Local Alignment Search Tool
°C	Degrees Celsius
C.I.	Coincidence interval
Cry1	Cryptochrome Circadian Regulator 1
Dio2/Dio3	Type II/III iodothyronine deiodinase (gene)
DIO2/3	Type II/III iodothyronine deiodinase (enzyme)
DNA	Deoxy-ribonucleic acid
°E	Degrees longitude (East)
e.g.	Example gratia – meaning "for example"
Eya3	Eyes absent 3, a transcription factor (gene)
FSH	Follicle stimulating hormone
F_{ST}	Fixation index
Gbp	giga base pairs 1000.000.000 base pairs (10^9)
GnRH	Gonadotropin releasing hormone
Gpr50	G protein-coupled receptor 50
h	Hours
H_P	Heterozygosity score
HS	Mean heterozygosity between populations
HT	Total heterozygosity, calculated through considering individual populations as one.
ICER	Inducible cAMP early repressor
ipRGC	Intrinsically photosensitive retinal ganglion cell
ILM	Internal limiting membrane
Kbp	Kilo base pairs: 1000 base pairs (10^3)
8L/16L/...L	8, 16 or x hours of light in of 24 hours day-night cycles.
LD	Long day
LH	Luteinizing hormone
LP	Long photoperiod (simulates summer)
MBH	Mediobasal hypothalamus
Mbp	Mega base pairs: 1.000.000 base pairs (10^6)
6-MBOA	6-methoxy-2-benzoxazolinone
ME	Medial eminence of hypothalamus
pPCR	Quantitative polymerase chain reaction
mRNA	Messenger ribonucleic acid
MT1, MT2	Melatonin receptor 1 (gene name *Mtnr1a*) and 2 (*Mtnr1b*)
MYA	Million years ago
°N	Degrees latitude (north)
n	Sample size
p50	Post weaning age of 50 days
PCR	Polymerase chain reaction
PD	*Pars distalis* of the pituitary gland
Per2	Period 2 gene
PNES	Photo neuroendocrine system
PT	Pars tuberalis of the pituitary gland
PVN	Paraventricular nucleus

Raldh1/Raldh2	Retinaldehyde dehydrogenase 1 or 2. Alternative name for *Aldh1a1* and *Aldh1a2* genes.
RALDH1/RALDH2	Retinaldehyde dehydrogenase 1 or 2 enzymes.
RAR	Retinoic acid response element
RFRP	RFamide related peptides
RXR	Retinoid X receptors
°S	Degrees latitude (South)
SCG	Superior cervical ganglion
SCN	Suprachiasmatic nuclei
SD	Short day
Sd	Standard deviation
SNP	Single nucleotide polymorphism
SP	Short photoperiod (simulates winter)
T_3	Triiodothyronine
T_4	Thyroxine
T_a	Ambient temperature
TEF	Thyrotroph embryonic factor (transcription factor)
TSH	Thyroid stimulating hormone
Tshβ	Thyroid stimulating hormone gene, β subunit
TSHr	Thyroid stimulating hormone receptor
TR	Thyroid hormone receptor
°W	Degrees longitude (West)
WGS	Whole genome sequencing

1. Introduction

1.1 Living with the seasons

1.1.1 A cycling environment

No environment on Earth remains constant. Temperature, weather and light conditions constantly change due to the motion of the Earth relative to the Sun and Moon. This creates a dynamic system of a cyclically changing environment that affects life on the planet on multiple levels. The rotation of the Earth on its own axis causes the 24 hours day-night cycle whereas the 23 degrees tilt in the Earth's axis is responsible for the seasons (Fig.1). Due to this tilt, the northern and southern hemispheres are illuminated unequally throughout the Earth's yearly orbit around the Sun (Fig.1). This gives rise to annual variation in day length at non-equatorial latitudes and the seasonal temperature fluctuations. In addition to the day-night and seasonal cycles, the gravitational pull on water bodies by the Moon orbiting the Earth creates tidal cycles, lunar cycles and semi-lunar cycles of spring and nape tides affecting marine life in various ways (Neumann 2014). Nocturnal moonlight is also reported to affect behaviour (e.g. fouraging, predator avoidance) and reproduction in some terrestrial animals (for review: Raible, Takekata and Tessmar-Raible (2017)). These complex interactions between the Sun, Earth and Moon resonate in spatio-temporal variation in temperature, rainfall and light conditions (DeCoursey 2004). In this thesis, I will focus on seasonal rhythmicity in mammals related to latitude. Global climate change and increasing temperatures affect the seasonal environment (Visser and Both 2005; Bronson 2009; Helm et al. 2013) and may impose adaptive challenges for seasonal mammals at all latitudes.

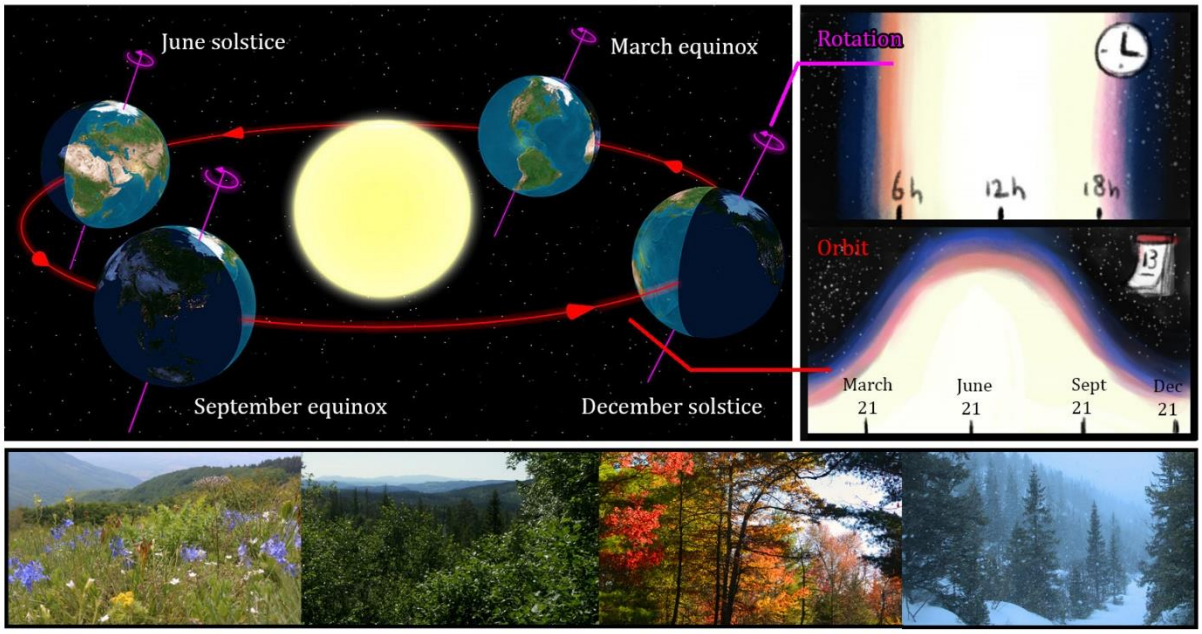

Figure 1. Seasonality on Earth. Seasons depend on the Earth's axis relative to the sun as it orbits around the sun while the rotation of the Earth creates the day-night cycle. During the equinoxes, the axis is parallel to the sun, resulting in an equal day length all over the planet while during the solstices, the axis is in the same line as the sun. During the December solstice, the northern hemisphere is tilted away from the sun, which causes the shorter days and longer nights and the following seasonal temperature fluctuations (see chapter 1.3.1). Photos and day length (rotation, orbit) illustrations to the right by M.J.van Dalum.

In seasonal environments, the ambient temperature, precipitation (e.g. snow cover) and food availability varies strongly throughout the year. For organisms living there, it pays off to match life cycle events with the most favourable conditions (Bradshaw and Holzapfel 2007; DeCoursey 2004). This favours the survival and reproduction of individuals who time events such as growth, reproduction, migration, molt and hibernation with the appropriate seasons. That makes environmental seasonality an ultimate driver of natural selection for biological seasonality. Organisms have therefore evolved mechanisms to synchronize physiology and behavior with the seasons. One of the most conspicuous seasonal adaptations is the change in coat- or plumage colour, which is relevant for camouflage in both predator and prey (Fig. 2).

Figure 2. Seasonal phenotype changes. Coat colour and plumage change to match the seasonally changing environment. Good camouflage is important for the survival of both predator and prey. Art by M.J.van Dalum.

Natural selection operates on phenotypes within a population and favours individuals exhibiting the most optimal phenotype in a given environment. These individuals have a higher survival chance, may produce more progeny, and thus have a higher fitness compared to less well-adapted conspecifics (Freeman and Herron 2004). For example, individual great tits (*Parus major)* whose chicks hatch right when caterpillars (an important food source) emerge are more likely to raise a next generation compared to individuals who had missed this food peak (Both and Visser 2001; Visser, Holleman, and Gienapp 2006)

1.1.2 Predicting upcoming seasonal changes

Growing a winter coat (Fig.2) and building fat-reserves are time-consuming changes that need to be initiated long before ambient temperatures actually drop. Gonadal growth must also take place in advance of the breeding season and in mammals with long gestation times, mating must occur long before environmental conditions are favorable for birth. These time-consuming life cycle preparations impose a time-lag between the decision to start preparing and the actual event. Once a 'decision' is made, and preparation has started, certain life-cycle events (e.g. pregnancy) cannot be reversed until they are completed (Bradshaw and Holzapfel 2007). Anticipatory timing is therefore essential for survival and successful reproduction in a seasonal environment (Hastings et al. 1985; Goldman et al. 2004; Bradshaw and Holzapfel 2007).

Animals can use several cues to predict upcoming seasonal changes and prepare accordingly. These cues serve as direct proximate stimuli. Annual ambient temperature fluctuations, food

availability or rainfall, are relatively noisy signals with great year-to-year variation and are therefore unreliable for precise timing of life cycle events. Only the annual day length cycle (photoperiod) follows the exact same pattern every year and is therefore the best cue to serve as a calendar (Bradshaw and Holzapfel 2007; Bronson 1988; Hut et al. 2013)

1.1.3 Photoperiodism: the use of day length

Organisms that respond to photoperiod to time life cycle events are called photoperiodic (Goldman et al. 2004). The first evidence for photoperiodism came from plants in which day length was demonstrated to affect the timing of flowering (Garner and Allard 1920). Early observations of photoperiodism in animals came from plant lice (Marcovitch 1924), followed by birds (Rowan 1925). The earliest evidence in mammals revealed that 9 hours versus 15 hours of day light alone could reduce the number of pups born in field voles (*Microtus agrestis*) (Baker and Ranson 1932). In the same year, a study on ferrets showed a photoperiodic response in seasonal sexual activity (Bissonette 1932).

The way in which mammals respond to photoperiod, depends on the species' life history and a good example is the difference in gestation time between species. In most seasonal species, birth takes place in summer, when food is most abundant. Species with a long gestation time mate in autumn or winter, under short photoperiods (Fig.3). In these short-day breeding species, short days stimulate gonadal growth and mating behavior. For example sheep *(Ovies aries)* have a gestation time of five months and mate in autumn to give birth in spring (Hazlerigg and Simonneaux 2015; Woodfill et al. 1994). On the contrary, mammals with short gestation times mate in spring and summer and give birth during the same season. In these long-day breeders, long days stimulate gonadal growth and reproductive activity (Hastings et al. 1985). Good examples are rodents such as voles and hamsters with short gestation times of about three weeks. They start breeding from spring to early autumn and can give birth to several litters throughout summer (Bronson and Perrigo 1987).

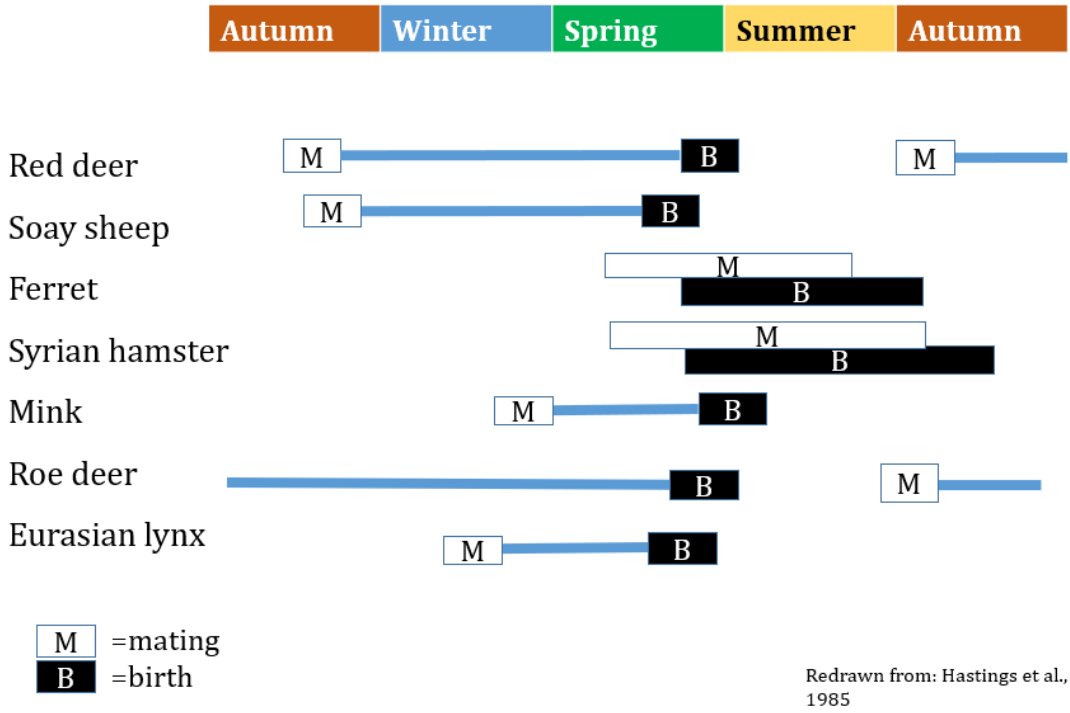

Figure 3. **Delay between mating and birth.** Depending on the duration of pregnancy, mating has to take place in advance of birth, before seasonal conditions are most favourable. Photoperiod serves herein as predictor for upcoming seasonal changes, enabling animals to prepare in advance.

The observation *that* mammals respond to photoperiod for seasonal synchronization also raised the questions of *how* photoperiod is used for time measurement and what the underlying causal mechanisms are. One of the early theories was the hourglass model that was mostly used to explain photoperiodism in insects (Saunders, Lewis, and Warman 2004). According to this model, a non-circadian biological component accumulates during the light- or dark phase and reaches a certain day length threshold that initiates seasonal changes (Lees 1973; Veerman 2001). An alternative model hinges on a circadian sensitivity to day light (Fig. 4). Erwin Bünning and Collin Pittendrigh were pioneers in the development of external- and internal circadian rhythm based models for photoperiodism. The external coincidence model describes a light sensitive window or a photo-inducible phase within the 24 hours cycle. For example, if this photo-inducible phase were 12 hours after sunset, then light would hit this window in nights shorter than 12 hours (Fig. 4). This window could act as an on/off switch for seasonal changes. In this model, it is not the total duration of the light phase that matters but rather *when* the light phase happens in the day-night cycle. The internal coincidence describes the interaction between two internal circadian oscillators; one tracing the onset (sunrise) and the other tracing the offset (sunset) of the light phase. The phase relation between these two oscillators could thereby regulate the seasonal response (Fig. 4).

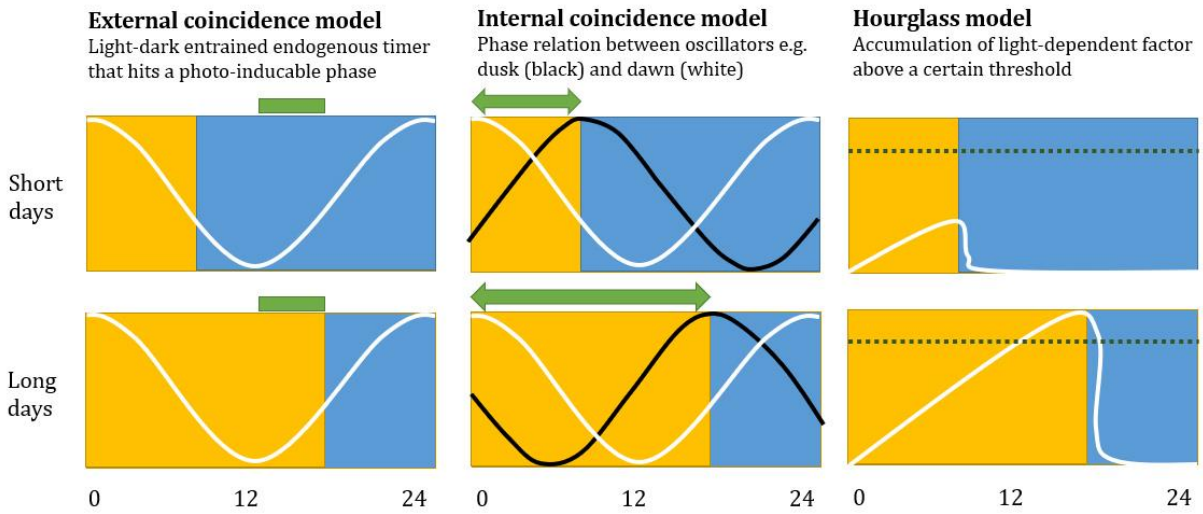

Figure 4. Circadian based models describing photoperiodism. Internal day length measurement and the initiation of a seasonal response. Illustration by M.J.van Dalum.

Hourglass like mechanism cannot be excluded in explaining mammalian photoperiodism but circadian based models are supported with most evidence (Goldman 1999), especially in situations when photoperiodic information is absent or intermittent. This is the case in hibernators such as European hamsters (*Cricetus cricetus)* retreating in a burrow (Hut, Dardente, and Riede 2014) or tundra voles (*Microtus oeconomus)* that spend the winter in tunnels under the snow (Korslund 2006). No detectible light can penetrate snow cover deeper than 30 to 50 cm (Evernden and Fuller 1972), which is common at high latitudes and altitudes.

Registration of absolute day length alone is insufficient to distinguish between the increasing photoperiods in spring and decreasing photoperiods in autumn and this makes the difference between the start (spring) or end (autumn) of the breeding season in long-day breeders such as many rodents. Therefore, they need to have registered what photoperiod preceded the current photoperiod and detect the *directional change*. (Horton 1984a, 1984b; Prendergast, Gorman, and Zucker 2000; Sáenz de Miera et al. 2017). The term used for this ability is photoperiodic history dependence. Indeed, vole pups born early in the breeding season, during increasing day lengths, grow fast and mature fast in order to breed in the same season as their mother. On the contrary, pups born late in the breeding season, with decreasing day lengths, grow slowly and prepare for overwintering instead of breeding (Gliwicz 1996; Goldman 2003; Horton 1984a; Prévot-Julliard et al. 1999). This shows that voles behave as if directional change is perceived, but leaves open the question of how this is achieved. This suggests the presence of an internal time keeping mechanism that keeps track of the seasons even photoperiodic information is intermittent (e.g. in burrows) or ambiguous (e.g. the equinox).

1.1.4 Circannual rhythms

A circannual rhythm that is produced by an internal circannual oscillator persists even under constant conditions (Fig. 5b). Whether or not a circannual rhythm in for example body mass, estrus cycles and molting originates from an endogenous circannual rhythm, depends on a three criteria for internal oscillators to serve as a clock or calendar. Such an oscillator must *generate* a rhythm that can *drive* the oscillation (Fig. 5c) of various output parameters such as body mass. The oscillator must have be self-sustained, meaning that the oscillation sustains under constant conditions with a constant amplitude and an internally determined free-running period (the duration of one cycle, Fig. 5a). Secondly, it must be entrainable to external cues (*Zeitgebers*) such as photoperiod and it must thus have a phase relationship with the annual day-length cycle. To achieve this phase-relationship, it must have a phase-response, meaning that the oscillator's rhythm can shift to earlier or later in response to *Zeitgebers* (Fig. 5a). Thirdly, the oscillator must be temperature compensated so that the period remains constant under a range of temperatures (Johnson et al. 2004).

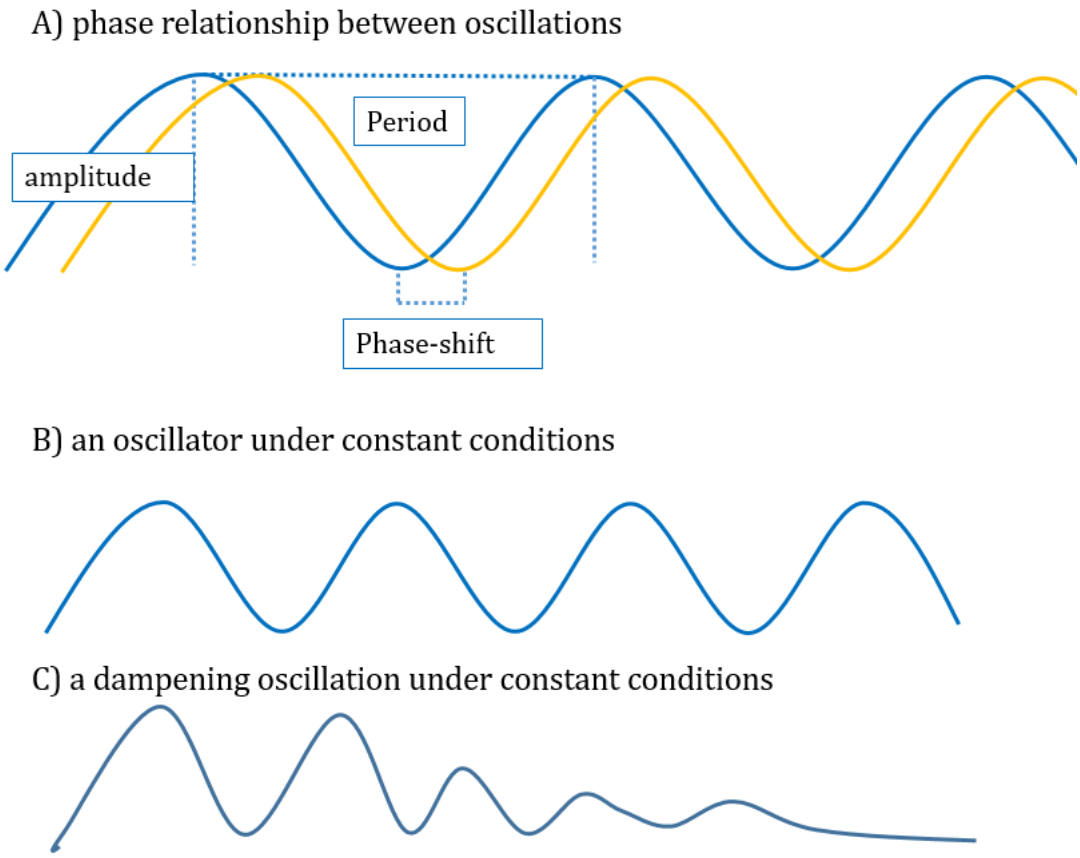

Figure 5. Characteristics of oscillators and oscillations. A) Two oscillations in phase-relation, showing identical amplitude period, but a phase difference (phase-shift). B) an oscillator continuing under constant conditions. C) a dampening oscillation. Illustration by M.J.van Dalum.

The first evidence for an endogenous, internally generated circannual rhythm came from hibernating ground squirrels (*Citellus lateralis*) who were kept under constant light and temperature conditions for four years (Pengelley, Asmundson, Barnes, et al. 1976; Pengelley, Aloia, and Barnes 1978)(Fig.6) . In addition, non-hibernating ground squirrels (*Citellus leucurus)* expressed robust circannual rhythms in body mass under constant light and temperature conditions (Pengelley, Asmundson, Aloia, et al. 1976).

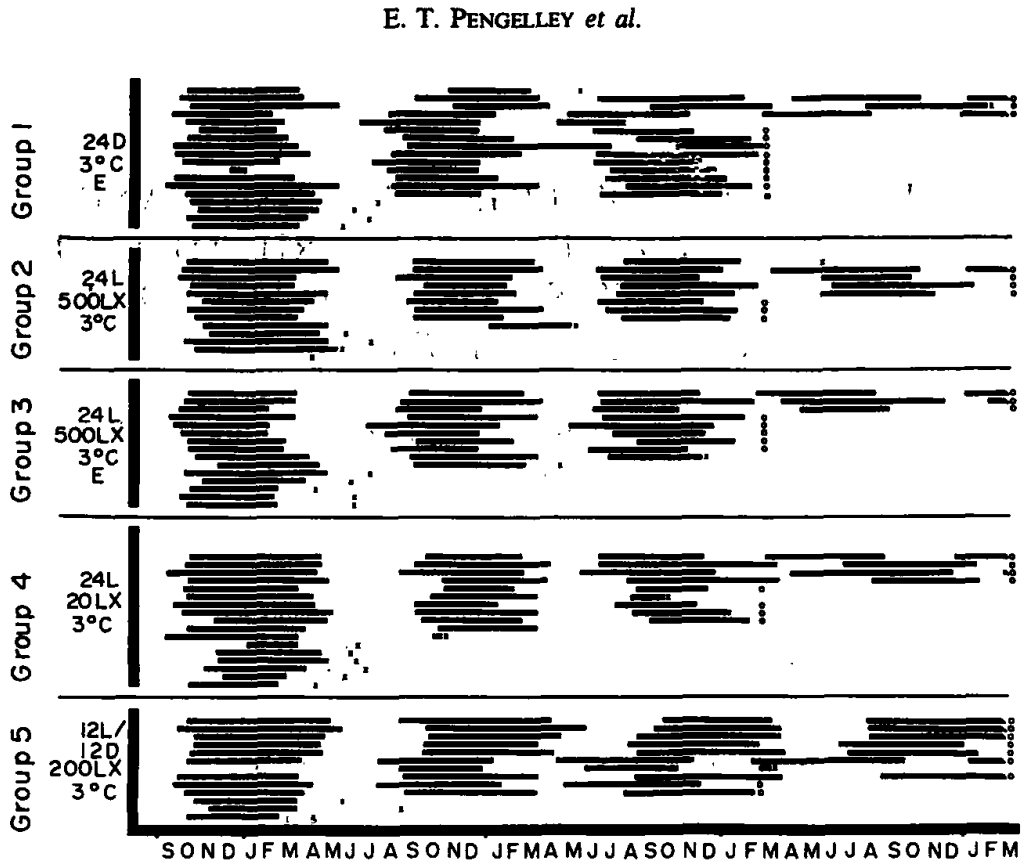

Figure 6. Circannual rhythms in hibernation periods in ground squirrels. They were kept under five different constant day length regimes and temperatures (Y-axis) for four subsequent years (X-axis). Black bars indicate the hibernation bouts of individual squirrels. Data from Pengelley, Asmundson, Barnes, et al. (1976).

Later research revealed that the degree of internal rhythmicity and the requirement for external stimuli to maintain the rhythm varies greatly between species with type 1 and type 2 circannual rhythms being at the ends of a continuum (Goldman et al. 2004; Prendergast, Nelson, and Zucker 2009). Both types are synchronized by photoperiod (Fig. 7a) but the main difference is that type 1 rhythms also require photoperiod as a *driver* while type 2 rhythms continue independently of photoperiod and only require it as a *synchronizer*.

Type 1 rhythms (Fig. 7b) still contain some form of internal rhythmicity, but these need photoperiodic input in order to complete an annual cycle (Lincoln et al. 2005). Siberian hamsters (*Phodopus sungorus*) kept under continuous short photoperiods (LD 8:16, 8 hours of light and 16 hours of darkness) have a winter coat and regressed gonads. However, after 12-38 weeks, they spontaneously change to a summer pelage and restored gonadal growth. They had become photorefractory so they no longer responded to the inhibitory effects of short photoperiods. This suggests that they have some form of internal timing mechanism; however, when retained on short photoperiods, they maintained a summer phenotype and never changed back to a winter phenotype. These type 1 circannual rhythms require to be 'reset' through long-day exposure followed by short days again, in order for the cycle to be completed and restore a winter phenotype (Lincoln, Andersson, and Loudon 2003).

Type 2 rhythms on the other hand, (Fig. 7c) are fully endogenous and only need external cues for entrainment (Goldman et al. 2004). These rhythms continue to cycle even in the absence of any other cue. This was first demonstrated in hibernating ground squirrels and later in several other species such as sheep in which prolactin levels continue to express a circannual cycle even under continuous long photoperiods (Lincoln, Andersson, and Loudon 2003). These type 2 rhythms tend to occur more in long-lived species whereas type-1 rhythms are more common in short-lived.

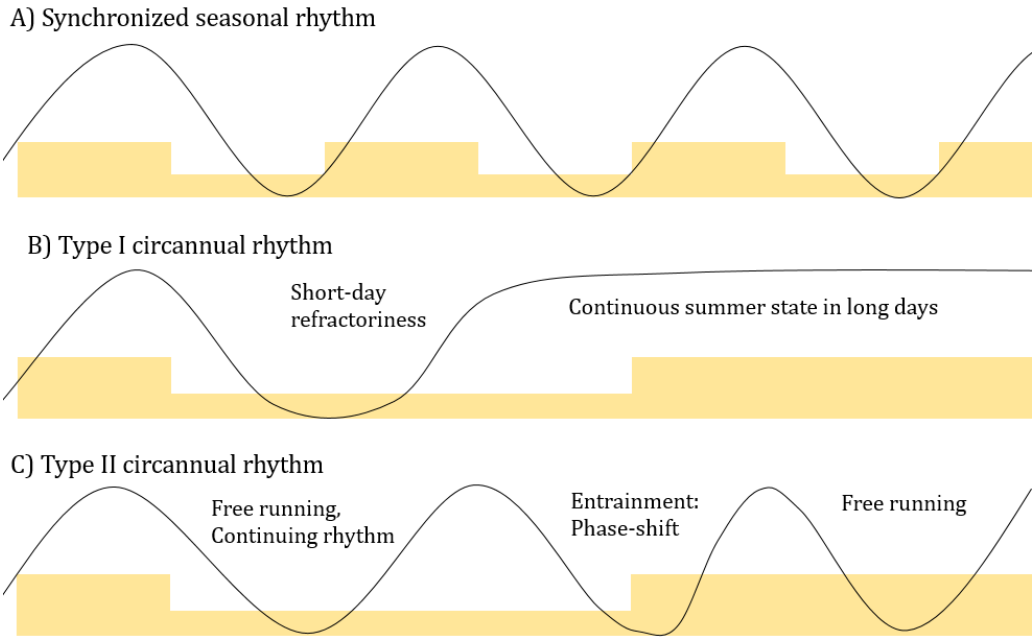

Figure 7. Circannual rhythms under artificial conditions. A) A seasonal rhythm synchronized to alternating periods of long days (high yellow bars) and short days (low yellow bars). B) Type 1 circannual rhythms show in short day refractoriness and spontaneous return to a summer state. However, in the absence of photoperiodic input, cycling would stop and animals remain in summer state. C) Type II rhythms continue to cycle (free running) under constant conditions and only need photoperiodic input for synchronization through entrainment. Illustration by M.J.van Dalum.

The type 1 versus type 2 dichotomy can be conceptually useful but biological variation is a continuum. The relative importance of an endogenous circannual rhythm and the dependence on environmental cues to maintain the oscillation varies per species and in some species, even per individual (Pengelley, Asmundson, Barnes, et al. 1976). Several life-history factors are suggested to affect to what extent a species is purely opportunistic or favours a rigid circannual rhythm to time life history events (Fig. 8). For example, long gestation times and a long lifespan favours stronger reliance on photoperiod for circannual timing whereas animals with short gestation times and short lifespans favour more flexible and opportunistic breeding. Short-lived species that experience only reproductive period in their lives cannot afford to be strict and must 'gamble' more with their reproduction than long-lived species, even at surprisingly high latitudes (Bronson 1988).

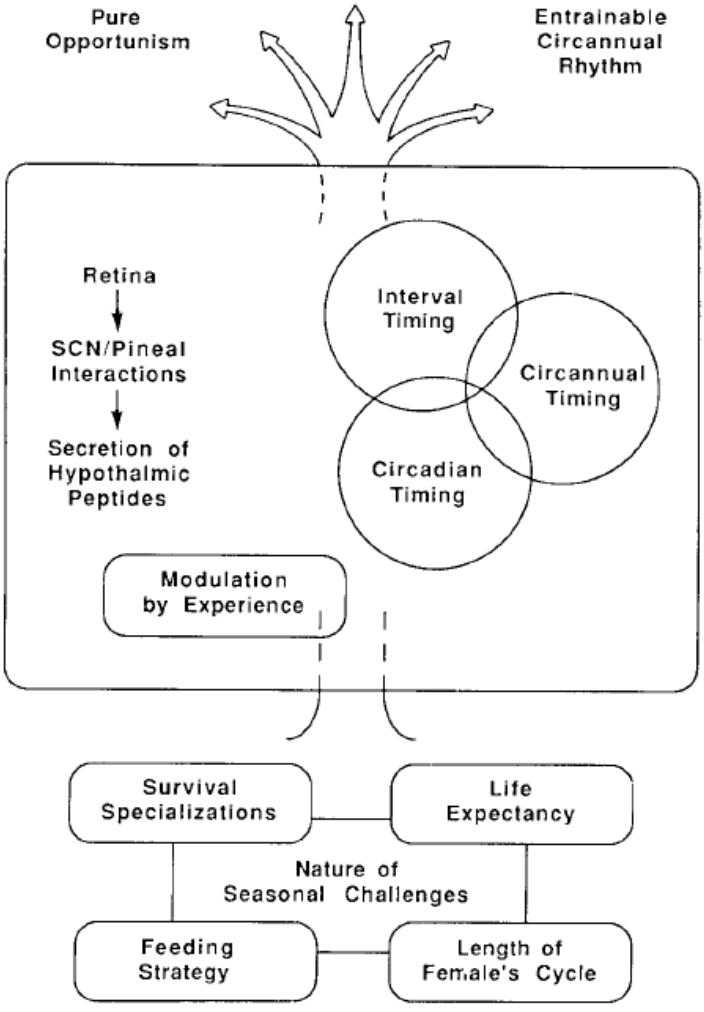

Figure 8. Life history factors determining the extent of opportunism or reliance on internal circannual rhythms regarding timing of reproduction in mammals. Shorter-lived mammals with short gestation times are more likely to rely on opportunism whereas long-lived mammals may favour a stronger circannual rhythm. Figure from Bronson (1988).

Availability of environmental cues also affects to what extent a species may rely an internal circannual rhythm for seasonal timing of life history events. Endogenous, self-sustaining seasonal rhythms are favourable in strongly seasonal environments yet when photoperiodic cue availability is intermittent (Helm et al. 2013) like in migratory birds or burrowing or hibernating mammals (Fig. 9). Still, these species need to entrain their rhythms to match it with the environment and have certain time-windows for photosensitivity such as the summer solstice (Monecke et al. 2009).

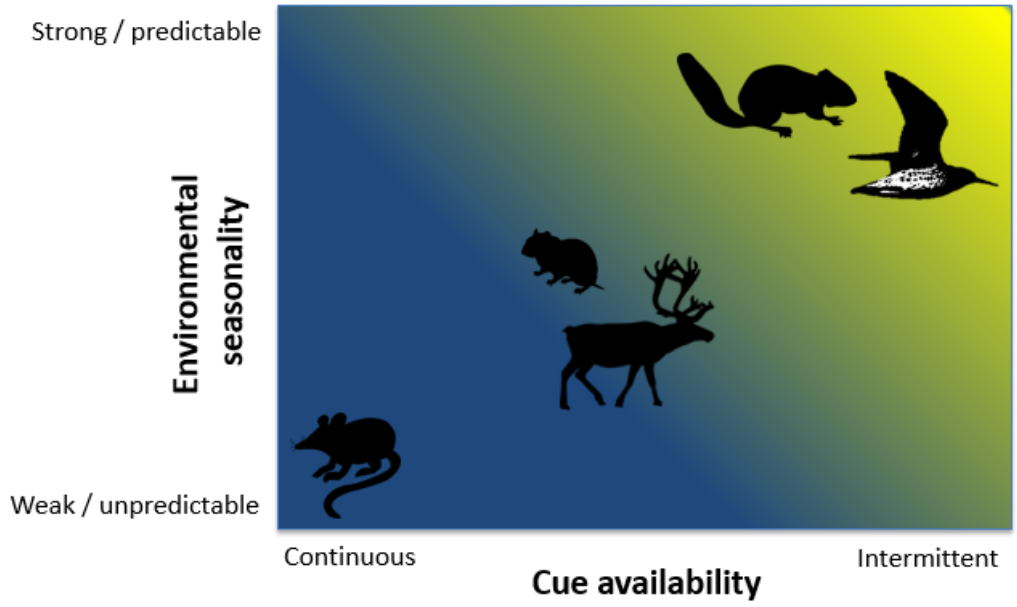

Figure 9. Requirement for a strong internal circannual rhythm in relation to cue availability and environmental seasonality. Blue represents the likelihood for animals to rely on opportunism whereas yellow represents strong reliance on an internal circannual rhythm. Unpublished figure from D.G.Hazlerigg.

When cues availability is more constant, animals can afford to rely more on photoperiod to maintain their seasonal cycles and depend less on endogenous timing. Above the Arctic Circle, the environment is relatively constant during the summer – and winter months, which are characterized by continuous light and continuous darkness respectively. Truly arctic species such as reindeer (Lu et al. 2010; Stokkan et al. 2007) and Svalbard ptarmigan (Appenroth et al. 2020) lose circadian rhythmicity during these periods, yet maintain strong circannual rhythmicity and the mechanisms behind this are still to be unraveled.

The question of *how* animals register day length and synchronize their life history traits with the seasons has been under investigation for several decades now and more recent research has focused on the causal molecular mechanisms underneath: the photoneuroendocrine system (PNES).

1.2 Seasonal phenotype and the photoneuroendocrine system

1.2.1 Tracing the changing day lengths

In order to register day length, organisms must sense when it is light and when it is dark. Mammals only register light through photoreceptors in the retina of the eyes (rods and cones) and a special type of retinal ganglion cells that produce the pigment melanopsin (Hattar et al. 2003). These intrinsically photosensitive retinal ganglion cells (ipRGCs) stand in direct synaptic connection with the superchiasmatic nucleus (SCN), located in the anterior hypothalamus; the mammalian circadian master clock (Hattar et al. 2002; Berson, Dunn, and Takao 2002). These ganglion cells alone can cause phase shifts in the circadian oscillation of clock genes within the SCN (Foster et al. 1991; Hattar et al. 2003). However, rod- and cone photoreceptors can also entrain the SCN when ipRGCs are rendered dysfunctional, suggesting that both photoreceptors contribute to light mediated entrainment of the SCN (Panda et al. 2003). The SCN governs other circadian rhythms within the body such as the nocturnal secretion of the hormone melatonin from the pineal gland (Fig. 10).

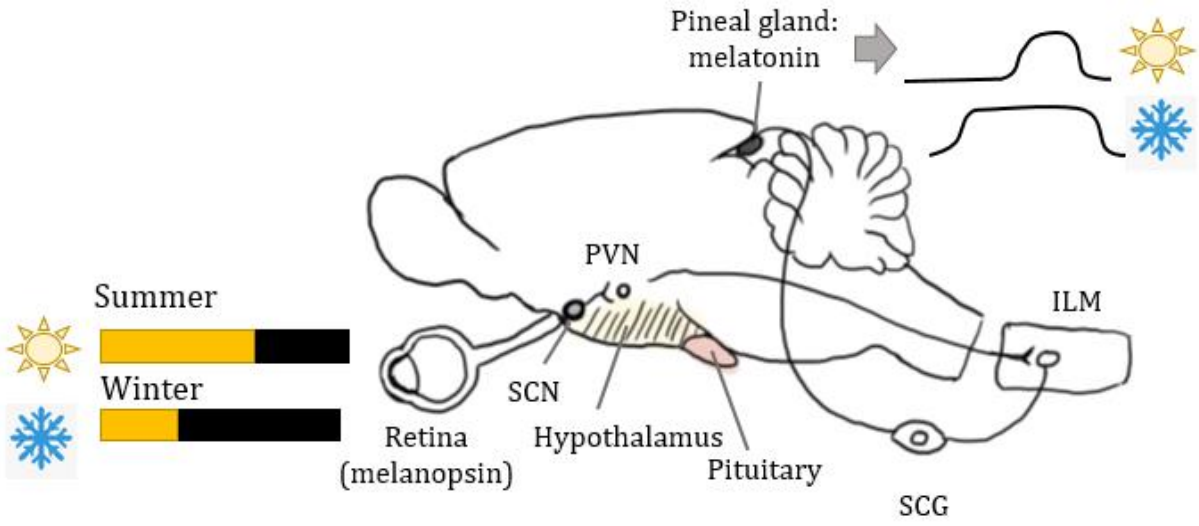

Figure 10. The photoneuroendocrine system driving nocturnal melatonin release. Light is sensed by photoreceptors (rods, cones and retinal ganglion cells producing melanopsin). Photosensitive ganglion cell nerve ends are directly coupled to the SCN, the mammalian circadian master clock which controls the nocturnal secretion of melatonin from the pineal gland, via a synaptic pathway passing by the paraventricular nucleus of the hypothalamus (PVN), the intermediolateral cells of the spinal cord and the superior cervical ganglia (SCG). Illustration by M.J.van Dalum.

Plasma melatonin levels follow the onset and offset of the night (Morgan et al. 1994; Morgan and Williams 1989) but the melatonin onset varies widely between species and also the function of photoperiod (Stehle et al. 2001). The daily light-dark cycle mostly affects the *duration* of melatonin secretion, rather than the level. This means that the melatonin signal is shorter during

the short nights of summer and consequently longer during the long nights of winter (review: Bartness et al. (1993). Removal of the pineal gland (pinealectomy) or knock out of the melatonin synthesis pathway as in c57 mice, shows that clock gene rhythms in the SCN oscillate independently of melatonin and that it is not required for circadian entrainment. However, pinealectomized sheep no longer synchronized their free-running annual estrus cycle and prolactin cycle with photoperiodic changes (Lincoln et al. 2006). Yet programmable melatonin infusions timed between the summer solstice and autumnal equinox could re-entrain the estrus cycle (Woodfill et al. 1994). Similar studies have also been performed in rodents (Goldman et al. 1979; Horton and Stetson 1992, 1990). This indicates that melatonin plays a key role in the regulation of mammalian seasonal reproduction (review: Hazlerigg and Simonneaux, (2015)).

In mammals, melatonin binds to two types of high affinity G-protein coupled receptors: melatonin receptor 1 (MT1) and 2 (MT2) (Klosen et al. 2019), produced by the genes *Mtnr1a* and *Mtnr1b* respectively. Non-mammalian vertebrates have a third melatonin receptor, *Mel1c*, and the mammalian paralogue is *Gpr50*. However, *Gpr50* does not bind melatonin yet its expression is highly photoperiodic (Barrett et al. 2006; Hand 2012). MT1 seems to be the most widely expressed receptor in mammals and it is the main melatonin receptor in the circadian and seasonal system (Weaver, Liu, and Reppert 1996; Von Gall et al. 2002). Melatonin receptors are expressed in a wide variety of tissues, including several regions of the brain such as (SCN) and the *pars tuberalis* (PT) of the pituitary gland, located beneath the hypothalamus (Fig. 12) (Klosen et al. 2002; Dardente et al. 2003; Johnston et al. 2003).

1.2.2. Processing of day length information in the pituitary and hypothalamus

The *pars tuberalis* and the medial eminence (ME) of the hypothalamus are so far considered as the main centres of seasonal time keeping in mammals (Nakao et al. 2008; Hanon et al. 2010; Lincoln and Hazlerigg 2010; Yoshimura 2010; S. M. Dupré et al. 2011). Interestingly, the *pars distalis* of the pituitary accounts for seasonal secretion of prolactin but it lacks melatonin receptors in adults of the species investigated (Hanon et al. 2008; Dardente 2007). Prolactin is involved in regulation of moulting cycles (Lincoln and Ebling 1985; Martinet, Allain, and Weiner 1984) and paracrine signalling from the *pars tuberalis* is potentially responsible for the seasonally oscillating prolactin secretion (Dardente 2007; Hanon et al. 2008).

In the PT, melatonin receptors are expressed by thyrotrophic cells that secrete thyroid-stimulating hormone (TSH) into the median eminence (ME) of the hypothalamus. The median eminence forms the interface between the hypothalamus and the pituitary gland, from which hormonal secretion takes place. Hypothalamic TSH production is highly photoperiodic and

responsible for downstream seasonal phenotype changes (Nakao et al. 2008; Dardente et al. 2010; Dardente, Hazlerigg, and Ebling 2014). TSH consists of a TSHBβ and GSUα subunit (Dardente et al. 2003): the GSUα is continuously expressed but transcription of the THSβ-subunit is turned on by the transcription factor eyes-absent 3 (*Eya3*), which is in turn repressed by melatonin. *Eya3* expression peaks 12 hours after the onset of the dark phase, only in the absence of melatonin during long summer (Fig. 11a) and this promotes high THSβ levels. However, if melatonin is still present (e.g. short days in winter), this *Eya3* expression peak is suppressed and THSβ is not transcribed resulting in an absence of hypothalamic TSH. *Eya3* expression acts thereby act as a seasonal switch for the production of hypothalamic TSH (Dardente et al. 2010; Masumoto et al. 2010; Hut 2011).

Interestingly, in sheep the phase-relationship between two clock genes in the PT also varies with day length. The gene *Period 2 (Per2)* peaks shortly after sunrise whereas the expression of *crytochrome circadian regulator 1 (Cry1)* peaks shortly after sunset (Lincoln et al. 2002; Johnston et al. 2006). Together, these gene products produce a dimer that regulates the expression of downstream seasonal genes (reviews: Hazlerigg and Wagner (2006); Wood and Loudon (2014)). In short summer nights, the time gap between sunset and sunrise and thus the start of *Per2* and *Cry1* expression, is short and overlap in expression allows for dimerization. In winter, the time gap is too long for expression overlap between *Per2* and *Cry1* and there is no dimer formation (Fig. 11b). In hamsters, the amplitude of *Per2* expression is higher in long days and so is the expression of an early response gene (ICER) (Lincoln, Andersson, and Loudon 2003), see figure 11c. However, the causal relations between these photoperiodically expressed clock genes and downstream seasonal responses remains unclear as *per 2* mutant mice still show robust TSH signalling (Ikegami and Yoshimura 2013).

The current molecular working model (Fig. 14) is centred around the interaction between melatonin, *Eya3* and the photoperiodic expression of THSβ in the PT. TSH is received by the TSH-receptor (TSHr) expressed on tanycytes, a special type of glia cells present in the median eminence (Nakao et al. 2008; Hanon et al. 2008). Tanycyte cell bodies are lined up against the third ventricle in the mediobasal hypothalamus and they have dendrites reaching to capillaries in the median eminence and to other hypothalamic neurons (Rodríguez et al. 2005; Bolborea and Dale 2013; Lewis and Ebling 2017).

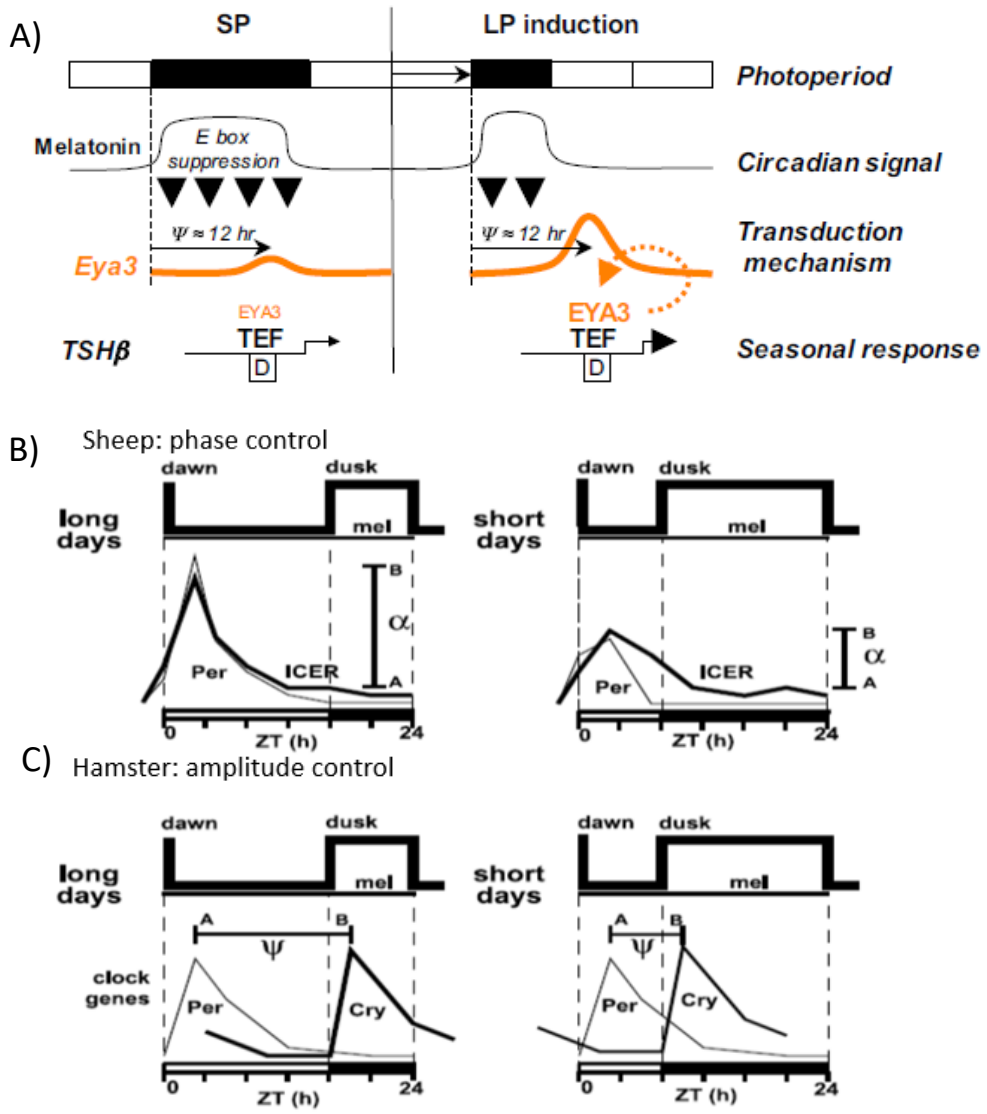

Figure 11. Encoding day length in the *Pars tuberalis* through melatonin signalling. A) Expression of transcription factor Eyes-absent 3 (EYA3) is inhibited by melatonin. In the absence of melatonin (long days), *Eya3* expression peaks 12 hours after melatonin onset at dawn and regulates expression of the TSHβ, together with thyrotroph embryonic factor (TEF). Figure from Dardente et al. (2010). B) In sheep, the clock gene *per* follows the onset of dawn and *Cry1* follows the onset of dusk. The phase relationship and the following dimerization of the two gene products during periods of overlapping expression may regulate downstream seasonal gene expression. C) Melatonin supressing the amplitude of clock gene *Period2 (Per2)* under short days in hamsters. (Panel B and C from Lincoln et al. (2003)).

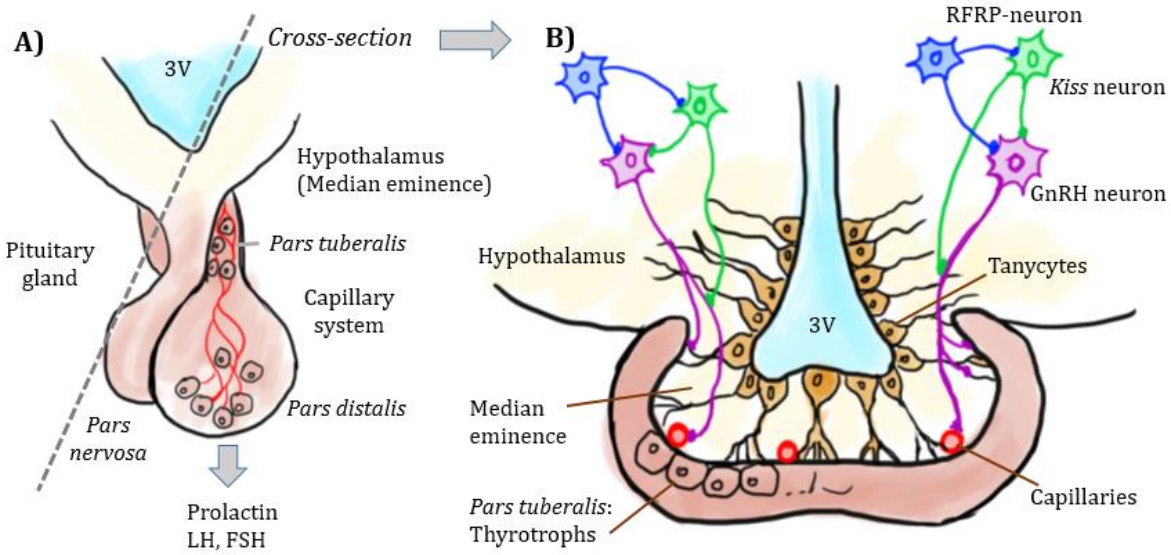

Figure 12. Anatomy of the pituitary and medial eminence of the hypothalamus. A) Overview illustration of the pituitary gland and hypothalamus with the third ventricle (3V). B) Cross section of this brain region showing parts of the *Pars tuberalis* (pale red) containing thyrotrophs cells. Tanycytes (orange) located in the median eminence of the hypothalamus (pale yellow) are lining the third ventricle (3V) and have dendrites reaching the PT and blood capillaries (red circles). Gonadotropin releasing hormone neurons (purple) have nerve ends reaching the capillary system of the PT to which they secrete GnRH. *Kiss* neurons (green) and RFRP neurons (blue) receive signals from tanycytes and have synaptic connections that regulate GnRH neurons. Illustration by M.J.van Dalum.

High levels of TSH (long days) initiate expression of iodothyronine deiodinase type-2 (DIO2) which turns then thyroxine (T4, biologically inactive) into triiodothyronine (T3, biologically active). T4 is produced by the thyroid gland and circulates in the bloodstream, which reaches the medial eminence through the third ventricle. Low TSH levels under short days switch on iodothyronine deiodinase type-3 (DIO3). DIO3 turns active T3 into the biologically inactive reverse-T3. Taken together, the seasonally fluctuating DIO2/DIO3 expression forms a molecular switch resulting in either a summer or winter phenotype (Fig. 13) (Ono et al. 2008; Nakao, Ono, and Yoshimura 2008; Hanon et al. 2008; Dardente et al. 2010). The hypothalamic thyroid hormone signalling pathway is considered as the main pathway regulating the seasonal phenotype. However, there may be a second, potentially equally important pathway that involves retinoic acid (RA) signalling from tanycytes (Shearer et al. 2010; Helfer et al. 2012; Stoney et al. 2016).

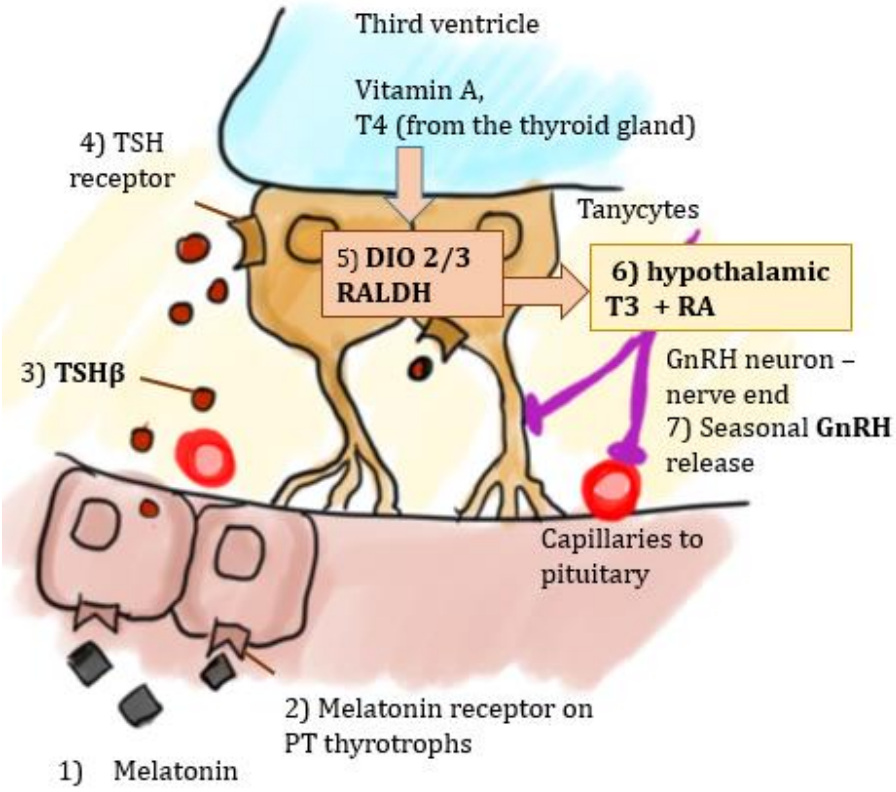

Figure 13. Interaction between PT thyrotrophs and hypothalamic tanycytes. PT thyrotrophs receive melatonin through MT1 melatonin receptors. Under long days, they secrete TSHβ into the median eminence, which is received by tanycytes through TSH-receptors. TSHβ then regulates *Dio2/Dio3* and *Raldh* expression in tanycytes. Long day expressed DIO2 turns T4 into active T3. Short-day expressed DIO3 turns T4 into inactive reverse-T3. RALDH synthesizes retinoic acid (RA) from retinol (vitamin A) that circulates in the blood stream. Tanycytes secrete RA and T3 into the median eminence from where the downstream seasonal phenotype is regulated for example via seasonal release of GnRH. Illustration by M.J.van Dalum.

Retinoic acid (RA) acts as a transcription factor in tissues such as the testes and ovaries, and it plays a key role in embryonic development of for example the eyes, forebrain and limb. It is also involved in neurogenesis in brain regions like the hippocampus (For reviews, see: Shearer et al. (2012); Ransom et al. (2014); Ghyselinck and Duester, (2019)). RA signalling in tanycytes (Shearer et al. 2010; Shearer, Stoney, Nanescu, et al. 2012; Stoney et al. 2016) is highly photoperiodic, mostly through the photoperiodic regulation of its synthesis enzymes: retinaldehyde dehydrogenase 1 (ALDH1A1 , sometimes referred to as RALDH1*)* and 2 (ALDH1A2, or RALDH2*).* Both enzymes turn retinaldehyde (shortened as retinal) into retinoic acid (Sobreira et al. 2011), which is then secreted into the ME of the hypothalamus. Retinal is formed from vitamin A (retinol) and this is taken up from the third ventricle and transported into the tanycyte cell body. Several genes involved in RA transport (*Stra6, Ttr*), binding (*Crabp1, Crabp2*), and synthesis (*Aldh1a1, Aldh1a2*), but also RA-receptors (*RAR, RXRγ*) are regulated by

photoperiod in rodents (Shearer, Stoney, Morgan, et al. 2012). Hypothalamic *Aldh1a1* expression is directly upregulated by T3 (Stoney et al. 2016) and Ebling (2014) suggested a direct relation between the TSH signalling and *Aldh1a1* expression in tanycytes. Retinoid acid degrading enzyme (CYP26B1) does respond to photoperiod as well but is regulated less rapidly or secondarily (Helfer et al. 2012). Interestingly, thyroid hormone receptors (TRs), retinoid X receptors (RXR) and retinoic acid response elements (RARs) interact through dimerization and control transcription of various downstream genes (Ross et al. 2005; Wu and Koenig 2000).

The exact role of summer-associated RA-signalling in the regulation of seasonal phenotypes is unclear but it is potentially involved in regulation of body mass and appetite through seasonal hypothalamic neurodegeneration and neurogenesis (Helfer, Barrett, and Morgan 2019). Cyclical histogenesis in certain regions of the hypothalamus and pituitary could lay at the basis of internal circannual rhythmicity, but this is still a rather unexplored theory (Hazlerigg and Lincoln 2011).

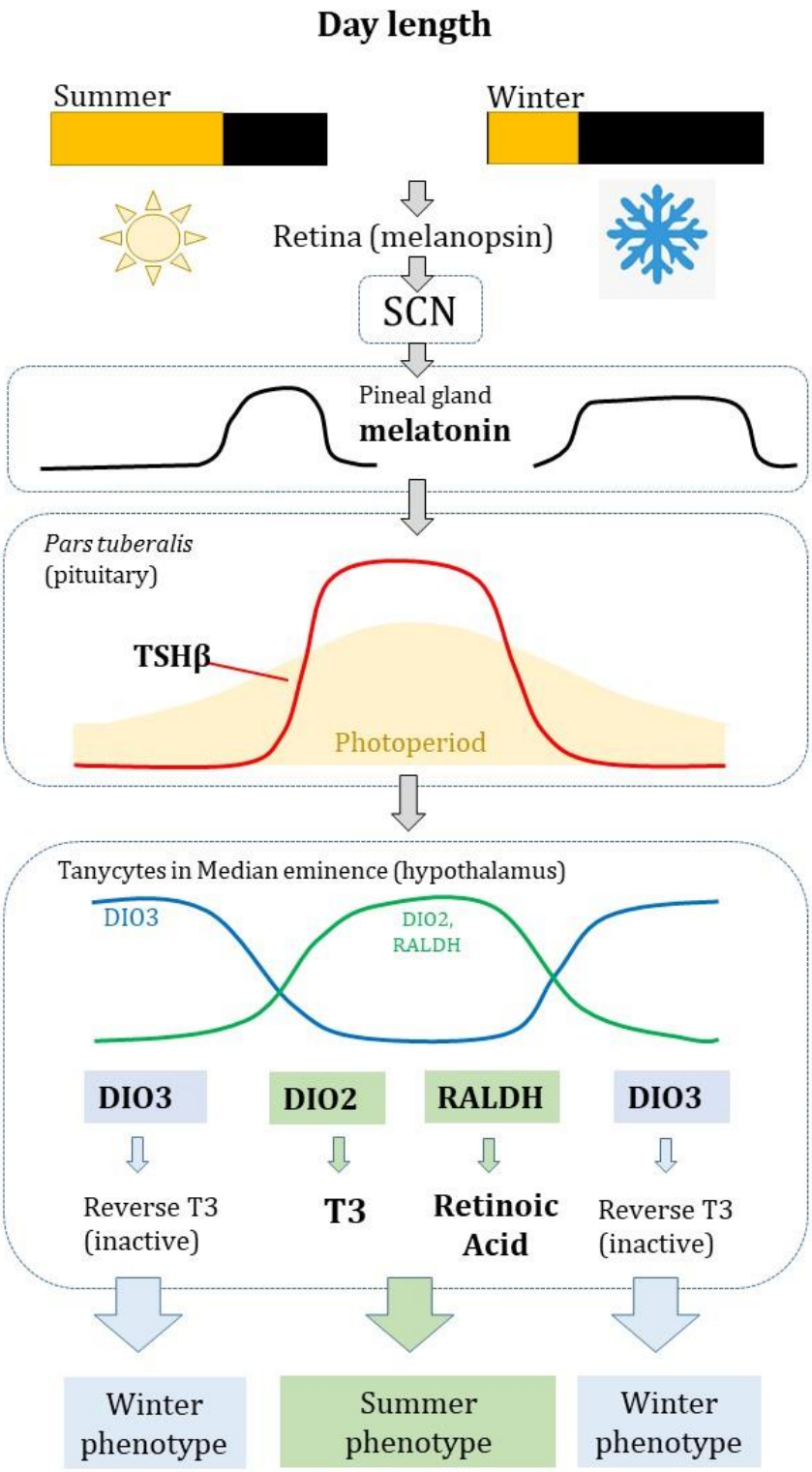

Figure14. Current model of the mammalian photo neuroendocrine system (PNES). Melanopsin from special ganglion cells in the retina register light. This input is received by the pineal gland, which secretes melatonin in the dark phase, and the duration of the signal follows the annual day length cycle. Short melatonin signals in summer stimulate the *pars tuberalis* of the pituitary to secrete thyroid-stimulating hormone (TSH) into the median eminence of the hypothalamus. There, tanycytes respond with photoperiodic regulation of *Dio2/Dio3, Raldh*. DIO2 turns thyroid produced T4 that reaches the hypothalamus through the third ventricle into active T3. RALDH synthesizes retinoic acid (RA) from circulating vitamin A (retinol). Both T3 and RA regulate the summer phenotype. Illustration by M.J.van Dalum.

1.2.3 Downstream regulation of the seasonal phenotype

Most research on the functioning of the PNES in mammals is based on studies in rodents and sheep. These species have provided a consistent picture of the upstream mechanisms in the hypothalamus and PT. In all species investigated so far, TSH signalling rigidly follows photoperiod with elevated expression in long days. The second upstream seasonal RA signalling pathway has so far only been studied in rodents (Shearer, Stoney, Morgan, et al. 2012) but there is no evidence for this pathway in sheep (Lomet et al. 2018).

Downstream regulation of the seasonal phenotype is more species- and even gender specific. The cell bodies of gonadotropin releasing hormone (GnRH) neurons are located in the rostral hypothalamus (preoptic area and organum vaculosum of lamina terminalis (Lehman et al. 1997). They regulate gonadal growth, gonadal activity and sex steroid production through the release of GnRH that in turn stimulates the release of follicle stimulating hormone (FSH) and luteinizing hormone (LH) from the anterior pituitary. The number of GnRH neurons does not seem to vary with the season in hamsters (Urbanski, Doan, and Pierce 1991) but GnRH release does respond to photoperiod in a species- and gender specific manner (Kriegsfeld et al. 2006; Hahn et al. 2009). Sex steroids such as testosterone negatively feedback on GnRH release but seemingly not directly onto the GnRH neurons themselves, but rather through interneuron pathways. Several coupling systems between melatonin and seasonal GnRH release have been investigated, such as involvement of RF-amide (arginine-phenylalanine-amide) peptides secreted from kisspeptin neurons and RFRP-neurons (Klosen et al. 2013; Simonneaux 2020) (Fig. 12b).

Seasonal changes in body mass and appetite seems to be regulated separately from acute energy homeostasis. For example, leptin is associated with adipose tissue and appetite regulation but it is not responsible for seasonal weight regulation in hamsters (Rousseau et al. 2002). In tundra voles, leptin was not affected by photoperiod but did correlate with body mass (Wang, Zhang, and Wang 2006). However, short days induced an upregulation of VGF polypeptide, which is associated with weight loss in hamsters (Ebling and Barrett 2008). When infused into the ventricular system of the hypothalamus, it supressed food intake and reduced body mass (Jethwa and Ebling 2008). There is also a potential role for growth hormone (GH) released from the pituitary in short photoperiods. Seasonal fluctuations in growth hormone (GH) release from the pituitary affects body mass in deer (Webster et al. 1999), golden hamsters and Siberian hamsters (Dumbell et al. 2015). Growth hormone releasing hormone (GHRH) from hypothalamic neurons promote GH release while this is inhibited by somatostatin, also produced by hypothalamic neurons. Both factors are regulated by photoperiod (Dumbell et al. 2015). The exact causal mechanism of body mass regulation remains unresolved but short photoperiod

induced downregulation of RA signalling pathway components (receptors RAR, RXRy and transporters CRBP, CRABP2) in the dorsomedial posterior arcuate nucleus of the hypothalamus, and this was associated with seasonally reduced body mass in hamsters (Ebling and Barrett 2008). As discussed before, thyroid hormone and retinoic acid mediated neurogenesis and neurodegradation in hypothalamic regions, may lay at the basis for downstream seasonal regulation of energy metabolism (Helfer, Barrett, and Morgan 2019).

The coupling between the upstream PNES and variation in for example seasonal immune function, stress response (Walton, Weil, and Nelson 2011; Davis and Maney 2018) and behaviour also remains unclear. Oxytocin and vasopressin can affect social behaviour and mate choice in mammals (Bielsky and Young 2004; C. E. Barrett et al. 2013). The bird oxytocin homologue is also associated with sexual and social behaviour and this was higher during the breeding season compared to the mating season in ravens (Stocker et al. 2021). Taken together, the downstream regulation of the seasonal phenotype is complex and flexible which allows natural selection to shape locally adapted phenotypes.

1.3 Adaptation to local seasonal environments

1.3.1 Photoperiod- temperature relations at different latitudes

In the previous section, I have summarised what is currently known about the mammalian photoneuroendocrine system (PNES). The components are rather well characterized but the sources of variation that enables animals to adapt to local seasonal conditions are largely unknown. Environmental seasonality varies greatly with latitude, altitude and the distance from the coast and this creates variable selection pressures that shape adaptations to the local seasonal environment.

The Earth's tilted axis is responsible for seasonality on Earth, which is particularly prominent at higher latitudes. Annual day length variation increases with latitude towards periods of continuous light in summer and periods of continuous darkness in winter near the poles (Fig. 15). Solar rays reach the Earth under a nearly right angle around the equator while this angle flattens towards the poles, spreading out over larger surface areas. This decreases the radiation dose per surface area unit and lowers ambient temperatures (Hartmann 2016). However, the annual day length variation is mostly responsible for the lower mean annual temperatures and larger seasonal temperature fluctuations at higher latitudes. The mean annual temperature also decreases with increasing altitude and the distance from the coast leads to larger annual temperature fluctuations as ocean currents stabilize temperatures on coastal regions. This creates a relatively mild climate compared to more extreme continental climate at the same latitude and altitude (Hartmann 2016).

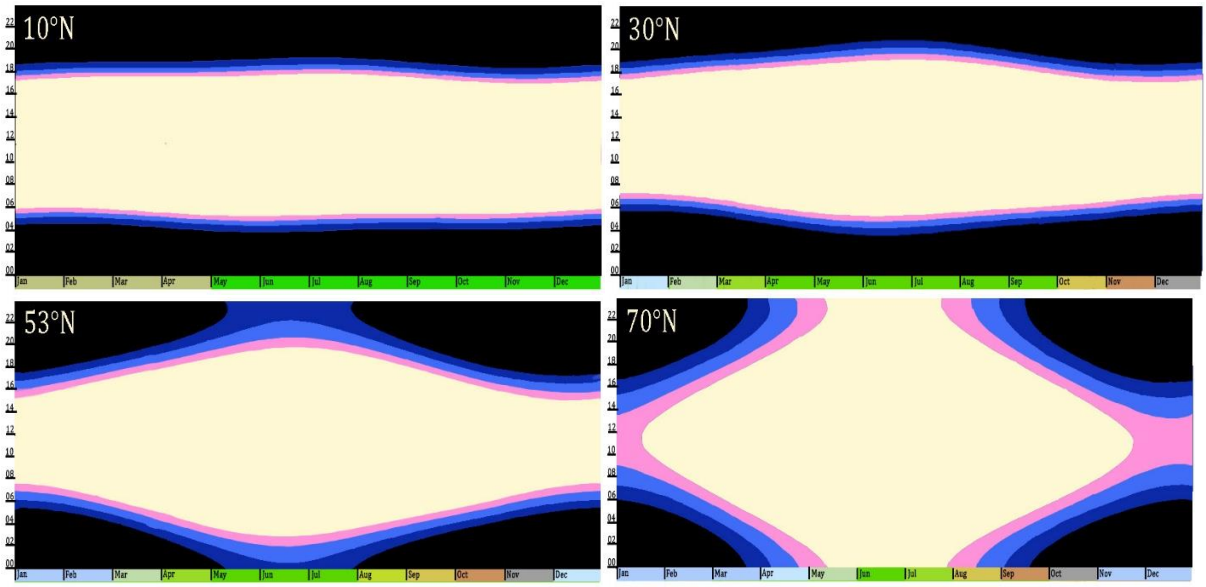

Figure 15. Annual variation in photoperiod at various latitudes. Y-axis: hours of the day, X-axis: months of the year. Yellow: period of day light. Pink: civil twilight, light blue: nautical twilight, dark blue: astronomical twilight. Illustration by M.J.van Dalum.

As mentioned earlier, organisms living at higher latitudes or altitudes must not only cope with cold winters, they must also optimize timing of reproduction in a fluctuating environment through the use of photoperiod as a time cue (Bronson 1988). Photoperiod correlates with ambient temperature fluctuations and this relation is elliptic (Fig.16). The elliptic shape with lower spring than autumn temperatures is caused by the delay in surface warming in winter and surface cooling in autumn (Hut et al. 2013).

The relation between photoperiod, temperature and timing becomes clear when we consider a hypothetical autumn temperature threshold of 10°C that would stimulate growth of a winter coat. This threshold corresponds with about 19 hours at this latitude 65°N but with 14 hours at latitude 55°N (Fig.16). In other words: the critical photoperiod associated with the right temperature to start growth of a winter coat varies per latitude, altitude and distance to the coast (Hut et al. 2013). Animals native to lower latitudes might see a 12 hour day length as a go-signal to turn "summer mode" on whereas a northern species remains in "winter mode" at exactly the same day length. This implies that organisms must 'read' day length information according to the latitude at which they live, which leads to the question whether animals require a different internal calendar. In other words, is their PNES 'calibrated differently' in order to match the local photoperiod-temperature relation?

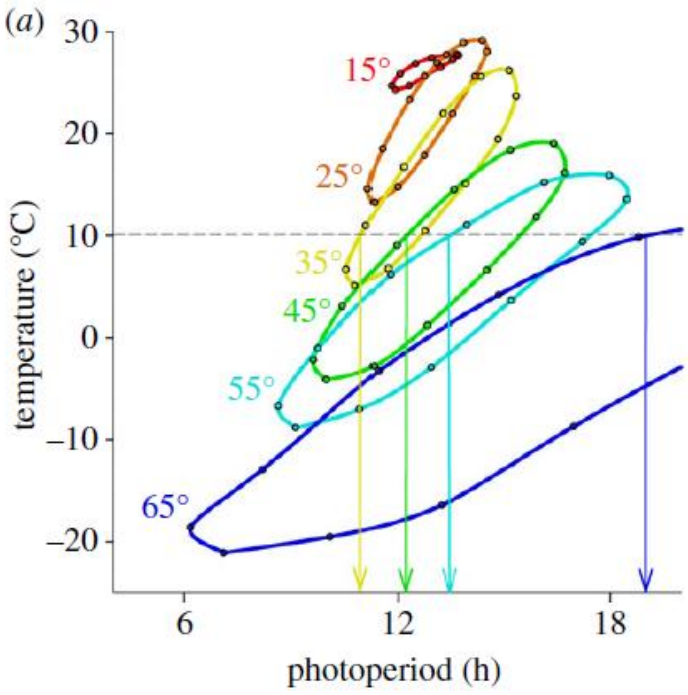

Figure 16. Photoperiod – temperature ellipses. The elliptical relation between monthly temperature fluctuations (y) and photoperiod (x) at various latitudes. Surface warming causes the higher temperatures in autumn (upper half of the ellipse) versus spring (lower half of the ellipse). A hypothetic autumn temperature threshold at 10°C shows how the corresponding photoperiod lengthens with latitude.

1.3.2 Latitudinal cline studies

One would expect to see a gradient, or a cline, in traits such as shortening of the breeding season, across latitudes. Several studies have assessed the effect of latitude on timing of reproduction although not many studies have focused on mammals. One of the first studies that considered latitude as a factor affecting seasonal timing came from Elizabeth Whetham (1933). She studied egg production in domestic chickens across a range of latitudes and longitudes and found that egg production correlated with increasing photoperiod at both the northern and southern hemisphere while it nearly continuous at low latitudes of 10°N. Franklin H. Bronson (1985) neatly demonstrated the narrowing of the breeding season with increasing latitude in deer mice (*Peromyscus sp.*) and lagomorphs (Fig. 17), yet the figure also shows variation between populations from the same latitude. Timing of birth was also significantly later in Eurasian lynx (*Lynx lynx)* from Northern Norway (69-70°N) compared to lynx from Southern Norway (60-61°N) with an average birth date on the 9th of June versus the 30th of May, respectively (van Dalum 2013).

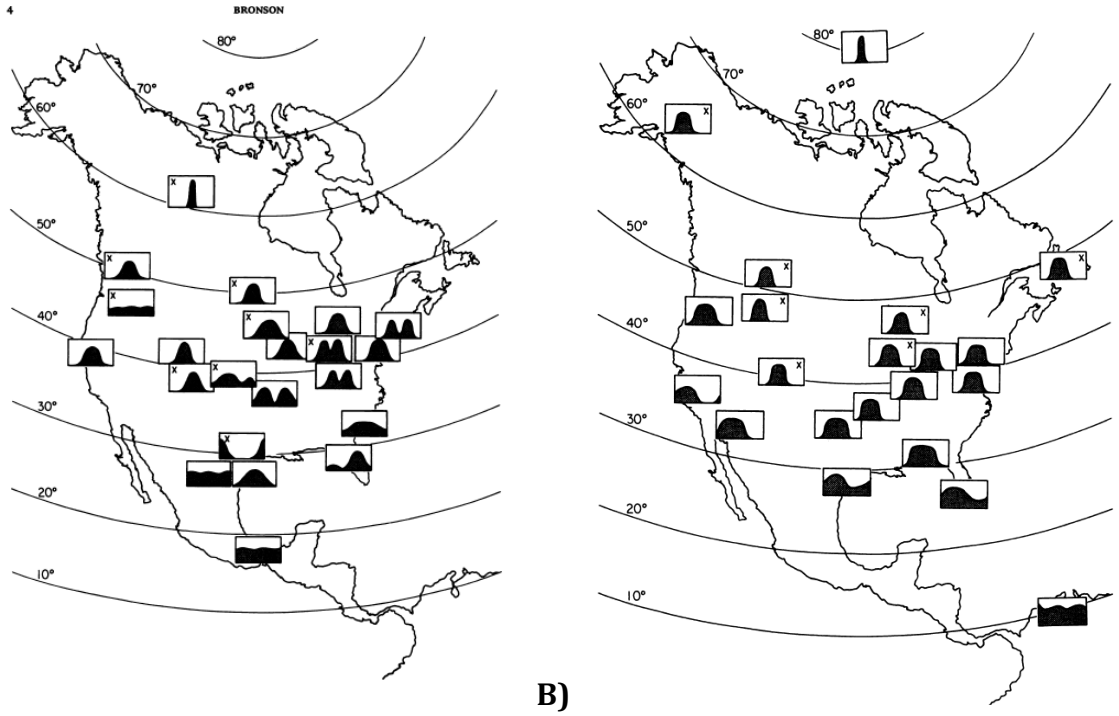

A) **B)**

Figure 17. **Breeding season in deer mice and lagomorphs.** Local variation in the number of pregnant females caught in deer mice (*Peromyscus*) (A) and lagomorphs (B). There is a general trend of a shortening breeding season with increasing latitude. The *X* in the left corner of some squares indicates patterns from the eastern deer mouse (*Peromyscus maniculatus*) (A) and the snowshoe hare (*Lepus americanus*) (B) Figures from Bronson 1985.

These observations do not provide answers whether seasonal *timing* mechanisms vary with latitude, since these could be passive responses to the declining winter temperatures and restricted energy available for reproduction. Photoperiod response studies provide more insight

in whether or not animals maintain different internal calendars or photoperiod-temperature calibrations. One such method is through assessing the critical photoperiod, or threshold day length that induces seasonal phenotype changes between species or populations from various latitudes. As expected from figure 16, critical photoperiod would increase with latitude for both spring induced summer preparations and for autumn induced winter preparations, which effectively shortens the overall breeding season. Most studies have been done on diapause (winter dormancy) induction in insects and collectively, these studies indeed show longer critical photoperiods with increasing latitude (populations below 800m altitude, reviewed by Hut et al. (2013)). Critical photoperiod has also been studied in several vertebrates like fish (Strand, Hazlerigg, and Jørgensen 2018), birds (Silverin, Massa, and Stokkan 1993) and mammals (Hoffmann 1982; Hazlerigg et al. 2018) but population differences and the potential effect of latitude has rarely been assessed. Although one study on non-migratory great tits (*Parus major*) from Tromsø (69°N), Göteborg (57°N) and Italy (45°N) showed that birds from Tromsø required 12h light for the induction of testes growth while birds from Italy responded to 11h and those from Göteborg needed 11-12h light (B. Silverin, Massa, and Stokkan 1993).

Some studies on mammals suggest that long-day breeding rodents from northern latitudes require longer photoperiods to induce or maintain the reproductive apparatus. For example, deer mice *(P.maniculatus*) from Chihuahua (27°N) and South Dakota (44°N) grew large testes when transferred from short days (10L) to longer days (14L) while mice from Manitoba (55°N) needed at least 16 hours for testicular growth (Dark et al. 1983) . Wild caught *P.leucopus* from Maine (44°N) and Connecticut (41°N) regressed their testes when transferred from natural summer photoperiods to shorter (9L) photoperiods while those from Georgia (33°N) remained reproductively competent, suggesting that photo-induced gonadal regression is more pronounced in the North (Lynch, Heath, and Johnston 1981). Photoperiod also evoked opposite immune responses in meadow voles (*Microtus pennsylvanicus)* from 62°N versus 39°N with short days enhancing delayed-type hypersensitivity responses in the southern population but suppressing it in the northern population (Pyter, Weil, and Nelson 2005). Interestingly, short photoperiods had no effect on body mass and the gonadal response was similar between both populations. This suggests a differential sensitivity to photoperiod at various physiological aspects, which may be associated with latitude.

The last three examples also suggest that these mammals *do* respond to photoperiod in a location-dependent fashion as we have seen in phenotypic variation that is supposedly adaptive to the local environment. However, these observations do not provide insight in the mechanisms behind this phenotypic variation.

1.3.3 Variation in the seasonal response mechanisms

As discussed in the first section, short-lived mammals such as voles may be more flexible in the timing of reproduction than long-lived animals since they have only one chance to reproduce in their lifetimes. One would therefore expect to see opportunistic and year-round breeding at relatively high latitudes compared to longer-lived species from similar latitudes that rely more on circannual timing (Fig. 18) (Bronson 1988).

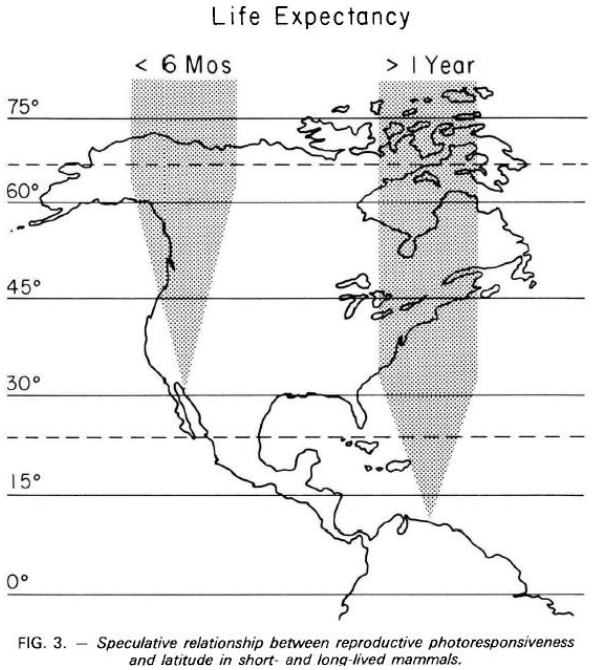

FIG. 3. — *Speculative relationship between reproductive photoresponsiveness and latitude in short- and long-lived mammals.*

Figure 18. Suggested relation between reproductive photoresponsiveness, life expectancy and latitude. The width of the grey bar shows relevance of photoperiod in the timing of reproduction, versus pure opportunistic timing. Short-lived mammals often have only once chance in a life time to reproduce and may therefore favour more opportunistic than long-lived mammals from the same latitude. Figure from Bronson (1988).

This opportunism shows as year-to-year variation in the onset and offset of breeding, both between individuals in a population and within individuals (Ergon, Lambin, and Stenseth 2001). This suggests that these species are responsive to a number of environmental factors that can alter their seasonal phenotype. Where and how this flexibility occurs in the PNES, remains a question to investigate. Understanding the extent of flexibility within the neuroendocrine response and its underlying causes could provide more insight in how selection can shape seasonal phenotypes and would enhance our ability to predict the adaptive potential is of a species or population in the face of environmental change (Lessells 2008; Visser et al. 2010).

On the other hand, when we observe changes in seasonal timing within a population, we cannot be sure about the mechanisms underlying a population's response without understanding the source of flexibility at the individual level. The concept of reaction norms can form a bridge between an individual's physiology and genetics and the evolutionary ecology of a population.

Reaction norms (Fig. 19) quantify the sensitivity to a particular environmental factor (selection pressure) and the ability to change certain features of the phenotype within an individual or within a population (West-Eberhard 2008). At the individual neuroendocrine level, one can envisage a quantitative analysis to evaluate how specific elements in the chain of neuroendocrine signaling change in response to for example photoperiod and temperature.

Different genotypes shape individual responses to a changing environment and individuals vary in their degree of phenotypic plasticity (Fig 19a). Phenotypic plasticity is the capacity of an individual genotype to produce multiple phenotypes in response to environmental change (Pigliucci, Murren, and Schlichting 2006). Phenotypic plasticity in seasonal timing could translate in the ability of an individual to modulate the photoperiodic response in for example reproduction with other non-photic cues such as ambient temperature (Kriegsfeld, Trasy, and Nelson 2000; Nelson et al. 1989; Visser, Holleman, and Caro 2009; Silverin et al. 2008), food availability (Haapakoski, Sundell, and Ylönen 2012), activity (Kerbeshian and Bronson 1996), predation (Haapakoski, Sundell, and Ylönen 2012; Gliwicz 2007) and social environment (Trainor et al. 2006). For example, low temperatures further stimulated gonadal regression in prairie voles (*Microtus ochrogaster*) kept on short photoperiods (Nelson et al. 1989) compared to individuals from the same population on higher temperatures. In a constantly changing and unpredictable environment, individuals need to be flexible and opportunistic in their seasonal response and selection may favour genotypes that can produce multiple phenotypes (Pigliucci, Murren, and Schlichting 2006; Lessells 2008).

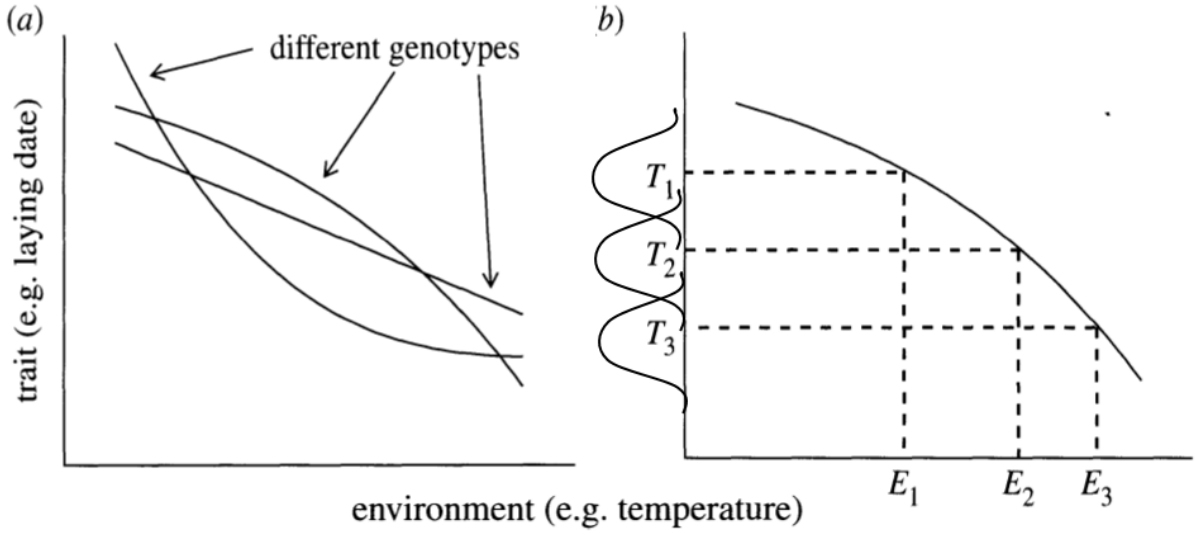

Figure 19. Reaction norms from the endocrine and evolutionary perspective. A: The endocrine perspective considers the response to environmental change within individuals with different genotypes. B: The ecological perspective considers changes in phenotype occurrence (the Gaussian curves on the Y-axis) within a population. Figure modified from Lessells (2008).

Reaction norms at the population level reflect shifts in phenotype occurrence in response to environmental change (Lessells 2008) (Fig. 19b). For example, the proportion of individuals engaging in winter breeding or the onset of the breeding season changes as a function of temperature (Nelson et al. 1989). Reaction norms are heritable and a shift in phenotypes occurring in a population may not be the result of individual phenotypic plasticity alone as individuals vary genetically (Postma and van Noordwijk 2005). Heritability can translate in persistent differential photoperiodic responses between populations kept under similar environmental conditions. For example, three generations of artificial selection on photosensitive breeding or on photoperiodic non-responsiveness in *Peromyscus leucopus* native to 37°N, resulted in a line in which 80% of the individuals responded to short photoperiods with gonadal regression whereas in the other line this was on 16% (Heideman et al. 1999). Similar experiments also showed heritability of photoperiodic response in *P.leucopus*, particularly to short days (Sharp et al. 2015) and red backed voles (*Myodes rutilus*) (Stevenson, van Tets, and Nay 2009). Hybrids between northern and southern viceroy butterflies *(Limenitis archippus)* with long versus short critical photoperiods showed an intermediate critical photoperiod (Hong and Platt 1975). Although heritability of phenotypes does not necessarily mean that there is difference in genetic coding as gene expression patterns can inherit epigenetically (through heritable methylation patterns) for several generations (Bossdorf, Richards, and Pigliucci 2008).

Yet evolution of populations through selection on individual seasonal reaction norms, can in turn alter the occurrence of certain genetic variants in PNES response elements within a population. Attempts have been made to find correlations between variants of genes involved in the PNES and environmental factors such as latitude. These studies have mostly targeted clock genes involved in the circadian system. Variation in a functionally significant paralogue of *Clock* correlated with latitude in blue tits (*Cyanistes caeruleus*) (Johnsen et al. 2007). A similar latitudinal gradient in length variants of *OtsClock1b* was found in salmon (*Oncorhynchus tshawytscha*) and these variants also correlated with latitudinal variation in reproductive timing (O'Malley and Banks 2008). However, population specific signatures of positive selection on the clock gene *period 2 (Per2)* in humans did not correlate with latitude (Cruciani et al. 2008). In common voles, local photoperiod-temperature relations correlated with intronic and exonic variation around the hinge region of the TSH receptor (van Rosmalen, 2021). A source of caution is the relatively small genomic regions assessed; only parts of one gene of interest. On the contrary, genome wide screenings for genes under selection between populations provide an unbiased, bottom-up approach. This has already revealed selection on the TSH-receptor in domestic chickens (Rubin et al. 2010). Chicken domestication may have led to alternations of TSHr that allow for photoperiod independent year-round breeding (Rubin et al. 2010).

1.3.4 Detecting signatures of selection in the genome

Genome wide screening for signatures of selection can provide insight in the evolutionary history of wild populations at the genetic level. A signature of selection is a change in genetic variation in a specific genomic region occurring as a consequence of environmental selection pressures that have led to functional differences between populations (Bertolini et al. 2018). Genes that carry a signature of selection are likely to have functional relevance in relation to divergent selection pressures and warrant further investigation (Vitti, Grossman, and Sabeti 2013). Genetic variation originates from mutations such as deletions, insertions or single nucleotide polymorphisms (SNPs) (Freeman and Herron 2004). Such mutations can alter gene expression when they occur in regions with promoters, enhancers or introns or they can alter structure of the actual gene product when they fall in coding regions (exons) of a gene (Freeman and Herron 2004). Mutations that fall in the exonic regions do not always alter the protein structure of the final products since several three-base pair combinations can encode the same amino acid. Mutations that do not change the amino acid structure of a protein are therefore called synonymous mutations. Synonymous mutations may nonetheless affect expression levels of the gene product because of codon-bias under which translation rates depend on levels and activity of synonymous tRNAs carrying different triplet codons (Freeman and Herron 2004). Non-synonymous mutations change the amino acids built into the protein and this may change and three-dimensional structure and functionality (e.g. enzyme activity) (S. Freeman and Herron 2004).

Signatures of selection in the genome (Fig.20) are the consequence of several forms of natural selection operating on the phenotypes present in a population. Positive, or in other words, directional selection is mostly associated with adaptation as it favours certain features in one population but not the other (Freeman and Herron 2004; Holsinger and Weir 2009). Negative or purifying selection reduces the occurrence of deleterious mutations in a population whereas balancing selection maintains a certain level of individual variation through preserving allelic variants in the gene pool (Casillas and Barbadilla 2017; S. Freeman and Herron 2004). Positive selection leaves the clearest signature of selection, which is detectible through searching for locations (loci) with reduced genetic variation (Fig.20). Positive selection namely favours certain alleles of a gene and drives these to higher allele frequencies within a given population. Under strong selection pressures, these alleles can reach complete fixation, leaving all individuals homozygous for this particular allele (Holsinger and Weir 2009; Vitti, Grossman, and Sabeti 2013; Messer and Petrov 2013). Genes on the same chromosome are inherited together and neighbouring yet functionally unrelated regions are also 'swept to fixation' and leave a *selective sweep* in the genome (Fig. 20b, c). The selected gene and its neighbours are in linkage disequilibrium and these genes co-inherit until crossing-over during meiosis dissolves the

association (Messer and Petrov 2013; Vitti, Grossman, and Sabeti 2013). Strong and recent selection pressures leave hard selective sweeps with a strong local reduction in genetic diversity. Milder or older selection pressures leave soft sweeps with only a mild reduction (Fig.20a). Soft sweeps are much harder to distinguish statistically from background variation (Messer and Petrov 2013; Vitti, Grossman, and Sabeti 2013).

A frequently used method to detect selective sweeps between two populations is through calculating the fixation index (F_{ST}). Directional selection between two populations can alter allele frequencies by driving an allele to fixation in one population, but not the other (Holsinger and Weir 2009; S. Freeman and Herron 2004). This index represents the genetic distance between two populations of the same species at any given locus. It is based on the Hardy-Weinberg principle (Freeman and Herron 2004), which states that allele frequencies of a given allele are constant from one generation to the next *in the absence* of any evolutionary processes. Any changes in these allele frequencies reveal ongoing selection or genetic drift (Holsinger and Weir 2009). The fixation index evaluates the deviation from neutrality and thus potential influence of evolutionary processes by comparing changes in heterozygosity scores at any given locus between two populations (Vitti, Grossman, and Sabeti 2013). Therefore, any differentiation greater than by chance would lead to a higher local F_{ST} value (Fig. 20d). The calculation and application is further explained in the extended method section. Genome-wide calculations of the F_{ST} can provide more insight in the evolution of populations from different environments and reveal novel genes under selection. With the sequencing costs diminishing, this is becoming an increasingly accessible approach. Several populations of livestock (Guo et al. 2018; Amaral et al. 2011; Choi et al. 2015) have already been screened for selection signatures but this has not yet been widely applied on wild populations.

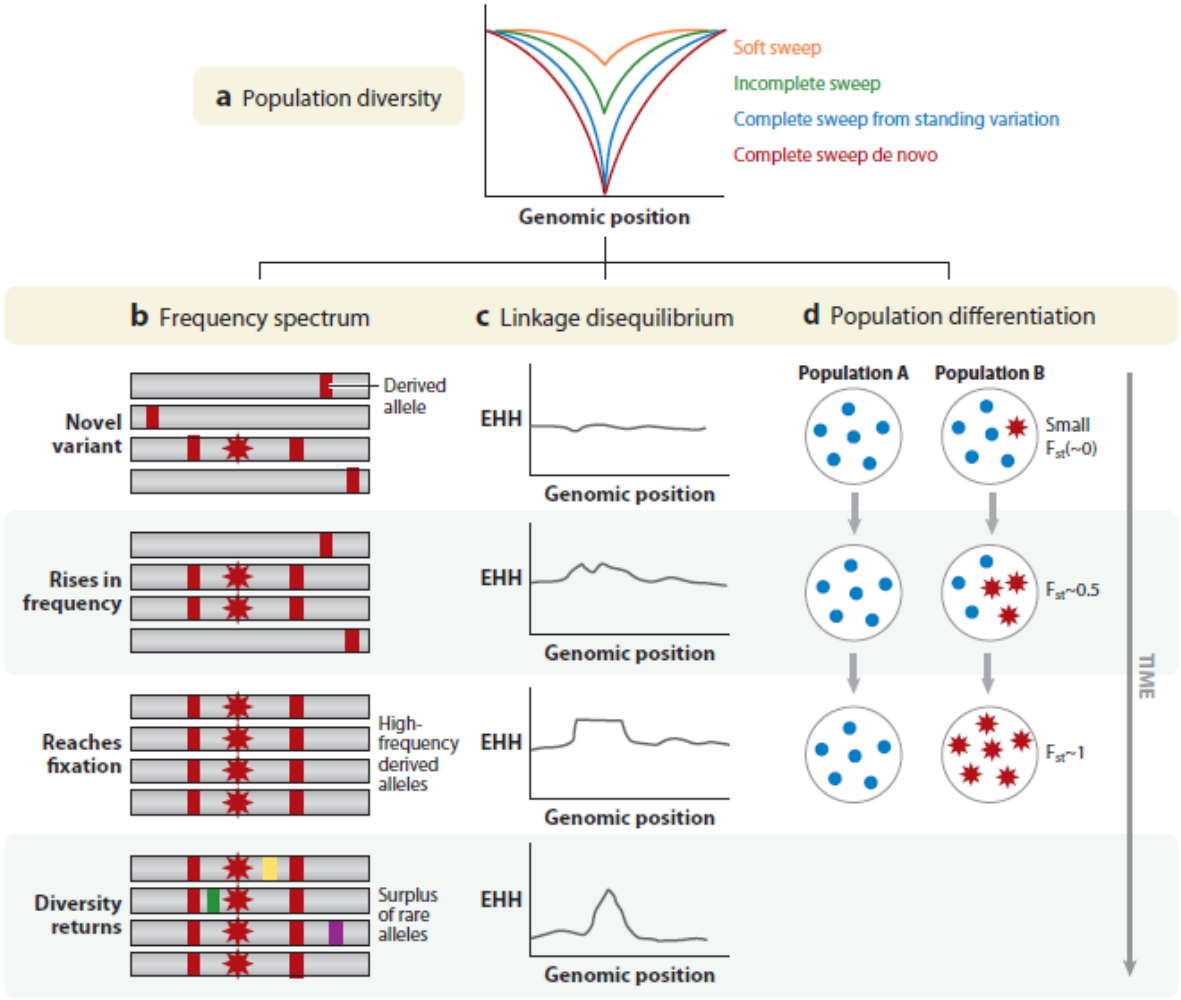

Figure 20. **Detection of selective sweeps in genomic data.** A: selection favouring a particular allele causes a population wide reduction of genetic diversity at the selected genomic position. B) A beneficial mutation (red star) would drive neighbouring alleles (bars) to high frequency due to linkage disequilibrium (coupled heritage). C) A selective sweep causes local extended haplotype homozygosity (EHH). D) Differences in frequency of the selected allele between populations causes the fixation index (F_{ST}) to increase as selection drives the new allele to fixation in one of the two populations. Figure from Vitti et al. (2013)

1.4 Voles: a seasonal species with a wide distribution range

In order to study variation and plasticity within the PNES and local adaption to variable seasonal environments in mammals, we need a suitable study species. Ideally, these will be seasonal species, with a wide distribution range and documented flexibility regarding the timing of reproduction. Based on these criteria, voles of the *Microtus* genus make excellent candidates.

1.4.1 Evolution of Microtus

Microtus is one of the most speciose mammalian genera within the family *Cricetidae (*subfamily *Arvicolinae)* and the order *Rodentia.* Currently there are more than 60 *Microtus* species, occupying a range stretching from the tropics (*M. guatemalensis* at 14°N) to the arctic (*M. levis* on Svalbard: 78°N), in both Eurasia as North America (IUCN 2021). *Microtus* originated from the Pleistocene genus *Allophaiomys* that is thought to have originated around 2 million years ago (Chaline et al. 1999). This widespread fossil genus was present in both Eurasia and North America but may have originated 2.3-2.4 million years ago in China (Zheng and Zhang 2000). The first fossils of true *Microtus* species did not appear in the fossil record before 0.5-0,7 million years ago and the lineage possibly originated in central Asia (Chaline et al. 1999).

The speciation rate in *Microtus* is currently 60-100 times higher than in most other mammals, with about 30 speciation events per million years (Triant and DeWoody 2006). The diploid chromosome number in this genus varies from 17 to 64 and karyotype studies estimate 4-32 chromosomal rearrangements per million years (Sitnikova et al. 2007). The increased gene density around chromosomal break points (Murphy et al. 2005) provides a source of genetic diversity, potentially facilitating rapid *Microtus* evolution. Unclear within- and between species genetic distances and large variation in mitochondrial *cytochrome b* sequences further suggests rapid evolution of this genus (Jaarola et al. 2004). Current molecular data supports the presence of four lineages within *Microtus* (Fig.21) that represent a western Eurasian lineage (*Microtus)*, a predominantly southern European lineage *(Terricola)* a Northern American lineage (Nearctic species) and a predominantly Asian lineage. The former two have the strongest molecular support (Jaarola et al. 2004).

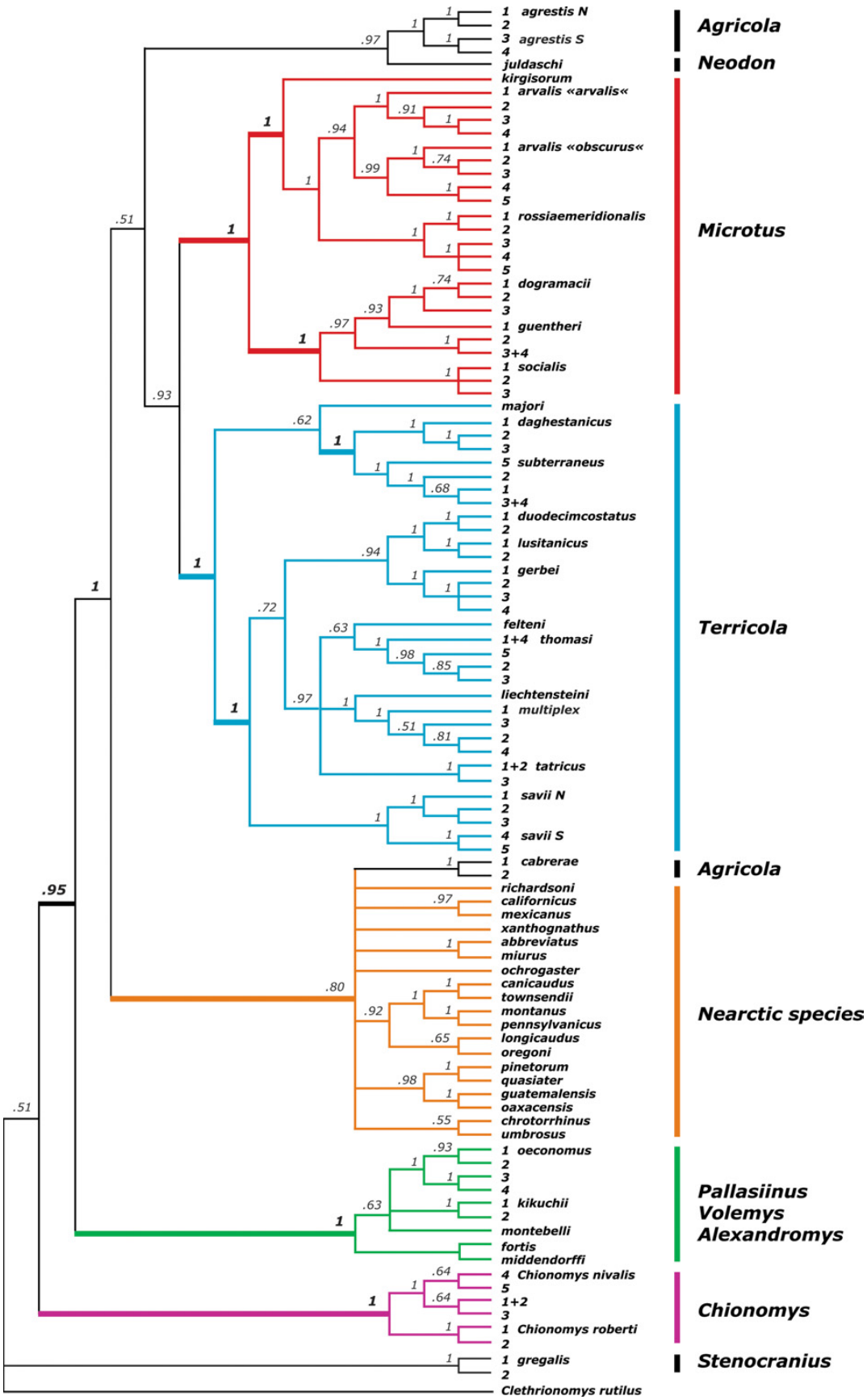

Figure 21. Phylogenetic tree of *Mictrotus* species. The tree is based on *cytochrome b* sequence homology. The bootstrapping scores given in the tree show four well supported phylogroups. *Chinomys* (snow voles) and the *Clethrionomys* (or *Myodes*) *rutilus* (red-backed vole) was used as an outgroup for *Microtus*. Figure from Jaarola et al. (2004).

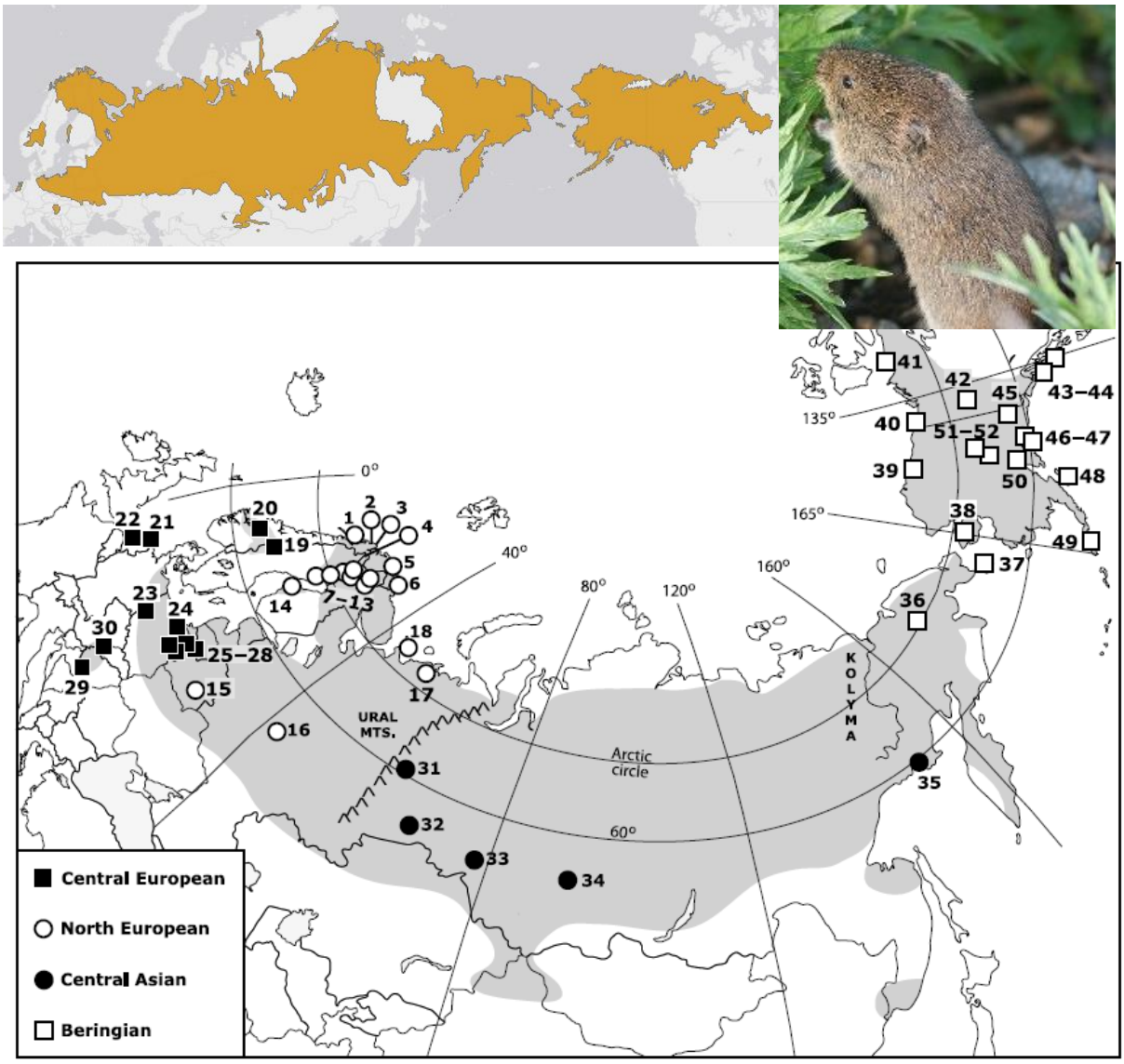

Figure 22. Tundra vole distribution range. Global range and image of the tundra vole (*Microtus oeconomus*) and an overview of the four different phylogroups (symbols) of tundra voles samples studied by Brunhoff et al. (2003).

In this thesis, we focused on the tundra vole or root vole (*Microtus oeconomus*) and the common vole (*Microtus arvalis*) (Pallas, 1776, Pallas 1778). Tundra voles belong to the 'Asian' lineage (subgenus *Pallassiius)* (Haring, Sheremetyeva, and Kryukov 2011) and are the most widespread species of *Microtus* (Fig.22), living in both Eurasia as well as North West America, with a latitudinal range of 43°N in Kazakhstan and China up to 74°N in Russia (Linzey et al. 2016). The diploid chromosome number is 30 and karyotype evolution is higher in *M.oeconomus* than in other *Microtus* species (Lemskaya et al. 2010). There are four distinct phylogroups within the species; a Northern European (Northern Scandinavia and West Russia), a central European (central Europe and Southern Scandinavia), an Asian and a Beringian group. The genetic distances (mtDNA) between the groups varies from 2 to 3.5 % (Brunhoff et al. 2003). The origin

of the species remains unclear but it could have taken place in central Asia (Rausch 1963). The European lineages are estimated to have split between 0,2-0,33 million years ago and have possibly originated in the Urals. Tundra voles colonized Europe via Northern and Southern routes and central European tundra voles were already present before the last glacial maximum. The Asian group East of the Ural mountains has a more diverse origin and may have split from the two European lineages between 0,29-0,49 million years ago. It is unclear when tundra voles colonized Alaska, but the high genetic similarity with far eastern Russian voles suggest a rather recent colonization during the last glacial period (Brunhoff et al. 2003).

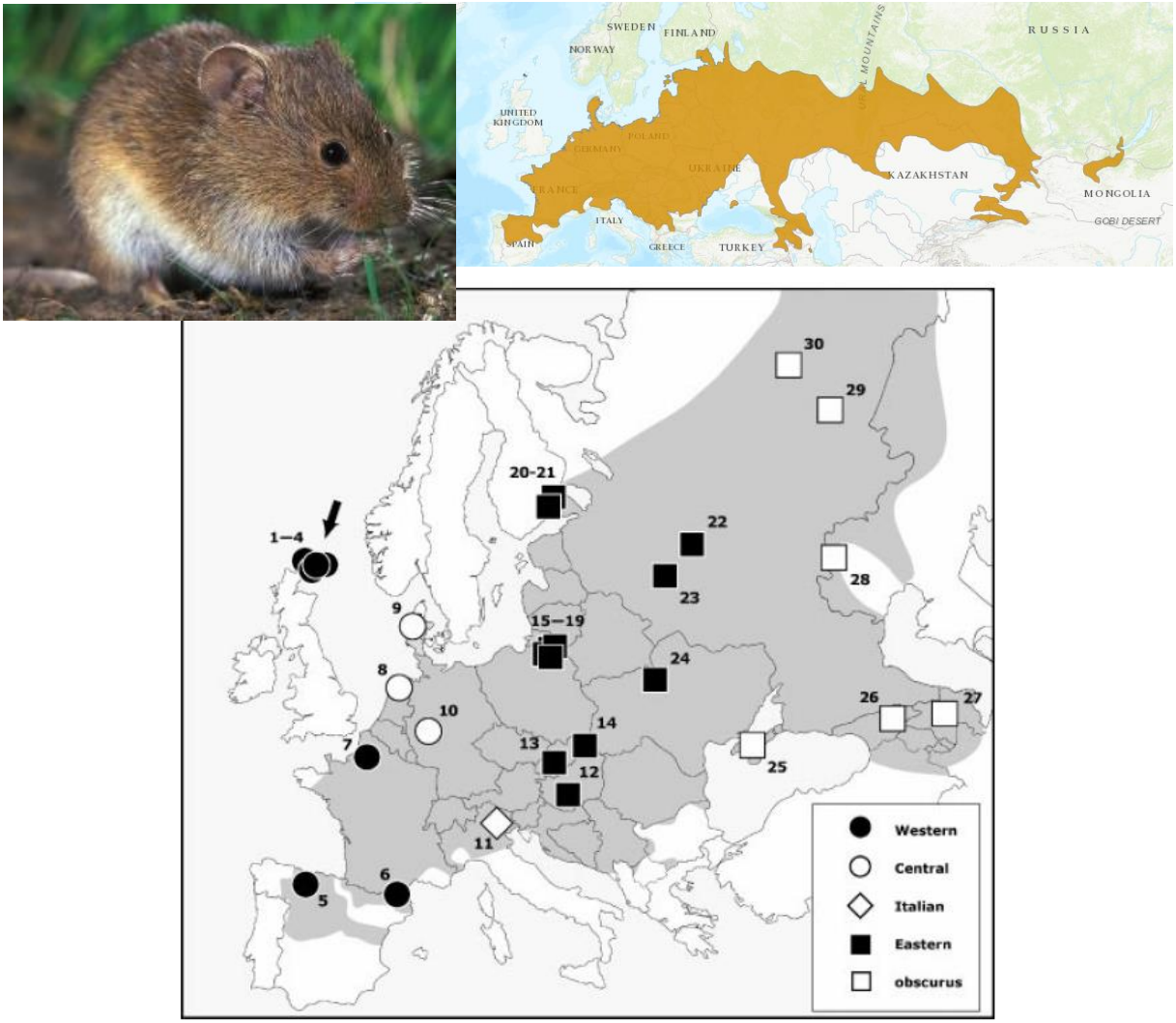

Figure 23. Common vole distribution range. Global range and image of the common vole (*Microtus arvalis*) and an overview of the five different phylogroups (symbols) of common voles samples studied by Haynes, Jaarola and Searle, (2003).

Common voles (Fig. 23) are mostly endemic to Europe and their range goes from 38°N in Spain to 62°N in Finland and Western Russia (Haynes, Jaarola, and Searle 2003). There are five phylogroups within the species; an Italian, and Eastern, a Central a Western European group.

The last Asian group is by some authors considered as a different species: *M. obscurus* (Haynes, Jaarola, and Searle 2003). The Asian *obscurus* group has a different karyotype than the other groups but close genetic distances make it debatable whether this is a separate species or a subspecies. The range of the latter group reaches as far east as to Lake Baikal (Yigit et al. 2016). Mitochondrial DNA analysis suggests a recent colonization of Northern Europe from several Southern refuge areas during the last glacial maximum (Heckel et al. 2005). However, common voles may have migrated from North East to Southern Europe before the last glacial maximum (Heckel et al. 2005).

Summed up, the tundra vole has a more northern paleogeographic history than the common vole and the center of the European distribution range is 60°N for the tundra vole and 53°N for the common vole.

1.4.2 Microtus *life history*

Despite the rapid evolution rate and great genetic variation on both the nucleotide and chromosome level, voles show surprising little superficial phenotypic variation: they are all small brown-grey rodents weighing roughly between 20 and 80 gr. Vole species generally live in meadow like habitats at various altitudes; from tundra to dry steppe regions and some species live predominantly subterraneous (Fig.24). Many *Microtus* populations cycle strongly in density with several years interval depending on the species and location (Mihok, Turner, and Iverson 1985; Lambin, Bretagnolle, and Yoccoz 2006; Zub et al. 2012).

Figure 24. Distribution range of the *Microtus* genus (data from IUCN Red List).

Voles are active, small herbivorous, mostly grass-eating rodents, which require frequent foraging to uphold their high metabolic rates (Nieminen, Hohtola, and Mustonen 2013). In contrast to many other rodents living in temperate regions, voles do not hibernate in winter and stay active year round. At higher latitudes, they live in tunnels under the snow and huddle together to cope with the cold (Korslund 2006). Social behavior may vary with the season and

for example, common voles (*M.arvalis*) are more social in winter than during the breeding months in summer, when they exhibit stronger territoriality (Eccard and Herde 2013). Activity patterns and body temperature rhythms of tundra voles and common voles can vary from strictly nocturnal to ultradian with nocturnal bias to ultradian without diurnal or nocturnal bias (Nieminen, Hohtola, and Mustonen 2013; Halle 1995; Gerkema and Verhulst 1990). Ultradian activity patterns seem to be more common in autumn and winter (Halle 1995) and can be induced in the lab by simulated food scarcity and low temperature (van Rosmalen and Hut, 2021)

The mating systems observed in *Microtus* varies from promiscuity, polygyny to predominantly monogamy in *M.ochrogaster* (Getz and Hofmann 1986). The mating system varies both between- as well as within species, with *M.oeconomus* (Tast 1966; Morgan and Williams 1989; Viitala et al. 1996) showing both promiscuity as well as monogamy. Female voles have either spontaneous or induced ovulation and form a vaginal plug after mating (Breed 1967; Moffatt, Nelson, and Devries 1993). The gestation time is short (~3 weeks) and most species breed seasonally in summer (Fig. 25). In colder regions at higher latitudes or altitudes, breeding season shortens and is confined to the summer months. Breeding also ceases during hot and dry periods, resulting in a bimodal breeding pattern, as observed in reed voles (*M.fortis*) (Zhengjun 1996), in which breeding activity is highest in spring and autumn. Species native to lower latitudes and altitudes breed year round (Fig. 25). The timing and length of the breeding season varies greatly between species and even between years, as observed in *M.oeconomus* (Tast 1966) and *M.agrestis* (Ergon et al. 2001). Many vole species are highly opportunistic and flexible regarding reproduction and even the more northern seasonally breeding species are capable of winter breeding under favorable conditions, as has been observed in *M.oeconomus* (Tast and Kaikusalo 1976), *M.pennsylvanicus* (Kerbeshian, Bronson, and Bellis 1994), *M.townsendii*, (Lambin and Krebs 1991), *M.ochrogaster* (Nelson et al. 1989) *M.arvalis* (Baláž 2010a) and *M.agrestis* (Tast and Kaikusalo 1976). The successful establishment of a sibling vole population (*M. levis*, native to Eastern Europe) on Svalbard (78°N) further underlines the adaptive stretch of *Microtus* (Yoccoz, Ims, and Steen 1993).

In seasonally breeding species, the breeding season starts with the overwintering cohort coming to reproductive maturity first in spring. Then breeding occurs in several cohorts during summer until and it stops again in autumn, leaving a generation of small, pre-mature voles to overwinter and reproduce in the next season (Fig.26). That makes voles typical long-day breeders.

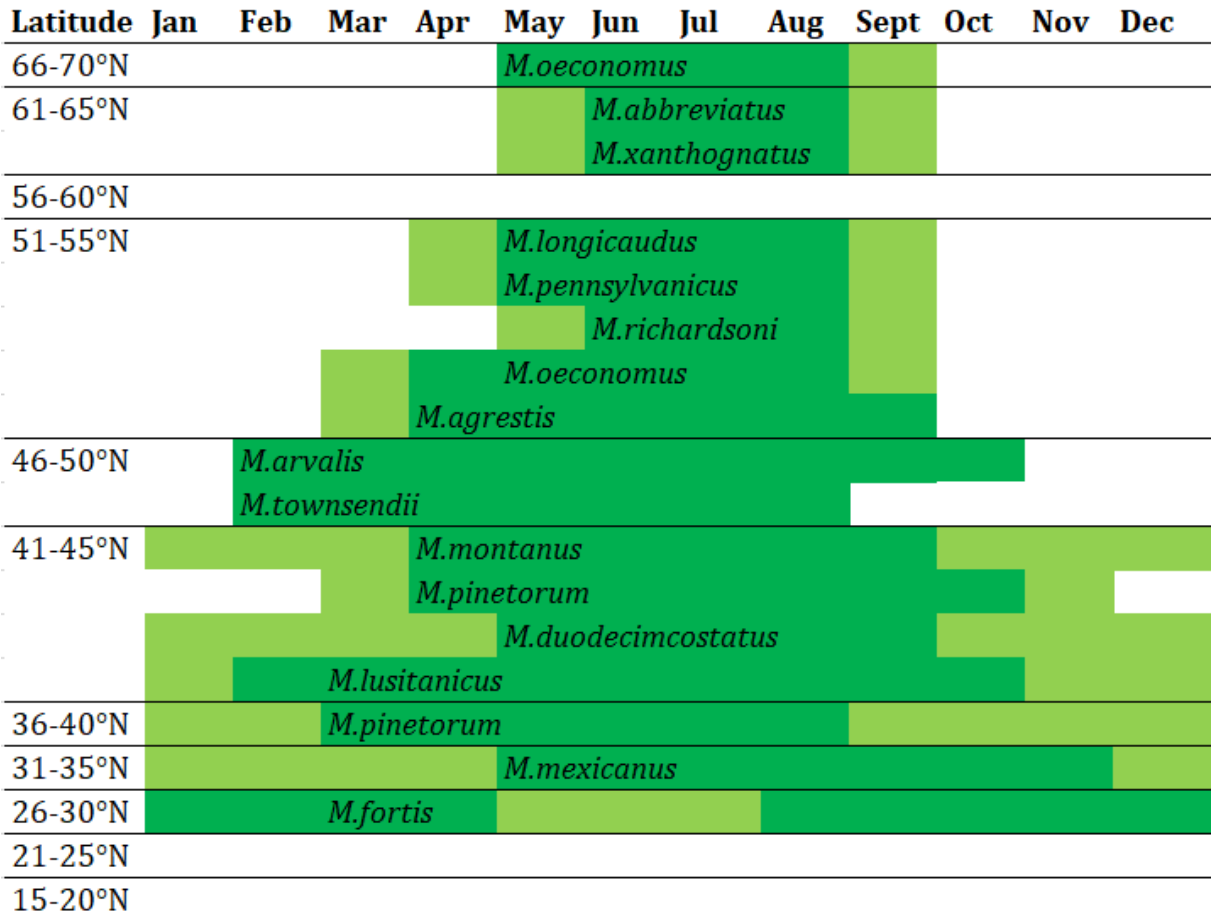

Figure 25. Timing of breeding in *Microtus*. Overview of breeding activity in various vole species at different latitudes based on literature. Dark green is when the majority of the individuals was caught in a reproductively active state (males with large testes, pregnant females). Light green is when breeding still occasionally occurs. This figure does not include rare instances of winter breeding at higher latitudes. Illustration by M.J.van Dalum.

References for the figure:

M.oeconomus (Tast 1966; Lambin, Krebs, and Scott 1992; Gliwicz 1996), *M.abbreviatus* (Raush and Raush, Virginia 1968), *M.xantoghanatus* (Wolff and Lidicker Jr. 1980), *M.longicaudus* (van Horne 1982), *M.pennsylvanicus* (Innes and Millar 1990), *M.richardsoni* (Ludwig 1988), *M.agrestis* (Ergon et al. 2001) *M.arvalis* (Baláž 2010a), *M.townsendii* (Lambin and Krebs 1991), *M.montanus* (Sera and Early 2003), *M.pinetorum* (Miller and Getz 1969), *M.duedecimcostatus* (Paradis and Guédon 1993), *M.lusitanicus* (Ventura, Jiménez, and Gisbert 2010), *M.pinetorum* (Smolen 1981), *M.mexicanus* (Hilton 1992), *M.fortis* (Zhengjun 1996).

Tundra voles are one the largest of the genus and are well adapted to the cold (Nieminen, Hohtola, and Mustonen 2013). In Northern Canada, they live mostly in wet sedge meadows, cotton grass marches, near tundra lakes (Lambin, Krebs, and Scott 1992) or near willow thickets, as was observed in Northern Norway (Ims 1997). Dependent on the region, they spend several months of the year under the snow, exhibiting free running ultradian rhythms and social synchronization (Korslund 2006). In Northern Canada, there was little competition with collared lemmings (*Dicrostonyx groenlandicus*) as they do not occupy the same wet areas as tundra voles (Lambin, Krebs, and Scott 1992).

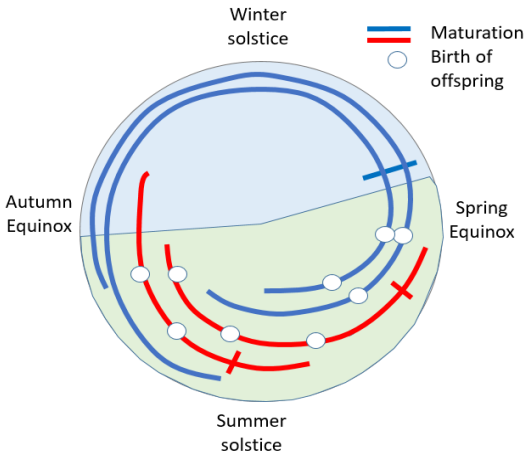

Figure 26. The vole life cycle. Diagram based on data from tundra voles in Poland (53°N) (Gliwicz 1996). Breeding starts with the overwintering cohorts (blue) coming to reproductive maturity and producing the first spring born cohort (red). The short gestation time allows for several subsequent cohorts to be born in the same season (red). However, late born cohorts delay growth and maturation in order to overwinter (blue). Cohorts consisting of mature individuals that have bred in summer are unlikely to survive the winter. Illustration by M.J.van Dalum.

Population density cycles of tundra voles vary in length and intensity; in Finnmark, the interval is about 3-5 years (Ims 1997) while in Poland this was 3 years (Zub et al. 2012). High predation risk increases female reproductive performance (Gliwicz 2007) whereas high population densities reduced this (Gliwicz 2007; Bian et al. 2015). The latter is also suggested to influence the offset of the breeding season (Tast 1966). The mating system of tundra voles is predominantly polygynous or promiscuous (Tast 1966; Gliwicz 1997) but voles can shift to monogamy in patchy habitats when mortality is high and populations are in decline (Viitala et al. 1996). Male parental investment was stronger in Northern tundra voles (Norway, 70°N) compared to southern populations (Norway, 61°N) (Ims 1997) and these results indicate that some biparental care occurs within the species.

The onset and offset of the breeding season in tundra voles ranges from early May to early September in Kilpisjärvi (69°N), Northern Finland (Tast 1966) and at the Northern Canadian coastline (69°N) (Lambin, Krebs, and Scott 1992). In Poland (53°N), near lake Ros, breeding started already in early March and lasted until early September (Gliwicz 1996). Several populations investigated in Lithuania (54°-56°N) were reproductively active from April until the end of October (Balčiauskas, Balčiauskiene, and Janonyte 2012). Under favourable conditions, winter breeding might occur as far north as Northern Finland (Tast and Kaikusalo 1976). Litter size and birth weight of tundra voles seems to vary with latitude. In central Norway (61°N) litter

size was larger but neonates were smaller compared to voles from Northern Norway (70°N). Body mass of overwintering voles was also 51% higher in the North Norwegian population compared to the central one. Crossbreeding and cross-fostering between these two populations resulted in an intermediate phenotype, which suggests that body mass has a genetic basis (Ims 1997).

Common voles were found on grasslands and farmlands in France (Dellatre 1992) and near cultural steppe regions agricultural areas in Slovakia, up to 1900 m altitude (Baláž 2010b). Like in the tundra vole, common vole populations cycle with an interval of 3-5 years with the amplitude of density fluctuations being higher in Northern populations (50-55°N) than in Southern populations (41-44°N). Some southern populations showed irregular non-cyclic oscillations in density (Mackin -Rogalska 1990). Their activity pattern is ultradian and is synchronized within a population which may enhance safety from predators (safety in numbers) and facilitates communication of predator presence to other voles (Gerkema and Verhulst 1990).

Common voles also exhibit seasonal breeding in cohorts (Eccard and Herde 2013) with breeding starting with the overwintering cohort. Females breed either in groups of on average three individuals or solitary. They make large burrows consisting of various chambers and expressed aggression and territoriality against unfamiliar individuals (Boyce and Boyce 1988). Females tend to form monogamous bonds but non-monogamous breeding also occurred (Ricankova, Sumbera, and Sedlacek 2007). Although females invested significantly more in parental care, the male was found in the nest, licking the pups, huddling in the nest and moving nest material (Gromov 2013).

In Slovakia (48°N), reproduction began in mid-February and lasted until mid-October or occasionally until November. In mild winters, females were also found pregnant in January (Baláž 2010a). The reproductive period was shorter in common voles from higher altitudes as compared to lower altitudes. Their body mass did not vary with altitude but the body length was shorter in high altitude voles, giving them stouter bodies. This was suggested as a cold adaptation as temperature explained variation in somatic data more directly then did altitude (Baláž 2010b).

1.4.3 Photoperiodic regulation of growth and reproduction in Microtus

Given the high year-to-year and individual (Fig. 27) variability in reproductive performance and the ability to reproduce in winter under favorable conditions, it was long unclear what role photoperiod plays in the timing of reproduction. Several factors such as food quality and quantity (Nelson and Blom 1993; Berger, Negus, and Rowsemitt 1987), ambient temperature (Nelson et al. 1989; Kriegsfeld, Trasy, and Nelson 2000; Dark and Zucker 1983), population density (Ergon et al. 2001; Bian et al. 2015), predation risk (Gliwicz 2007; Haapakoski, Sundell, and Ylönen 2012) or social cues (Trainor et al. 2006) have been suggested as factors affecting seasonal reproduction in voles more than photoperiod.

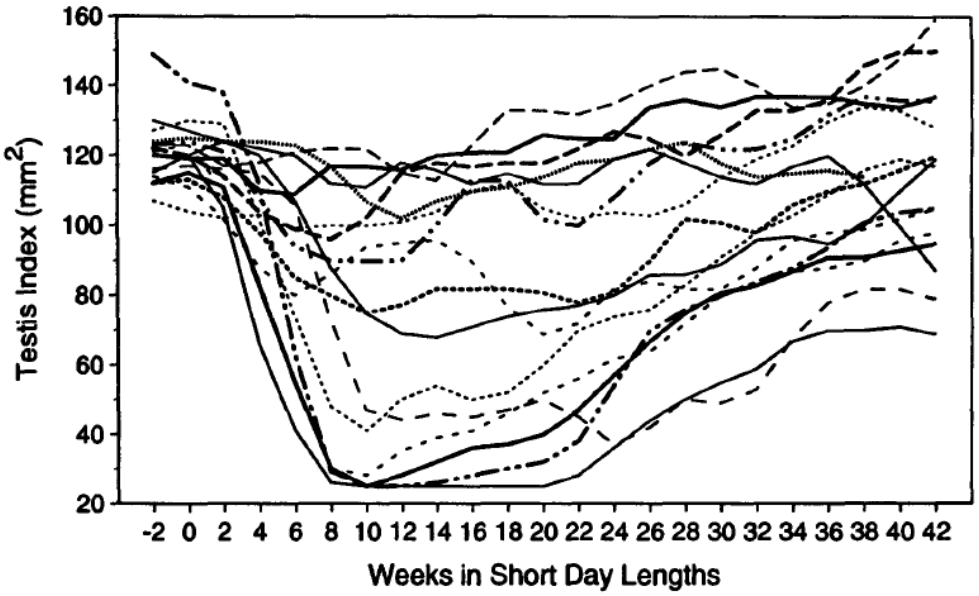

Figure 27. Strong individual variation in testicular regression. Data from wild caught adult, reproductively active meadow voles (*Microtus pennsylvanicus*) housed under short photoperiods in the laboratory. Figure from Kerbeshian, Bronson and Bellis (1994).

However, photoperiod can affect the vole life cycle at potentially three time points. Namely through spring activation of reproduction in overwintering sub-adults, through photoperiodic imprinting in the prenatal state, and through suppression of reproductive activity in mature adults at the end of the breeding season (Fig.28).

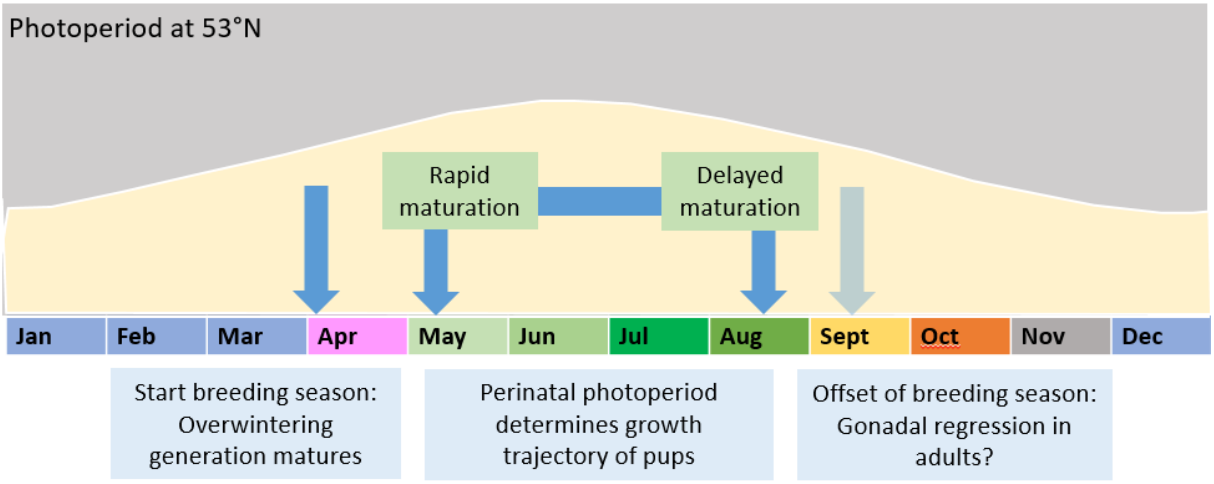

Figure 28. Potential timing effect of photoperiod in the vole life cycle. Increasing photoperiod may stimulate the overwintering generation to mature and reproduce. Pups experiencing an increasing photoperiod mature rapidly whereas pups experiencing decreasing photoperiods delay maturation until the next breeding season. Adults that have reproduce may regress their gonads and reduce body mass at the end of the breeding season. Illustration by M.J.van Dalum.

The overwintering generation - the onset of the breeding season

The overwintering cohort comes to reproductive maturity when photoperiods begin to increase in spring. They form the first generation that reproduces during the breeding season. Indeed, long days in field voles (*M.agrestis,* latitudinal range: 41-70°N) captured near Aberdeen, Scotland (57°N) induced an increase in body mass, which was largely due to increased gonadal growth (Król et al. 2005). Long days also enhanced proceptive behavior in female prairie voles (*M.ochrogaster*) under laboratory conditions (Moffatt and Nelson 1994). Although even in the absence of a long-day signal, meadow voles (*M.pennsylvanicus)* become refractory to the inhibitory effect of prolonged short photoperiods and spontaneously produce spring-ready offspring (Lee and Zucker 1988). Pups born from mothers who had been on short days for 2 weeks (mimicking late autumn/early winter) were small and had regressed gonads, whereas those born from mothers kept on short days for 26 weeks (mimicking late winter/early spring) grew much faster and had larger testes (Lee and Zucker 1988). This suggests that increasing photoperiod is a stimulating factor but not a requirement for spring breeding.

Photoperiodic imprinting in the perinatal phase – the growth trajectory

The photoperiod experienced before weaning shows the clearest relevance of seasonal timing in the vole life cycle. Voles born under increasing photoperiods grow and mature fast to breed during the same season whereas those born under decreasing photoperiods grow slowly and delay maturation until the next season. In field data from tundra voles studied in Poland (53°N) the first cohort, born from overwintering individuals, indeed grew and matured fast and reproduced during the same season. Following cohorts born in mid-July, when photoperiods

begin to decrease, showed a remarkable drop in growth rate. These individuals rarely sexually matured. Instead, they retained a low body mass, stayed in a pre-mature state and thereby formed the overwintering cohort (Gliwicz 1996). Lower body mass and increased metabolic rates were indeed associated with higher survival rates in tundra voles from Poland (Zub 2014) and Norway (Aars and Ims 2002). Lower a body mass is indeed associated with reduced energetic costs in small mammals (<100g) (Lovegrove 2005).

In this thesis, we focused on the effect of pre-weaning photoperiod on post weaning growth and reproduction. Given the relevance of photoperiodic imprinting in the perinatal phase for our research, we have written a review on this – **see chapter 7**(van Dalum et al. 2020).
As stated earlier in the introduction, it may be the directional change in photoperiod and thus the photoperiodic history that explains growth patterns in voles. This was neatly demonstrated in an experiment on Montane voles (*M.montanus*) (Horton 1984a). Pups were gestated and kept under either 8 (8L) or 16 (16L) hours of light per day until weaning. After weaning, they were divided over three post-weaning groups and exposed to either 8L, 14L or 16L. The intermediate photoperiod of 14L revealed the effect of pre-weaning photoperiod clearly. Pups from born in 8L experienced an increase in day length and were heavier with better developed reproductive tracts than those born in 16L, who experienced a decrease in day length. Here, both groups experienced the same post-weaning photoperiod, except that they had a different photoperiodic history. Further experiments demonstrated that the photoperiod *in utero*, during gestation, determined the pup's growth response in relation to various post-natal photoperiods (Horton 1984b). In order to exclude post-natal effects of the birth mother through milk, montane vole pups were transferred to foster mothers who had experienced either the same or the opposite photoperiod during pregnancy as the birth mother. The results clearly showed the effect of *maternal photoperiodic imprinting*: namely that the photoperiod (long or short) experienced by the birth mother determined the pup's growth response under intermediate photoperiods (Horton 1985). Cross-fostering experiments in meadow voles (*M.pennsylvanicus*) revealed the same pattern (Lee 1993) . Maternal photoperiodic imprinting also affects growth in Siberian hamster (*Phodopus sungorus*), and the effect of melatonin was assessed through housing pinealectomized hamsters under constant light. Melatonin administration (mimicking short days) could indeed restore the somatic and gonadal growth response offspring(Horton, Ray, and Stetson 1989). Long (16L) or short (8L) photoperiods experienced prior to weaning (21 days) affected the *dio2/dio3* expression pattern in tanycytes of Siberian hamsters exposed to intermediate post-weaning photoperiods (14 L) possibly through altered sensitivity to TSHβ (Sáenz de Miera et al. 2017). Plasticity in response to photoperiodic history may thus occur at the level of tanycytes. Since maternal photoperiodic imprinting and cohort breeding is similar

between hamsters and voles, these results form the basis for our experiments performed in **paper I, II and III** in this thesis.

Reproductive suppression in mature adults – the offset of the breeding season

Mature adults that have reproduced during the breeding season rarely survive the winter. Instead, the pre-mature cohort that delayed growth forms the majority of the overwintering voles that will reproduce the spring after (Zub et al. 2014; Gliwicz 1996; Eccard and Herde 2013). However, Ludwig, (1988) live-trapped two female water voles (*M. richardsoni)* in Alberta, Canada (51°N) that had reproduced during their birth season and in the breeding season a year later. Given the low winter survival chances of mature adults, short-lived species must be more opportunistic regarding breeding and they may retain reproductive activity regardless of decreasing photoperiods and temperatures in autumn (Bronson 1988).

Although adult reproductively active hamsters as well has voles have showed gonadal regression in response to short days and this opposes the hypothesis that once mature, they remain in a breeding state. In a lab colony of prairie voles (*M.ochrogaster*) originally trapped near Illinois (40N°), adult males (>45 days) reduced testes mass and seminal vesicle weight when transferred from long to short photoperiods compared to males maintained on long photoperiods. Immature males also had low testes mass under short photoperiods, possibly because of delayed maturation as described above. Photoperiod had no effect on reproductive performance on adult females. Interestingly, despite reduced testes mass, adult males remained fertile and produced the same number of offspring when housed with a female as did males with large testes housed under long photoperiods. However, immature males with small testes housed under short days, did not produce any offspring. Body mass was not affected by photoperiod in any case (Nelson 1985).

The degree of gonadal regression in response to short photoperiods varied strongly between wild meadow vole males from Pennsylvania (41°N) (Fig.27). All wild males were in breeding condition and had large testes before short day (8L) exposure in the lab. Body mass was also significantly reduced after 10 weeks under short photoperiods (Kerbeshian, Bronson, and Bellis 1994). Short day induced gonadal regression was not affected by age (3-30 weeks) in lab-reared males (Kerbeshian, Bronson, and Bellis 1994). Similarly, male field voles (*M.agrestis)* reared in the lab under LP to SP at an age of 35, 55 and 80 days all showed gonadal regression with no significant effect of age (Grocock 1980).

It is questionable why adult individuals of various species still respond with gonadal regression and in some cases with body mass reduction in shortening days. This may still be an 'attempt' to increase winter survival chances in case winter breeding opportunities occur under favourable conditions, as gonadal regression may not necessarily reduce fertility (Nelson 1985).

1.4.4 Photoperiodic regulation of non-reproductive parameters

Seasonal fluctuation in gonadal- and body mass is variable per species and is possibly affected by the local seasonal environment (as suggested in figure 17). In a seasonal environment, energy saving mechanisms and moult may be more obligatory for survival than is gonadal regression yet the exact role of photoperiod and temperature on these parameters is not entirely clear. Adult meadow voles (*M.pennsylvanicus* , latitudinal range 30-70°N) kept under laboratory conditions responded to short photoperiods with a reduction in body mass and food intake, as well as with gonadal regression and growth of winter pelage (Dark and Zucker 1983). Body mass and brown adipose tissue (BAT) was reduced by low temperature but not by photoperiod in prairie voles, although photoperiods but not temperature induced growth of winter pelage (Nelson 1985). Tundra voles (*M.oeconomus*)* from Tibetan plateau (37°N, altitude: 2275m) are exposed to extreme cold during the winter months and short day lengths alone significantly increased thermogenesis capacities and winter survival adaptations, such as lower body mass, increased energy intake, a higher basal metabolic rate and increased non-shivering thermogenesis (Wang, Zhang, and Wang 2006). Temperature can interact with photoperiod in regards to gonadal growth, body mass regulation and mount, yet how these factors interact with the PNES has not been studied extensively .

1.4.5. The PNES in voles

The *Dio2/Dio3* expression ratio in wild Brandt's voles (*Lasiopodomys brandtii*) from Inner Mongolia, China (45°N) was correlated with testes mass and followed photoperiod with an increase in *Dio2* in spring and an increase in *Dio3* in autumn. Body mass and testes mass was largest in overwintered adults. Juveniles and non-overwintered adults had smaller testes, which were further reduced towards the end of the breeding season in October. The age dependent gonadal development was reflected in altered *Kiss-1* and *Rfrp-3* expression, which may be governed by the photoperiodic control of the *Dio2*/*Dio3* expression ratios (Wang et al. 2019)

At the start of this thesis project, only one study by Król et al. (2012) has investigated the PNES in *Microtus.* They studied the effect of food quality and photoperiod on seasonal gene expression, gonadal growth and body mass in female common voles (*M.arvalis*) native to the Netherlands (53°N). The plant metabolite 6-methoxy-2-benzoxazolinone (6-MBOA) is present in early grass

shoots and this was hypothesized to enhance reproduction in voles (Meek, Lee, and Gallon 1995) but no effect was found in this study. Neither did 6-MBOA nor photoperiod affected body mass and long photoperiods only increased uterus and ovary mass slightly, although the effect was significant. However, photoperiod but not 6-MBOA, strongly affected expression of genes involved in the PNES. Voles of age 1-7 weeks were kept on 8L for 10 weeks and then either maintained on 8L until sampling 10 days later or transferred to 12L or 16L for 10 days.

Expression of *THSβ* and *Dio2* in the *pars tuberalis* of the pituitary stalk was largely increased under 16L but barely detectable under 8 or 12L. *Dio3*, however had the strongest expression in 8L, was still expressed in 12L but was absent in 16L. This demonstrates that the common vole PNES clearly processes photoperiod at the hypothalamic gene expression level but that downstream somatic- and gonadal effects are less clear. This study did not account for age dependent effect of photoperiod on the growth trajectory.

Taken together, these studies show that voles are flexible in their response to photoperiod and that other factors such as temperature can modulate the vole seasonal phenotype downstream of the PNES. The perinatal photoperiod in which maternal photoperiodic imprinting plays an important role, has the strongest seasonal timing relevance in vole development through which we examined plasticity of the vole PNES in relation to the paleogeographic history in the northern tundra vole and southern common vole .

*The distribution range map of *M.oeonomus* provided by IUCN red list, does not show occurrence of the species on the Tibetan plateau. The only *Microtus* species living there is the Lacustrine vole (*M.limnophilus*), which closely resembles *M.oeconomus* (IUCN 2021). Barcoding revealed that 8 of the 10 museum samples described *as M.oeconomus* from Mongolia, north of Tibet, were in fact *M.limnophilus*.

2. Research aim

The Dutch behavioural biologist Niko Tinbergen (1963) recognized that any biological problem, observation or trait, can be approached through asking four questions:

What is it for, how does this affect fitness?

How did it evolve through history?

How did it develop, what is the ontology of the trait?

How does it work, what are the causal mechanisms?

These four questions are still widely used to create a more complete understanding of biological phenomena. With these questions in mind, I aimed to study phenotypic and genetic variation in the mammalian seasonal time keeping mechanism in relation to latitude of origin. Tundra voles (*Microtus oeconomus)* native to higher latitudes (43-74°N) and common voles (*M.arvalis)* native to lower latitudes (38-62°N), served as model species.

This overall goal led to the following research questions:

1) Do tundra voles and common voles respond to photoperiod differently and if so, how does this phenotype develop with age?
2) Can we measure a critical photoperiod at different mechanistic levels for the expression of a summer phenotype and does temperature modulate the response?
3) Have tundra voles, native to higher latitudes, evolved different critical photoperiods and temperature modulation mechanisms than common voles?
4) Can we detect signatures of selection between tundra voles from high (70°N) versus lower latitudes (53°N) and do any observed signatures relate to known genetic mechanisms underlying photoperiodic time measurement?

We took a top-down approach to the first questions, looking for observable phenotype differences and searching for underlying neuroendocrine mechanisms, down to expression of genes in the brain and pituitary gland. Here we primarily assess Tinbergen's questions concerning causal mechanisms and ontology but also touch upon the evolutionary history between the species. The last question constitutes a bottom up approach in which we search for within-species genetic variation that could have originated from latitudinal selection affecting the seasonal phenotype. Hereby we consider Tinbergen's question regarding evolution. Taken together, I hope that these combined approaches will generate new insights into the evolution of seasonal time keeping mechanisms in mammals.

3. Methods extension: theory of sequencing and bioinformatics

3.1. *De novo* sequencing strategies

In order to detect signatures of selection between a Northern (Ifjordfjellet, Norway, 70°N) and Southern population (Białowieża, Poland 52°N) of tundra voles, we first needed a good reference genome of the species. We have achieved this through *de novo* sequencing (creating a reference genome of a species that has not been sequenced before) of one representative individual. Then we re-sequenced a pool of individuals from each population and compared this with the reference genome to screen for genetic variation between the populations (Fig. 29).

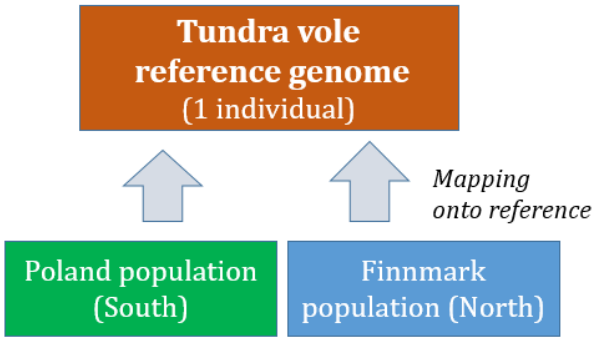

Figure 29. Schematic overview of the sequencing strategy. Genomic data from the two populations was mapped onto the *de novo* tundra vole reference genome to find loci under selection. Illustration by M.J.van Dalum.

Sequencing is the translation of genomic DNA base pairs (adenine, cytosine, guanine and thymine) into a sequence of letters (A,C,T,G). There are a number of sequencing methods available, each coming with costs and benefits (Giani et al. 2020). For this project, we combined next generation and third generation sequencing. Next generation sequencing (NGS) or also called second generation sequencing, is a collective term for high throughput massive parallel sequencing technologies that can sequence entire genomes per run by sequencing many small DNA fragments (<300 base pairs) simultaneously (Niedringhaus et al. 2011). Third generation sequencing is massive parallel sequencing of much longer fragments (up to the size of chromosomes). We chose the next generation sequencing technology provided by the company Illumina and the third generation by Oxford Nanopore Technologies.

3.1.1. Illumina paired-end sequencing

For sequencing with the Illumina technology (Fig. 30), DNA is first sheared into smaller fragments of variable sequence lengths (often 200-1000 bp). This is called library preparation. Then a DNA polymerase, which draws fluorescently labeled new base pairs from the solution in which the reaction takes place, amplifies these fragments. Each new base pair (bp) that is built in by the polymerase, gives off a light signal unique for the type of base pair (A,C,T,G). The machine then reads this signal (www.Illumina.com). Illumina machines can produce high quantity and high quality readings with relatively few sequencing errors (Pfeiffer et al. 2018; Tucker, Marra, and Friedman 2009). The drawback is that the machine is limited to produce sequence readings (called reads) of a limited length, often set between 50 to 300 bp. The tundra vole reference genome was sequenced on an Illumina HiSeq 2500 machine with 250 bp reads. When an entire genome consisting of 2.3 Gbp ($2.3 * 10^9$ bp) is sheared into smaller fragments of which only 250 bp is sequenced, any spatial information about gene locations is lost. However, algorithms can use the degree of overlap between individual reads and assemble them into longer continuous sequences called contigs (Brown 2002; Miller, Koren, and Sutton 2011). However, since the reads are so short, repetitive regions in the genome are difficult to map with using read overlap only. This still leaves many gaps where there is no continuous overlap between reads resulting in a large number of small contigs of which the actual location in the genome remains unknown.

DNA Fragment preparation

DNA fragments (orange) with forward (purple) and reverse (cyan) adaptors attached

Forward and reverse anchor points on the flow cell

Illumina flow cell with four lanes

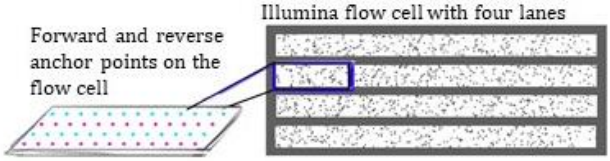

Cluster generation

1) Adaptors bind to anchor points on flow cell

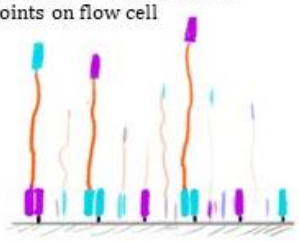

2) DNA fragment is copied (PCR) so that it is anchored to the flow cell

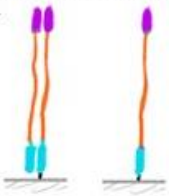

3) **Bridge amplification**: DNA fragment binds over to Neighbouring attachment point And the fragment is copied with PCR to create a large number clones of the DNA fragments

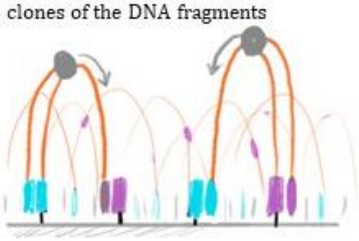

4) Many copies of the DNA fragments in forward and reverse direction, now anchored on the flow cell

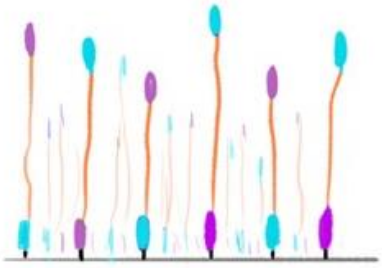

Sequencing by synthesis

5) Reverse fragments are washed off

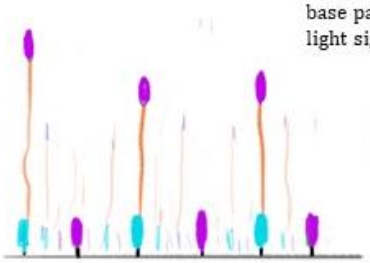

6) The **forward read** is generated from the DNA fragment through adding fluorescent, complementary base pairs that give off a light signal upon binding.

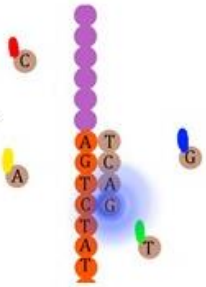

One base pair is added per cycle. The machine runs through 250 cycles to create 250bp reads. The machine reads the light signals on the flow cell from many reads simultaneously in each cycle.

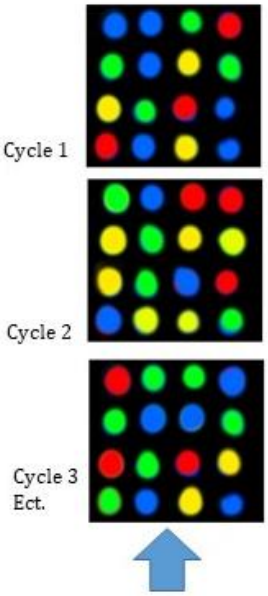

7) DNA fragments are amplified in reverse direction through bridge amplification

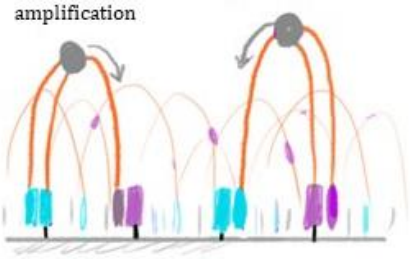

8) Now the forward reads are washed away

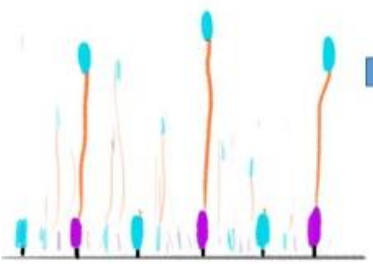

9) Generation of **reverse reads**, in cycles similar to the reverse reads

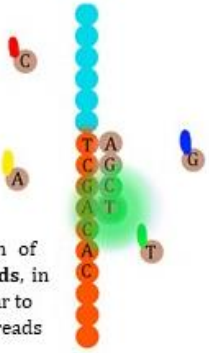

Figure 30. Illumina sequencing technique. Forward and reverse adaptors are attached to the double stranded DNA fragments. DNA is separated into single strands so that adapters bind to complementary anchor sequences on the flow cell. DNA folds to neighboring anchor points and forms a bridge. Strands are copied with PCR to form clusters of identical fragments in forward and reverse direction. Sequencing starts with DNA polymerase adding fluorescently tagged individual base pairs to the DNA fragment. This happens in cycles: during each cycle, one base pair is added to all the anchored fragments simultaneously. Each incorporation gives off a light signal indicating implementation of an A,C,T, or G base pair, which is read by the machine. The number of cycles determines how many base pairs are added to each strand and thus who long the sequence *reads* are. Illustration by M.J.van Dalum.

This number of gaps between contigs can be reduced through paired-end sequencing, which greatly improves the spatial quality of the genome assembly. Since DNA is double-stranded, it can be read in two directions: forward and reverse (Fig.30, Fig 31). The DNA fragments generated during library preparation are longer than the set 250 bp read length. They attach to the anchor points on the flow cell (Fig. 30) and are first sequenced in forward direction and then in reverse direction. The forward and reverse reads are generated in the same order and this way, we know which reads form pairs based on the read numbers. This gives a forward 250 bp read from a given fragment and a reverse 250 bp read from the same fragment with an unknown region in the middle (Fig 31). Based on the type of library preparation, the length of this unknown region can be estimated and this greatly improves the assembly of the reads, especially when the fragment length is long enough that the forward and reverse reads do not overlap in the middle (e.g. fragments longer than 500 bp).

Assembly algorithms can utilize this paired end information and close the gaps between some contigs. For example, when the read 1 of a pair is mapped at the end of one contig and read 2 of a pair at the beginning of another, we now know that they originated from the same DNA fragment and that these contigs can be tied together. These longer sequences generated through tying contigs together are called scaffolds (Fig.31) (Tucker, Marra, and Friedman 2009; Innes and Millar 1990).

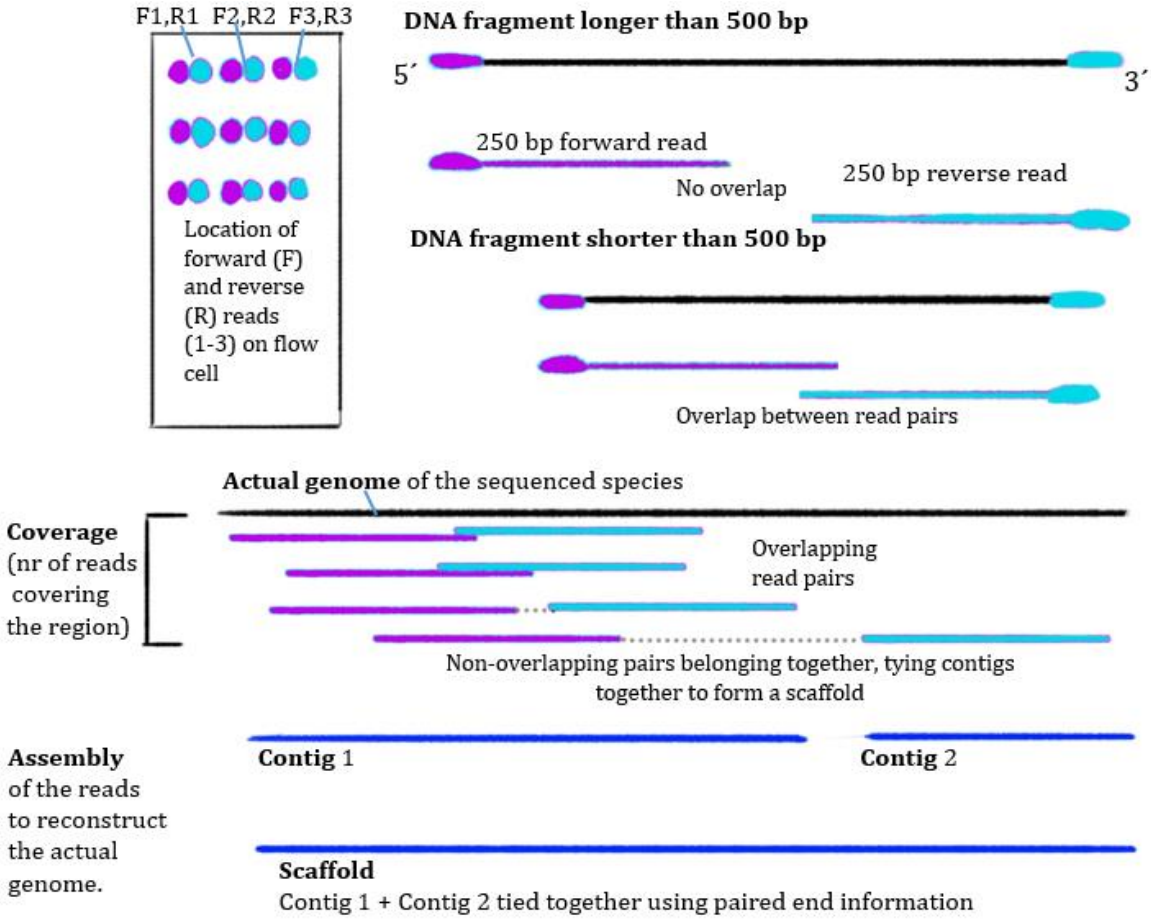

Figure 31. Steps behind assembling Illumina paired end sequence reads.
Genomic DNA consisting of chromosomes is sheared into small fragments of variable length. Adaptors (purple and cyan) are attached for the sequencing machine to recognize the fragments and sequence them to produce a set length (here 250 bp) reads. In pair-end sequencing, each fragment is sequenced both ends to generate a pair of two reads, forward (5' to 3') and reverse (3' to 5'). Forward and reverse pairs are located next to each other on a flow cell, which tells which pairs belong together. Reads are assembled based on sequence overlap to form contigs. The number of reads matching with a certain region is called coverage. Matching pairs can tie contigs together in places were no reads can be mapped or when mapping is difficult due to sequence repeat regions. Tied contigs are called scaffolds. Illustration by M.J.van Dalum.

Another important concept to know for understanding sequencing and genomics is coverage, also called sequencing depth. The sequencing machine generates reads of which the sum length exceeds the total length of the genome an X number of times. In the case of the tundra vole reference genome, this was 77x and we can say that the coverage was on average 77 fold. When all these reads are assembled together, they generate regions of overlap and the number of reads overlapping at a certain region of the genome is called the coverage of this location (Fig.31).

Several statistics indicate the quality of an assembly regarding the contig- and scaffold lengths (see below) (Miller, Koren, and Sutton 2011). The N50 is a good indicator for the overall contig- and scaffold length in an assembly. The scaffolds and contigs are arranged from longest to shortest and the length of the scaffold or contig that sits at 50% of the total genome length is the N50 (Fig.32).

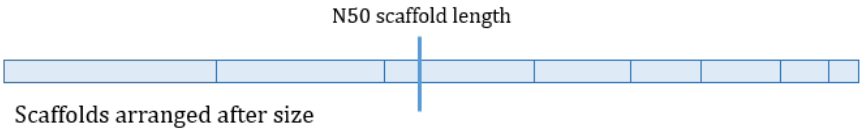

Figure 32. Visualization of the N50 statistic. Scaffolds and contigs are arranged after length and the length of the scaffold or contig located at 50% of the total genome length is the N50 contig/scaffold length.

The L50 is the smallest number of contigs/scaffolds of which the length sum is half the genome size. In figure 32, this is three. Table 1 summarises the statistics for the tundra vole reference genome generated with an Illumina HiSeq 2500 machine with 250 bp reads and a an average coverage of 77 fold.

Table 1. Statistics for *M.oeconomus de novo* assembly generated from Illumina sequence reads.
Kbp = kilo base pairs(10^3 bp), Mbp = mega base pairs (10^6 bp) , Gbp=giga base pairs (10^9 bp).

Nr of scaffolds	562436
Gaps between scaffolds	0
Longest scaffold	0.929 Mbp
Scaffold N50	0.115 Mpb
Scaffold L50	5556
Nr of contigs	589027
Contig N50	51,2 Kbp
Contig L50	13221
Longest contig	0.418 Mbp
Total sequence length	2.307 Gbp
Ns (= any base pair)	265,876,7
% Ns	0.12
GC content	42.17%

Table 1 shows that the reference genomes consisting of a large number of contigs/scaffolds with the longest scaffold being less than a million base pairs (0.92 Mbp).The genome is divided over a number of chromosomes that varies between species (2n=17-64, see overview in Lemskaya et al. (2010). The chromosome length of the sequenced prairie vole (*Microtus ochrogaster,* NCBI: txid79684*)* varies from 15.4 to 126.7 Mbp . The length of a gene varies strongly and longer genes can reach lengths of up to 0.39 Mbp (e.g. *Gria4*) which exceeded the length of most scaffolds in the assembly (Fig.34). As these lengths indicate, we ran into problems concerning downstream analysis of genes under selection

3.1.3 Oxford Nanopore sequencing

Therefore, we also performed third generation Oxford Nanopore sequencing (www.nanoporetech.com) on a PromethION machine. This generates much longer reads, up to the length of an entire chromosome. In this method, a single stranded DNA strand is pulled through small pores in a membrane using a voltage difference (Fig.33). As the base pairs of the single stranded DNA strand pass through the pore, they alter the ion flow within the pore that creates a readable current. An adaptor molecule attached to the pore reads these current alternations caused by passing DNA base pairs and sends these to a computer. The advantage of this method is the generation of very long sequence reads compared to the small reads produced by next generation technologies such as Illumina sequencing. A current drawback is the relatively high error rate (Lu, Giordano, and Ning 2016; Laver et al. 2015). Therefore, we have combined these two methods to generate a high quality tundra vole reference genome (Table 2) in which spatial information regarding gene positions is preserved.

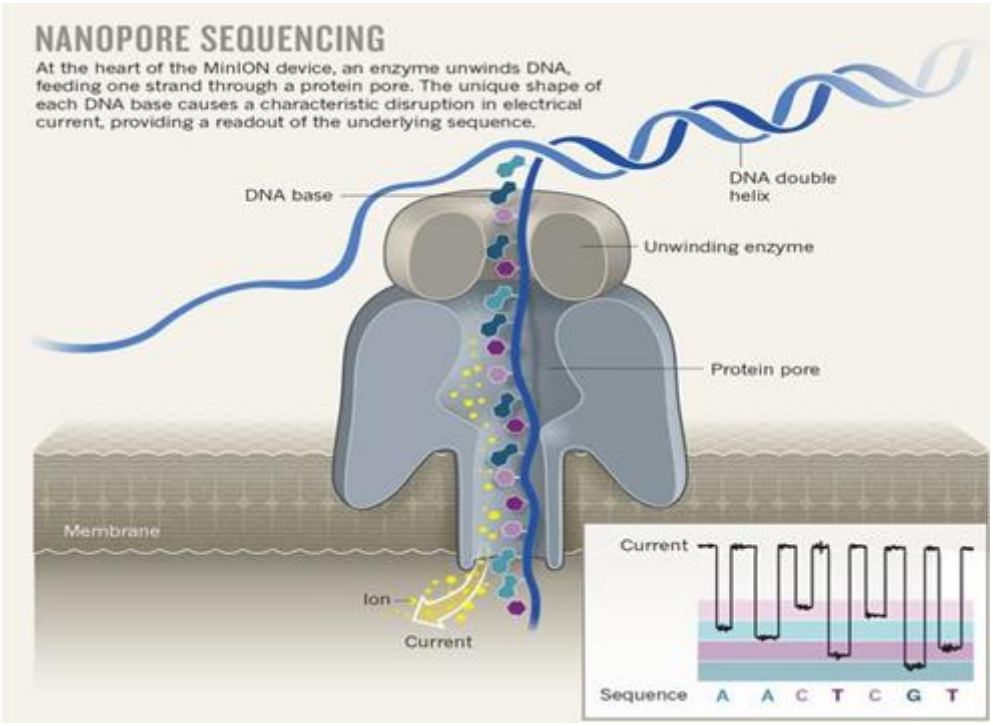

Figure 33. Nanopore sequencing. Entire chromosomes are is unwound and electric currents pull single stranded DNA strands through a protein pore embedded in a membrane. As the individual bases pass the pore, they alter the ion current in a way that is unique for each base pair. The voltage change over the membrane is registered by the machine.

Figure 33 shows the lengths of scaffolds generated by both sequencing methods, relative to the length of large genes and chromosomes.

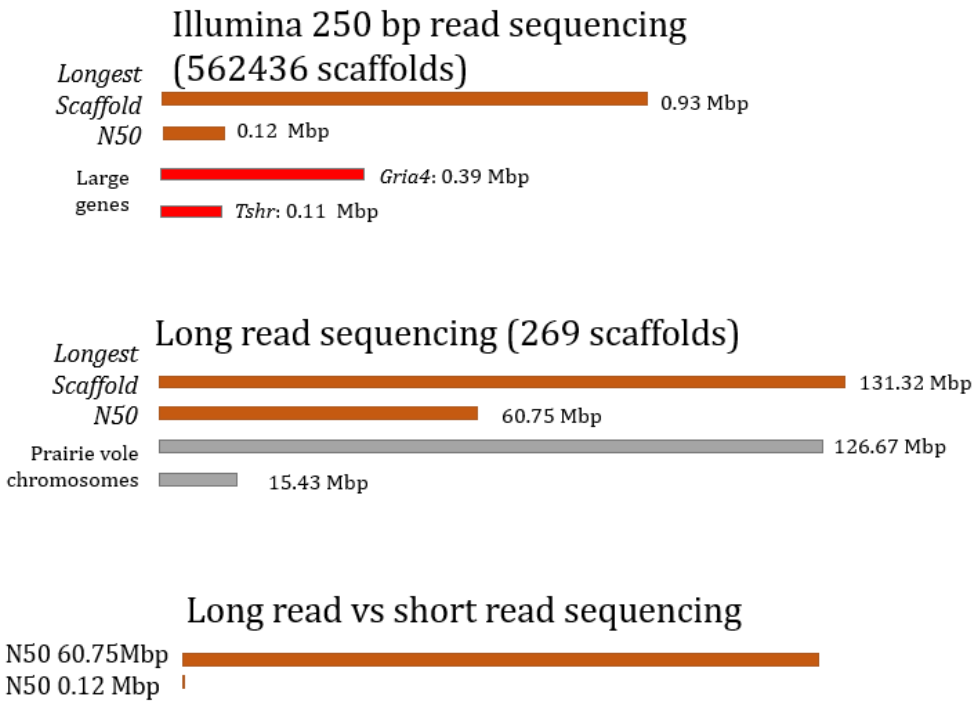

Figure 34. Variation in scaffold length between sequencing techniques. Length of the longest and N50 scaffold for Illumina and Nanopore sequencing (brown) relative to the length of large genes (red) and chromosomes (grey). Lengths are given in million base pairs (Mbp). Illustration by M.J.van Dalum.

Table2. Statistics for the *M.oeconomus* reference genome constructed with both Illumina short reads and nanopore long reads. Kbp = kilo base pairs(10^3 bp), Mbp = mega base pairs (10^6 bp) , Gbp=giga base pairs (10^9 bp).

Number of scaffolds and contigs	269
Longest scaffold	131.33 Mbp
Shortest contig	2143 bp
Number of scaffolds/contigs > 500 bp	269 - 100.0%
Number of scaffolds/contigs > 1Kbp	269 - 100.0%
Number of scaffolds/contigs > 10 Kbp	230 86.1%
Number of scaffolds/contigs > 100 Kbp	129 48.3%
Number of scaffolds/ contigs > 1Mbp	71 26.6%
Mean scaffold size	8.20 Mbp
Median scaffold size	0.91 Mbp
N50 scaffold length	60.75 Mbp
L50 scaffold count	13
%A	28.87
%C	21.15
%G	21.15
%T	28.87
%N	0.00

3.2. Pooled sequencing

With the tundra vole reference genome in place, we could perform whole genome sequencing of the two populations of interest and map this to the reference genome in order to search for genetic variation between the populations. DNA was extracted from 12 individuals representing the Northern population and 13 individuals representing the southern population (see **paper IV**) and these DNA sequences were pooled into two samples with equal DNA concentrations per individual vole.

Pooling individuals into one population sample saves costs for library preparation but individual information is lost in most methods (Fig.35). When the number of individuals is low (<40), this can cause problems for detecting rare genetic variants (Schlötterer et al. 2014). However Rubin et al. (2010) choose pools of 8 to 11 individuals with a coverage of 4-5x per pool. Amaral et al. (2011) used pools consisting of 23 to 36 individuals with a a mean coverage of 7.5-10x per pool. In these examples coverage was lower than the number of individuals per population pool which gives a relatively noisy allele frequency estimate. However, Atanur et al. (2013) performed individual sequencing for 27 individuals from various rat strains with a much higher coverage per individual (20x). Therefore, we increased the coverage to 190-200x per population with an average coverage of 15x per individual. This enables us to more easily distuinguish sequencing errors from minor alleles. The population size was still rather small for the detection of rare alleles but was sufficient (personal communication S.R Sandve) to find genes under strong selection pressures as this leads to fixation of an allele within one population but not the other (Vitti, Grossman, and Sabeti 2013).

We chose Illumina sequencing (HiSeq 3000 machine, 150 bp paired end reads) for the populations because of the relative low error rate. The Illumina machine generates output in the form of sequenced lanes in forward and reverse direction. Each lane yielded 110 Gbp sequence data and we had 4 lanes for each population.

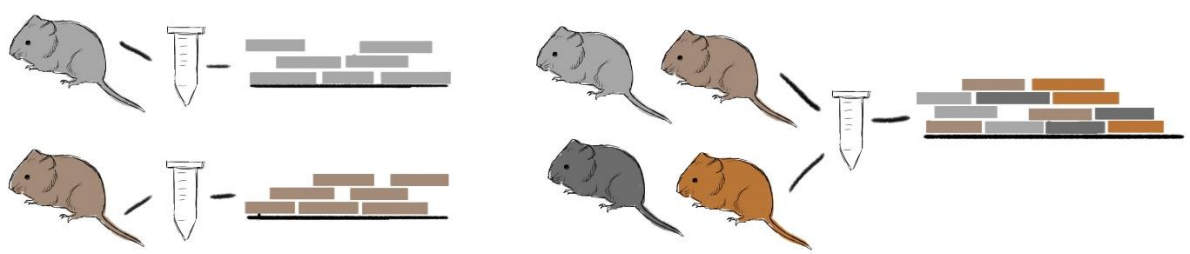

Figure 35. Unpooled versus pooled sequencing. The different colours represent reads coming from different indiviuals. Illustration by M.J.van Dalum.

3.3 Bioinformatics

3.2.1 Pipeline of mapping population data onto the reference genome

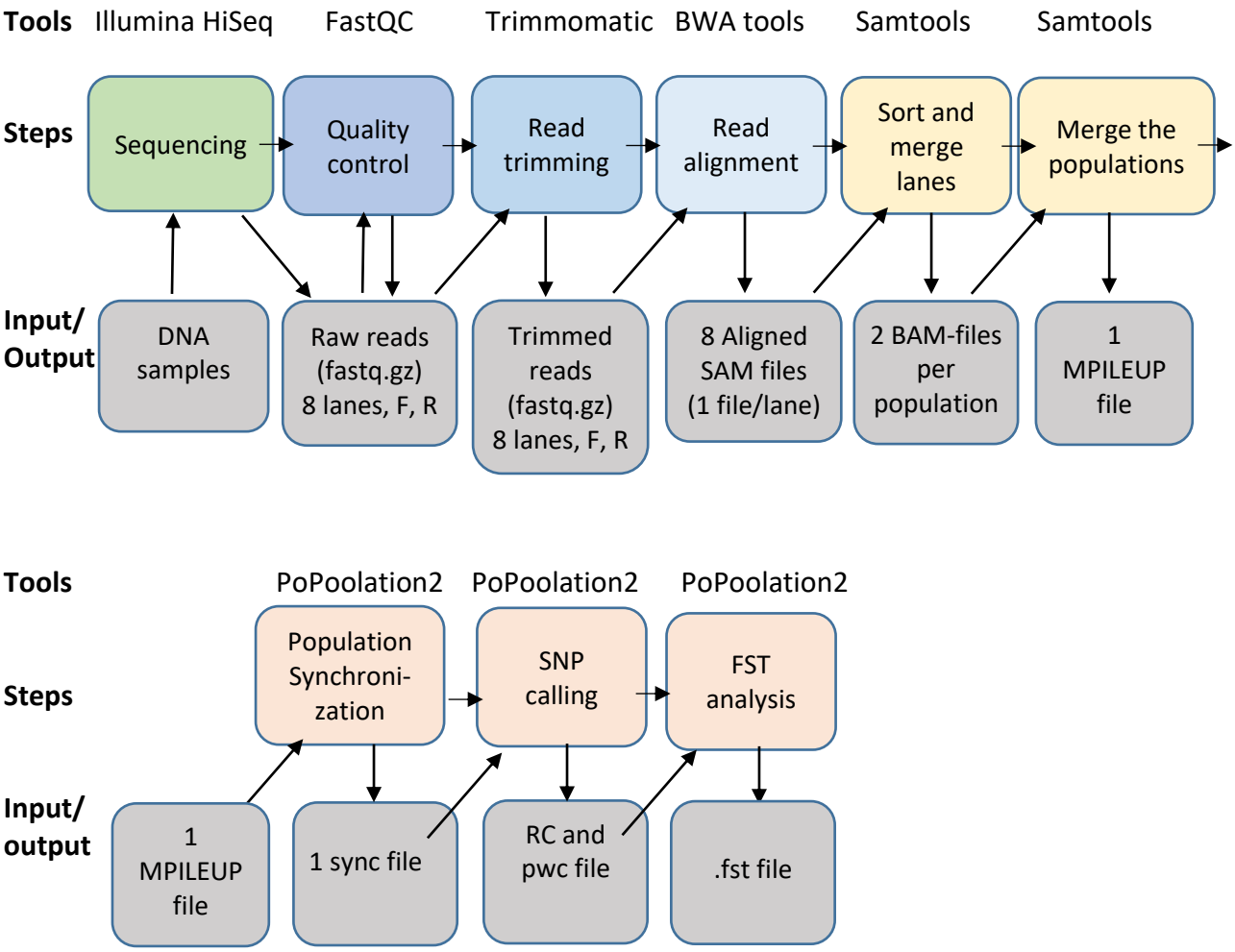

Figure 36. Bioinformatics pipeline showing the steps undertaken. The different coloured boxes represent steps undertaken with various software tools. The grey boxes show the input/output files generated. Illustration by M.J.van Dalum.

Figure 36 illustrates the bioinformatics steps undertaken to analyse the two populations. Details are described in **Paper IV**. In summary, the Illumina reads for each lane were quality checked and the poor quality starts and ends were cut off from each read (Fig.37). The trimmed reads were then mapped onto the tundra vole reference genome using BWA tools (Li and Durbin 2009) and the four lanes were merged into one file per population. Then each population was screened for base pair variants (SNPs, single nucleotide polymorphisms) across the genome and allele frequencies of each SNP (Fig. 37) were calculated between the populations using PoPoolation2 (Kofler, Pandey, and Schlötterer 2011). Alleles are variants of the same gene and

diploid organism possess two alleles for each gene. Diploid organisms have pairs of matching, nearly identical chromosomes. One of each pair is inherited from the mother and the other from the father. Therefore, the genes located on a chromosome, also have two variants, namely alleles. These alleles can be identical, making and individual homozygous for this gene or they can be different, which makes the individual heterozygous for this allele. The frequency of heterozygous individuals for a certain gene can be indicative for selection pressures affecting this particular genomic region.

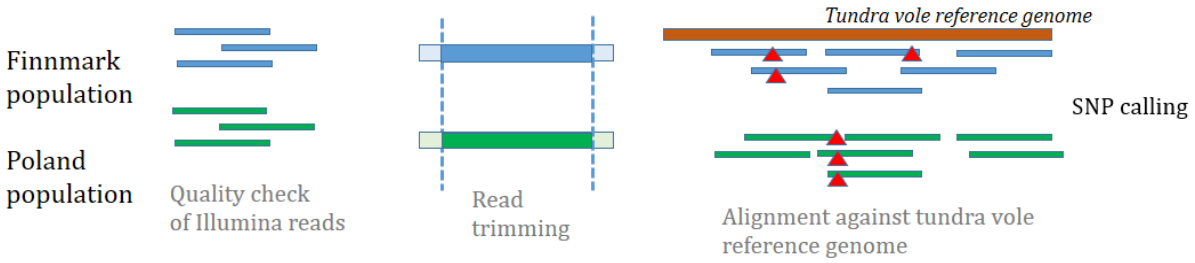

Figure 37. Read trimming and mapping of the reads. Reads from the two populations (blue and green) are mapped against the reference genome (brown) in order to search for single nucleotide polymorphisms (SNPs – red triangles. Illustration by M.J.van Dalum.

3.3.2 Calculating the heterozygosity (H_P) and fixation index (F_{ST})

As described in the introduction, we used the fixation index (F_{ST}) and heterozygosity index (H_P) to find regions and genes under selection between the two populations. The average F_{ST} and H_P was calculated for 20 000 base pairs (20 Kbp) non-overlapping windows across the entire genome (Fig.38). In addition, the F_{ST} and H_P were calculated for each single SNP separately.

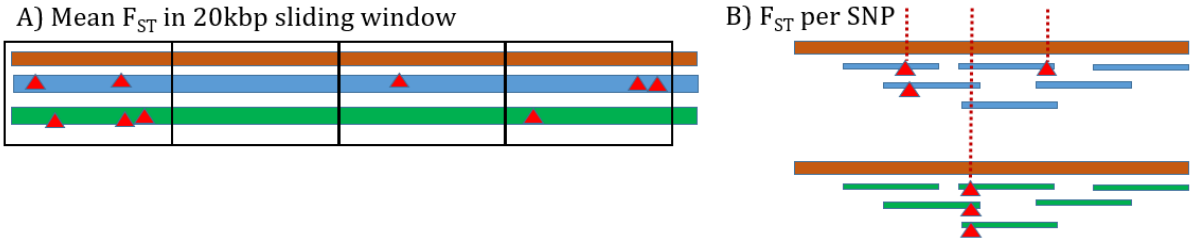

Figure 38. Calculation of F_{ST} with sliding windows and per SNP. Two approaches for calculating the fixation index (F_{ST}) and heterozygosity scores (H_P) of alleles between the two populations. A: the mean F_{ST} is calculated for non-overlapping 20 kbp sliding windows across the entire genome. B: calculation of the F_{ST} for each single SNP. Illustration by M.J.van Dalum.

The heterozygosity is calculated based on the frequency of base pairs occurring at each SNP position within each population (Jakobsson, Edge, and Rosenberg 2013; Meirmans and Hedrick 2011). With the allele frequencies of SNPs known, one can calculate what the proportion of homozygous or heterozygous individuals is within a population for any given gene by using the Hardy-Weinberg Equilibrium:

$p^2 + 2pq + q^2 = 1$
p= frequency of allele 1
q = is the frequency of allele 2.

Here, p^2 is the fraction of individuals homozygous for allele1, 2pq is the fraction of heterozygous individuals and q^2 is the fraction of individuals homozygous for allele 2.

Our dataset gave the coverage (total number of reads) and number of reads containing each base pair variant per SNP position for each population. With the coverage for each population given, we could calculate the allele frequencies within the population: e.g. allele 1 in population 1 divided by coverage of population 1. As the equilibrium states: the fraction of heterozygous individuals is 2pq. With this, the heterozygosity of both populations was calculated and the average between the two scores was taken, hereafter called HS. In addition, we calculated the total heterozygosity (HT) for both populations together through summation of the coverage and allele frequencies. The HT score is the heterozygosity of both populations taken together and treated as one.

The Hardy-Weinberg principle states that in the absence of evolutionary forces, allele frequencies and thus heterozygosity scores in a given population remain the same between generations (Freeman and Herron 2004). This means that without selection on one of the populations, the heterozygosity scores should be similar between the two populations. The F_{ST} is based on this principle and is therefore used to detect changes in heterozygosity *between* two populations.

The formula for two populations and two alleles:

$$F_{ST} = \frac{HT - HS}{HT}$$

In which:

HT = expected heterozygosity (2pq) of the total population (at one particular locus) in Hardy-Weinberg equilibrium

HS= observed average heterozygosity (2pq) in both populations

Positive selection tends to increase the frequency of the favoured allele and can drive it towards fixation, meaning that all individuals are homozygous for this selected allele (Freeman and Herron 2004). Consequently, heterozygosity scores approach zero. With strong direction selection (e.g. due to different environments) between two populations, allele 1 can be fixed in one population whereas allele 2 can be fixed in the other. Both populations would have a heterozygosity score of zero as they are homozygous for the opposite alleles. The average (HS) would then also be zero. However, the total heterozygosity (HT), in which both populations are considered as one, would be maximal as both alleles occur in equal frequencies. The F_{ST} index would therefore return 1. If there are no changes in allele frequency between the two populations, HS and HT are equal and the F_{ST} index is 0.

In this example, the fixation index only considered 2 alleles, but since there are four different base pairs, there can be up to four variants present at each SNP position. Therefore, the software used on our dataset calculated the fixation index slightly differently and is based on the equation given in "Hartl and Clark, (2007) *Principles of Population Genetics*"

$$F_{ST} = \frac{\pi_{total} - \pi_{within}}{\pi_{total}}$$

$$\pi_{within} = \frac{\pi p_{opulation1} + \pi_{population2}}{2}$$

$$\pi_{population1\ or\ 2} = \frac{C}{C-1} \times (1 - fA^2 - fT^2 - fC^2 - fG^2)$$

C= coverage

fN =frequencies of base pair A, T, C and G

π_{total} = the allele frequencies of the two populations are averaged and π is calculated as shown above.

3.3.3 Visualisation of the data and searching for genes

Data from the F_{ST} calculations for 20kbp windows as well as per single SNP, were visualized in the Interactive Genome Viewer (Robinson et al. 2011)(Fig.39) and mapped against the tundra vole reference genome. Data containing the location and names of genes (annotation) from the mouse (*Mus musculus,* Ensembl database CL57BL6) was applied to the tundra vole genome using the Liftoff software (Shumate and Salzberg 2021)(see **Paper IV**).

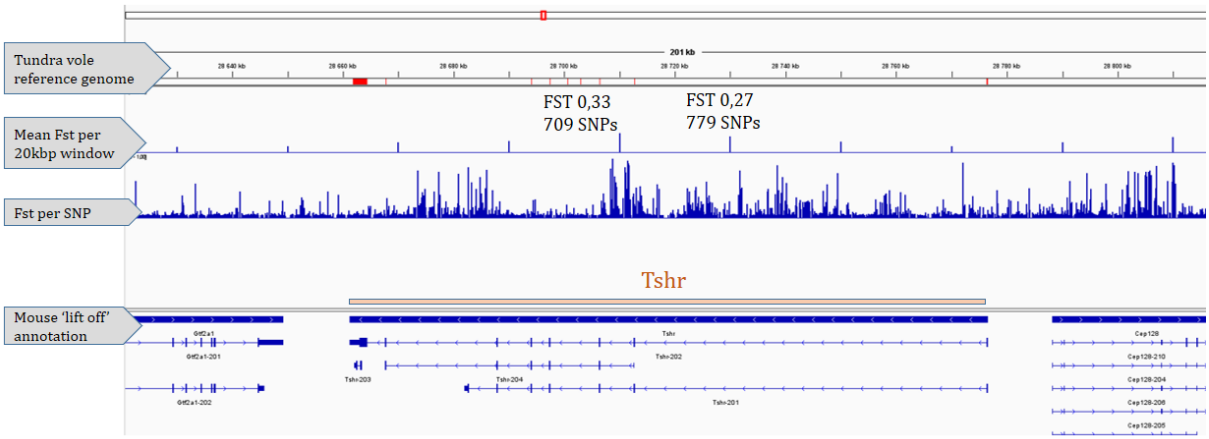

Figure 39. Visualization of the data in the Interactive Genome Browser (IGV). The tundra vole reference genome is in the top row, followed by the mean F_{ST} value for the two populations in 20 Kbp windows, the F_{ST} value for each single SNP and the gene annotation from the mouse applied onto the tundra vole using the Lift off software. Illustration by M.J.van Dalum.

3.3.4. BLAST

We checked the accuracy of the liftoff annotation through using BLAST (Basic Local Alignment Search Tool, (Altschul et al. 1990), in both directions (Fig. 40). First, the genomic sequence of 20 kbp windows with a significantly high mean F_{ST} value was selected from the tundra vole reference. This sequence was then mapped against the mouse reference in the Ensembl database (CL57BL6) (Howe et al. 2021), by using TblastX. This translates the genomic sequence into an amino acid sequence for all three possible reading frames and matches this with the mouse protein database. This greatly reduced the number of ambiguous matches and gave a clear indication of possible genes present in these 20kbp windows. This gave a list of candidate genes under selection. Of these genes, the mRNA sequence of either the prairie vole (*Microtus ochrogaster* NCBI:txid79684*)* or the mouse (NCBI:txid 10090) was downloaded from the NCBI (Sayers et al. 2021) database and then mapped with BLAST+ stand-alone (Camacho et al. 2009) against our tundra vole reference genome (Fig.40). This confirmed the presence of genes and as indicated by the LiftOff annotation.

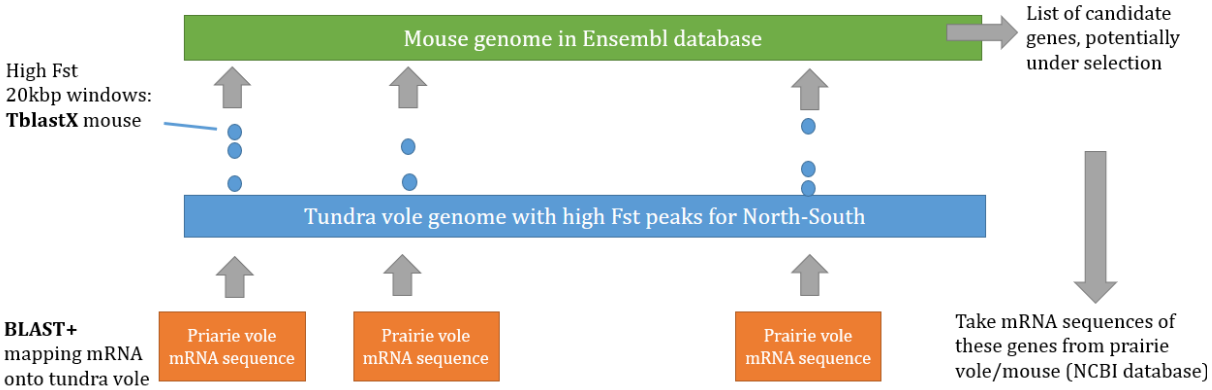

Figure 40. Schematic overview of the steps undertaken to explore genes under selection and check the accuracy of the Lift-off software. The genomic sequences in windows with high mean F_{ST} values were extracted from the reference genome. Through TblastX, against the mouse protein base, we found candidate genes. Of these genes, mRNA sequences were extracted from the prairie vole (*Microtus ochrogaster*) or mouse database and mapped back onto the tundra vole reference with BLAST+ to confirm the precise location of genes. Illustration by M.J.van Dalum.

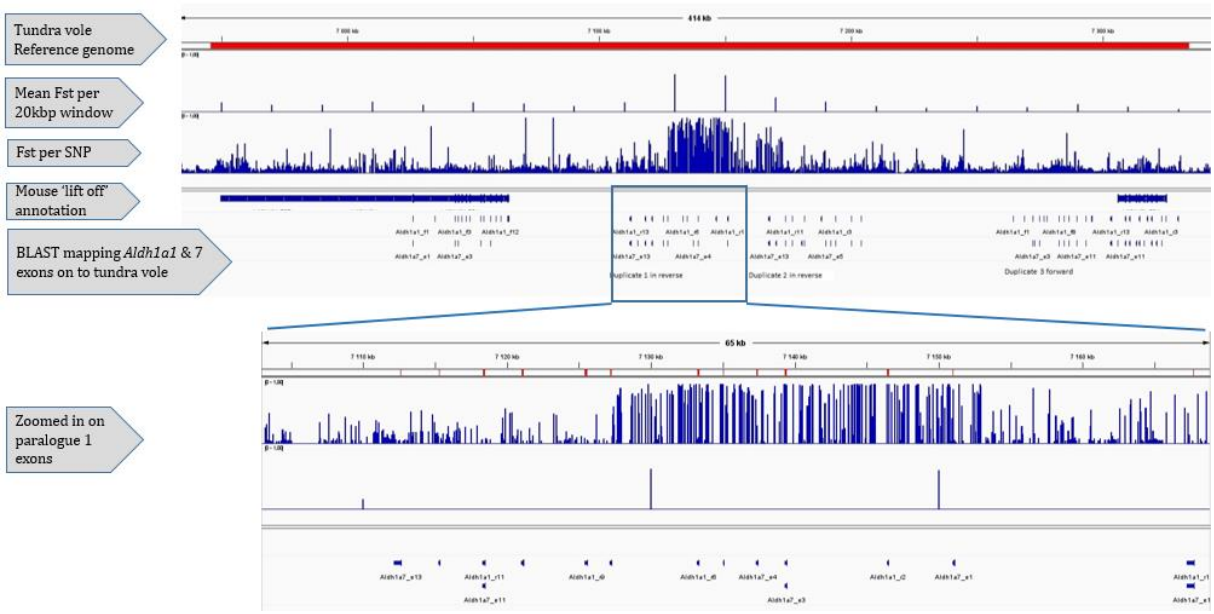

Figure 41. **Visualisation of *Aldh1a1* mapping onto the tundra vole genome.** Zoomed in example of the mapping of prairie vole *Aldh1a1* and mouse *Aldh1a7* mRNA sequences onto tundra vole reference genome, zooming in on a region with high F_{ST} values. The small bars indicate individual exons of the mRNA sequence matching onto the corresponding DNA sequence. Illustration by M.J.van Dalum.

3.3.5 Analysis of sequences

As described in detail in **Paper IV** and the results section, we found additional matches of prairie vole *Aldh1a1* and mouse *Aldh1a7* exon sequences in the tundra vole, between the *Aldh1a1* and *Aldh1a7* genomic positions (Fig. 41). Tundra vole genomic sequences of these additional *Aldh1a1/Aldh1a7* BLAST matches were extracted and translated into amino acid sequences from the reading frame that corresponds with the known *Aldh1a1* protein sequence (Fig.42). This gave a predicted amino acid sequence for these additional *Aldh1a* copies, which were then aligned with the protein sequence of prairie vole *Aldh1a1* and mouse *Aldh1a7* through using the online Clustal Omega Multiple Sequence Alignment tool (Madeira et al. 2019). This allowed us to screen for non-synonymous variants (genetic mutations that result in an altered amino acid sequence), areas of conservation and comparison of functional domains between these variants and *Aldh1a1* and *Aldh1a7* but also between the Northern and Southern population of tundra voles.

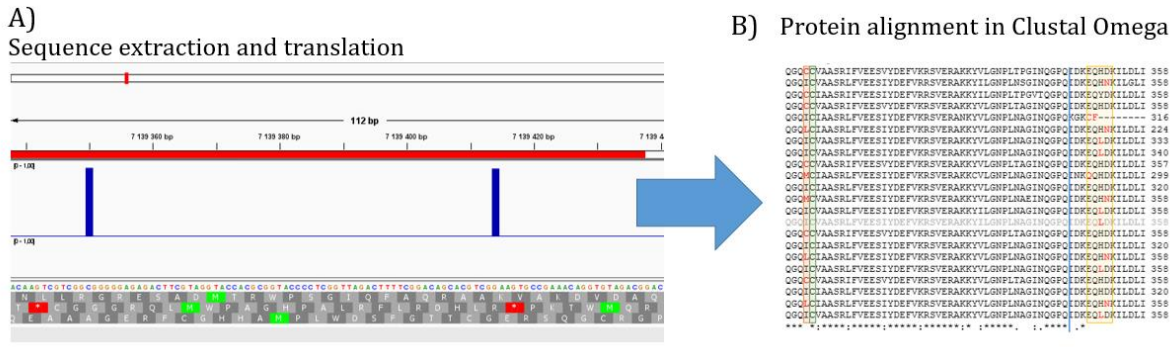

Figure 42. Exploration of translated sequences. (A) Translation of the exonic sequences of the *Aldh1a1*, *Aldh1a7* and discovered paralogues. The upper bar shows the genomic location in the tundra vole reference genome, the blue vertical bars are F_{ST} values for individual SNPs and the letters underneath are the amino acid translations in the three different reading frames. (B) Alignment of the *Aldh1a1*, *Aldh1a7* and paralogue amino acid sequences with the webtool Clustal Omega. Illustration by M.J.van Dalum.

We found *Aldh1a1*-like paralogues in other vole species (*M.fortis, M.arvalis, M.agrestis, M.ochrogaster*) as well and we extracted genomic sequences of *Aldh1a1, Aldh1a7* and the paralogues from these species. With these, we constructed a phylogenetic tree using the maximum likelihood algorithm in order to analyse sequence homology between the genes and the possible origin of these paralogues. See **paper IV** for more details.

4. Summary of findings

4.1 Paper I

Gonads or body? *Differences in gonadal and somatic photoperiodic growth response in two vole species*

In this paper, we investigated the development of the photoperiodic response in common voles (*Microtus arvalis),* native to 38-62°N, and tundra voles (*Microtus oeconomus)* native to 43-74°N. Photoperiods experienced early in life determine the rate of somatic and gonadal growth in small rodents like voles (Horton 1984a, 1984b; Lee 1993). The mammalian photoneuroendocrine system (PNES) has been well characterized (Dardente et al. 2010; D. Hazlerigg and Simonneaux 2015; Wood and Loudon 2014; Yoshimura 2010) but sources of variation within the system allowing for local adaptation are largely unknown. Photoperiod-temperature relations vary greatly with latitude and the photoperiod associated with favorable breeding temperatures is much longer at higher latitudes (Hut et al. 2013). Both vole species caught to establish the laboratory colony used for this study, came from the Netherlands. Common voles were obtained from the Lauwersmeer area and tundra voles were caught in four different locations the Netherlands (van de Zande et al. 2000). The latitude of the Netherlands (52-53°N) is in the center of the common vole's distribution range but is the southernmost boundary of the tundra vole. Different, potentially latitude dependent selection pressures, have resulted in genetic differentiation between the species and therefore we expected that they have adapted differently to the seasonal environment, reflecting their paleogeographic origins.

Voles from both species were kept on either short (SP: 8 hours of light) or long (LP: 16 hours of light) photoperiods from conception to 50 days of age (p50), which was the last sampling point. Body mass, gonadal mass and expression of PNES associated genes was assessed at 7, 15, 21, 30 and 42 days of age. Short photoperiods inhibited somatic growth, but not gonadal growth in tundra voles whereas in common voles, gonadal growth was inhibited but not somatic growth. The effect of photoperiod on body mass in tundra voles was first detectable at p30 and differences in the gonadal somatic index were already detectible at p15 in common voles. The photoperiodic response in gene expression was similar between the species with high *TSHβ* and *Dio2* expression and low expression of *Dio3* under LP. Under SP, we saw the opposite expression pattern. TSH receptor (*TSHr*) expression was significantly higher in tundra voles kept in SP whereas photoperiod had no effect on *TSHr* expression in common voles.

The results showed that photoperiodic programming occurs at the level of the TSH receptor in the tanycytes in the median eminence of the hypothalamus, modulating photosensitivity in a species-specific manner. The increased *TSHr* expression under SP in tundra voles could possibly make them more sensitive to photoperiod later in life. The species-specific response on either the gonadal (common vole) or somatic (tundra vole) axis occurred downstream of TSH signaling. This differential seasonal phenotype can reflect the evolutionary history at higher latitudes in the tundra voles, as winter temperatures are generally lower and favourable breeding periods shorter at higher latitudes. A reduction in body mass significantly reduces thermoregulatory costs (Lovegrove 2005) and the lack of a gonadal response in tundra voles could allow for opportunistic breeding outside of the breeding season (Tast and Kaikusalo 1976). However, due to the higher energetic costs of maintaining high gonadal mass, this may not have been selected for in common voles native to lower latitudes were breeding seasons are generally longer.

4.2 Paper II

Mechanisms of temperature modulation in mammalian seasonal time timing

In this paper, we studied the effect of ambient temperature on the critical photoperiod for summer phenotype development in spring and winter phenotype development in autumn. Voles show great year-to-year variation in the timing of breeding activity and several environmental factors such as ambient temperature have been shown to modulate the photoperiodic response (Nelson et al. 1989; Kriegsfeld, Trasy, and Nelson 2000; Dark and Zucker 1983). Earlier research demonstrated the relevance of photoperiodic history in voles; those born in under increasing photoperiods (spring) grow and mature fast and those born under decreasing photoperiods (autumn) grow and mature slowly to prepare for overwintering (Horton 1984a; Gliwicz 1996; Aars and Ims 2002). Yet it remained unclear how ambient temperature is integrated in the PNES and how this modulates the seasonal phenotype in relation to photoperiodic history.

Common voles were housed in SP (representing spring) or LP (representing autumn) at 21°C and gestation, birth and lactation took place under these conditions. At 21 days of age (p21, weaning), groups of pups were exposed to a range of photoperiods (6, 8, 10, 12, 14, 16 or 18 hours of light) at either 21°C or 10°C. We fitted dose-response curves (4-parameter log-logistic function) to the response parameters as function of post-weaning photoperiod. This enabled us to calculate the critical photoperiod (or reaction norm, see section 1.3.3. in the introduction), which was determined as the inflexion point or the ED50 of the fitted curve. The ED50 is the

photoperiod in which the response variable (e.g. gene expression) reaches 50% of its maximum measured value.

The higher temperature increased the long-day induced expression of *Dio2* in tanycytes while lower temperatures enhanced the short-lay induced *Dio3* expression. *TSHβ* expression was not affected by temperature. Downstream somatic and gonadal growth was enhanced in 10°C compared to voles in 21°C whereas testosterone levels were lower under short days and low temperatures. Critical photoperiods varied between the variables tested, depended largely on the gestational photoperiod and they varied in their sensitivity to temperature modulation. These results indicate that temperature modulation occurs at level of *Dio2*- and *Dio3* expressing tanycytes rather than in *TSHβ* expressing thyrotrophs located in the *pars tuberalis* (PT) of the pituitary.

Collectively, we demonstrate the effect of photoperiodic history and relevance of directional change on the post-weaning seasonal phenotype in common voles. Temperature modulation occurred at various levels in PNES and the various critical photoperiods in different response parameters indicate flexibility within this system. This flexibility is relevant for local adaptation to changing seasonal environments and the opportunism in breeding as observed in several vole species in the field.

4.3 Paper III

Differential effects of ambient temperature on the photoperiod-regulated spring and autumn growth programme in *Microtus oeconomus* and their relationship to the primary photoneuroendocrine response pathway.

In paper III, we used the same protocol as in paper II, this time in tundra voles, native to higher latitudes than common voles. Paper I demonstrated that tundra voles respond to short photoperiods primarily through reducing in somatic growth, whereas common voles reduced gonadal growth. The generally lower temperatures at higher latitudes may have enhanced the evolution of cold tolerance in tundra voles and this may have affected the integration of temperature and photoperiod as seasonal cues. Given the results of paper I, we expected that ambient temperature might modulate somatic growth.

We fitted a standard von Bertalanffy asymptotic growth function to individual vole growth trajectories which enabled us to calculate the individual growth potential (weight gain from weaning, p21, to sampling p50), and half-time. Half-time is the number of post-weaning days at which the 50% of the maximum weight (at p50) is reached. With these individual growth potentials and half-times we fitted dose-response curves to the photoperiod-temperature groups, as described in paper II.

The growth potential depended on the combined effect of gestational and post-weaning photoperiods with voles raised under short photoperiods followed by long (16L) post-weaning photoperiods (spring), showing the highest growth potential. Low temperatures further enhanced growth in spring born voles, but had no effect in the autumn groups. The gonadal axis remained insensitive to both photoperiod and temperature. In contrast to common voles, the critical photoperiod for *TSHβ* expression shortened significantly in 10°C, only in the autumn group experiencing decreasing photoperiods. *Dio2* expression was generally higher in spring than in autumn and was barely detectable in the 10°C group. *Dio3*, however, was generally higher in autumn and insensitive to temperature.

Sigmoid curves could be fitted to the *TSHβ* expression pattern in the PT but these fitted poorly with *Dio2* and *Dio3* expression and downstream variables (growth potential, gonadal mass, and testosterone). This confirmed the model for *TSHβ* functioning as photoperiodic readout with *Dio2/Dio3* responding in a more switch-like manner (Hugues Dardente et al. 2010). We were surprised that 10°C shortened the critical photoperiod of *TSHβ* expression in autumn (from 15.4 to 14h) since *TSHβ* was expected to be insensitive to non-photic cues. It is difficult to find a functional explanation and this could be due to circadian variation of *TSHβ* expression relative to sampling time. Pre-weaning photoperiod and ambient temperature modulated tanycyte *Dio2* and *Dio3* expression and growth potential which indicates that plasticity in the photoperiodic response occurs mostly downstream of the PT.

In comparison with common voles described in paper II, we did not detect a low temperature-induced lengthening of critical photoperiod in other parameters nor an increased photosensitivity in tundra voles. This suggest that tundra vole's evolutionary history at higher latitudes than common voles has favoured opportunistic breeding and flexibility in the photoperiodic response.

4.4 Paper IV

Evidence for repeated local gene duplication at the *Aldh1a1* locus in an herbivorous rodent (*Microtus oeconomus*).

In paper IV, we studied genetic differences *within* the tundra vole species: between a northern (70°N) and southern population (53°N). We screened for signatures of selection across the genomes, which could be the consequence of latitude-dependent selection pressures.
A signature of selection is a change in genetic variation in a specific genomic region occurring as a consequence of environmental selection pressures that have led to functional differences between populations (Bertolini et al. 2018). This study only assessed two populations but it provides a first indication of genes potentially under latitudinal selection.

To perform this study it was necessary to do *de novo* sequencing of the tundra vole, to generate a high quality reference genome for downstream analysis. DNA samples were collected from a population in Northern Norway, Ifjordfjellet (n=12) and Poland, Białowieża (n=13). Samples were pooled per population for whole-genome resequencing and the fixation index (F_{ST}) was calculated for non-overlapping 20kbp sliding windows. Fixation of an allele in one population but not the other indicates selection on this allele, which is reflected in a high F_{ST} value. We applied the mouse annotation onto the tundra vole reference genome to explore genes falling in regions with high F_{ST} values. The presence of these was double-checked through BLAST.

The heterozygosity scores were generally higher in the Northern population and we found immune system related genes, olfactory receptors and vomero-nasal receptors in windows with high F_{ST} values. The PNES related genes iodothyronine deiodinase 2 (*Dio2*) and the melatonin receptor 1b (*Mtnr1b*) were found directly neighboring windows with a high mean F_{ST} value. The most striking finding was a strong signature of selection between the neighbouring genes *Aldh1a1* and *Aldh1a7* (Aldehyde dehydrogenase 1 family member A1 an A7). Through BLAST, we found three seemingly functional *Aldh1a1*-like paralogues located between *Aldh1a1* and *Aldh1a7* and one paralogue was under strong selection as indicated by a high F_{ST} value. Similar *Aldh1a1*-like paralogues were also found in other voles: *M.fortis, M.ochrogaster , M.agrestis , M.arvalis*.

These *Aldh1a1*-like paralogues had the highest sequence homology with *Aldh1a7* but their function remains unclear. Previous research showed that *Aldh1a1* (*Raldh1*) is expressed in tanycytes under long photoperiods and is potentially involved in energy metabolism regulation through retinoic acid (RA) signaling (Shearer et al. 2010; Helfer, Barrett, and Morgan 2019).

Aldh1a7 is unique to rodents and despite its high similarity with *Aldh1a1;* it does not seem to be involved in RA signaling as it is not reported to process retinaldehyde (Hsu et al. 1999). Aldehyde dehydrogenases are involved in aldehyde detoxification associated with oxidative stress and red-backed voles (*Myodes rutilus)* living in a mild hypoxic environment under the snow had enhanced an ADH-ALDH metabolism (Kolosova and Kershengol'ts 2017). Selection on an *Aldh1a1*-paralogue could be associated with the long periods of snow cover experienced by tundra voles from Northern Norway but this requires further research.

4.5 Extension to paper IV: analysis of the *Aldh1a1*-paralogue sequences

Amino acid homology between ALDH1A1 and other ALDH-paralogues in the mouse varied between 90.62% to 16.96% (Table 3). For comparison: all ALDH1A1 paralogues in voles had a similarity between 87.6 – 89.9% with ALDH1A1 and 93.0 – 95.0% with ALDH1A7.

Table 3. Mouse ALDH paralogues. Percentage of amino acid sequence similarity between the various aldehyde dehydrogenases (ALDH) in the mouse, relative to ALDH1A1.

ALDH1A7	90.62 %
ALDH1A3	65.82 %
ALDH1A2	69.69 %
ALDH1B1	63.39 %
ALDH1L1	26.72 %
ALDH1L2	25.57 %
ALDH2	64.55 %
ALDH3A1	28.70 %
ALDH3A2	23.68 %
ALDH3B1	23.72 %
ALDH3B2	22.76 %
ALDH3B3	23.17 %
ALDH4A1	24.20 %
ALDH5A1	33.27 %
ALDH6A1	29.72 %
ALDH7A1	25.97 %
ALDH9A1	35.91 %
ALDH8A1	36.76 %
ALDH16A1	16.96 %

Most of the 13 *Aldh1a1* exons could be located in the paralogues by using BLAST, except exon 7 (See table SX of paper IV).

The functional domains as described by (Sobreira et al. 2011) were further assessed to provide insight in the possible function of these paralogues. In this paper, they identified three positions of the substrate entry channels in aldehyde dehydrogenases. These were the 'mouth' at position 124, the 'neck' at position 459 and 'bottom' at position 302, near the catabolic site. The size and charge of the amino acids present on these key positions could alter the channel from allowing large substrates. Amino acids with a small molecular volume create a wide substrate entry channel allowing large molecules such as retinaldehyde (for retinoic acid synthesis) to reach the catalytic site. Large amino acids present at these key positions make the channel much narrower, allowing only small molecules such as acetaldehyde to reach the catalytic site

(Sobreira et al. 2011). Small molecules can still be processed by large-channeled ALDHs but less effectively due to the wide channel compared to narrow channeled ALDHs.

Assessment of the amino acids present at these key positions in ALDH1A1, ALDH1A7 and the vole paralogues gave a rough estimation of the possible substrate entry channel size as summarized in tables 4 and 5. Both ALDH1A7 as well as the ALDH1A1-like paralogues seem to have a smaller substrate entry channel than ALDH1A1. Indeed ALDH1A7 does seem to process retinaldehyde (Hsu et al. 1999) and the paralogues may have a similar function as ALHD1A7.

Table 4. Amino acid characteristics of amino acids at key points in ALDH1A1 and the paralogues. Molecular volumes and class of the amino acids found at the key positions of the ALDH1A substrate entry channel, based on Sobreira et al. (2011). Molecular volumes come from http://www.imgt.org/IMGTeducation/Aide-memoire/_UK/aminoacids/abbreviation.html#refs, and are based on Zamyatnin, (1972).

Symbol	Name	Volume (Å^3)	class
Mouth, position 124			
E	Glutamic acid	138.4	charged, acidic
G	Glycine	60.1	non polar
D	Aspartic acid	111.1	charged, acidic
Neck, position 459			
L	Leucine	166.7	non polar
A	Alanine	88.6	non polar
V	Valine	140	non polar
M	Methionine	162.9	non polar
T	Threonine	116.1	polar
Bottom, position 302			
I	Isoleucine	166.7	non polar
L	Leucine	166.7	non polar
C	Cysteine	108.5	polar
M	Methionine	162.9	non polar

Protein	Amino acids at mouth (124), neck (459), bottom(302)
ALDH1A1	GVC
	GMC
ALDH1A7	EAI
	EAL
Paralogues	DAI
	DTI
	DAM
	GAM
	EAL
	EAI
	ELI

Table 5. Amino acids present at key points in the substrate entry channel of the various ALDH1A1 paralogues. These amino acids may determine the channel size in ALDH1A1, ALDH1A7 and paralogues of *Microtus .oeconomus, M.arvalis, M.ochrogaster, M.agrestis, M.fortis* and *Mus musculus*..

5. Discussion and conclusions

5.1 General discussion of the main findings

In this thesis, we studied phenotypic plasticity and genetic variation in the mammalian seasonal time keeping mechanism in relation to latitude origin, with voles (*Microtus*) as research species. We first approached this top-down, from phenotype down to the mechanisms underneath. Then we took a bottom-up approach focusing on genetic differences associated with living at a northern versus southern latitude. I will first discuss the differential photoperiodic response between the common vole (*Microtus arvalis*) and tundra vole (*Microtus oeconomus*) and then the plasticity within the vole PNES and the response to ambient temperature. Before I get deeper into genetics, I will discuss the occurrence of photoperiodic non-responders in rodents. The last topic will be about the genetic differences between the northern and southern tundra vole populations the *Aldh1a1*-like paralogue that carried a strong signature of selection.

5.1.1 The differential photoperiodic response in tundra voles and common voles from the same location

Common voles and tundra voles express different seasonal phenotypes in response to similar laboratory conditions. Tundra voles generally inhabit higher latitudes than common voles and are expected to have adapted to northern conditions. The lab colonies used in this study were established from wild populations both caught in the Netherlands (52-53°N). Any differential seasonal responses between the species can therefore be ascribed to genetic differences caused by species specific evolutionary histories. The northern species reduced somatic growth whereas the southern species reduced gonadal growth in response to continuous short photoperiods. This effect became noticeable during the period between weaning and puberty when voles either accelerate growth and maturation or delay this (Horton 1984a, Gliwicz 1996). In the wild, the population of overwintering voles consists mostly of subadults born late in the breeding season. In tundra voles and common voles, only a small proportion of mature adults may overwinter but most adults die at the end of the breeding season (Eccard and Herde 2013; Gliwicz 1996; Aars and Ims 2002). Overwintering subadults maintain low body- mass and gonadal mass but grow and mature in spring to form the first breeding cohort (Gliwicz 1996; Ergon 2007; Negus, Berger, and Brown 1986).

We have two hypothesis regarding the tundra vole's response to short photoperiods. The first is that they would respond more strongly to short photoperiods than common voles because of their more northern evolutionary history and the potentially more obligatory winter

adaptations. For example, adult prairie voles (*M.ochrogaster*) kept in the lab all responded to short photoperiods with pelage growth but the gonadal response was less clear. Winter pelage was suggested as a more obligatory winter adaptation than gonadal regression and indeed, about 30% or the males retained an active reproductive system (Nelson et al. 1989). The second hypothesis is that tundra voles would resort to more opportunistic breeding, which is characteristic for short-lived mammals even at temperate- to high latitudes (Bronson 1988). Figure 17 in the introduction shows that population of the Eastern deer mouse (*Peromyscus maniculatus*), in the figure marked with an *X*) at lower latitudes (30-40°N) breed year round while those at higher latitudes (50-60°N) breed seasonally. This species is thus capable of year-round breeding at favourable environmental conditions. Tundra voles in our lab colony came from the southernmost boundary of their European distribution range, and therefore, they may exhibit similar breeding opportunism relative to conspecifics from higher latitudes.

Indeed, our results show that tundra voles had no gonadal response to photoperiod, which supports the opportunistic breeding strategy that has indeed been documented in tundra voles (Tast and Kaikusalo 1976). Although winter breeding has been observed in common voles too (Baláž 2010a), gonadal growth inhibition in short days is much stronger in this species despite *ad libitum* food availability under laboratory conditions (21°C). Environmental unpredictability is suggested to increase the degree of opportunism versus strict photoperiodism (Prendergast, Kriegsfeld, and Nelson 2001). Siberian hamsters (*Phodopus sungorus*) living in more predictable environments than Campbell hamsters (*Phodopus campbelli*) and desert hamsters (*Phodopus roborovskii*) at the same latitude (48.1- 53.4° N), showed the strongest photoperiodic response and the lowest occurrence of photoperiodic non-responders (see section below) under lab-conditions (Müller et al. 2015). It could be that common voles have evolved under more predictable seasonal conditions than the higher latitude associated tundra vole, yielding them more responsive to photoperiod regarding the timing of breeding.

Tundra voles did respond to photoperiod but through reduction of the post-weaning growth potential, which was unaffected by photoperiod in common voles. Low body mass may enhance winter survival chances in small mammals as this lowers energy demands (Lovegrove 2005) and indeed, a lower body mass and higher whole body metabolic rates was associated with higher winter survival chances in tundra voles from Poland (53°N) (Zub et al. 2014). In Norway, the winter survival rate was also negatively correlated with body mass and lighter weight females had a higher survival chance than males (Aars and Ims 2002).This may be an essential survival strategy that has evolved in tundra voles. The lack of photoperiodic regulation of body mass in common voles suggests that winter conditions at lower latitudes do not require this. Moreover,

the long photoperiod induced high body mass in tundra voles could provide a competitive advance during the shorter breeding season at high latitudes since the larger individuals from the overwintering generation have bigger territories (Lambin, Krebs, and Scott 1992).

5.1.2 Plasticity in the photoperiodic response and integration of ambient temperature

Our next goal was to characterize sources of variation in the PNES of common voles and tundra voles. We therefore assessed critical photoperiods at different mechanistic levels for the expression of a summer phenotype in response to ambient temperature modulation (see **paper II and II)**.

There was a clearly detectable critical photoperiod for *TSHβ* expression in the *pars tuberalis*, which is the photoperiodic read-out relatively upstream in the mammalian PNES. This was unaffected by temperature nor photoperiodic history (e.g. spring or autumn born pups) in common voles but an ambient temperature of 10°C shortened the autumn critical photoperiod in the tundra vole from 15 (21°C) to 14.4 (10°C). This corresponds with the 11th of August (15h at 21°C) and the 21th of August (14.4h at 10°C) and at 53°N, where both lab colonies have been captured. This indicates that under lower temperatures, tundra voles maintain higher (summer associated) *TSHβ* levels further into autumn and a winter phenotype would be initiated *later*. As discussed in **paper III,** we have no functional explanation for this and a possible effect of sampling time relative to the circadian fluctuation in *TSHβ* expression (Masumoto et al. 2010) could have caused this critical photoperiod shift. However, the circadian expression peak of *TSHβ* relative to sampling time was taken into account in all groups equally. *TSHβ* expression is regulated by the transcription factor *Eya3,* which is inhibited by melatonin and together, these factors form a read-out of photoperiod, which serves as a calendar that is generally insensitive to non-photic cues (Masumoto et al. 2010; Dupré et al. 2010; Hut 2011). Melatonin receptor expression (*Mtnr1a)* in PT thyrotrophs was not affected by photoperiod (**paper I**) and it is unlikely to be affected by temperature as the main function of melatonin is to follow the onset and offset of the circadian dark phase (Stehle et al. 2001). Although we did not measure *Mtnr1* nor *Eya3* expression in relation to temperature so we cannot exclude this possibility.

Temperature modulation was most apparent downstream of PT *TSHβ* expression, at the level of *Dio2* and *Dio3* expression in hypothalamic tanycytes (Hugues Dardente et al. 2010; Wood and Loudon 2018). *Dio2* and *Dio3* expression in the median eminence of the hypothalamus act in a flip-flop switch like manner in which high *Dio2*, and low *Dio3* expression is associated with a summer phenotype and high *Dio3*, and low *Dio2* expression is associated with a winter phenotype. This switch-like *Dio2/Dio3* expression pattern resulted in poor sigmoid curve fits

and we could not determine a critical photoperiod. This, indeed, indicates that these genes are also sensitive to other factors than only photoperiod. We detected a clear effect of photoperiodic history at the *Dio2/Dio3* level as well as a temperature effect in both species.

Further downstream, we saw a species-specific differentiation on the gonadal- versus somatic axis which did not correlate directly with the *Dio2/Dio3* expression patterns. We did not find a correlation between testosterone and testes mass and neither did testosterone correlate with *Dio2/Dio3* expression. This indicates that parameters downstream of the PT and ME are orchestrated independently of each other as has been reviewed earlier (Hazlerigg and Simonneaux 2015). This allows for flexibility in the expression of seasonal phenotypes relative to environmental factors. Temperature modulation can potentially also happen downstream of *Dio2/Dio3* signaling, at the level of Gonadotropin releasing hormone (GnRH) release. GnRH initiates the secretion of LH and FSH from the pituitary, which in turn controls gametogenesis and steroid production in the gonads. GnRH mRNA production in prairie voles was not inhibited by low temperature or short days alone but both factors together reduced GnRH mRNA production (Kriegsfeld, Trasy, and Nelson 2000).

Taken together, our results show that the strongest effect of temperature modulations happens at the level of *Dio2/Dio3* expression in hypothalamic tanycytes but temperature modulation can potentially occur at the level of PT *TSHβ*-expression. Furthermore, we demonstrated a clear effect of photoperiodic history, which underlines the importance of directional change rather than a critical day length. Indeed, Whetham (1933) already stretched that it was not the absolute photoperiod but rather the directional change that coordinated the onset and offset of the egg production season in domestic chickens. This was later also neatly demonstrated in meadow voles (*M. pennsylvanicus*), montane voles (*M. montanus*) and Siberian hamsters (*Phodopus sungorus)* in which the direction change in photoperiod experienced by pups *in utero* relative to post weaning photoperiod affected growth rate and age of maturation (Lee 1993; Stetson, Elliott, and Goldman 1986; Horton 1985). See chapter 7 for a review on maternal photoperiodic imprinting.

5.1.3 Photoperiodic non-responders

In several seasonally breeding rodents investigated, a small proportion of the population does not respond to short photoperiods through gonadal regression or delayed maturation. These individuals remain reproductively active and are called photoperiodic non-responders (Prendergast, Gorman, and Zucker 2000). The distinction between a photoperiodic responder

and a non-responder is not always clear as individuals show variation in their short day response on different seasonal response parameters (Müller et al. 2015).

In this context, we had a tundra vole in the spring (pre-weaning 8L) 21°C group who had high *TSHβ* expression levels, even under short post-weaning photoperiods (post weaning 10L) , while other individuals had very low to no detectible *TSHβ* expression. This male also expressed near summer like levels of *Dio2* but also had high winter levels of *Dio3*. However, he was not heavier nor did he have larger testes than the other males in the group. We also had one common vole in the autumn (pre-weaning 16L) 21°C group who had higher *TSHβ* levels, larger testes and higher body mass under shortening (14L) photoperiods than the other males in both temperatures (21°C and 10°C). These two could be examples of photoperiodic non-responders and our data suggests that photoperiodic non-responsiveness can occur at the level of PT *TSHβ* expression. We did not test the melatonin levels of these voles but the melatonin profiles of non-responder Eastern deer mice still reflected short days, similar as in responders (Blank and Freeman 1991). Interestingly, Siberian hamsters generally had a longer circadian period (tau) than Campbell hamsters (*P.campbelli)* and desert hamsters (*P.roborovskii)*, who are less photoperiodic and more responsive to other environmental cues than Siberian hamsters (Müller et al. 2015). The occurrence of photoperiodic non-responders was higher in the latter two species with a shortest circadian period (Müller et al. 2015), which is in contrast with the findings that non-responsive Siberian hamsters had a longer circadian period than responsive individuals (Freeman and Goldman 1997a).

The degree of photoperiodic non-responsiveness on downstream response parameters varies greatly between individuals and species, which underlines the flexibility in the rodent seasonal phenotype. For example non-responder Eastern deer mice (*Peromyscus maniculatus)* males kept in SP with non-regressed testes still showed a short day response in wheel running activity and food intake, but had long-day like nest building activity and had LP body mass (Moffatt and Nelson 1994). Both responding and non-responding prairie voles (*M. ochrogaster*) had a similar reduction in food-intake and wheel-running activity compared to LP voles (Moffatt, Nelson, and Devries 1993). In a genetically selected non-responder line of Siberian hamsters, fewer individuals molted to winter pelage compared to a responder line (Freeman and Goldman 1997b).

Factors such as environmental unpredictability, increased ambient temperatures (Müller et al. 2015) and advanced age (Grocock 1980; Freeman and Goldman 1997b) can increase the proportion of non-responders whereas food restriction (Nelson 1992) and physical activity

(Freeman and Goldman 1997a) can reduce the occurrence of non-responders. The effect of age in relation to gonadal regression in adult voles has been discussed in the introduction. Given the short lifespan of voles and hamsters, one could expect an increase in the occurrence of photoperiodic non-responders with age, at the end of the breeding season (Freeman and Goldman 1997b; Prendergast, Kriegsfeld, and Nelson 2001). Most adults who have reproduced during the breeding season die before winter and photoperiodic non-responsiveness could be a form of opportunism. Siberian hamsters kept in SP for 8 week around weaning age (17-19 days) and then as adults again, did show that older age increases the occurrence of photoperiodic non-responsiveness to SP in maintenance of high gonadal mass as well as summer pelage (Freeman and Goldman 1997b). However, male field voles (*M. agrestis)* initially kept at LD 16:8 and then transferred to SP for 6 months at variable ages did not show any effect of age on testicular regression (Grocock 1980). Although in this study, the photoperiodic response measured in different groups was averaged, without looking individual non-responders. In our dataset, all voles were of similar age but differed in photoperiodic history that simulated the fast maturing spring- or delayed maturing autumn cohort. We had a non-responder in both groups, which indicates that non-responsiveness can occur regardless of photoperiodic history.

The balanced polyphenism theory described by Prendergast, Kriegsfeld and Nelson, (2001) suggests that a range of different reproductive phenotypes is maintained, so that at least a certain proportion of the population can survive under variable environmental conditions. This is in line with the hypothesis that short-lived species are more opportunistic in the timing of breeding as individuals generally experience only one breeding season in their lifetime (Bronson 1988). Indeed, under favourable conditions, rare winter breeding has been observed in the seasonally breeding voles tundra voles, field voles (Tast and Kaikusalo 1976) and in common voles (Baláž 2010a) which could have been due to survival of non-responding adults. Most studies on photoperiodic non-responders have been done in males. The occurrence of non-responsiveness in females may be rarer due to the higher costs of reproduction. Although the gonadal axis in both males and females of *M.oeconomus* responded only mildly to photoperiod and cases of winter breeding in wild vole populations suggest that photoperiodic non-responsiveness also occurs in females.

5.1.4. Within species genetic variation and local adaptation – selection on an *Aldh1a1*-like paralogue.

The term reaction norm to environmental cues has been discussed in the introduction and the degree of photoperiodic non-responsiveness is a good example of individually variable reaction norms within a population. It is reasonable to assume that differences in reaction norms at the phenotypic level come from differences at the genetic level. Artificial selection for photosensitivity in white-footed mice (*Peromyscus leucopus)* versus photo non-responsiveness shows that this trait is heritable (Heideman et al. 1999; Sharp et al. 2015). Aside from species-specific evolutionary histories associated phenotype differences as discussed above, it is also expected that species with a large distribution range adapt to the local (latitude dependent) photoperiod-temperature relations (Hut et al. 2013). Figure 17 indeed shows that the breeding season can vary strongly within species, depending on the geographic location of the population, which led to the question to what extent this has shaped genetic differentiation underlying seasonal timekeeping mechanisms.

These considerations led us to perform a genome-wide screening for signatures of selection between a Northern (70°N) and Southern population (53°N) of tundra voles **(see paper IV**). This was the start of a wider study (see the next section) through which we sought a first impression of genetic differences between the populations. The most striking finding was a clear selection signature on the *Aldh1a1-Aldh1a7* locus. *Aldh1a1* (*Raldh1)* expression in PT tanycytes is under photoperiodic control (Shearer, Stoney, Nanescu, et al. 2012; Helfer, Barrett, and Morgan 2019; Stoney et al. 2016). ALDH1A1 synthesizes retinoic acid (RA); a key transcription regulator in embryonic developmental and neurogenesis in brain areas such as the hippocampus (Ransom et al. 2014). It may play a key role in the mammalian PNES, similar as TSHβ (Helfer et al. 2012). In rodents, long day associated RA signaling increases body mass and food intake through production of chemerin (an inflammatory chemokine) in tanycytes, which is encoded by the *Rarres2* (retinoic acid receptor responder2) gene (Helfer et al. 2016). In peripheral tissues, chemerin increases adiposity (Helfer and Wu 2018).

Closer inspection of the *Aldh1a1-Aldh1a7* locus revealed that this strong selection pressure fell upon an *Aldh1a1*-like paralogue, directly downstream of the *Aldh1a1* gene. Moreover, we found three additional *Aldh1a1*-like paralogues, situated between the *Aldh1a1* and the rodent-specific *Aldh1a7* gene. These paralogues are highly similar to both *Aldh1a1* and even more so to *Aldh1a7* and the predicted translation indicated that these are functional genes. Despite the high sequence homology with ALDH1A1, ALDH1A7 does not synthesize retinoid acid (Hsu et al. 1999). Investigation of amino acids present at critical locations of the substrate entry channel

(Sobreira et al. 2011) indicate that ALDH1A7 and the vole ALDH1A1-like paralogues have a substrate entry channel unsuitable for large molecules such as retinaldehyde. ALDH1A7 and the ALDH1A1-like paralogues may be more similar to the narrow-channeled ALDH2, which oxidizes smaller molecules like acetaldehyde derived from ethanol metabolism (Sobreira et al. 2011; Koppaka et al. 2012). So far, *Aldh1a7* has only been found rodents (Touloupi et al. 2019). Similar *Aldh1a1*-like paralogues were also present in other *Microtus* species but have not been found in any other species except in two marsupial species, the South American opossum (*Monodelphis domestica*) and Australian Tasmanian devil (*Sacrophilus harrisii*) (Holmes 2015, 2009). This suggests independent gene duplications of *Aldh1a1* and possible convergent evolution in response to potentially similar selection pressures. However, the genomes of a number of mammals are available publicly and further exploration of the mammalian *Aldh1a1* locus could shed more light on the evolution of Aldh1a1-like paralogues.

5.2 Ongoing and future research

The profound difference in gonadal versus somatic growth investment between the two vole species raised the question whether this is detectable in altered somatostatin and growth hormone releasing hormone (GHRH) production from hypothalamic neurons. These are under photoperiodic control and both factors regulate seasonal body mass fluctuations in Siberian hamsters (Dumbell et al. 2015). Expression of these factors as well as chemerin (Helfer et al. 2016) under the various photoperiods and the two temperatures as done in **paper II** and **paper III** can possibly provide more insight in the observed species differences in body mass regulation. We still have tissue samples available from these experiments, which can be used for further gene expression analysis.

The ambient temperatures used in the experiments described in **paper II** and **III** were 10°C and 21°C. The lowest possible temperature in our climate chambers was 10°C, which may not have been low enough to induce a photoperiodic response in gonadal growth in tundra voles.
In most parts of the tundra vole's distribution range, mean monthly winter temperatures are lower than 10°C and the species may have evolved a thermal neutral zone below 10°C. Therefore, it would be interesting to measure the thermal neutral zones for both species in response to photoperiod as done by Balin, Haim and Arad (1994). They measured rest metabolic rate (oxygen consumption), core body temperature, non-shivering thermogenesis and overall thermal conductance in Levant voles (*M. guentheri)*. This species lives under hot and dry summer conditions in the Mediterranean region and were expected to experience heat stress in

summer. Voles kept under long photoperiods (16L) had lower rest metabolic rates and thermal conductance but a higher upper critical point in the thermoneutral zone than voles under short days (8L) (Balin, Haim and Arad 1994). Such a study could give more clarification about individual- and general species-specific reaction norms to environmental factors and it would give a clearer answer to whether the northern species has evolved higher cold tolerance than the southern species.

The brain samples taken in the photoperiod-temperature experiments can also be used to explore seasonal expression of *Aldh1a1* (*Raldh1*), its sister gene *Aldh1a2* (*Raldh2*) and the rodent specific gene *Aldh1a7* in the tanycytes. The seasonal histogenesis hypothesis as proposed by Hazlerigg and Lincoln (2011) is yet to be explored further and *Aldh1a1* and A*ldh1a2* may play a role in this. RA induced the cytoskeleton protein vimentin (via chemerin) which indicates hypothalamic remodeling (Helfer and Wu 2018). The short-day decrease in hypothalamic TH and RA signaling is proposed to cause local neurodegeneration, which may initiate a reduction body mass and appetite. This neurodegeneration induces compensatory proliferation in the tanycyte niche and newborn cells can differentiate to various types of neuronal phenotypes which may lay at the basis for seasonal variation in energy balance and reproduction (Helfer, Barrett, and Morgan 2019).

The function and expression pattern of *Aldh1a7* has not been investigated in depth and its relation with photoperiod is unclear. RNA sequencing of various tissues under variable seasonal conditions (e.g. photoperiods and temperatures) can clarify the role of *Aldh1a7* and whether it is associated with seasonal phenotype regulation. Moreover, our sequencing results suggest that the *Aldh1a* paralogues in *Microtus* are additional copies of *Aldh1a7*. The strong signature of selection on one of these paralogues suggests functional relevance for the tundra vole populations investigated. The predicted amino acid structure indicates that these paralogues produce functional proteins but we cannot confirm this without RNA sequencing and further in *vitro* expression studies to assess the function (such as such as *in situ* hybridization or qPCR).

The signatures of selection detected between the two tundra vole populations are a first indication of potential latitudinal selection. However, these population differences can also originate from selection pressures independent of latitude since we have only assessed two populations. Therefore, we need to sequence more vole populations from various latitudes and longitudes to see if we can find the same genes under selection. Our particular interest goes to the outstanding *Aldh1a* paralogue. We have already collected several *Microtus oeconomus* museum samples from different longitudes and latitudes (Fig. 43). Other voles from the *Microtus*

genus also possess these paralogues and it would be interesting to see if these are also under latitudinal selection. As indicated on the map, we already have samples from various *Microtus* species available. Phylogenetic analysis of a more complete dataset could provide better insight in *Microtus* evolutionary history in relation to latitudinal adaptation and the potential role of *Aldh1a1*-like genes. Ideally, these genomic studies could be supported with phenotypic data from the investigated populations.

We have only studied seasonal gene expression under laboratory conditions and so far there is one study in which this has been assessed in wild mammals (Wang et al. 2019). In order to bring the laboratory results together with our sequencing data, we could study seasonal gene expression and other seasonal phenotype parameters (e.g. body mass, gonadal mass, sex steroid levels) in wild populations from various locations with different photoperiod-temperature relations.

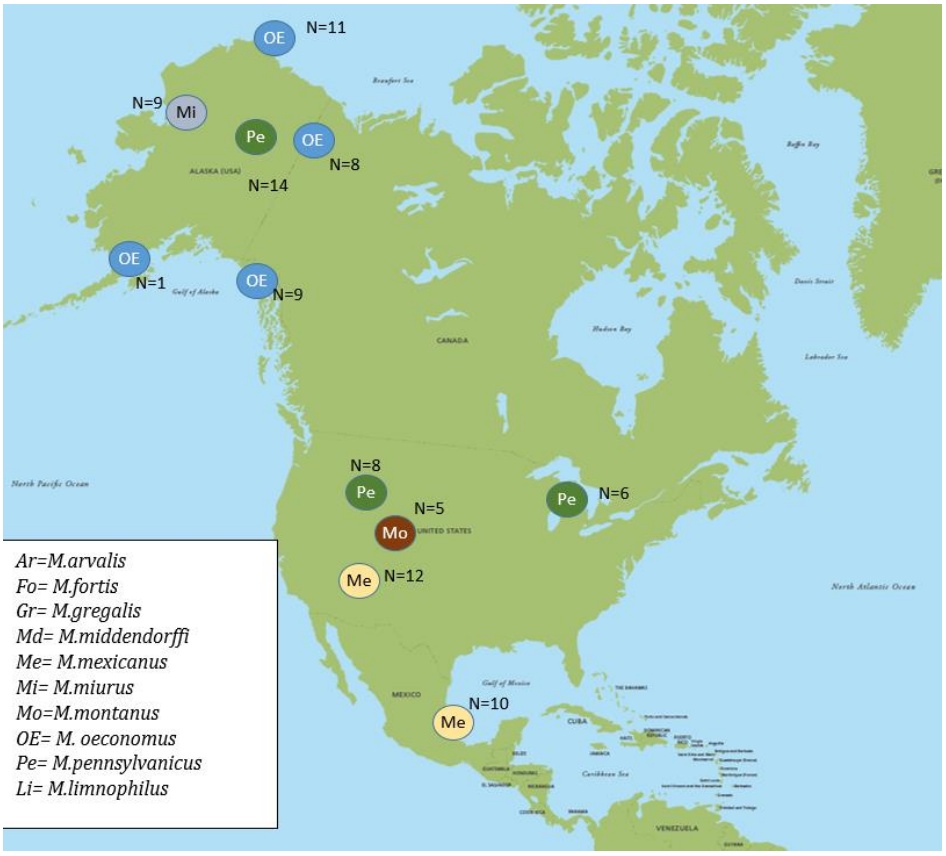

Figure 43. Locations of other vole DNA samples collected. N represents the number of individuals and the letters the species.

5.3 Conclusion

We have seen that photoperiodic history and ambient temperature modulate the mammalian photoneuroendocrine system at the level of the hypothalamic tanycytes and potentially even in the *pars tuberalis* as well as downstream in a species-specific manner (Fig. 44). This may be caused by genetic differences between the common vole and tundra vole as a consequence of their evolutionary history at higher versus lower latitudes. **Paper I** showed that long photoperiods stimulate somatic growth in tundra voles native to higher latitudes while common voles native to lower latitudes, favour gonadal growth. In **paper II and II** we demonstrated that these differential responses are modulated by photoperiodic history and ambient temperature at the level of *Dio2/Dio3* expression and in tundra voles even in PT TSHβ expression. Here we also demonstrated that the PNES is hierarchically structured and that selection can affect different components independently.

In **paper IV** we provided evidence for *within* species selection pressures between a southern and northern population of tundra voles. The most striking finding was selection on an *Aldh1a1*-like paralogue directly downstream of the photoperiodically expressed *Aldh1a1* gene. The three *Aldh1a1*-like paralogues are predicted to be functional and are also present in other voles (*Microtus)* but have so far not been detected in other rodents.

Plasticity in the photoperiodic response in two vole species.

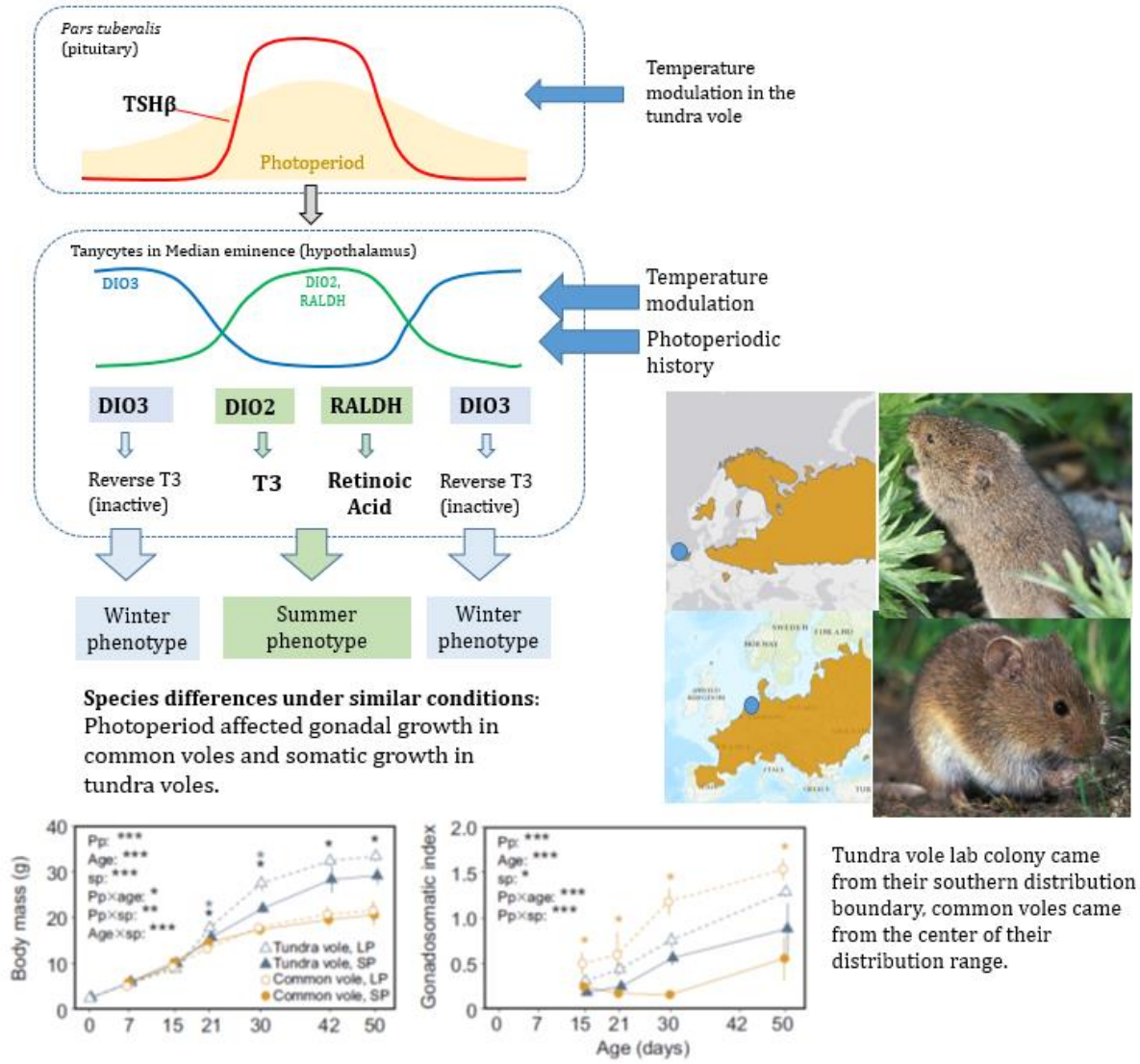

Genetic variation between a population of northern and southern tundra voles.

Figure 44. Visual summary of the findings and conclusions.

6. References

Aars, Jon, and Rolf A. Ims. 2002. "Intrinsic and Climatic Determinants of Population Demography: The Winter Dynamics of Tundra Voles." *Ecology* 83 (12): 3449. https://doi.org/10.2307/3072093.

Altschul, S., W. Gish, W. Miller, E.W. Meyers, and D.J. Lipman. 1990. "Basic Local Alignment Search Tool." *Journal of Molecular Biology* 215: 403–10. https://doi.org/10.1006/jmbi.1990.9999.

Amaral, Andreia J., Luca Ferretti, Hendrik Jan Megens, Richard P.M.A. Crooijmans, Haisheng Nie, Sebastian E. Ramos-Onsins, Miguel Perez-Enciso, Lawrence B. Schook, and Martien A.M. Groenen. 2011. "Genome-Wide Footprints of Pig Domestication and Selection Revealed through Massive Parallel Sequencing of Pooled DNA." *PLoS ONE* 6 (4). https://doi.org/10.1371/journal.pone.0014782.

Appenroth, Daniel, Vebjørn J. Melum, Alexander C. West, Hugues Dardente, David G. Hazlerigg, and Gabriela C. Wagner. 2020. "Photoperiodic Induction without Light-Mediated Circadian Entrainment in a High Arctic Resident Bird." *Journal of Experimental Biology*. https://doi.org/10.1242/jeb.220699.

Atanur, Santosh S., Ana Garcia Diaz, Klio Maratou, Allison Sarkis, Maxime Rotival, Laurence Game, Michael R. Tschannen, et al. 2013. "XGenome Sequencing Reveals Loci under Artificial Selection That Underlie Disease Phenotypes in the Laboratory Rat." *Cell* 154 (3): 691–703. https://doi.org/10.1016/j.cell.2013.06.040.

Baker, John R., and R. M. Ranson. 1932. "Factors Affecting the Breeding of the Field Mouse (Microtus Agrestis). Part I. --Light." *Proceedings of the Royal Society of London. Series B, Containing Papers of a Biological Character* 110 (767): 313–22.

Baláž, Ivan. 2010a. "Somatic Characteristics and Reproduction of Common Vole, Microtus Arvalis (Mammalia: Rodentia) Populations in Slovakia." *Biologia* 65 (6): 1064–71. https://doi.org/10.2478/s11756-010-0122-7.

———. 2010b. "The Influence of the Altitude on Somatic Characteristics Size of Common Vole (Microtus Arvalis) in Slovakia." *Ekologia Bratislava* 29 (2): 174–81. https://doi.org/10.4149/ekol_2010_02_174.

Balčiauskas, Linas, Laima Balčiauskiene, and Agne Janonyte. 2012. "Reproduction of the Root Vole (Microtus Oeconomus) at the Edge of Its Distribution Range." *Turkish Journal of Zoology* 36 (5): 668–75. https://doi.org/10.3906/zoo-1111-20.

Balin, Daniel, Abraham Haim, and Zeev Arad. 1994. "Metabolism and Thermoregulation in the Levant Vole Microtus Guentheri: The Role of Photoperiodicity." *Journal of Thermal Biology* 19 (1): 55–62.

Barrett, Catherine E., Alaine C. Keebaugh, H Todd, Ahern, Caroline E. Bass, Ernest F. Terwilliger, and Larry J. Young. 2013. "Variation in Vasoperessin Receptor (Avpr1a) Expression Creates Diversity in Behaviors Related to Monogamy in Prairie Voles." *Hormones and Behavior* 63 (3): 518–26. https://doi.org/10.1016/j.yhbeh.2013.01.005.Variation.

Barrett, Perry, Elena Ivanova, E. Scott Graham, Alexander W. Ross, Dana Wilson, Helene Plé, Julian G. Mercer, et al. 2006. "Photoperiodic Regulation of Cellular Retinoic Acid-Binding Protein 1, GPR50 and Nestin in Tanycytes of the Third Ventricle Ependymal Layer of the Siberian Hamster." *Journal of Endocrinology* 191 (3): 687–98. https://doi.org/10.1677/joe.1.06929.

Bartness, Timothy J., J. Bradley Powers, Michael H. Hastings, Eric L. Bittman, and Bruce D. Goldman. 1993. "The Timed Infusion Paradigm for Melatonin Delivery: What Has It Taught Us about the Melatonin Signal, Its Reception, and the Photoperiodic Control of Seasonal Responses?" *Journal of Pineal Research* 15 (4): 161–90. https://doi.org/10.1111/j.1600-079X.1993.tb00903.x.

Berger, P. J., N. C. Negus, and C. N. Rowsemitt. 1987. "Effect of 6-Methoxybenzoxazolinone on Sex Ratio and Breeding Performance in Microtus Montanus." *Biology of Reproduction* 36 (2): 255–60. https://doi.org/10.1095/biolreprod36.2.255.

Berson, David M., Felice A. Dunn, and Motoharu Takao. 2002. "Phototransduction by Retinal Ganglion Cells That Set the Circadian Clock." *Science*. https://doi.org/10.1126/science.1067262.

Bertolini, Francesca, Bertrand Servin, Andrea Talenti, Estelle Rochat, Eui Soo Kim, Claire Oget, Isabelle Palhière, et al. 2018. "Signatures of Selection and Environmental Adaptation across the Goat Genome Post-Domestication 06 Biological Sciences 0604 Genetics." *Genetics Selection Evolution* 50 (1): 1–24. https://doi.org/10.1186/s12711-018-0421-y.

Bian, Jiang Hui, Shou Yang Du, Yan Wu, Yi Fan Cao, Xu Heng Nie, Hui He, and Zhi Bing You. 2015. "Maternal Effects and Population Regulation: Maternal Density-Induced Reproduction Suppression Impairs Offspring Capacity in Response to Immediate Environment in Root Voles Microtus Oeconomus." *Journal of Animal Ecology* 84 (2): 326–36. https://doi.org/10.1111/1365-2656.12307.

Bielsky, Isadora F., and Larry J. Young. 2004. "Oxytocin, Vasopressin, and Social Recognition in Mammals."

Peptides 25 (9): 1565–74. https://doi.org/10.1016/j.peptides.2004.05.019.
Bissonette, Thomas Hume. 1932. "Modification of Mammalian Sexual Cycles ; Reactions of Ferrets (Putorius Vulgaris) of Both Sexes to Electric Light Added after Dark in November and December." *Royal Society* 110 (767): 322–36.
Blank, J. L., and D. A. Freeman. 1991. "Differential Reproductive Response to Short Photoperiod in Deer Mice: Role of Melatonin." *Journal of Comparative Physiology A* 169 (4): 501–6. https://doi.org/10.1007/BF00197662.
Bolborea, Matei, and Nicholas Dale. 2013. "Hypothalamic Tanycytes: Potential Roles in the Control of Feeding and Energy Balance." *Trends in Neurosciences* 36 (2): 91–100. https://doi.org/10.1016/j.tins.2012.12.008.
Bossdorf, Oliver, Christina L. Richards, and Massimo Pigliucci. 2008. "Epigenetics for Ecologists." *Ecology Letters* 11 (2): 106–15. https://doi.org/10.1111/j.1461-0248.2007.01130.x.
Both, Christiaan, and Marcel E. Visser. 2001. "Adjustment to Climate Change Is Constrained by Arrival Date in a Long-Distance Migrant Bird." *Nature* 411 (6835): 296–98. https://doi.org/10.1038/35077063.
Boyce, Christine C., and Jesse L. Boyce. 1988. "Population Biology of Microtus Arvalis . III . Regulation of Numbers and Breeding Dispersion of Females." *Journal of Animal Ecology* 57 (3): 737–54.
Bradshaw, William E., and Christina M. Holzapfel. 2007. "Evolution of Animal Photoperiodism." *Annual Review of Ecology, Evolution, and Systematics* 38: 1–25. https://doi.org/10.1146/annurev.ecolsys.37.091305.110115.
Breed, W. G. 1967. "Ovulation in the Genus Microtus." *Nature* 214: 826. https://doi.org/10.1038/214826a0.
Bronson, Franklin H. 1985. "Mammalian Reproduction: An Ecological Perspective." *Biology of Reproduction* 32 (1): 1–26. https://doi.org/10.1095/biolreprod32.1.1.
———. 1988. "Mammalian Reproductive Strategies: Genes, Photoperiod and Latitude." *Reproduction Nutrition Developpement* 28 (2 B): 335–47. https://doi.org/10.1051/rnd:19880301.
———. 2009. "Climate Change and Seasonal Reproduction in Mammals." *Philosophical Transactions of the Royal Society B: Biological Sciences* 364 (1534): 3331–40. https://doi.org/10.1098/rstb.2009.0140.
Bronson, Franklin H., and Glenn Perrigo. 1987. "Seasonal Regulation of Reproduction in Muroid Rodents." *Integrative and Comparative Biology* 27 (3): 929–40. https://doi.org/10.1093/icb/27.3.929.
Brown, Terence A. 2002. *Genomes*. Oxford:Wiley-Liss.
Brunhoff, Cecilia, K. E. Galbreath, V. B. Fedorov, J. A. Cook, and M. Jaarola. 2003. "Holarctic Phylogeography of the Root Vole (Microtus Oeconomus): Implications for Late Quaternary Biogeography of High Latitudes." *Molecular Ecology* 12 (4): 957–68. https://doi.org/10.1046/j.1365-294X.2003.01796.x.
Camacho, Christiam, George Coulouris, Vahram Avagyan, Ning Ma, Jason Papadopoulos, Kevin Bealer, and Thomas L. Madden. 2009. "BLAST+: Architecture and Applications." *BMC Bioinformatics*. https://doi.org/10.1186/1471-2105-10-421.
Casillas, Sònia, and Antonio Barbadilla. 2017. "Molecular Population Genetics." *Genetics* 205 (3): 1003–35. https://doi.org/10.1534/genetics.116.196493.
Chaline, Jean, Patrick Brunet-Lecomte, Sophie Montuire, Laurent Viriot, and Frédéric Courant. 1999. "Anatomy of the Arvicoline Radiation (Rodentia): Palaeogeographical, Palaeoecological History and Evolutionary Data." *Annales Zoologici Fennici* 36 (4): 239–67.
Choi, Jung Woo, Bong Hwan Choi, Seung Hwan Lee, Seung Soo Lee, Hyeong Cheol Kim, Dayeong Yu, Won Hyong Chung, et al. 2015. "Whole-Genome Resequencing Analysis of Hanwoo and Yanbian Cattle to Identify Genome-Wide SNPs and Signatures of Selection." *Molecules and Cells* 38 (5): 466–73. https://doi.org/10.14348/molcells.2015.0019.
Cruciani, Fulvio, Beniamino Trombetta, Damian Labuda, David Modiano, Antonio Torroni, Rodolfo Costa, and Rosaria Scozzari. 2008. "Genetic Diversity Patterns at the Human Clock Gene Period 2 Are Suggestive of Population-Specific Positive Selection." *European Journal of Human Genetics* 16 (12): 1526–34. https://doi.org/10.1038/ejhg.2008.105.
Dalum, Jayme van, Vebjørn J. Melum, Shona H. Wood, and David G. Hazlerigg. 2020. "Maternal Photoperiodic Programming: Melatonin and Seasonal Synchronization Before Birth." *Frontiers in Endocrinology* 10 (January): 1–7. https://doi.org/10.3389/fendo.2019.00901.
Dalum, Mattis Jayme Van. 2013. "Postnatal Behaviour in Eurasian Lynx Females in Norway: Space Use and Activity." Utrecht University. https://scandlynx.nina.no/Portals/Scandlynx/Dokumenter/Postnatal behaviour of Eurasian lynx females in Norway_MJvanDalum_FINAL.pdf?ver=eGTYWW6HBSV8F_e1ZJ_iVA%3D%3D.
Dardente, H., P. Klosen, P. Pévet, and M. Masson-Pévet. 2003. "MT1 Melatonin Receptor MRNA Expressing Cells in the Pars Tuberalis of the European Hamster: Effect of Photoperiod." *Journal of Neuroendocrinology* 15 (8): 778–86. https://doi.org/10.1046/j.1365-2826.2003.01060.x.

Dardente, Hugues. 2007. “Does a Melatonin-Dependent Circadian Oscillator in the Pars Tuberalis Drive Prolactin Seasonal Rhythmicity?” *Journal of Neuroendocrinology* 19 (8): 657–66. https://doi.org/10.1111/j.1365-2826.2007.01564.x.

Dardente, Hugues, David G. Hazlerigg, and Francis J.P. Ebling. 2014. “Thyroid Hormone and Seasonal Rhythmicity.” *Frontiers in Endocrinology* 5 (FEB): 1–11. https://doi.org/10.3389/fendo.2014.00019.

Dardente, Hugues, Cathy A. Wyse, Mike J. Birnie, Sandrine M. Dupré, Andrew S.I. Loudon, Gerald A. Lincoln, and David G. Hazlerigg. 2010. “A Molecular Switch for Photoperiod Responsiveness in Mammals.” *Current Biology* 20 (24): 2193–98. https://doi.org/10.1016/j.cub.2010.10.048.

Dark, J., P. G. Johnston, M. Healy, and I. Zucker. 1983. “Latitude of Origin Influences Photoperiodic Control of Reproduction of Deer Mice (Peromyscus Maniculatus).” *Biology of Reproduction* 28 (1): 213–20. https://doi.org/10.1095/biolreprod28.1.213.

Dark, John, and Irving Zucker. 1983. “Short Photoperiods Reduce Winter Energy Requirements of the Meadow Vole, Microtus Pennsylvanicus.” *Physiology and Behavior* 31 (5): 699–702. https://doi.org/10.1016/S0031-9384(83)80006-7.

Davis, Andrew K., and Donna L. Maney. 2018. “The Use of Glucocorticoid Hormones or Leucocyte Profiles to Measure Stress in Vertebrates: What’s the Difference?” *Methods in Ecology and Evolution* 9 (6): 1556–68. https://doi.org/10.1111/2041-210X.13020.

DeCoursey, Patricia J. 2004. “The Behavioral Ecology and Evolution of Biological Timing Systems.” In *Chronobiology: Biological Timekeeping*, edited by Jay C. Dunlap, Jennifer J. Loros, and Patricia J. DeCoursey, 27–65. Sunderland, Mass: Sinauer Associates.

Dumbell, R. A., F. Scherbarth, V. Diedrich, H. A. Schmid, S. Steinlechner, and P. Barrett. 2015. “Somatostatin Agonist Pasireotide Promotes a Physiological State Resembling Short-Day Acclimation in the Photoperiodic Male Siberian Hamster (Phodopus Sungorus).” *Journal of Neuroendocrinology* 27 (7): 588–99. https://doi.org/10.1111/jne.12289.

Dupré, S. M., H. Dardente, M. J. Birnie, A. S.I. Loudon, G. A. Lincoln, and D. G. Hazlerigg. 2011. “Evidence for Rgs4 Modulation of Melatonin and Thyrotrophin Signalling Pathways in the Pars Tuberalis.” *Journal of Neuroendocrinology* 23 (8): 725–32. https://doi.org/10.1111/j.1365-2826.2011.02168.x.

Dupré, Sandrine M., Katarzyna Miedzinska, Chloe V. Duval, Le Yu, Robert L. Goodman, Gerald A. Lincoln, Julian R.E. Davis, Alan S. McNeilly, David D. Burt, and Andrew S.I. Loudon. 2010. “Identification of Eya3 and TAC1 as Long-Day Signals in the Sheep Pituitary.” *Current Biology* 20 (9): 829–35. https://doi.org/10.1016/j.cub.2010.02.066.

Ebling, Francis J.P. 2014. “On the Value of Seasonal Mammals for Identifying Mechanisms Underlying the Control of Food Intake and Body Weight.” *Hormones and Behavior* 66 (1): 56–65. https://doi.org/10.1016/j.yhbeh.2014.03.009.

Ebling, Francis J.P., and P. Barrett. 2008. “The Regulation of Seasonal Changes in Food Intake and Body Weight.” *Journal of Neuroendocrinology* 20 (6): 827–33. https://doi.org/10.1111/j.1365-2826.2008.01721.x.

Eccard, Jana A., and Antje Herde. 2013. “Seasonal Variation in the Behaviour of a Short-Lived Rodent.” *BMC Ecology* 13. https://doi.org/10.1186/1472-6785-13-43.

Ergon, T., Xavier Lambin, and Nils Christian Stenseth. 2001. “Life-History Traits of Voles in a Fluctuating Population Respond Directly to Environmental Change.” *Nature* 411 (1996): 1043–45.

Ergon, T., J. L. MacKinnon, N. Chr Stenseth, R. Boonstra, and X. Lambin. 2001. “Mechanisms for Delayed Density-Dependent Reproductive Traits in Field Roles, Microtus Agrestis: The Importance of Inherited Environmental Effects.” *Oikos* 95 (2): 185–97. https://doi.org/10.1034/j.1600-0706.2001.950201.x.

Ergon, Torbjörn. 2007. “Optimal Onset of Seasonal Reproduction in Stochastic Environments: When Should Overwintering Small Rodents Start Breeding?” *Ecoscience* 14 (3): 330–46. https://doi.org/10.2980/1195-6860(2007)14[330:OOOSRI]2.0.CO;2.

Evernden, L. N., and W. A. Fuller. 1972. “Light Alteration Caused by Snow and Its Importance to Subnivean Rodents.” *Canadian Journal of Zoology* 50 (7): 1023–32. https://doi.org/10.1139/z72-137.

Foster, R. G., I. Provencio, D. Hudson, S. Fiske, W. De Grip, and M. Menaker. 1991. “Circadian Photoreception in the Retinally Degenerate Mouse (Rd/Rd).” *Journal of Comparative Physiology A* 169 (1): 39–50. https://doi.org/10.1007/BF00198171.

Freeman, David A., and Bruce D. Goldman. 1997a. “Evidence That the Circadian System Mediates Photoperiodic Nonresponsiveness in Siberian Hamsters: The Effect of Running Wheel Access on Photoperiodic Responsiveness.” *Journal of Biological Rhythms* 12 (2): 100–109. https://doi.org/10.1177/074873049701200202.

———. 1997b. “Photoperiod Nonresponsive Siberian Hamsters: Effect of Age on the Probability of Nonresponsiveness.” *Journal of Biological Rhythms* 12 (2): 110–21.

https://doi.org/10.1177/074873049701200203.
Freeman, Scott, and Jon C. Herron. 2004. *Evolutionary Analysis*. Third edit. Pearson Eductaion, Inc.
Gall, Charlotte Von, Martine L. Garabette, Christian A. Kell, Sascha Frenzel, Faramarz Dehghani, Petra Maria Schumm-Draeger, David R. Weaver, Horst Werner Korf, Michael H. Hastings, and Jörg H. Stehle. 2002. "Rhythmic Gene Expression in Pituitary Depends on Heterologous Sensitization by the Neurohormone Melatonin." *Nature Neuroscience*. https://doi.org/10.1038/nn806.
Garner, W.W., and H.A. Allard. 1920. "Effect of the Relative Length of Day and Night and Other Factors of the Environment on Growth and Reproduction in Plants." *Journal of Agricultural Research* 18: 553–606.
Gerkema, Menno P., and Simon Verhulst. 1990. "Warning against an Unseen Predator: A Functional Aspect of Synchronous Feeding in the Common Vole, Microtus Arvalis." *Animal Behaviour* 40 (6): 1169–78. https://doi.org/10.1016/S0003-3472(05)80183-6.
Getz, Lowell L., and Joyce E. Hofmann. 1986. "Social Organization in Free-Living Prairie Voles, Microtus Ochrogaster." *Behavioral Ecology and Sociobiology* 18 (4): 275–82. https://doi.org/10.1007/BF00300004.
Ghyselinck, Norbert B., and Gregg Duester. 2019. "Retinoic Acid Signaling Pathways." *Development (Cambridge)* 146 (13): 1–7. https://doi.org/10.1242/dev.167502.
Giani, Alice Maria, Guido Roberto Gallo, Luca Gianfranceschi, and Giulio Formenti. 2020. "Long Walk to Genomics: History and Current Approaches to Genome Sequencing and Assembly." *Computational and Structural Biotechnology Journal* 18: 9–19. https://doi.org/10.1016/j.csbj.2019.11.002.
Gliwicz, Joanna. 1996. "Life History of Voles: Growth and Maturation in Seasonal Cohorts of the Root Vole." *Miscellania Zoologica* 19 (1): 1–12.
———. 1997. "Space Use in the Root Vole: Basic Patterns and Variability." *Ecography* 20 (4): 383–89. https://doi.org/10.1111/j.1600-0587.1997.tb00383.x.
———. 2007. "Increased Reproductive Effort as a Life History Response of Microtus to Predation." *Ecoscience* 14 (3): 314–17. https://doi.org/10.2980/1195-6860(2007)14[314:IREAAL]2.0.CO;2.
Goldman, B., V. Hall, C. Hollister, P. Roychoudhury, L. Tamarkin, and W. Westrom. 1979. "Effects of Melatonin on the Reproductive System in Intact and Pinealectomized Male Hamsters Maintained under Various Photoperiods." *Endocrinology*. https://doi.org/10.1210/endo-104-1-82.
Goldman, Bruce D. 1999. "The Circadian Timing System and Reproduction in Mammals." *Steroids* 64 (9): 679–85. https://doi.org/10.1016/S0039-128X(99)00052-5.
———. 2003. "Pattern of Melatonin Secretion Mediates Transfer of Photoperiod Information from Mother to Fetus in Mammals." *Science's STKE : Signal Transduction Knowledge Environment* 2003 (192): 1–4. https://doi.org/10.1126/scisignal.1922003pe29.
Goldman, Bruce D., Eberhard Gwinner, Fred J. Karsch, David Saunders, Irving Zucker, and Gregory F. Ball. 2004. "Circannual Rhythms and Photoperiodism." In *Chronobiology: Biological Timekeeping*, edited by Jay C. Dunlap, Jennifer J. Loros, and Patricia J. DeCoursey, 107–42. Sunderland, Mass: Sinauer Associates.
Grocock, C. A. 1980. "Effects of Age on Photo-Induced Testicular Regression, Recrudescence, and Refractoriness in the Short-Tailed Field Vole Microtus Agrestis." *Biology of Reproduction* 23 (1): 15–20. https://doi.org/10.1095/biolreprod23.1.15.
Gromov, V. S. 2013. "Care of Young and the Effect of the Presence of a Male on Parental Behavior in the Common Vole (Microtus Arvalis) in Captivity." *Contemporary Problems of Ecology* 6 (3): 330–35. https://doi.org/10.1134/S1995425513030086.
Guo, Jiazhong, Haixi Tao, Pengfei Li, Li Li, Tao Zhong, Linjie Wang, Jinying Ma, Xiaoying Chen, Tianzeng Song, and Hongping Zhang. 2018. "Whole-Genome Sequencing Reveals Selection Signatures Associated with Important Traits in Six Goat Breeds." *Scientific Reports* 8 (1): 1–11. https://doi.org/10.1038/s41598-018-28719-w.
Haapakoski, Marko, Janne Sundell, and Hannu Ylönen. 2012. "Predation Risk and Food: Opposite Effects on Overwintering Survival and Onset of Breeding in a Boreal Rodent." *Journal of Animal Ecology* 81 (6): 1183–92. https://doi.org/10.1111/j.1365-2656.2012.02005.x.
Hahn, Thomas P., Heather E. Watts, Jamie M. Cornelius, Kathleen R. Brazeal, and Scott A. MacDougall-Shackleton. 2009. "Evolution of Environmental Cue Response Mechanisms: Adaptive Variation in Photorefractoriness." *General and Comparative Endocrinology* 163 (1–2): 193–200. https://doi.org/10.1016/j.ygcen.2009.04.012.
Halle, Stefan. 1995. "Diel Pattern of Locomotor Activity in Populations of Root Voles, Microtus Oeconomus" 10 (3): 211–24.
Hand, Laura. 2012. "The Biology of GPR50, the Melatonin-Related Receptor." The University of Manchester. https://www.research.manchester.ac.uk/portal/en/theses/the-biology-of-gpr50-the-

melatoninrelated-receptor(167ef6b9-269e-4015-999a-13ca7813329e).html.
Hanon, E. A., K. Routledge, H. Dardente, M. Masson-Pévet, P. J. Morgan, and D. G. Hazlerigg. 2010. "Effect of Photoperiod on the Thyroid-Stimulating Hormone Neuroendocrine System in the European Hamster (Cricetus Cricetus)." *Journal of Neuroendocrinology* 22 (1): 51–55. https://doi.org/10.1111/j.1365-2826.2009.01937.x.
Hanon, Elodie A., Gerald A. Lincoln, Jean Michel Fustin, Hugues Dardente, Mireille Masson-Pévet, Peter J. Morgan, and David G. Hazlerigg. 2008. "Ancestral TSH Mechanism Signals Summer in a Photoperiodic Mammal." *Current Biology* 18 (15): 1147–52. https://doi.org/10.1016/j.cub.2008.06.076.
Haring, Elisabeth, Irina N. Sheremetyeva, and Alexey P. Kryukov. 2011. "Phylogeny of Palearctic Vole Species (Genus Microtus, Rodentia) Based on Mitochondrial Sequences." *Mammalian Biology* 76 (3): 258–67. https://doi.org/10.1016/j.mambio.2010.04.006.
Hartl, Daniel L., and Andrew G. Clark. 2007. *Principles of Population Genetics*. Fourth Edi. Sunderland, Mass. : Sinauer Associates.
Hartmann, Dennis L. 2016. "The Energy Balance of the Surface." In *Global Physical Climatology*, edited by Dennis L. Hartmann, Second Edi, 95–130. Elsevier. https://doi.org/https://doi.org/10.1016/C2009-0-00030-0.
Hastings, M. H., J. Herbert, N. D. Martensz, and A. C. Roberts. 1985. "Annual Reproductive Rhythms in Mammals: Mechanisms of Light Synchronization." *Annals of the New York Academy of Sciences* 453 (1): 182–204. https://doi.org/10.1111/j.1749-6632.1985.tb11810.x.
Hattar, S., H. W. Liao, M. Takao, D. M. Berson, and K. W. Yau. 2002. "Melanopsin-Containing Retinal Ganglion Cells: Architecture, Projections, and Intrinsic Photosensitivity." *Science*. https://doi.org/10.1126/science.1069609.
Hattar, S., R. J. Lucas, N. Mrosovsky, S. Thompson, R. H. Douglas, M. W. Hankins, J. Lem, et al. 2003. "Melanopsin and Rod—Cone Photoreceptive Systems Account for All Major Accessory Visual Functions in Mice." *Nature*. https://doi.org/10.1038/nature01761.
Haynes, Susan, Maarit Jaarola, and Jeremy B. Searle. 2003. "Phylogeography of the Common Vole (Microtus Arvalis) with Particular Emphasis on the Colonization of the Orkney Archipelago." *Molecular Ecology* 12 (4): 951–56. https://doi.org/10.1046/j.1365-294X.2003.01795.x.
Hazlerigg, David G., and Gerald A. Lincoln. 2011. "Hypothesis: Cyclical Histogenesis Is the Basis of Circannual Timing." *Journal of Biological Rhythms* 26 (6): 471–85. https://doi.org/10.1177/0748730411420812.
Hazlerigg, David G., and Gabriela C. Wagner. 2006. "Seasonal Photoperiodism in Vertebrates: From Coincidence to Amplitude." *Trends in Endocrinology and Metabolism* 17 (3): 83–91. https://doi.org/10.1016/j.tem.2006.02.004.
Hazlerigg, David, Didier Lomet, Gerald Lincoln, and Hugues Dardente. 2018. "Neuroendocrine Correlates of the Critical Day Length Response in the Soay Sheep." *Journal of Neuroendocrinology* 30 (9): 1–7. https://doi.org/10.1111/jne.12631.
Hazlerigg, David, and Valerie Simonneaux. 2015. *Seasonal Regulation of Reproduction in Mammals*. *Knobil and Neill's Physiology of Reproduction*. Fourth. Elsevier. https://doi.org/10.1016/C2011-1-07288-0.
Heckel, Gerald, Reto Burri, Sabine Fink, Jean-François Desmet, and Laurent Excoffier. 2005. "Genetic Structure and Colonization Processes in European Populations of the Common Vole, Microtus Arvalis." *Evolution* 59 (10): 2231. https://doi.org/10.1554/05-255.1.
Heideman, Paul D., Todd A. Bruno, Jeff W. Singley, and Jeremy V. Smedley. 1999. "Genetic Variation in Photoperiodism in Peromyscus Leucopus: Geographic Variation in AN Alternative Life-History Strategy." *Journal of Mammalogy* 80 (4): 1232–42. https://doi.org/10.2307/1383173.
Helfer, Gisela, Perry Barrett, and Peter J. Morgan. 2019. "A Unifying Hypothesis for Control of Body Weight and Reproduction in Seasonally Breeding Mammals." *Journal of Neuroendocrinology* 31 (3): 1–12. https://doi.org/10.1111/jne.12680.
Helfer, Gisela, Alexander W. Ross, Laura Russell, Lynn M. Thomson, Kirsty D. Shearer, Timothy H. Goodman, Peter J. McCaffery, and Peter J. Morgan. 2012. "Photoperiod Regulates Vitamin A and Wnt/β-Catenin Signaling in F344 Rats." *Endocrinology* 153 (2): 815–24. https://doi.org/10.1210/en.2011-1792.
Helfer, Gisela, Alexander W. Ross, Lynn M. Thomson, Claus D. Mayer, Patrick N. Stoney, Peter J. McCaffery, and Peter J. Morgan. 2016. "A Neuroendocrine Role for Chemerin in Hypothalamic Remodelling and Photoperiodic Control of Energy Balance." *Scientific Reports* 6 (February): 1–12. https://doi.org/10.1038/srep26830.
Helfer, Gisela, and Qing Feng Wu. 2018. "Chemerin: A Multifaceted Adipokine Involved in Metabolic Disorders." *Journal of Endocrinology* 238 (2): R79–94. https://doi.org/10.1530/JOE-18-0174.

Helm, Barbara, Rachel Ben-Shlomo, Michael J. Sheriff, Roelof A. Hut, Russell Foster, Brian M. Barnes, and Davide Dominoni. 2013. "Annual Rhythms That Underlie Phenology: Biological Time-Keeping Meets Environmental Change." *Proceedings of the Royal Society B: Biological Sciences* 280 (1765). https://doi.org/10.1098/rspb.2013.0016.
Hilton, Barry L. 1992. "Reproduction in the Mexican Vole, Microtus Mexicanus." *Journal of Mammalogy* 73 (3): 586–90.
Hoffmann, Klaus. 1982. "The Critical Photoperiod in the Djungarian Hamster." In *Vertebrate Circadian Systems*, edited by Jürgen Aschoff, Serge Daan, and Gerard A. Groos, 297–304. Springer-Verlag Berlin Heidelberg.
Holmes, Roger S. 2009. "Opossum Aldehyde Dehydrogenases: Evidence for Four ALDH1A1-like Genes on Chromosome 6 and ALDH1A2 and ALDH1A3 Genes on Chromosome 1." *Biochemical Genetics* 47 (9–10): 609–24. https://doi.org/10.1007/s10528-009-9245-3.
———. 2015. "Comparative and Evolutionary Studies of Vertebrate ALDH1A-like Genes and Proteins." *Chemico-Biological Interactions* 234: 4–11. https://doi.org/10.1016/j.cbi.2014.11.002.
Holsinger, Kent E., and Bruce S. Weir. 2009. "Genetics in Geographically Structured Populations: Defining, Estimating and Interpreting FST." *Nature Reviews Genetics* 10 (9): 639–50. https://doi.org/10.1038/nrg2611.
Hong, James W., and Austin P. Platt. 1975. "Critical Photoperiod and Daylength Threshold Differences between Northern and Southern Populations of the Butterfly Limenitis Archippus." *Journal of Insect Physiology* 21 (5): 1159–65. https://doi.org/10.1016/0022-1910(75)90129-8.
Horne, B. Van. 1982. "Demography of the Longtail Vole Microtus Longicaudus in Seral Stages of Coastal Coniferous Forest, Southeast Alaska." *Canadian Journal of Zoology* 60 (7): 1690–1709. https://doi.org/10.1139/z82-222.
Horton, T. H. 1984a. "Growth and Maturation in Microtus Montanus: Effects of Photoperiods before and after Weaning." *Canadian Journal of Zoology* 62 (9): 1741–46. https://doi.org/10.1139/z84-256.
———. 1984b. "Growth and Reproductive Development of Male Microtus Montanus Is Affected by the Prenatal Photoperiod." *Biology of Reproduction* 31 (3): 499–504. https://doi.org/10.1095/biolreprod31.3.499.
———. 1985. "Cross-Fostering of Voles Demonstrates in Utero Effect of Photoperiod." *Biology of Reproduction*. https://doi.org/10.1095/biolreprod33.4.934.
Horton, T. H., S. L. Ray, and M. H. Stetson. 1989. "Maternal Transfer of Photoperiodic Information in Siberian Hamsters. III. Melatonin Injections Program Postnatal Reproductive Development Expressed in Constant Light." *Biology of Reproduction* 41 (1): 34–39. https://doi.org/10.1095/biolreprod41.1.34.
Horton, Teresa H., and Milton H. Stetson. 1990. "Maternal Programming of the Fetal Brain Dictates the Response of Juvenile Siberian Hamsters to Photoperiod: Dissecting the Information Transfer System." *Journal of Experimental Zoology* 256 (4 S): 200–202. https://doi.org/10.1002/jez.1402560443.
———. 1992. "Maternal Transfer of Photoperiodic Information in Rodents." *Animal Reproduction Science* 30 (1–3): 29–44. https://doi.org/10.1016/0378-4320(92)90004-W.
Howe, Kevin L., Premanand Achuthan, James Allen, Jamie Allen, Jorge Alvarez-Jarreta, M. Ridwan Amode, Irina M. Armean, et al. 2021. "Ensembl 2021." *Nucleic Acids Research* 49 (D1): D884–91. https://doi.org/10.1093/nar/gkaa942.
Hsu, Lily C., Wen Chung Chang, Ines Hoffmann, and Gregg Duester. 1999. "Molecular Analysis of Two Closely Related Mouse Aldehyde Dehydrogenase Genes: Identification of a Role for Aldh1, but Not Aldh-Pb, in the Biosynthesis of Retinoic Acid." *Biochemical Journal*. https://doi.org/10.1042/0264-6021:3390387.
Hut, Roelof A. 2011. "Photoperiodism: Shall EYA Compare Thee to a Summers Day?" *Current Biology* 21 (1): R22–25. https://doi.org/10.1016/j.cub.2010.11.060.
Hut, Roelof A., Hugues Dardente, and Sjaak J. Riede. 2014. "Seasonal Timing: How Does a Hibernator Know When to Stop Hibernating?" *Current Biology* 24 (13): R602–5. https://doi.org/10.1016/j.cub.2014.05.061.
Hut, Roelof A., Silvia Paolucci, Roi Dor, Charalambos P. Kyriacou, and Serge Daan. 2013. "Latitudinal Clines: An Evolutionary View on Biological Rhythms." *Proceedings of the Royal Society B: Biological Sciences*. https://doi.org/10.1098/rspb.2013.0433.
Ikegami, Keisuke, and Takashi Yoshimura. 2013. "Seasonal Time Measurement during Reproduction." *Journal of Reproduction and Development* 59 (4): 327–33. https://doi.org/10.1262/jrd.2013-035.
Ims, Rolf Anker. 1997. "Determinants of Geographic Variation in Growth and Reproductive Traits in the Root Vole." *Ecology* 78 (2): 461–70. https://doi.org/10.1890/0012-

9658(1997)078[0461:DOGVIG]2.0.CO;2.
Innes, Duncan G L, and John S Millar. 1990. “Numbers of Litters, Litter Size and Survival in Two Species of Microtines at Two Elevations.” *Nordic Society Oikos* 13 (3): 207–16.
IUCN. 2021. “The IUCN Red List of Threatened Species.” 2021. https://www.iucnredlist.org/.
Jaarola, Maarit, Natália Martínková, Islam Gündüz, Cecilia Brunhoff, Jan Zima, Adam Nadachowski, Giovanni Amori, et al. 2004. “Molecular Phylogeny of the Speciose Vole Genus Microtus (Arvicolinae, Rodentia) Inferred from Mitochondrial DNA Sequences.” *Molecular Phylogenetics and Evolution* 33 (3): 647–63. https://doi.org/10.1016/j.ympev.2004.07.015.
Jakobsson, Mattias, Michael D. Edge, and Noah A. Rosenberg. 2013. “The Relationship between FST and the Frequency of the Most Frequent Allele.” *Genetics* 193 (2): 515–28. https://doi.org/10.1534/genetics.112.144758.
Jethwa, Preeti H., and Francis J.P. Ebling. 2008. “Role of VGF-Derived Peptides in the Control of Food Intake, Body Weight and Reproduction.” *Neuroendocrinology* 88 (2): 80–87. https://doi.org/10.1159/000127319.
Johnsen, A., A. E. Fidler, S. Kuhn, K. L. Carter, A. Hoffmann, I. R. Barr, C. Biard, et al. 2007. “Avian Clock Gene Polymorphism: Evidence for a Latitudinal Cline in Allele Frequencies.” *Molecular Ecology* 16 (22): 4867–80. https://doi.org/10.1111/j.1365-294X.2007.03552.x.
Johnson, Carl Hirschie, Jeffrey Elliot, Russell G. Foster, Ken-Ichi Honma, and Richard Kronauer. 2004. “Fundamental Properties of Circadian Rhythms.” In *Chronobiology: Biological Timekeeping*, edited by Jay C Dunlap, Jennifer J Loros, and Patricia J DeCoursey, 67–106. Sinauer Associates, Inc.Publishers.
Johnston, J. D., S. Messager, P. Barrett, and David G. Hazlerigg. 2003. “Melatonin Action in the Pituitary: Neuroendocrine Synchronizer and Developmental Modulator?” *Journal of Neuroendocrinology* 15 (4): 405–8. https://doi.org/10.1046/j.1365-2826.2003.00972.x.
Johnston, Jonathan D., Benjamin B. Tournier, Håkan Andersson, Mireille Masson-Pévet, Gerald A. Lincoln, and David G. Hazlerigg. 2006. “Multiple Effects of Melatonin on Rhythmic Clock Gene Expression in the Mammalian Pars Tuberalis.” *Endocrinology* 147 (2): 959–65. https://doi.org/10.1210/en.2005-1100.
Kerbeshian, M. C., F. H. Bronson, and E. D. Bellis. 1994. “Variation in Reproductive Photoresponsiveness in a Wild Population of Meadow Voles.” *Biology of Reproduction* 50 (4): 745–50. https://doi.org/10.1095/biolreprod50.4.745.
Kerbeshian, Marie C., and Franklin H. Bronson. 1996. “Running-Induced Testicular Recrudescence in the Meadow Vole: Role of the Circadian System.” *Physiology and Behavior* 60 (1): 165–70. https://doi.org/10.1016/0031-9384(95)02244-9.
Klosen, Paul, Christele Bienvenu, Olivier Demarteau, Hugues Dardente, Hilda Guerrero, Paul Pévet, and Mireille Masson-Pévet. 2002. “The Mt1 Melatonin Receptor and RORβ Receptor Are Co-Localized in Specific TSH-Immunoreactive Cells in the Pars Tuberalis of the Rat Pituitary.” *Journal of Histochemistry and Cytochemistry* 50 (12): 1647–57. https://doi.org/10.1177/002215540205001209.
Klosen, Paul, Sarawut Lapmanee, Carole Schuster, Beatrice Guardiola, David Hicks, Paul Pevet, and Marie Paule Felder-Schmittbuhl. 2019. “MT1 and MT2 Melatonin Receptors Are Expressed in Nonoverlapping Neuronal Populations.” *Journal of Pineal Research* 67 (1): 1–19. https://doi.org/10.1111/jpi.12575.
Klosen, Paul, Marie Emilie Sébert, Kamontip Rasri, Marie Pierre Laran-Chich, and Valérie Simonneaux. 2013. “TSH Restores a Summer Phenotype in Photoinhibited Mammals via the RF-Amides RFRP3 and Kisspeptin.” *FASEB Journal* 27 (7): 2677–86. https://doi.org/10.1096/fj.13-229559.
Kofler, Robert, Ram Vinay Pandey, and Christian Schlötterer. 2011. “PoPoolation2: Identifying Differentiation between Populations Using Sequencing of Pooled DNA Samples (Pool-Seq).” *Bioinformatics* 27 (24): 3435–36. https://doi.org/10.1093/bioinformatics/btr589.
Kolosova, O. N., and B. M. Kershengol’ts. 2017. “Endogenous Ethanol and Acetaldehyde in the Mechanisms of Adaptation of Small Mammals to Northern Conditions.” *Russian Journal of Ecology* 48 (1): 68–72. https://doi.org/10.1134/S1067413617010088.
Koppaka, Vindhya, David C. Thompson, Ying Chen, Manuel Ellermann, Kyriacos C. Nicolaou, Risto O. Juvonen, Dennis Petersen, Richard A. Deitrich, Thomas D. Hurley, and Vasilis Vasiliou Dr. 2012. “Aldehyde Dehydrogenase Inhibitors: A Comprehensive Review of the Pharmacology, Mechanism of Action, Substrate Specificity, and Clinical Application.” *Pharmacological Reviews* 64 (3): 520–39. https://doi.org/10.1124/pr.111.005538.
Korslund, Lars. 2006. “Activity of Root Voles (Microtus Oeconomus) under Snow: Social Encounters Synchronize Individual Activity Rhythms.” *Behavioral Ecology and Sociobiology* 61 (2): 255–63. https://doi.org/10.1007/s00265-006-0256-3.

Kriegsfeld, L. J., A. G. Trasy, and R. J. Nelson. 2000. “Temperature and Photoperiod Interact to Affect Reproduction and GnRH Synthesis in Male Prairie Voles.” *Journal of Neuroendocrinology* 12 (6): 553–58. https://doi.org/10.1046/j.1365-2826.2000.00485.x.

Kriegsfeld, Lance J., Dan Feng Mei, George E. Bentley, Takayoshi Ubuka, Alex O. Mason, Kasuhiko Inoue, Kazuyoshi Ukena, Kasuyoshi Tsutsui, and Rae Silver. 2006. “Identification and Characterization of a Gonadotropin-Inhibitory System in the Brains of Mammals.” *Proceedings of the National Academy of Sciences of the United States of America* 103 (7): 2410–15. https://doi.org/10.1073/pnas.0511003103.

Król, E., P. Redman, P. J. Thomson, R. Williams, C. Mayer, J. G. Mercer, and J. R. Speakman. 2005. “Effect of Photoperiod on Body Mass, Food Intake and Body Composition in the Field Vole, Microtus Agrestis.” *Journal of Experimental Biology* 208 (3): 571–84. https://doi.org/10.1242/jeb.01429.

Król, Elzbieta, Alex Douglas, Hugues Dardente, Mike J. Birnie, Vincent van der Vinne, Willem G. Eijer, Menno P. Gerkema, David G. Hazlerigg, and Roelof A. Hut. 2012. “Strong Pituitary and Hypothalamic Responses to Photoperiod but Not to 6-Methoxy-2-Benzoxazolinone in Female Common Voles (Microtus Arvalis).” *General and Comparative Endocrinology* 179 (2): 289–95. https://doi.org/10.1016/j.ygcen.2012.09.004.

Lambin, Xavier, Vincent Bretagnolle, and Nigel G. Yoccoz. 2006. “Vole Population Cycles in Northern and Southern Europe: Is There a Need for Different Explanations for Single Pattern?” *Journal of Animal Ecology* 75 (2): 340–49. https://doi.org/10.1111/j.1365-2656.2006.01051.x.

Lambin, Xavier, and Charles J. Krebs. 1991. “Spatial Organization and Mating System of Microtus Townsendii.” *Behavioral Ecology and Sociobiology* 28 (5): 353–63. https://doi.org/10.1007/BF00164385.

Lambin, Xavier, Charles J. Krebs, and Beth Scott. 1992. “Spacing System of the Tundra Vole (Microtus Oeconomus) during the Breeding Season in Canada’s Western Arctic.” *Canadian Journal of Zoology* 70: 2068–72.

Laver, T., J. Harrison, P. A. O’Neill, K. Moore, A. Farbos, K. Paszkiewicz, and D. J. Studholme. 2015. “Assessing the Performance of the Oxford Nanopore Technologies MinION.” *Biomolecular Detection and Quantification* 3: 1–8. https://doi.org/10.1016/j.bdq.2015.02.001.

Lee, T. M. 1993. “Development of Meadow Voles Is Influenced Postnatally by Maternal Photoperiodic History.” *American Journal of Physiology - Regulatory Integrative and Comparative Physiology* 265 (4 34-4). https://doi.org/10.1152/ajpregu.1993.265.4.r749.

Lee, T. M., and I. Zucker. 1988. “Vole Infant Development Is Influenced Perinatally by Maternal Photoperiodic History.” *American Journal of Physiology - Regulatory Integrative and Comparative Physiology* 255 (5). https://doi.org/10.1152/ajpregu.1988.255.5.r831.

Lees, A. D. 1973. “Photoperiodic Time Measurement in the Aphid Megoura Viciae.” *Journal of Insect Physiology* 19 (12): 2279–2316. https://doi.org/10.1016/0022-1910(73)90237-0.

Lehman, Michael N., Robert L. Goodman, Fred J. Karsch, Gary L. Jackson, Sandra J. Berriman, and Heiko T. Jansen. 1997. “The GnRH System of Seasonal Breeders: Anatomy and Plasticity.” *Brain Research Bulletin* 44 (4): 445–57. https://doi.org/10.1016/S0361-9230(97)00225-6.

Lemskaya, Natalia A., Svetlana A. Romanenko, Feodor N. Golenishchev, Nadezhda V. Rubtsova, Olga V. Sablina, Natalya A. Serdukova, Patricia C.M. O’Brien, et al. 2010. “Chromosomal Evolution of Arvicolinae (Cricetidae, Rodentia). III. Karyotype Relationships of Ten Microtus Species.” *Chromosome Research* 18 (4): 459–71. https://doi.org/10.1007/s10577-010-9124-0.

Lessells, Cate M. 2008. “Neuroendocrine Control of Life Histories: What Do We Need to Know to Understand the Evolution of Phenotypic Plasticity?” *Philosophical Transactions of the Royal Society B: Biological Sciences* 363 (1497): 1589–98. https://doi.org/10.1098/rstb.2007.0008.

Lewis, Jo E., and Francis J.P. Ebling. 2017. “Tanycytes as Regulators of Seasonal Cycles in Neuroendocrine Function.” *Frontiers in Neurology* 8 (MAR): 1–7. https://doi.org/10.3389/fneur.2017.00079.

Li, Heng, and Richard Durbin. 2009. “Fast and Accurate Short Read Alignment with Burrows-Wheeler Transform.” *Bioinformatics* 25 (14): 1754–60. https://doi.org/10.1093/bioinformatics/btp324.

Lincoln, G. A., and F. J.P. Ebling. 1985. “Effect of Constant-Release Implants of Melatonin on Seasonal Cycles in Reproduction, Prolactin Secretion and Moulting in Rams.” *Journal of Reproduction and Fertility* 73 (1): 241–53. https://doi.org/10.1530/jrf.0.0730241.

Lincoln, Gerald A., Håkan Andersson, and Andrew S.I. Loudon. 2003. “Clock Genes in Calendar Cells as the Basis of Annual Timekeeping in Mammals - A Unifying Hypothesis.” *Journal of Endocrinology* 179 (1): 1–13. https://doi.org/10.1677/joe.0.1790001.

Lincoln, Gerald A., Iain J. Clarke, Roelof A. Hut, and David G. Hazlerigg. 2006. "Characterizing a Mammalian Circannual Pacemaker." *Science 3*14 (5807): 1941-1944. https://doi.org/10.1126/science.1132009

Lincoln, Gerald A., and David. G. Hazlerigg. 2010. “Mammalian Circannual Pacemakers.” *Society of*

Reproduction and Fertility Supplement 67: 171–86. https://doi.org/10.7313/upo9781907284991.015.
Lincoln, Gerald A., Jonathan D. Johnston, Håkan Andersson, Gabriela Wagner, and David G. Hazlerigg. 2005. "Photorefractoriness in Mammals: Dissociating a Seasonal Timer from the Circadian-Based Photoperiod Response." *Endocrinology* 146 (9): 3782–90. https://doi.org/10.1210/en.2005-0132.
Lincoln, Gerald, Sophie Messager, Håkan Andersson, and David Hazlerigg. 2002. "Temporal Expression of Seven Clock Genes in the Suprachiasmatic Nucleus and the Pars Tuberalis of the Sheep: Evidence for an Internal Coincidence Timer." *Proceedings of the National Academy of Sciences of the United States of America* 99 (21): 13890–95. https://doi.org/10.1073/pnas.212517599.
Linzey, A.V., S. Shar, D. Lkhagvasuren, R. Juškaitis, B. Sheftel, Meinig H., G. Amori, and H. Henttonen. 2016. "Microtus Oeconomus." The IUCN Red List of Threatened Species 2016. 2016. https://doi.org/https://dx.doi.org/10.2305/IUCN.UK.2016-3.RLTS.T13451A22347188.en.
Lomet, Didier, Juliette Cognié, Didier Chesneau, Emeric Dubois, David Hazlerigg, and Hugues Dardente. 2018. "The Impact of Thyroid Hormone in Seasonal Breeding Has a Restricted Transcriptional Signature." *Cellular and Molecular Life Sciences* 75 (5): 905–19. https://doi.org/10.1007/s00018-017-2667-x.
Lovegrove, Barry G. 2005. "Seasonal Thermoregulatory Responses in Mammals." *Journal of Comparative Physiology B: Biochemical, Systemic, and Environmental Physiology* 175 (4): 231–47. https://doi.org/10.1007/s00360-005-0477-1.
Lu, Hengyun, Francesca Giordano, and Zemin Ning. 2016. "Oxford Nanopore MinION Sequencing and Genome Assembly." *Genomics, Proteomics and Bioinformatics* 14 (5): 265–79. https://doi.org/10.1016/j.gpb.2016.05.004.
Lu, Weiqun, Qing Jun Meng, Nicholas J.C. Tyler, Karl Arne Stokkan, and Andrew S.I. Loudon. 2010. "A Circadian Clock Is Not Required in an Arctic Mammal." *Current Biology* 20 (6): 533–37. https://doi.org/10.1016/j.cub.2010.01.042.
Ludwig, Daniel R. 1988. "Reproduction and Population Dynamics of the Water Vole, Microtus Richardsoni." *American Society of Mammalogists* 69 (3): 532–41.
Lynch, G. R., H. W. Heath, and C. M. Johnston. 1981. "Effect of Geographical Origin on the Photoperiodic Control of Reproduction in the White-Footed Mouse, Peromyscus Leucopus." *Biology of Reproduction* 25 (3): 475–80. https://doi.org/10.1095/biolreprod25.3.475.
Madeira, Fábio, Young Mi Park, Joon Lee, Nicola Buso, Tamer Gur, Nandana Madhusoodanan, Prasad Basutkar, et al. 2019. "The EMBL-EBI Search and Sequence Analysis Tools APIs in 2019." *Nucleic Acids Research* 47 (W1): W636–41. https://doi.org/10.1093/nar/gkz268.
Marcovitch, S. 1924. "The Migration of the Aphididae and the Appearance of the Sexual Forms as Affected by the Relative Length of Daily Light Exposure." *Journal of Agricultural Research* XXVII: 513–22.
Martinet, L., D. Allain, and C. Weiner. 1984. "Role of Prolactin in the Photoperiodic Control of Moulting in the Mink (Mustela Vison)." *Journal of Endocrinology* 103 (1): 9–15. https://doi.org/10.1677/joe.0.1030009.
Masumoto, Koh Hei, Maki Ukai-Tadenuma, Takeya Kasukawa, Mamoru Nagano, Kenichiro D. Uno, Kaori Tsujino, Kazumasa Horikawa, Yasufumi Shigeyoshi, and Hiroki R. Ueda. 2010. "Acute Induction of Eya3 by Late-Night Light Stimulation Triggers TSHβ Expression in Photoperiodism." *Current Biology* 20 (24): 2199–2206. https://doi.org/10.1016/j.cub.2010.11.038.
Meek, Leslie R., Theresa M. Lee, and Jill F. Gallon. 1995. "Interaction of Maternal Photoperiod History and Food Type on Growth and Reproductive Development of Laboratory Meadow Voles (Microtus Pennsylvanicus)." *Physiology and Behavior* 57 (5): 905–11. https://doi.org/10.1016/0031-9384(94)00356-A.
Meirmans, Patrick G., and Philip W. Hedrick. 2011. "Assessing Population Structure: FST and Related Measures." *Molecular Ecology Resources* 11 (1): 5–18. https://doi.org/10.1111/j.1755-0998.2010.02927.x.
Messer, Philipp W., and Dmitri A. Petrov. 2013. "Population Genomics of Rapid Adaptation by Soft Selective Sweeps." *Trends in Ecology and Evolution* 28 (11): 659–69. https://doi.org/10.1016/j.tree.2013.08.003.
Mihok, Steve, Brian N Turner, and Stuart L Iverson. 1985. "The Characterization of Vole Population Dynamics." *Ecological Monographs* 55 (4): 399–420. https://doi.org/10.2307/2937129.
Miller, Donald H., and Lowell L. Getz. 1969. "Life-History Notes on Microtus Pinetorum in Central Connecticut." *Journal of Mammalogy* 50 (4): 777. https://doi.org/10.2307/1378256.
Miller, Jason R, Sergey Koren, and Granger Sutton. 2011. "Genome Sequencing Algorithms." *Genomics* 95 (6): 315–27. https://doi.org/10.1016/j.ygeno.2010.03.001.Assembly.
Moffatt, Christopher A., Randy J. Nelson, and A. Courtney Devries. 1993. "Winter Adaptations of Male Deer

Mice (Peromyscus Maniculatus) and Prairie Voles (Microtus Ochrogaster) That Vary in Reproductive Responsiveness to Photoperiod." *Journal of Biological Rhythms* 8 (3): 221–32. https://doi.org/10.1177/074873049300800305.
Moffatt, Christopher, and Randy J. Nelson. 1994. "Day Length Influences Proceptive Behavior of Female Prairie Voles." *Physiology & Behavior* 55 (6): 1163–65.
Monecke, Stefanie, Michel Saboureau, Andŕ Malan, Daniel Bonn, Mireille Masson-Ṕvet, and Paul Ṕvet. 2009. "Circannual Phase Response Curves to Short and Long Photoperiod in the European Hamster." *Journal of Biological Rhythms* 24 (5): 413–26. https://doi.org/10.1177/0748730409344502.
Morgan, P. J., and L. M. Williams. 1989. "Central Melatonin Receptors: Implications for a Mode of Action." *Experientia*. https://doi.org/10.1007/BF01953053.
Morgan, Peter J., Perry Barrett, H. Edward Howell, and Rachel Helliwell. 1994. "Melatonin Receptors: Localization, Molecular Pharmacology and Physiological Significance." *Neurochemistry International*. https://doi.org/10.1016/0197-0186(94)90100-7.
Müller, D., J. Hauer, K. Schöttner, P. Fritzsche, and D. Weinert. 2015. "Seasonal Adaptation of Dwarf Hamsters (Genus Phodopus): Differences between Species and Their Geographic Origin." *Journal of Comparative Physiology B: Biochemical, Systemic, and Environmental Physiology* 185 (8): 917–30. https://doi.org/10.1007/s00360-015-0926-4.
Murphy, William J., Denis M. Larkin, Annelie Everts-van der Wind, Guillaume Bourque, Glenn Tesler, Loretta Auvil, Jonathan E. Beever, et al. 2005. "Evolution: Dynamics of Mammalian Chromosome Evolution Inferred from Multispecies Comparative Maps." *Science* 309 (5734): 613–17. https://doi.org/10.1126/science.1111387.
Nakao, Nobuhiro, Hiroko Ono, Takashi Yamamura, Tsubasa Anraku, Tsuyoshi Takagi, Kumiko Higashi, Shinobu Yasuo, et al. 2008. "Thyrotrophin in the Pars Tuberalis Triggers Photoperiodic Response." *Nature* 452 (7185): 317–22. https://doi.org/10.1038/nature06738.
Nakao, Nobuhiro, Hiroko Ono, and Takashi Yoshimura. 2008. "Thyroid Hormones and Seasonal Reproductive Neuroendocrine Interactions." *Reproduction* 136 (1): 1–8. https://doi.org/10.1530/REP-08-0041.
Negus, N. C., P. J. Berger, and B. W. Brown. 1986. "Microtine Population Dynamics in a Predictable Environment." *Canadian Journal of Zoology* 64 (3): 785–92. https://doi.org/10.1139/z86-117.
Nelson, R. J. 1985. "Photoperiod Influences Reproduction in the Prairie Vole. (Microtus Ochrogaster)." *Biology of Reproduction* 33 (3): 596–602. https://doi.org/10.1095/biolreprod33.3.596.
Nelson, R. J., D. Frank, L. Smale, and S. B. Willoughby. 1989. "Photoperiod and Temperature Affect Reproductive and Nonreproductive Functions in Male Prairie Voles (Microtus Ochrogaster)." *Biology of Reproduction* 40 (3): 481–85. https://doi.org/10.1095/biolreprod40.3.481.
Nelson, Randy J., and Joan M. C. Blom. 1993. " 6-Methoxy-2-Benzoxazolinone and Photoperiod: Prenatal and Postnatal Influences on Reproductive Development in Prairie Voles (Microtus Ochrogaster Ochrogaster) ." *Canadian Journal of Zoology* 71 (4): 776–89. https://doi.org/10.1139/z93-103.
Neumann, Dietrich. 2014. "Timing in Tidal, Semilunar and Lunar Rhythms." In *Annual, Lunar and Tidal Clocks. Patterns and Mechanims of Nature's Enigmatic Rhythms*, edited by Hideharu Numata and Barbara Helm, 3–24. Springer Japan.
Niedringhaus, Thomas P., Denitsa Milanova, Matthew B. Kerby, Michael P. Snyder, and Annelise E. Barron. 2011. "Landscape of Next-Generation Sequencing Technologies." *Analytical Chemistry* 83 (12): 4327–41. https://doi.org/10.1021/ac2010857.
Nieminen, Petteri, Esa Hohtola, and Anne Mari Mustonen. 2013. "Body Temperature Rhythms in Microtus Voles during Feeding, Food Deprivation, and Winter Acclimatization." *Journal of Mammalogy* 94 (3): 591–600. https://doi.org/10.1644/12-MAMM-A-219.1.
O'Malley, Kathleen G., and Michael A. Banks. 2008. "A Latitudinal Cline in the Chinook Salmon (Oncorhynchus Tshawytscha) Clock Gene: Evidence for Selection on PolyQ Length Variants." *Proceedings of the Royal Society B: Biological Sciences* 275 (1653): 2813–21. https://doi.org/10.1098/rspb.2008.0524.
Ono, Hiroko, Yuta Hoshino, Shinobu Yasuo, Miwa Watanabe, Yusuke Nakane, and Atsushi Murai. 2008. "Involvement of Thyrotropin in Photoperiodic Signal Transduction in Mice. - Proceedings of the National Academy of Sciences of the United States of America.Pdf." *Pnas* 105 (47): 18238–42.
Panda, Satchidananda, Ignacio Provencio, Daniel C. Tu, Susana S. Pires, Mark D. Rollag, Ana Maria Castrucci, Mathew T. Pletcher, et al. 2003. "Melanopsin Is Required for Non-Image-Forming Photic Responses in Blind Mice." *Science* 301 (5632): 525–27. https://doi.org/10.1126/science.1086179.
Paradis, E., and G. Guédon. 1993. "Demography of a Mediterranean Microtine: The Mediterranean Pine Vole, Microtus Duodecimcostatus." *Oecologia* 95 (1): 47–53. https://doi.org/10.1007/BF00649505.
Pengelley, E. T., Roland C. Aloia, and Brian Barnes. 1978. "Circannual Rhythmicity in the Hibernating

Ground Squirrel Citellus Lateralis Under Constant Light and Hyperthermic Ambient Temperature." *Comparative Biochemistry and Physiology - A Molecular and Integrative Physiology* 61A: 599–603.
Pengelley, E. T., Sally J. Asmundson, Roland C. Aloia, and Brian Barnes. 1976. "Circannual Rhythmicity in a Non-Hibernating Ground Squirrel, Citellus Leucurus." *Comparative Biochemistry and Physiology - A Molecular and Integrative Physiology* 54A: 233–37.
Pengelley, E. T., Sally J. Asmundson, Brian Barnes, and Roland C. Aloia. 1976. "Relationship of Light Intensity and Photoperiod to Circannual Rhythmicity in the Hibernating Ground Squirrel, Citellus Lateralis." *Comparative Biochemistry and Physiology -- Part A: Physiology* 53 (3): 273–77. https://doi.org/10.1016/S0300-9629(76)80035-7.
Pfeiffer, Franziska, Carsten Gröber, Michael Blank, Kristian Händler, Marc Beyer, Joachim L. Schultze, and Günter Mayer. 2018. "Systematic Evaluation of Error Rates and Causes in Short Samples in Next-Generation Sequencing." *Scientific Reports* 8 (1): 1–14. https://doi.org/10.1038/s41598-018-29325-6.
Pigliucci, Massimo, Courtney J. Murren, and Carl D. Schlichting. 2006. "Phenotypic Plasticity and Evolution by Genetic Assimilation." *Journal of Experimental Biology* 209 (12): 2362–67. https://doi.org/10.1242/jeb.02070.
Postma, Erik, and Arie J. van Noordwijk. 2005. "Genetic Variation for Clutch Size in Natural Populations of Birds from a Reaction Norm Perspective." *Ecology* 86 (9): 2344–57. https://doi.org/10.1890/04-0348.
Prendergast, B. J., R. J. Nelson, and I. Zucker. 2009. "Mammalian Seasonal Rhythms: Behavior and Neuroendocrine Substrates." *Hormones, Brain and Behavior Online*, 507–40. https://doi.org/10.1016/B978-008088783-8.00014-0.
Prendergast, Brian J., Michael R. Gorman, and Irving Zucker. 2000. "Establishment and Persistence of Photoperiodic Memory in Hamsters." *Proceedings of the National Academy of Sciences of the United States of America*. https://doi.org/10.1073/pnas.100098597.
Prendergast, Brian J., Lance J. Kriegsfeld, and Randy J. Nelson. 2001. "Photoperiodic Polyphenisms in Rodents: Neuroendocrine Mechanisms, Costs and Functions." *Quarterly Review of Biology* 73 (3): 293–325.
Prendergast, Brian J, Lance J Kriegsfeld, and Randy J Nelson. 2001. "Photoperiodic Polyphenisms in Rodents: Neuroendocrine Mechanisms, Costs and Functions." *The Quarterly Review of Biology* 76 (3): 293–325.
Prévot-Julliard, Anne Caroline, Heikki Henttonen, Nigel G. Yoccoz, and Nils Chr Stenseth. 1999. "Delayed Maturation in Female Bank Voles: Optimal Decision or Social Constraint?" *Journal of Animal Ecology* 68 (4): 684–97. https://doi.org/10.1046/j.1365-2656.1999.00307.x.
Pyter, L. M., Z. M. Weil, and R. J. Nelson. 2005. "Latitude Affects Photoperiod-Induced Changes in Immune Response in Meadow Voles (Microtus Pennsylvanicus)." *Canadian Journal of Zoology* 83 (10): 1271–78. https://doi.org/10.1139/z05-121.
Raible, Florian, Hiroki Takekata, and Kristin Tessmar-Raible. 2017. "An Overview of Monthly Rhythms and Clocks." *Frontiers in Neurology* 8 (MAY): 1–14. https://doi.org/10.3389/fneur.2017.00189.
Ransom, Jemma, Peter J. Morgan, Peter J. McCaffery, and Patrick N. Stoney. 2014. "The Rhythm of Retinoids in the Brain." *Journal of Neurochemistry* 129 (3): 366–76. https://doi.org/10.1111/jnc.12620.
Rausch, Robert L. 1963. "A Review of the Distribution of Holarctic Recent Mammals." *Faculty Publications from the Harold W. Manter Laboratory of Parasitology* 518.
Raush, Robert L., and R. Raush, Virginia. 1968. "On the Biology and Systematic Position of Microtus Abbreviatus Miller, a Vole Endemic to the St.Matthew Islands, Bering Sea." *Zeitschrift Für Säugetierkunde : Im Auftrage Der Deutschen Gesellschaft Für Säugetierkunde e.V.* 33: 65–99.
Ricankova, V., R. Sumbera, and F. Sedlacek. 2007. "Familiarity and Partner Preferences in Female Common Voles, Microtus Arvalis." *Journal of Ethology* 25 (1): 95–98. https://doi.org/10.1007/s10164-006-0211-9.
Robinson, James T., Helga Thorvaldsdóttir, Wendy Winckler, Mitchell Guttman, Eric S. Lander, Gad Getz, and Jill P. Mesirov. 2011. "Integrative Genomics Viewer." *Nature Biotechnology* 29: 24–26. https://doi.org/10.1038/nbt.1754.
Rodríguez, Esteban M., Juan L. Blázquez, Francisco E. Pastor, Belén Peláez, Patricio Peña, Bruno Peruzzo, and Pedro Amat. 2005. "Hypothalamic Tanycytes: A Key Component of Brain-Endocrine Interaction." *International Review of Cytology* 247 (05): 89–164. https://doi.org/10.1016/S0074-7696(05)47003-5.
Rosmalen, Laura van and Roelof A. Hut. 2021. "Negative Energy Balance Enhances Ultradian Rhythmicity in Spring-Programmed Voles." *Journal of Biological Rhythms* 36 (4): 359-368.

https://doi.org/10.1177/07487304211005640
Rosmalen, Laura van. 2021. "Photoperiodism in voles. A neurobiological perspective on seasonal ecology". University of Groningen, PhD dissertation. https://research.rug.nl/nl/publications/photoperiodism-in-voles-a-neurobiological-perspective-on-seasonal
Ross, Alexander W., Lynn M. Bell, Pauline A. Littlewood, Julian G. Mercer, Perry Barrett, and Peter J. Morgan. 2005. "Temporal Changes in Gene Expression in the Arcuate Nucleus Precede Seasonal Responses in Adiposity and Reproduction." *Endocrinology* 146 (4): 1940–47. https://doi.org/10.1210/en.2004-1538.
Rousseau, Karine, Zeenat Atcha, Felino Ramon A. Cagampang, Philippe Le Rouzic, J. Anne Stirland, Tina R. Ivanov, Francis J.P. Ebling, Martin Klingenspor, and Andrew S.I. Loudon. 2002. "Photoperiodic Regulation of Leptin Resistance in the Seasonally Breeding Siberian Hamster (Phodopus Sungorus)." *Endocrinology* 143 (8): 3083–95. https://doi.org/10.1210/endo.143.8.8967.
Rowan, William. 1925. "Relation of Light to Bird Migration and Developmental Changes." *Nature* 115: 494–95.
Rubin, Carl Johan, Michael C. Zody, Jonas Eriksson, Jennifer R.S. Meadows, Ellen Sherwood, Matthew T. Webster, Lin Jiang, et al. 2010. "Whole-Genome Resequencing Reveals Loci under Selection during Chicken Domestication." *Nature* 464 (7288): 587–91. https://doi.org/10.1038/nature08832.
Sáenz de Miera, Cristina, Béatrice Bothorel, Catherine Jaeger, Valérie Simonneaux, and David Hazlerigg. 2017. "Maternal Photoperiod Programs Hypothalamic Thyroid Status via the Fetal Pituitary Gland." *Proceedings of the National Academy of Sciences of the United States of America* 114 (31): 8408–13. https://doi.org/10.1073/pnas.1702943114.
Saunders, D. S., R. D. Lewis, and G. R. Warman. 2004. "Photoperiodic Induction of Diapause: Opening the Black Box." *Physiological Entomology* 29 (1): 1–15. https://doi.org/10.1111/j.1365-3032.2004.0369.x.
Sayers, Eric W., Jeffrey Beck, Evan E. Bolton, Devon Bourexis, James R. Brister, Kathi Canese, Donald C. Comeau, et al. 2021. "Database Resources of the National Center for Biotechnology Information." *Nucleic Acids Research* 49 (D1): D10–17. https://doi.org/10.1093/nar/gkaa892.
Schlötterer, Christian, Raymond Tobler, Robert Kofler, and Viola Nolte. 2014. "Sequencing Pools of Individuals-Mining Genome-Wide Polymorphism Data without Big Funding." *Nature Reviews Genetics* 15 (11): 749–63. https://doi.org/10.1038/nrg3803.
Sera, By Wendy E, and Cathleen N Early. 2003. "Microtus Montanus." *American Society of Mammalogists*, no. 716: 1–10.
Sharp, Kathy, Donna Bucci, Paul K. Zelensky, Alanna Chesney, Wendy Tidhar, David R. Broussard, and Paul D. Heideman. 2015. "Genetic Variation in Male Sexual Behaviour in a Population of White-Footed Mice in Relation to Photoperiod." *Animal Behaviour* 104: 203–12. https://doi.org/10.1016/j.anbehav.2015.03.026.
Shearer, Kirsty D., Timothy H. Goodman, Alexander W. Ross, Laura Reilly, Peter J. Morgan, and Peter J. McCaffery. 2010. "Photoperiodic Regulation of Retinoic Acid Signaling in the Hypothalamus." *Journal of Neurochemistry* 112 (1): 246–57. https://doi.org/10.1111/j.1471-4159.2009.06455.x.
Shearer, Kirsty D., Patrick N. Stoney, Peter J. Morgan, and Peter J. McCaffery. 2012. "A Vitamin for the Brain." *Trends in Neurosciences* 35 (12): 733–41. https://doi.org/10.1016/j.tins.2012.08.005.
Shearer, Kirsty D., Patrick N. Stoney, Sonia E. Nanescu, Gisela Helfer, Perry Barrett, Alexander W. Ross, Peter J. Morgan, and Peter McCaffery. 2012. "Photoperiodic Expression of Two RALDH Enzymes and the Regulation of Cell Proliferation by Retinoic Acid in the Rat Hypothalamus." *Journal of Neurochemistry* 122 (4): 789–99. https://doi.org/10.1111/j.1471-4159.2012.07824.x.
Shumate, Alaina, and Steven L Salzberg. 2021. "Liftoff: Accurate Mapping of Gene Annotations." *Bioinformatics*. https://doi.org/10.1093/bioinformatics/btaa1016.
Silverin, B., R. Massa, and K. A. Stokkan. 1993. "Photoperiodic Adaptation to Breeding at Different Latitudes in Great Tits." *General and Comparative Endocrinology*. https://doi.org/10.1006/gcen.1993.1055.
Silverin, Bengt, John Wingfield, Karl Arne Stokkan, Renato Massa, Antero Järvinen, Nils Åke Andersson, Marcel Lambrechts, Alberto Sorace, and Donald Blomqvist. 2008. "Ambient Temperature Effects on Photo Induced Gonadal Cycles and Hormonal Secretion Patterns in Great Tits from Three Different Breeding Latitudes." *Hormones and Behavior* 54 (1): 60–68. https://doi.org/10.1016/j.yhbeh.2008.01.015.
Simonneaux, Valérie. 2020. "A Kiss to Drive Rhythms in Reproduction." *European Journal of Neuroscience* 51 (1): 509–30. https://doi.org/10.1111/ejn.14287.
Sitnikova, Natalia A., Svetlana A. Romanenko, Patricia C.M. O'Brien, Polina L. Perelman, Beiyuan Fu, Nadezhda V. Rubtsova, Natalya A. Serdukova, et al. 2007. "Chromosomal Evolution of Arvicolinae

(Cricetidae, Rodentia). I. The Genome Homology of Tundra Vole, Field Vole, Mouse and Golden Hamster Revealed by Comparative Chromosome Painting." *Chromosome Research* 15 (4): 447–56. https://doi.org/10.1007/s10577-007-1137-y.
Smolen, Michael J. 1981. "Microtus Pinetorum." *American Journal of Mammalogists*, no. 147: 1–7.
Sobreira, Tiago J.P., Ferdinand Marlétaz, Marcos Simões-Costa, Deborah Schechtman, Alexandre C. Pereira, Frédéric Brunet, Sarah Sweeney, et al. 2011. "Structural Shifts of Aldehyde Dehydrogenase Enzymes Were Instrumental for the Early Evolution of Retinoid-Dependent Axial Patterning in Metazoans." *Proceedings of the National Academy of Sciences of the United States of America* 108 (1): 226–31. https://doi.org/10.1073/pnas.1011223108.
Stehle, Jörg H., Charlotte Von Gall, Christof Schomerus, and Horst Werner Korf. 2001. "Of Rodents and Ungulates and Melatonin: Creating a Uniform Code for Darkness by Different Signaling Mechanisms." *Journal of Biological Rhythms* 16 (4): 312–25. https://doi.org/10.1177/074873001129002033.
Stetson, M. H., J. A. Elliott, and B. D. Goldman. 1986. "Maternal Transfer of Photoperiodic Information Influences the Photoperiodic Response of Prepubertal Djungarian Hamsters (Phodopus Sungorus Sungorus)." *Biology of Reproduction* 34 (4): 664–69. https://doi.org/10.1095/biolreprod34.4.664.
Stevenson, K. T., I. G. Van Tets, and L. A.I. Nay. 2009. "The Seasonality of Reproduction in Photoperiod Responsive and Nonresponsive Northern Red-Backed Voles (Myodes Rutilus) in Alaska." *Canadian Journal of Zoology* 87 (2): 152–64. https://doi.org/10.1139/Z08-147.
Stocker, Martina, Jonathan Prosl, Lisa Claire Vanhooland, Lisa Horn, Thomas Bugnyar, Virginie Canoine, and Jorg J.M. Massen. 2021. "Measuring Salivary Mesotocin in Birds - Seasonal Differences in Ravens' Peripheral Mesotocin Levels." *Hormones and Behavior* 134 (June): 105015. https://doi.org/10.1016/j.yhbeh.2021.105015.
Stokkan, Karl Arne, Bob E.H. van Oort, Nicholas J.C. Tyler, and Andrew S.I. Loudon. 2007. "Adaptations for Life in the Arctic: Evidence That Melatonin Rhythms in Reindeer Are Not Driven by a Circadian Oscillator but Remain Acutely Sensitive to Environmental Photoperiod." *Journal of Pineal Research* 43 (3): 289–93. https://doi.org/10.1111/j.1600-079X.2007.00476.x.
Stoney, Patrick N., Gisela Helfer, Diana Rodrigues, Peter J. Morgan, and Peter Mccaffery. 2016. "Thyroid Hormone Activation of Retinoic Acid Synthesis in Hypothalamic Tanycytes." *Glia* 64 (3): 425–39. https://doi.org/10.1002/glia.22938.
Strand, Jo E.T., David Hazlerigg, and Even H. Jørgensen. 2018. "Photoperiod Revisited: Is There a Critical Day Length for Triggering a Complete Parr–Smolt Transformation in Atlantic Salmon Salmo Salar?" *Journal of Fish Biology* 93 (3): 440–48. https://doi.org/10.1111/jfb.13760.
Tast, Johan. 1966. "The Root Vole, Microtus Oeconomus (Pallas) as an Inhabitant of Seasonally Flooded Land." *Annales Zoologici Fennici* 3 (3): I27-I7I.
Tast, Johan, and Asko Kaikusalo. 1976. "Winter Breeding of the Root Vole , Microtus Oeconomus , in 1972 / 1973 at Kilpisjärvi , Finnish Lapland" 13 (3): 174–78.
Tinbergen, Niko. 1963. "On Aims and Methods of Ethology." *Zeitschrift Für Tierpsychologie*. https://doi.org/10.1111/j.1439-0310.1963.tb01161.x.
Touloupi, Katerina, Jenni Küblbeck, Angeliki Magklara, Ferdinand Molnár, Mika Reinisalo, Maria Konstandi, Paavo Honkakoski, and Periklis Pappas. 2019. "The Basis for Strain-Dependent Rat Aldehyde Dehydrogenase 1A7 (ALDH1A7) Gene Expression." *Molecular Pharmacology* 96 (5): 655–63. https://doi.org/10.1124/mol.119.117424.
Trainor, Brian C., Lynn B. Martin, Kelly M. Greiwe, Joshua R. Kuhlman, and Randy J. Nelson. 2006. "Social and Photoperiod Effects on Reproduction in Five Species of Peromyscus." *General and Comparative Endocrinology* 148 (2): 252–59. https://doi.org/10.1016/j.ygcen.2006.03.006.
Triant, Deborah A., and J. Andrew DeWoody. 2006. "Accelerated Molecular Evolution in Microtus (Rodentia) as Assessed via Complete Mitochondrial Genome Sequences." *Genetica* 128 (1–3): 95–108. https://doi.org/10.1007/s10709-005-5538-6.
Tucker, Tracy, Marco Marra, and Jan M. Friedman. 2009. "Massively Parallel Sequencing: The Next Big Thing in Genetic Medicine." *American Journal of Human Genetics* 85 (2): 142–54. https://doi.org/10.1016/j.ajhg.2009.06.022.
Urbanski, H. F., A. Doan, and M. Pierce. 1991. "Immunocytochemical Investigation of Luteinizing Hormone-Releasing Hormone Neurons in Syrian Hamsters Maintained under Long or Short Days." *Biology of Reproduction* 44 (4): 687–92. https://doi.org/10.1095/biolreprod44.4.687.
Veerman, Alfred. 2001. "Photoperiodic Time Measurement in Insects and Mites: A Critical Evaluation of the Oscillator-Clock Hypothesis." *Journal of Insect Physiology*. https://doi.org/10.1016/S0022-1910(01)00106-8.
Ventura, Jacint, Laia Jiménez, and Julio Gisbert. 2010. "Breeding Characteristics of the Lusitanian Pine Vole, Microtus Lusitanicus." *Animal Biology* 60 (1): 1–14.

https://doi.org/10.1163/157075610X12610595764011.
Viitala, J, J Pusenius, H Ylönen, T Mappes, and H Hakkarainen. 1996. "Social Organization and Life History Strategy in Microtines." *Proceedings of the European Congress of Mammalogy*, no. April 2016: 151–161.
Visser, Marcel E., and Christiaan Both. 2005. "Shifts in Phenology Due to Global Climate Change: The Need for a Yardstick." *Proceedings of the Royal Society B: Biological Sciences* 272 (1581): 2561–69. https://doi.org/10.1098/rspb.2005.3356.
Visser, Marcel E., Samuel P. Caro, Kees van Oers, Sonja V. Schaper, and Barbara Helm. 2010. "Phenology, Seasonal Timing and Circannual Rhythms: Towards a Unified Framework." *Philosophical Transactions of the Royal Society B: Biological Sciences* 365 (1555): 3113–27. https://doi.org/10.1098/rstb.2010.0111.
Visser, Marcel E., Leonard J.M. Holleman, and Samuel P. Caro. 2009. "Temperature Has a Causal Effect on Avian Timing of Reproduction." *Proceedings of the Royal Society B: Biological Sciences* 276 (1665): 2323–31. https://doi.org/10.1098/rspb.2009.0213.
Visser, Marcel E., Leonard J.M. Holleman, and Phillip Gienapp. 2006. "Shifts in Caterpillar Biomass Phenology Due to Climate Change and Its Impact on the Breeding Biology of an Insectivorous Bird." *Oecologia* 147 (1): 164–72. https://doi.org/10.1007/s00442-005-0299-6.
Vitti, Joseph J., Sharon R. Grossman, and Pardis C. Sabeti. 2013. "Detecting Natural Selection in Genomic Data." *Annual Review of Genetics* 47: 97–120. https://doi.org/10.1146/annurev-genet-111212-133526.
Walton, James C., Zachary M. Weil, and Randy J. Nelson. 2011. "Influence of Photoperiod on Hormones, Behavior, and Immune Function." *Frontiers in Neuroendocrinology* 32 (3): 303–19. https://doi.org/10.1016/j.yfrne.2010.12.003.
Wang, Dawei, Ning Li, Lin Tian, Fei Ren, Zhengguang Li, Yan Chen, Lan Liu, et al. 2019. "Dynamic Expressions of Hypothalamic Genes Regulate Seasonal Breeding in a Natural Rodent Population." *Molecular Ecology* 28 (15): 3508–22. https://doi.org/10.1111/mec.15161.
Wang, Jian Mei, Yan Ming Zhang, and De Hua Wang. 2006. "Photoperiodic Regulation in Energy Intake, Thermogenesis and Body Mass in Root Voles (Microtus Oeconomus)." *Comparative Biochemistry and Physiology - A Molecular and Integrative Physiology* 145 (4): 546–53. https://doi.org/10.1016/j.cbpa.2006.08.034.
Weaver, David R., Chen Liu, and Steven M. Reppert. 1996. "Nature's Knockout: The Mel1b Receptor Is Not Necessary for Reproductive and Circadian Responses to Melatonin in Siberian Hamsters." *Molecular Endocrinology*. https://doi.org/10.1210/mend.10.11.8923472.
Webster, James R., Ian D. Corson, Roger P. Littlejohn, Shirley K. Stuart, and James M. Suttie. 1999. "Effects of Photoperiod on the Cessation of Growth during Autumn in Male Red Deer and Growth Hormone and Insulin-like Growth Factor-I Secretion." *General and Comparative Endocrinology*. https://doi.org/10.1006/gcen.1998.7230.
West-Eberhard, M. J. 2008. "Phenotypic Plasticity." *Encyclopedia of Ecology, Five-Volume Set*, 2701–7. https://doi.org/10.1016/B978-008045405-4.00837-5.
Whetham, Elizabeth O. 1933. "Factors Modifying Egg Production with Special Reference to Seasonal Changes." *The Journal of Agricultural Science* 23 (3): 383–418. https://doi.org/10.1017/S0021859600053284.
Wolff, J. O., and W. Z. Lidicker Jr. 1980. " Population Ecology of the Taiga Vole, Microtus Xanthognathus , in Interior Alaska ." *Canadian Journal of Zoology* 58 (10): 1800–1812. https://doi.org/10.1139/z80-247.
Wood, Shona, and Andrew Loudon. 2014. "Clocks for All Seasons: Unwinding the Roles and Mechanisms of Circadian and Interval Timers in the Hypothalamus and Pituitary." *Journal of Endocrinology* 222 (2). https://doi.org/10.1530/JOE-14-0141.
———. 2018. "The Pars Tuberalis: The Site of the Circannual Clock in Mammals?" *General and Comparative Endocrinology* 258: 222–35. https://doi.org/10.1016/j.ygcen.2017.06.029.
Woodfill, C. J.I., N. L. Wayne, S. M. Moenter, and F. J. Karsch. 1994. "Photoperiodic Synchronization of a Circannual Reproductive Rhythm in Sheep: Identification of Season-Specific Time Cues." *Biology of Reproduction* 50 (4): 965–76. https://doi.org/10.1095/biolreprod50.4.965.
Wu, Yifei, and Ronald J. Koenig. 2000. "Gene Regulation by Thyroid Hormone." *Trends in Endocrinology and Metabolism* 11 (6): 207–11. https://doi.org/10.1016/S1043-2760(00)00263-0.
Yigit, N., R. Hutterer, B. Krystufek, and G. Amori. 2016. "Microtus Arvalis." He IUCN Red List of Threatened Species 2016. 2016. https://doi.org/https://dx.doi.org/10.2305/IUCN.UK.2016-2.RLTS.T13488A22351133.en.
Yoccoz, N. G., R. A. Ims, and H. Steen. 1993. "Growth and Reproduction in Island and Mainland Populations

of the Vole Microtus Epiroticus." *Canadian Journal of Zoology* 71 (12): 2518–27. https://doi.org/10.1139/z93-345.
Yoshimura, Takashi. 2010. "Neuroendocrine Mechanism of Seasonal Reproduction in Birds and Mammals." *Animal Science Journal* 81 (4): 403–10. https://doi.org/10.1111/j.1740-0929.2010.00777.x.
Zamyatnin, A. A. 1972. "Protein Volume in Solution." *Progress in Biophysics and Molecular Biology* 24 (C): 107–23. https://doi.org/10.1016/0079-6107(72)90005-3.
Zande, L. van de, R. C. van Apeldoorn, A. F. Blijdenstein, D. de Jong, W. van Delden, and R. Bijlsma. 2000. "Microsatellite Analysis of Population Structure and Genetic Differentiation within and between Populations of the Root Vole, Microtus Oeconomus in the Netherlands." *Molecular Ecology* 9 (10): 1651–56. https://doi.org/10.1046/j.1365-294X.2000.01051.x.
Zheng, S.-H., and Z..Q Zhang. 2000. "Late Miocene–Early Pleistocene Micromammals from Wenwanggou of Lingtai, Gansu, China." *Vertebrata Paleasiatica* 38: 58–71.
Zhengjun, Wu. 1996. "Growth and Development of Yangtze Vole (Microtus Fortis Calamorum) in Dongting Lake Area." *Chinese Journal of Zoology* 31 (5): 26–30.
Zub, K., B. Jędrzejewska, W. Jędrzejewski, and K. A. Bartoń. 2012. "Cyclic Voles and Shrews and Non-Cyclic Mice in a Marginal Grassland within European Temperate Forest." *Acta Theriologica* 57 (3): 205–16. https://doi.org/10.1007/s13364-012-0072-2.
Zub, Karol, Zbigniew Borowski, Paulina A. Szafrańska, Monika Wieczorek, and Marek Konarzewski. 2014. "Lower Body Mass and Higher Metabolic Rate Enhance Winter Survival in Root Voles, Microtus Oeconomus." *Biological Journal of the Linnean Society* 113 (1): 297–309. https://doi.org/10.1111/bij.12306.

7. Papers and manuscripts

Review

frontiers in Endocrinology

REVIEW
published: 10 January 2020
doi: 10.3389/fendo.2019.00901

Maternal Photoperiodic Programming: Melatonin and Seasonal Synchronization Before Birth

*Jayme van Dalum†, Vebjørn J. Melum†, Shona H. Wood and David G. Hazlerigg**

Department of Arctic and Marine Biology, UiT – the Arctic University of Norway, Tromsø, Norway

This mini-review considers the phenomenon of maternal photoperiodic programming (MPP). In order to match neonatal development to environmental conditions at the time of birth, mammals use melatonin produced by the maternal pineal gland as a transplacental signal representing ambient photoperiod. Melatonin acts via receptors in the fetal pituitary gland, exerting actions on the developing medio-basal hypothalamus. Within this structure, a central role for specialized ependymal cells known as tanycytes has emerged, linking melatonin to control of hypothalamic thyroid metabolism and in turn to pup development. This review summarizes current knowledge of this programming mechanism, and its relevance in an eco-evolutionary context. Maternal photoperiodic programming emerges as a useful paradigm for understanding how *in utero* programing of hypothalamic function leads to life-long effects on growth, reproduction, health and disease in mammals, including humans.

Keywords: melatonin, pars tuberalis, tanycyte, fetal programming, thyrotropin (TSH—thyroid-stimulating hormone), photoperiodic history, deiodinase, thyroid hormone (T3)

OPEN ACCESS

Edited by:
Claudia Torres-Farfan, Austral University of Chile, Chile

Reviewed by:
Chandana Haldar, Banaras Hindu University, India
Laura Bennet, The University of Auckland, New Zealand

***Correspondence:**
David G. Hazlerigg
david.hazlerigg@uit.no

† These authors share joint first authorship

Specialty section:
This article was submitted to Translational Endocrinology, a section of the journal Frontiers in Endocrinology

Received: *30 September 2019*
Accepted: *10 December 2019*
Published: *10 January 2020*

Citation:
van Dalum J, Melum VJ, Wood SH and Hazlerigg DG (2020) Maternal Photoperiodic Programming: Melatonin and Seasonal Synchronization Before Birth. Front. Endocrinol. 10:901. doi: 10.3389/fendo.2019.00901

INTRODUCTION

Life on a rotating planet brings predictable daily and seasonal environmental challenges to the balancing of energy budgets for biological fitness. Because thermo-energetic challenges are inversely related to body size, the capacity to predict the cyclical environmental changes is of special importance for small animals (1), presumably this is crucial in the neonatal/juvenile period. The light-dark cycle and annually changing day lengths (photoperiod), are the most predictable information sources regarding the time of the day and time of the year. Adult mammals are in direct contact with the photic environment, and translate this signal via the hormone melatonin, to time their own changes in physiology and behavior. Contrastingly, the fetus is isolated from photoperiodic information both because light levels *in utero* are much lower than in the surrounding environment, and light sensing pathways are not fully developed until after birth in many cases (2, 3). To deal with this challenge, mammals use maternal melatonin as a transplacental signal (4), through which the fetus gains information about time of day [for review see (5, 6), and references therein], and about time of year [for review see (7), and references therein]. Several articles in this review series deal with the former aspect, and so we focus here on the latter, which we describe as maternal photoperiodic programming (MPP). We first discuss

the eco-evolutionary importance of MPP; then we go on to review current understanding of how MPP takes place, focussing on the sites of action of melatonin during the fetal and neonatal period.

THE EVOLUTIONARY DRIVERS FOR MPP

While seasonal conditions at any given point in the annual cycle may vary considerably from year to year, photoperiod is the most reliable cue for position in the annual cycle, and hence is a predictor of forthcoming environmental challenges. This in essence is the ultimate evolutionary reason for the evolution of melatonin-based photoperiodic synchronization in mammals. It is also important to appreciate that absolute day length alone is insufficient as a synchronizing signal because all variations in day length, except the solsticial maxima and minima, occur twice in every solar year. Hence the use of photoperiod as a cue must be dependent on prior history of photoperiodic exposure: intermediate photoperiods preceded by the long days of summer presage autumn and winter, whereas intermediate photoperiods preceded by the short days of winter presage spring and summer (**Figure 1A**) [for review see (8)].

This importance of integrating photoperiodic history into the use of photoperiod as a cue is made abundantly clear by a consideration of reproductive development and life-history strategy in short lived rodent species including voles and hamsters (9–11). In such animals the time from conception to reproductive maturity is potentially <2 months, and so multiple generations are typically born within a single annual breeding season. Nonetheless, the optimal life-history strategy for individuals born in the spring is entirely different from that for individuals born late in the breeding season (**Figure 1A**). For the former a "live fast, die young" strategy with fitness success based on producing progeny within the same summer season is appropriate because within the same season there will continue to be sufficient resources for lactation and rearing young. Contrastingly, young born later in the season do not have time for breeding and rearing of young before the autumn decline in resources and increased thermo-energetic demand occurs. As consequence these late born pups delay reproduction until the following year, conserving resources for investment in overwintering survival. In the field, the use of these two alternate life-history strategies as a function of time of birth reveals itself as a bimodal age distribution in wild caught individuals (9–11).

CHARACTERIZATION OF MPP IN THE LABORATORY

In the laboratory it is possible to reveal these alternate strategies simply by manipulation of artificial photoperiod. In the Montane vole (*Microtus montanus*), pups gestated and raised under long photoperiods (16L:8D) delay growth and maturation when exposed to shorter, intermediate photoperiods (14L:10D) at weaning, whereas pups gestated under short photoperiods (8L:16D) undergo accelerated growth and maturation when exposed to the same intermediate photoperiod (12, 13). The use of intermediate photoperiods is a powerful paradigm to show that weaned offspring have a "memory" of prior photoperiodic history. Determining if this "memory" is encoded *in utero* or neonatally, was a challenge addressed by a series of elegant studies by Milton Stetson, Teresa Horton and colleagues, which dissected the origins of this photoperiodic history, both through cross-fostering experiments and by resolving photoperiodic manipulation into gestational, neonatal and post-weaning phases [(12, 14, 15), reviewed in (7, 16)].

Cross fostering experiments in Montane voles demonstrate that the *in utero* environment is where the programming of developmental trajectories occurs (14). Pregnant mothers were kept under long (16L:8D) or short (8L:16D) photoperiods. At birth, half of the young were given to a foster mother who had experienced the same photoperiod as the birth-mother and the other half of the young went to a foster mother who had experienced the opposite photoperiod during pregnancy, compared to the birth-mother. All young were raised under intermediate (14L:10D) photoperiods after birth. The accelerated growth and sexual maturation of short-day gestated voles compared to long-day gestated voles clearly demonstrated the *in utero* transfer of photoperiodic information by the actual birth-mother. The foster mother's photoperiodic history had no effect on the offspring after birth, which excludes the effect of maternal signals transferred through milk. Similar effects of maternal photoperiodic programming have been shown in Siberian hamsters (*Phodopus sungorus*) (15, 17), collared lemmings (*Dicrostonyx groenlandicus*) (18), and meadow voles (*Microtus pennsylvanicus*) (19, 20).

The clear conclusion from these studies is that photoperiod influences reproductive development in a manner dependent on the interaction between photoperiod exposure *in utero* and photoperiod exposure post-weaning. Photoperiod exposure in the intervening neonatal period has little influence, and constitutes a "dead zone" for MPP, probably because at this stage the photo-neuroendocrine system (PNS) is not fully light-responsive and pups typically remain in subterranean nests (21).

MPP IN NON-RODENT SPECIES

Longer-lived, larger mammals also show evidence of MPP. Sexual maturity of red deer gestated under short photoperiods is advanced compared to long photoperiods (22). The effect of gestation is also evident in the prolactin levels of sheep lambs at the time of birth, with levels being lower in short-day gestated lambs than in long-day gestated lambs (23). Moreover, subsequent responses to intermediate (LD12:12) photoperiods after birth were quite different, with prolactin levels rapidly increased in short-day gestated lambs but decreased in long-day gestated lambs. Under natural conditions sheep and other ungulates have a single round of reproduction in a given year,

Abbreviations: Dio2, type 2 deiodinase; Dio3, type 3 deiodinase; MBH, medio basal hypothalamus; MPP, maternal photoperiodic programing; MT1, type 1 melatonin receptor; 3V, 3rd ventricle; PNS, photoneuroendocrine system; PD, pars distalis; PT, pars tuberalis; Px, pinealectomy; SCN, suprachiasmatic nucleus; SCG, superior cervical ganglion; T3, triiodothyronine; T4, thyroxine; TSH, thyroid stimulating hormone.

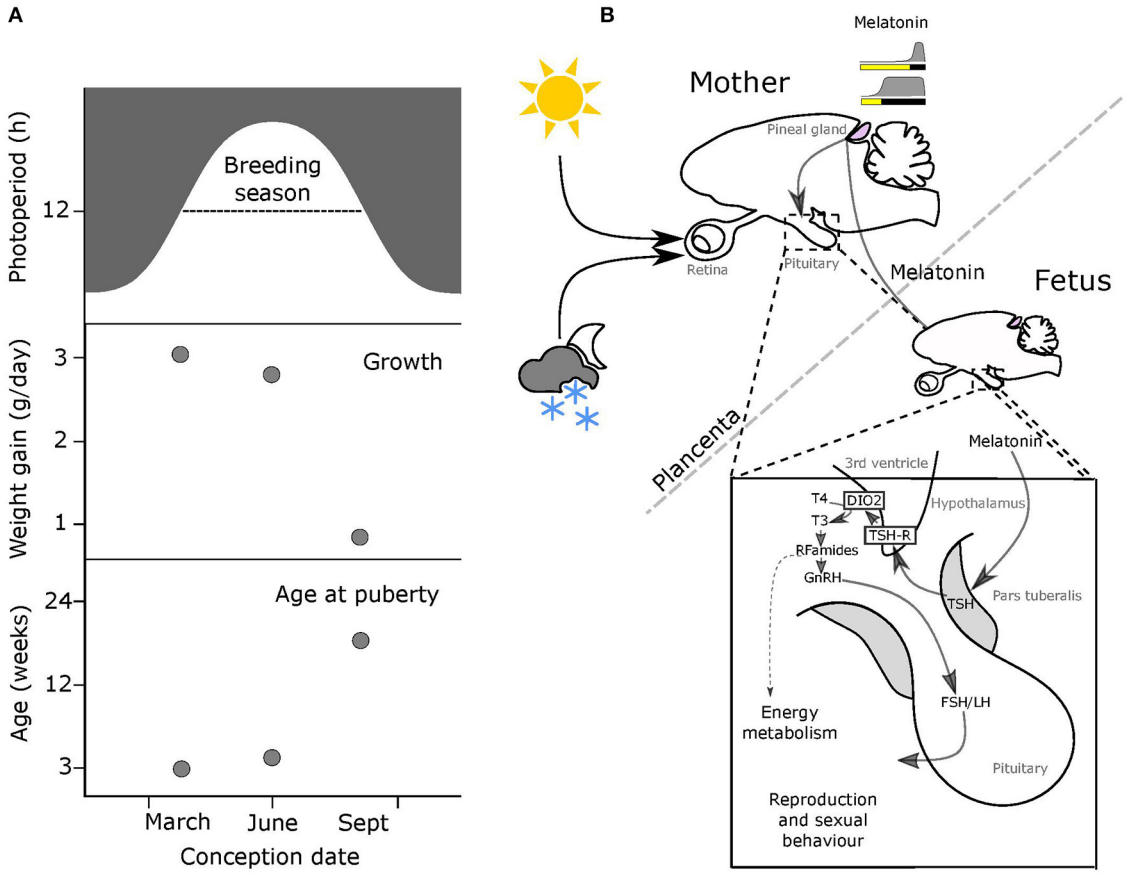

FIGURE 1 | Melatonin-mediated transplacental relay of photoperiodic information. **(A)** The breeding season for small rodents runs from spring through to early autumn (top panel, dashed line). Middle & bottom panels: offspring born early in the breeding season on increasing photoperiods grow fast and breed in the same season, while pups born later on declining photoperiods grow slowly and delay breeding to the following year. **(B)** Actions of maternal melatonin via the pars tuberalis (PT). In both the mother and the fetus, thyrotrophs in the *pars tuberalis* (PT) contain melatonin receptors (MT1), and in response to shorter melatonin signals representing intermediate to long photoperiods these cells secrete thyroid stimulating hormone (TSH). Tanycytes lining the 3rd ventricle, express TSH receptors, and respond to changing levels of PT TSH secretion by modulating relative levels of expression of two thyroid hormone deiodinase enzymes (dio2 and dio3). This affects the local thyroid environment in the MBH, with relatively increased dio2 expresison causing a relative increase in levels of T3 (the active form of TH). This in turn determines the reproductive behavior and energy metabolism of the adult animal.

and this is tightly constrained to an autumn period to ensure that young are born in the spring. Hence in contrast to voles and hamsters, an evolutionary narrative based on alternate life-history strategies cannot apply. Rather it is likely that *in utero* programming establishes the phase for calendar timer mechanisms from birth which then continue throughout life.

ROLE OF MELATONIN IN MPP

Except in early development, the pineal gland of mammals secretes melatonin in a light responsive fashion. The photic input pathway from the retina to the suprachiasmatic nucleus (SCN) drives rhythmic melatonin production from the pineal gland and this melatonin signal is sculpted by photoperiod to provide an internal endocrine representation for external photoperiod, this is the PNS (**Figure 1B**) [for review see (8, 24)]. Through this means, short (winter) photoperiods are represented by increased duration of nocturnally elevated plasma melatonin titers and long (summer) photoperiods by shorter duration for nocturnally elevated titers (**Figure 1B**).

The pivotal role of maternal pineal melatonin production in MPP was first demonstrated by a series of studies in Siberian hamsters (*P. sungorus*) [(17, 25–27), for review see (28)]. Injection of melatonin to pineal-intact mothers caused a suppression of pup testicular growth, dependent on the phase of melatonin injection relative to the light dark cycle. Specifically, injections in afternoon were most effective, because melatonin delivered at this phase extended the endogenous maternal melatonin signal to give it a profile mimicking a short photoperiod (25). Complete removal of the maternal melatonin signal by pinealectomy (px) blocked the effect of *in utero* photoperiod manipulations on pup development (26), as did fitting of pineal-intact mothers with continuous release

melatonin implants (27). Collectively, these studies reveal that maternal pineal melatonin production relays information about ambient photoperiod to the developing fetus.

MELATONIN SITES OF ACTION IN THE DEVELOPING FETUS

The use of the radio-analog of melatonin, 2-iodo-melatonin (29), led to the identification of melatonin binding sites in a range of central and peripheral fetal tissues (30). In fetal rodents, melatonin binding sites representing high affinity G–protein coupled receptors are consistently observed in the pars tuberalis (PT) and pars distalis (PD) of the pituitary and in the SCN [(31–33), for review see (30, 34)]. While type 1 melatonin receptor (mt1) expression disappears from the PD within a few days of birth (35), expression in the PT persists, and this site has emerged as the key site for the seasonal actions of melatonin in adult mammals [for review see (8, 30, 36–38)].

The PT shows the highest concentration of melatonin receptors of all mammalian tissues, and these mediate photoperiodic control of TSH production by the PT through a circadian-based "coincidence timer" mechanism (39, 40). TSH produced by the PT acts locally on the TSH receptors (TSHR) expressed in tanycyte cells lining the third ventricle of the hypothalamus (41, 42). Ligand binding to TSHR regulates the expression of deiodinase seleno-enzymes (Dio2 and Dio3), which in turn controls the local metabolism of thyroid hormone within the mediobasal hypothalamus (MBH), driving seasonal adaptations (**Figure 1B**) [(41, 42), for review see (24, 43)].

FETAL PT AS A TARGET FOR THE MATERNAL MELATONIN SIGNAL

Based on the paradigm emerging in adult mammals, Sáenz de Miera and colleagues have explored the involvement of the PT and MBH in MPP (44). This study demonstrates that in the Siberian hamster, expression of *TSH* in the fetal PT at the time of birth depends on maternal photoperiod, with high expression in pups gestated on LP but low expression in pups gestated on SP. These effects on PT *TSH* gene expression persisted through the perinatal period. As in adult mammals, *TSHR* expression is found in the ependymal region, and corresponding effects of photoperiod on the expression of dio2 and dio3 were observed (i.e., high *dio2* and low *dio3* in LP gestated pups and the converse in SP gestated pups). These studies provide evidence that the fetal PT mediates seasonal programming effects of maternal melatonin.

MPP ESTABLISHES PHOTOPERIODIC HISTORY-DEPENDENCE AT THE LEVEL OF THE TANYCYTES

Maternal photoperiod not only sets neonatal levels of TSH and deiodinase gene expression, associated with different trajectories for gonadal development, it also influences the sensitivity of MBH deiodinase gene expression to photoperiod exposure post-weaning. Specifically SP-gestation was associated with more dio2 and less dio3 expression in response to intermediate photoperiods than was the case for LP-gestated pups (**Figure 2**). Hence MPP is seen in hypothalamic expression of the key enzymes controlling thyroid status in the developing hypothalamus.

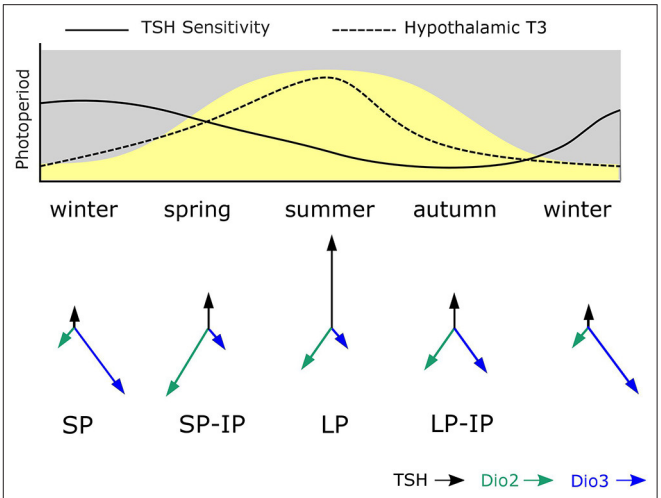

FIGURE 2 | Model for photoperiodic history-dependence through shifting tanycyte sensitivity to TSH. The solid line in the upper panel shows how tanycyte sensitivity to TSH is presumed to change during the course of the year. During winter PT TSH secretion is photoperiodically inhibited and TSH-sensitivity becomes heightened. In spring increased TSH production is a potent stimulus for increased dio2 expression due to high TSH sensitivity established in the winter phase. As spring becomes summer, sensitivity to TSH in the tanycytes declines and so high dio2 expression is not maintained despite continued exposure to long photoperiods. Then in autumn, the combination of declining TSH secretion and reduced sensitivity to TSH established in the summer phase leads to loss of dio2 expression and increased dio3 expression. The system then resets to the winter. The predicted consequences of this for hypothalamic T3 levels is shown as a dashed line—the asymmetry of this relative to the curve for photoperiod represents photoperiodic history-dependence. The lower panel shows the predicted consequences of this process for TSH, dio2 and dio3 expression—where arrow lengths represent strength of expression.

This effect does not seem to derive from downstream programming of both melatonin synthesis in the weaned pups, and sensitivity to melatonin at the level of the pup PT, but rather, it derives from history-dependent differences in sensitivity to TSH produced by the pup PT. This was demonstrated by icv injection of exogenous TSH which had a bigger inductive effect on *dio2* expression in SP- than in LP-gestated pups (**Figure 2**). Since no overt changes in *TSHR* expression in the MBH were seen in these experiments (44), other causes for this apparent shift in TSH sensitivity must be sought.

The identification of tanycytes as the site at which MPP generates photoperiodic history dependence echoes data from studies in the Soay sheep (45). Here, the onset of refractoriness to SP-exposure, i.e., another example of photoperiodic history-dependence, also appears at the level of *dio2/dio3* expression in tanycytes independently of changes in *TSH* expression in the PT.

FUNCTIONAL ROLES FOR HYPOTHALAMIC TANYCYTES

If the significance of these programming phenomena are to be properly understood it is imperative that attention focuses on tanycyte function. Tanycytes are a specialized form of ependymal cell derived from a glial cell lineage shared with microglial cells—for review see (46–49). They differ morphologically from the cuboidal epithelial cells that line most of the ventricular walls in that they have a bipolar morphology with extensive processes projecting into the parenchymal tissue surrounding the ependymal zone. Detailed analysis suggests that hypothalamic tanycytes may be subclassified based upon their anatomical location and upon their expression profiles (50)—but how these differences relate to differences in function remains uncertain. Much has been written on the possible functions of these cells, and at least three broad classes of cellular process have emerged: metabolic sensing (48, 51–53) regulation of blood/CSF/brain interfaces (50) and neurogenesis (54). The regulation of deiodinase gene expression and consequent effects on the local thyroid environment is but one molecular function of tanycytes, and may impact on any or all of the above cellular processes. At one level dio2/dio3 are regulators of uptake of active thyroid hormone into the circumventricular environment, and so serve a role as enzymatic "gatekeepers" (55). At another level, because T3 levels in the hypothalamus interact with the AMP-kinase dependent energy sensing pathways (56), shifts in deiodinase expression may be linked to metabolic sensing and responses. Thirdly, because T3 is strongly implicated in neurogenic pathways (57–59), shifts in T3 status dependent on photoperiodic history may impact in neurogenesis-dependent neural plasticity in the basal hypothalamus (54, 60, 61). Much remains to be done to establish an integrated view on the consequences of photoperiodic programming of tanycyte function.

MPP IN THE WIDER CONTEXT OF PROGRAMMING BY EARLY LIFE EXPERIENCE

The life-long consequences of early life experience is a topic of major biomedical importance. Epidemiological studies in humans demonstrate a positive correlation between low birthweight and susceptibility to obesity and cardiovascular health problems in adult life (62–66). Attempts to understand the mechanisms behind this phenomenon have led to studies in rats, in which maternal undernutrition leads to a chronic increase in susceptibility to weight gain when fed a "cafeteria" diet (67). Remarkably, this effect is completely reversed by treatment with the lipostatic hormone, leptin, in a narrow window in the neonatal period, which has closed by 10 days post-partum [(67), for review see (68)]. The mechanisms behind this effect of leptin remain unclear, it is probably not a coincidence that the ependymal zone of the MBH expresses high levels of leptin receptor at post-natal day 4, which then decline rapidly over the following week (69). This pattern is the inverse of that seen in the arcuate nuclei, and points to a transient role for leptin in establishing energy regulatory circuits in the neonatal period. The mapping of leptin receptor expression to the region encompassing the tanycytes involved in MPP suggests that this region is at the crux of mechanisms through which hypothalamic control circuits are established in early life. For this reason, we suggest that MPP, which relies on a harmless and non-invasive environmental perturbation (i.e., light) and acts through a well-defined pharmacological pathway (i.e., MT1 receptors in the PT), is a useful experimental paradigm for investigating the mechanisms through which early life experience establishes long term patterns of hypothalamic regulation.

AUTHOR CONTRIBUTIONS

All authors listed have made a substantial, direct and intellectual contribution to the work, and approved it for publication.

FUNDING

VM was supported by the Tromsø forskningsstiftelse (TFS) starter grant TFS2016SW, fonds Paul-Mandel pour les neurosciences, and the Norwegian research council Aurora travel grant, awarded to SW. JD was supported by HFSP program grant RGP0030/2015-C301 Evolution of seasonal timers, awarded to DH. The publication charges for this article have been funded by a grant from the publication fund of UiT The Arctic University of Norway.

REFERENCES

1. Hazlerigg DG, Tyler NJC. Activity patterns in mammals: circadian dominance challenged. *PLoS Biol.* (2019) 17:e3000360.doi: 10.1371/journal.pbio.3000360
2. Moore RY. Development of the suprachiasmatic nucleus. In: Klein DC, Moore RY, Reppert SM, editors. *Reppert Suprachiasmatic Nucleus: The Mind's Clock*. Oxford: University Press (1991). p. 391–404.
3. Ribelayga C, Gauer F, Pévet P, Simonneaux V. Ontogenesis of hydroxyindole-O-methyltransferase gene expression and activity in the rat pineal gland. *Dev Brain Res.* (1998) 110:235–9.doi: 10.1016/S0165-3806(98)00114-X
4. Yellon SM, Longo LD. Melatonin rhythms in fetal and maternal circulation during pregnancy in sheep. *Am J Physiol.* (1987) 252:E799–802.doi: 10.1152/ajpendo.1987.252.6.E799
5. Davis FC. Melatonin: role in development. *J Biol Rhythms.* (1997) 12:498–508.doi: 10.1177/074873049701200603
6. Hassell KJ, Reiter RJ, Robertson NJ. Melatonin and its role in neurodevelopment during the perinatal period: a review. *Fetal Matern Med Rev.* (2013) 24:76–107.doi: 10.1017/S0965539513000089
7. Horton TH. Fetal origins of developmental plasticity: animal models of induced life history variation. *Am J Hum Biol.* (2005) 17:34–43.doi: 10.1002/ajhb.20092
8. West AC, Wood SH. Seasonal physiology: making the future a thing of the past. *Curr Opin Physiol.* (2018) 5:1–8.doi: 10.1016/j.cophys.2018.04.006
9. Negus NC, Berger PJ, Forslund LG. Reproductive strategy of microtus montanus. *J Mammal.* (1977) 58:347–53.doi: 10.2307/1379333

10. Negus NC, Berger PJ, Brown BW. Microtine population dynamics in a predictable environment. *Can J Zool.* (1986) 64:785–92.doi: 10.1139/z86-117
11. Negus NC, Berger PJ, Pinter AJ. Phenotypic plasticity of the montane vole (*Microtus montanus*) in unpredictable environments. *Can J Zool.* (1992) 70:2121–4.doi: 10.1139/z92-285
12. Horton TH. Growth and reproductive development of male microtus montanus is affected by the prenatal photoperiod. *Biol Reprod.* (1984) 31:499–504.doi: 10.1095/biolreprod31.3.499
13. Horton TH. Growth and maturation in *Microtus montanus* : effects of photoperiods before and after weaning. *Can J Zool.* (1984) 62:1741–6.doi: 10.1139/z84-256
14. Horton TH. Cross-fostering of voles demonstrates *in utero* effect of photoperiod. *Biol Reprod.* (1985) 33:934–9.doi: 10.1095/biolreprod33.4.934
15. Stetson MH, Elliott JA, Goldman BD. Maternal transfer of photoperiodic information influences the photoperiodic response of prepubertal djungarian hamsters (Phodopus Sungorus Sungorus)1. *Biol Reprod.* (1986) 34:664–9.doi: 10.1095/biolreprod34.4.664
16. Horton TH, Stetson MH. Maternal transfer of photoperiodic information in rodents. *Anim Reprod Sci.* (1992) 30:29–44.doi: 10.1016/0378-4320(92)90004-W
17. Stetson MH, Ray SL, Creyaufmiller N, Horton TH. Maternal transfer of photoperiodic information in Siberian hamsters. II. the nature of the maternal signal, time of signal transfer, and the effect of the maternal signal on peripubertal reproductive development in the absence of photoperiodic input1. *Biol Reprod.* (1989) 40:458–65.doi: 10.1095/biolreprod40.3.458
18. Gower BA, Nagy TR, Stetson MH. Pre- and postnatal effects of photoperiod on collared lemmings (*Dicrostonyx groenlandicus*). *Am J Physiol.* (1994) 267:R879–87.doi: 10.1152/ajpregu.1994.267.4.R879
19. Lee TM, Spears N, Tuthill CR, Zucker I. Maternal melatonin treatment influences rates of neonatal development of meadow vole pups1. *Biol Reprod.* (1989) 40:495–502.doi: 10.1095/biolreprod40.3.495
20. Lee TM. Development of meadow voles is influenced postnatally by maternal photoperiodic history. *Am J Physiol.* (1993) 265:R749–55.doi: 10.1152/ajpregu.1993.265.4.R749
21. Gruder-Adams S, Getz LL. Comparison of the mating system and paternal behavior in microtus ochrogaster and *M. pennsylvanicus*. *J Mammal.* (1985) 66:165–7.doi: 10.2307/1380976
22. Adam CL, Kyle CE, Young P. Influence of prenatal photoperiod on postnatal reproductive development in male red deer (*Cervus elaphus*). *J Reprod Fertil.* (1994) 100:607–11.doi: 10.1530/jrf.0.1000607
23. Ebling FJP, Wood RI, Suttie JM, Adel TE, Foster DL. Prenatal photoperiod influences neonatal prolactin secretion in the sheep. *Endocrinology.* (1989) 125:384–91.doi: 10.1210/endo-125-1-384
24. Dardente H, Wood S, Ebling F, Sáenz de Miera C. An integrative view of mammalian seasonal neuroendocrinology. *J Neuroendocrinol.* (2019) 31:e12729.doi: 10.1111/jne.12729
25. Horton TH, Lynn Ray S, Stetson MH. Maternal transfer of photoperiodic information in Siberian hamsters. III. Melatonin injections program postnatal reproductive development expressed in constant lights1. *Biol Reprod.* (1989) 41:34–9.doi: 10.1095/biolreprod41.1.34
26. Horton TH, Stachecki SA, Stetson MH. Maternal transfer of photoperiodic information in Siberian hamsters. IV. Peripubertal reproductive development in the absence of maternal photoperiodic signals during gestation1. *Biol Reprod.* (1990) 42:441–9.doi: 10.1095/biolreprod42.3.441
27. Horton TH, Lynn Ray S, Rollag MD, Yellon SM, Stetson MH. Maternal transfer of photoperiodic information in Siberian hamsters. V. Effects of melatonin implants are dependent on photoperiod. *Biol Reprod.* (1992) 47:291–6.doi: 10.1095/biolreprod47.2.291
28. Horton TH, Stetson MH. Maternal programming of the fetal brain dictates the response of juvenile Siberian hamsters to photoperiod: dissecting the information transfer system. *J Exp Zool.* (1990) 256:200–2.doi: 10.1002/jez.1402560443
29. Vakkuri O, Lämsä E, Rahkamaa E, Ruotsalainen H, Leppäluoto J. Iodinated melatonin: preparation and characterization of the molecular structure by mass and 1H NMR spectroscopy. *Anal Biochem.* (1984) 142:284–9.doi: 10.1016/0003-2697(84)90466-4
30. Morgan PJ, Barrett P, Howell HE, Helliwell R. Melatonin receptors: localization, molecular pharmacology and physiological significance. *Neurochem Int.* (1994) 24:101–46.doi: 10.1016/0197-0186(94)90100-7
31. Rivkees SA, Reppert SM. Appearance of melatonin receptors during embryonic life in Siberian hamsters (*Phodopus sungorous*). *Brain Res.* (1991) 568:345–9.doi: 10.1016/0006-8993(91)91424-Y
32. Vanecek J. The melatonin receptors in rat ontogenesis. *Neuroendocrinology.* (1988) 48:201–3.doi: 10.1159/000125008
33. Williams LM, Martinoli MG, Titchener LT, Pelletier G. The ontogeny of central melatonin binding sites in the rat. *Endocrinology.* (1991) 128:2083–90.doi: 10.1210/endo-128-4-2083
34. Vanecek J. Cellular mechanisms of melatonin action. *Physiol Rev.* (1998) 78:687–721.doi: 10.1152/physrev.1998.78.3.687
35. Johnston JD, Messager S, Ebling FJP, Williams LM, Barrett P, Hazlerigg DG. Gonadotrophin-releasing hormone drives melatonin receptor down-regulation in the developing pituitary gland. *Proc Natl Acad Sci USA.* (2003) 100:2831–5.doi: 10.1073/pnas.0436184100
36. Dardente H. Does a melatonin-dependent circadian oscillator in the pars tuberalis drive prolactin seasonal rhythmicity? *J Neuroendocrinol.* (2007) 19:657–66.doi: 10.1111/j.1365-2826.2007.01564.x
37. Wood S, Loudon A. Clocks for all seasons: unwinding the roles and mechanisms of circadian and interval timers in the hypothalamus and pituitary. *J Endocrinol.* (2014) 222:R39–59.doi: 10.1530/JOE-14-0141
38. Wood SH. How can a binary switch within the pars tuberalis control seasonal timing of reproduction? *J Endocrinol.* (2018) 239:R13–25.doi: 10.1530/JOE-18-0177
39. Dardente H, Wyse CA, Birnie MJ, Dupré SM, Loudon ASI, Lincoln GA, et al. A molecular switch for photoperiod responsiveness in mammals. *Curr Biol.* (2010) 20:2193–8.doi: 10.1016/j.cub.2010.10.048
40. Masumoto K, Ukai-Tadenuma M, Kasukawa T, Nagano M, Uno KD, Tsujino K, et al. Acute induction of Eya3 by late-night light stimulation triggers TSHβ expression in photoperiodism. *Curr Biol.* (2010) 20:2199–206.doi: 10.1016/j.cub.2010.11.038
41. Hanon EA, Lincoln GA, Fustin J-M, Dardente H, Masson-Pévet M, Morgan PJ, et al. Ancestral TSH mechanism signals summer in a photoperiodic mammal. *Curr Biol.* (2008) 18:1147–52.doi: 10.1016/j.cub.2008.06.076
42. Ono H, Hoshino Y, Yasuo S, Watanabe M, Nakane Y, Murai A, et al. Involvement of thyrotropin in photoperiodic signal transduction in mice. *Proc Natl Acad Sci USA.* (2008) 105:18238–42.doi: 10.1073/pnas.0808952105
43. Dardente H, Hazlerigg DG, Ebling FJP. Thyroid hormone and seasonal rhythmicity. *Front Endocrinol.* (2014) 5:19.doi: 10.3389/fendo.2014.00019
44. Sáenz de Miera C, Bothorel B, Jaeger C, Simonneaux V, Hazlerigg D. Maternal photoperiod programs hypothalamic thyroid status via the fetal pituitary gland. *Proc Natl Acad Sci USA.* (2017) 114:8408–13.doi: 10.1073/pnas.1702943114
45. Sáenz de Miera C, Hanon EA, Dardente H, Birnie M, Simonneaux V, Lincoln GA, et al. Circannual variation in thyroid hormone deiodinases in a short-day breeder. *J Neuroendocrinol.* (2013) 25:412–21.doi: 10.1111/jne.12013
46. Rodríguez EM, Blázquez JL, Pastor FE, Peláez B, Peña P, Peruzzo B, Amat P. Hypothalamic tanycytes: a key component of brain–endocrine interaction. *Int Rev Cytol.* (2005) 247:89–164.doi: 10.1016/S0074-7696(05)47003-5
47. Rodríguez EM, Blá Zquez B JL, Guerra M. The design of barriers in the hypothalamus allows the median eminence and the arcuate nucleus to enjoy private milieus: the former opens to the portal blood and the latter to the cerebrospinal fluid. *Peptides.* (2010) 31:757–76.doi: 10.1016/j.peptides.2010.01.003
48. Bolborea M, Dale N. Hypothalamic tanycytes: potential roles in the control of feeding and energy balance. *Trends Neurosci.* (2013) 36:91–100.doi: 10.1016/j.tins.2012.12.008
49. Lewis JE, Ebling FJP. Tanycytes as regulators of seasonal cycles in neuroendocrine function. *Front Neurol.* (2017) 8:79.doi: 10.3389/fneur.2017.00079
50. Prevot V, Dehouck B, Sharif A, Ciofi P, Giacobini P, Clasadonte J. The versatile tanycyte: a hypothalamic integrator of reproduction and energy metabolism. *Endocr Rev.* (2018) 39:333–68.doi: 10.1210/er.2017-00235
51. Frayling C, Britton R, Dale N. ATP-mediated glucosensing by hypothalamic tanycytes. *J Physiol.* (2011) 589:2275–86.doi: 10.1113/jphysiol.2010.202051

52. Lazutkaite G, Soldà A, Lossow K, Meyerhof W, Dale N. Amino acid sensing in hypothalamic tanycytes via umami taste receptors. *Mol Metab.* (2017) 6:1480–92.doi: 10.1016/j.molmet.2017.08.015
53. Balland E, Dam J, Langlet F, Caron E, Steculorum S, Messina A, et al. Hypothalamic tanycytes are an ERK-gated conduit for leptin into the brain. *Cell Metab.* (2014) 19:293–301.doi: 10.1016/j.cmet.2013.12.015
54. Rizzoti K, Lovell-Badge R. Pivotal role of median eminence tanycytes for hypothalamic function and neurogenesis. *Mol Cell Endocrinol.* (2017) 445:7–13.doi: 10.1016/j.mce.2016.08.020
55. Barrett P, Ebling FJP, Schuhler S, Wilson D, Ross AW, Warner A, et al. Hypothalamic thyroid hormone catabolism acts as a gatekeeper for the seasonal control of body weight and reproduction. *Endocrinology.* (2007) 148:3608–17.doi: 10.1210/en.2007-0316
56. López M, Varela L, Vázquez MJ, Rodríguez-Cuenca S, González CR, Velagapudi VR, et al. Hypothalamic AMPK and fatty acid metabolism mediate thyroid regulation of energy balance. *Nat Med.* (2010) 16:1001–8.doi: 10.1038/nm.2207
57. Lezoualc'h F, Seugnet I, Monnier AL, Ghysdael J, Behr JP, Demeneix BA. Inhibition of neurogenic precursor proliferation by antisense alpha thyroid hormone receptor oligonucleotides. *J Biol Chem.* (1995) 270:12100–8.doi: 10.1074/jbc.270.20.12100
58. López-Juárez A, Remaud S, Hassani Z, Jolivet P, Pierre Simons J, Sontag T, et al. Thyroid hormone signaling acts as a neurogenic switch by repressing sox2 in the adult neural stem cell niche. *Cell Stem Cell.* (2012) 10:531–43.doi: 10.1016/j.stem.2012.04.008
59. Remaud S, Gothié JD, Morvan-Dubois G, Demeneix BA. Thyroid hormone signaling and adult neurogenesis in mammals. *Front Endocrinol.* (2014) 5:62.doi: 10.3389/fendo.2014.00062
60. Migaud M, Batailler M, Segura S, Duittoz A, Franceschini I, Pillon D. Emerging new sites for adult neurogenesis in the mammalian brain: a comparative study between the hypothalamus and the classical neurogenic zones. *Eur J Neurosci.* (2010) 32:2042–52.doi: 10.1111/j.1460-9568.2010.07521.x
61. Migaud M, Batailler M, Pillon D, Franceschini I, Malpaux B. Seasonal changes in cell proliferation in the adult sheep brain and pars tuberalis. *J Biol Rhythms.* (2011) 26:486–96.doi: 10.1177/0748730411420062
62. Barker DJ, Godfrey K, Gluckman P, Harding J, Owens J, Robinson J. Fetal nutrition and cardiovascular disease in adult life. *Lancet.* (1993) 341:938–41.doi: 10.1016/0140-6736(93)91224-A
63. Barker D, Eriksson J, Forsén T, Osmond C. Fetal origins of adult disease: strength of effects and biological basis. *Int J Epidemiol.* (2002) 31:1235–9.doi: 10.1093/ije/31.6.1235
64. Bateson P, Barker D, Clutton-Brock T, Deb D, D'Udine B, Foley RA, et al. Developmental plasticity and human health. *Nature.* (2004) 430:419–21.doi: 10.1038/nature02725
65. Gluckman PD, Hanson MA. Living with the past: evolution, development, and patterns of disease. *Science.* (2004) 305:1733–6.doi: 10.1126/science.1095292
66. Roseboom T, de Rooij S, Painter R. The dutch famine and its long-term consequences for adult health. *Early Hum Dev.* (2006) 82:485–91.doi: 10.1016/j.earlhumdev.2006.07.001
67. Vickers MH, Gluckman PD, Coveny AH, Hofman PL, Cutfield WS, Gertler A, et al. Neonatal leptin treatment reverses developmental programming. *Endocrinology.* (2005) 146:4211–6.doi: 10.1210/en.2005-0581
68. Vickers MH. Developmental programming and adult obesity: the role of leptin. *Curr Opin Endocrinol Diabetes Obes.* (2007) 14:17–22.doi: 10.1097/MED.0b013e328013da48
69. Cottrell EC, Cripps RL, Duncan JS, Barrett P, Mercer JG, Herwig A, et al. Developmental changes in hypothalamic leptin receptor: relationship with the postnatal leptin surge and energy balance neuropeptides in the postnatal rat. *Am J Physiol Integr Comp Physiol.* (2009) 296:R631–9.doi: 10.1152/ajpregu.90690.2008

Conflict of Interest: The authors declare that the research was conducted in the absence of any commercial or financial relationships that could be construed as a potential conflict of interest.

Paper I

© 2020. Published by The Company of Biologists Ltd | Journal of Experimental Biology (2020) 223, jeb230987. doi:10.1242/jeb.230987

RESEARCH ARTICLE

Gonads or body? Differences in gonadal and somatic photoperiodic growth response in two vole species

Laura van Rosmalen[1,*], Jayme van Dalum[2], David G. Hazlerigg[2] and Roelof A. Hut[1]

ABSTRACT

To optimally time reproduction, seasonal mammals use a photoperiodic neuroendocrine system (PNES) that measures photoperiod and subsequently drives reproduction. To adapt to late spring arrival at northern latitudes, a lower photoperiodic sensitivity and therefore a higher critical photoperiod for reproductive onset is necessary in northern species to arrest reproductive development until spring onset. Temperature–photoperiod relationships, and hence food availability–photoperiod relationships, are highly latitude dependent. Therefore, we predict PNES sensitivity characteristics to be latitude dependent. Here, we investigated photoperiodic responses at different times during development in northern (tundra or root vole, *Microtus oeconomus*) and southern vole species (common vole, *Microtus arvalis*) exposed to constant short (SP) or long photoperiod (LP). Although the tundra vole grows faster under LP, no photoperiodic effect on somatic growth is observed in the common vole. In contrast, gonadal growth is more sensitive to photoperiod in the common vole, suggesting that photoperiodic responses in somatic and gonadal growth can be plastic, and might be regulated through different mechanisms. In both species, thyroid-stimulating hormone β-subunit (*Tshβ*) and iodothyronine deiodinase 2 (*Dio2*) expression is highly increased under LP, whereas *Tshr* and *Dio3* decrease under LP. High *Tshr* levels in voles raised under SP may lead to increased sensitivity to increasing photoperiods later in life. The higher photoperiodic-induced *Tshr* response in tundra voles suggests that the northern vole species might be more sensitive to thyroid-stimulating hormone when raised under SP. In conclusion, species differences in developmental programming of the PNES, which is dependent on photoperiod early in development, may form different breeding strategies as part of latitudinal adaptation.

KEY WORDS: Latitudinal adaptation, *Microtus*, Pars tuberalis, Photoperiodism, Seasonality

INTRODUCTION

Organisms use intrinsic annual timing mechanisms to adaptively prepare behavior, physiology and morphology for the upcoming season. In temperate regions, decreased ambient temperature is associated with reduced food availability during winter, which will impose increased energetic challenges that may, dependent on the species, prevent the possibility of successfully raising offspring. Annual variation in ambient temperature shows large fluctuations between years, with considerable day-to-day variations, whereas annual changes in photoperiod provide a consistent year-on-year signal for annual phase. This has led to convergent evolutionary processes in many organisms to use day length as the most reliable cue for seasonal adaptations.

In mammals, the photoperiodic neuroendocrine system (PNES) measures photoperiod and subsequently drives annual rhythms in physiology and reproduction (Fig. 1) (for review, see Dardente et al., 2018; Hut, 2011; Nakane and Yoshimura, 2019). The neuroanatomy of this mechanism has been mapped in detail, and genes and promoter elements that play a crucial role in this response pathway have been identified in several mammalian species (Dardente et al., 2010; Hanon et al., 2008; Hut, 2011; Masumoto et al., 2010; Nakao et al., 2008; Ono et al., 2008; Sáenz De Miera et al., 2014; Wood et al., 2015), including the common vole (Król et al., 2012).

Voles are small grass-eating rodents with a short gestation time (i.e. 21 days). They can have several litters a year, while their offspring can reach sexual maturity within 40 days during spring and summer. Overwintering voles may, however, delay reproductive activity by as much as 7 months (Wang et al., 2019). In small rodents, photoperiods experienced early in development determine growth rate and reproductive development. Photoperiodic reactions to intermediate day lengths depend on prior photoperiodic exposure (Hoffmann, 1978; Horton, 1984, 1985; Horton and Stetson, 1992; Prendergast et al., 2000; Sáenz de Miera et al., 2017; Stetson et al., 1986; Yellon and Goldman, 1984). By using information about day length early in life, young animals will be prepared for the upcoming season. Presumably, crucial photoperiod-dependent steps in PNES development take place in young animals to secure an appropriate seasonal response later in life (Sáenz de Miera et al., 2017, 2020; Sáenz De Miera, 2019; van Dalum et al., 2020). In Siberian hamsters, photoperiodic programming takes place downstream of melatonin secretion at the level of *Tshr*, with expression increased in animals born under short photoperiod (SP), associated with subsequent increases in thyroid-stimulating hormone (TSH) sensitivity (Sáenz de Miera et al., 2017).

Primary production in the food web of terrestrial ecosystems is temperature dependent (Robson, 1967; Peacock, 1976; Malyshev et al., 2014). Small herbivores may therefore show reproductive development either as a direct response to temperature increases (opportunistic response), or as a response to photoperiod that forms an annual proxy for seasonal temperature changes (photoperiodic response), or a combination of the two (Caro et al., 2013). *Microtus* species adjust their photoperiodic response such that reproduction in spring starts when primary food production starts (Baker, 1938).

Photoperiodically induced reproduction should start at longer photoperiods in more northern populations, as a specific ambient spring temperature at higher latitudes coincides with longer photoperiods compared with lower latitudes (Hut et al., 2013). To adapt to late spring arrival at northern latitudes, a lower sensitivity to

[1]Chronobiology Unit, Groningen Institute for Evolutionary Life Sciences, University of Groningen, 9747 AG Groningen, The Netherlands. [2]Department of Arctic and Marine Biology, UiT – the Arctic University of Norway, NO-9037 Tromsø, Norway.

*Author for correspondence (l.van.rosmalen@rug.nl)

L.v., 0000-0003-1273-1225

Received 12 June 2020; Accepted 2 September 2020

Journal of Experimental Biology (2020) 223, jeb230987. doi:10.1242/jeb.230987

List of abbreviations

Dio2	iodothyronine deiodinase 2
Dio3	iodothyronine deiodinase 3
Kiss1	Kisspeptin
LP	long photoperiod
Mtnr1a (*Mt1*)	melatonin receptor 1a
Npvf (*Rfrp3*)	neuropeptide VF precursor
PNES	photoperiodic neuroendocrine system
SP	short photoperiod
Tshβ	thyroid-stimulating hormone β-subunit
Tshr	thyroid-stimulating hormone receptor

photoperiod, and therefore a longer critical photoperiod, is expected to be necessary in northern species. This is crucial to arrest reproductive development until arrival of spring. Moreover, (epi)genetic adaptation to local annual environmental changes may create latitudinal differences in photoperiodic responses and annual timing mechanisms.

Microtus is a genus of voles found in the northern hemisphere, ranging from close to the equator to arctic regions, which makes it an excellent genus to study latitudinal adaptation of photoperiodic responses (for review, see Hut et al., 2013). In order to understand the development of the PNES for vole species with different paleogeographic origins, we investigated photoperiodic responses at different time points during development by exposing northern [tundra or root vole, *Microtus oeconomus* (Pallas 1776)] and southern vole species [common vole, *Microtus arvalis* (Pallas 1778)] to constant short or long photoperiods in the laboratory. Animals from our two vole laboratory populations originate from the same latitude in the Netherlands (53°N) where both populations overlap. This is for the common vole the center (mid-latitude) of its distribution range (38–62°N), while our laboratory tundra voles originate from a postglacial relict population at the southern boundary of its European geographical range (48–72°N). Assuming that the latitudinal distribution range is limited by seasonal adaptation, it is expected that latitudinal adaptation is optimal at the center of the distribution and suboptimal towards the northern and southern boundaries. Although this assumption remains to be confirmed at genetic and physiological levels, it does lead to the expectation that the PNES of the common vole is better adapted to the local annual environmental changes of the Netherlands (53°N, distribution center) than that of the tundra vole which is at its southern distribution boundary. Because lower latitudes have higher spring temperatures at a specific photoperiod (Hut et al., 2013), we hypothesize that gonadal activation through PNES signaling occurs under shorter photoperiods in common voles than in tundra voles.

MATERIALS AND METHODS

Animals and experimental procedures

All experimental procedures were carried out according to the guidelines of the animal welfare body (IvD) of the University of Groningen, and all experiments were approved by the Centrale Commissie Dierproeven of the Netherlands (CCD, license number: AVD1050020171566). The Groningen common vole breeding colony started with voles (*M. arvalis*) obtained from the Lauwersmeer area (Netherlands, 53°24′N, 6°16′E) (Gerkema et al., 1993), and was occasionally supplemented with wild caught voles from the same region to prevent the laboratory population from inbreeding. The Groningen tundra vole colony started with voles (*M. oeconomus*) obtained from four different regions in the Netherlands (described in Van de Zande et al., 2000). Both breeding colonies were maintained at the University of Groningen

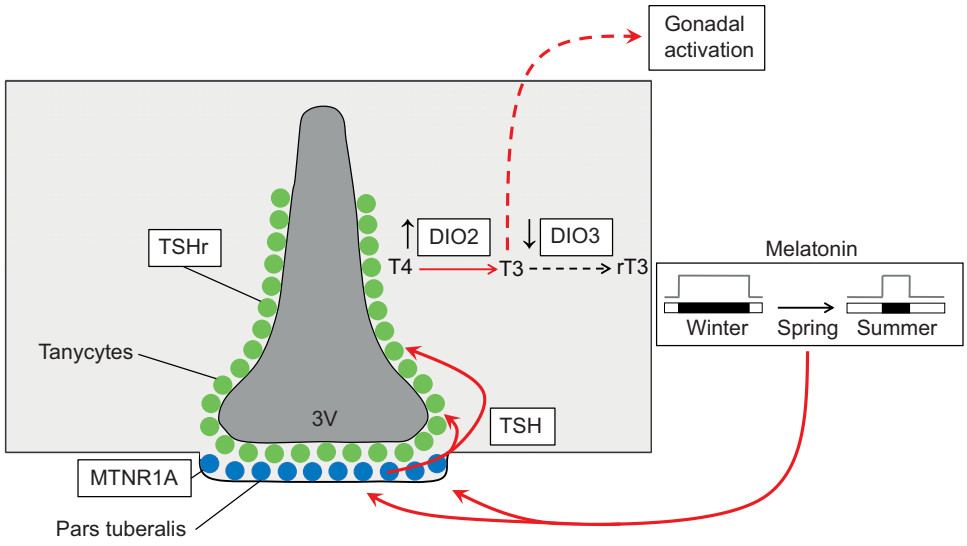

Fig. 1. The photoperiodic neuroendocrine system of a long-day breeding mammal. Light is perceived by specialized mammalian non-visual retinal photoreceptors that signal to the suprachiasmatic nucleus (SCN). The SCN acts via the paraventricular nucleus on the pineal gland, such that the duration of melatonin production during darkness changes over the year to represent the inverse of day length. Melatonin binds to its receptor (MTNR1A/ MT1) in the pars tuberalis (PT) of the anterior lobe of the pituitary gland (von Gall et al., 2002, 2005; Klosen et al., 2019; Williams and Morgan, 1988). Under long days, pineal melatonin is released for a short duration and thyroid-stimulating hormone β-subunit (Tshβ) is increased in the PT, forming an active dimer (TSH) with chorionic gonadotropin α-subunit (αGSU) (Magner, 1990). PT-derived TSH acts locally through TSH receptors (TSHr) found in the tanycytes in the neighboring mediobasal hypothalamus. The tanycytes produce increased iodothyronine deiodinase 2 (DIO2) and decreased DIO3 levels (Guerra et al., 2010; Hanon et al., 2008; Nakao et al., 2008), which leads to higher levels of the active form of thyroid hormone (T3) and lower levels of inactive forms of thyroid hormone (T4 and rT3) (Lechan and Fekete, 2005). In small mammals, it is likely that T3 acts 'indirectly', through KNDy (kisspeptin, neurokinin B and dynorphin) neurons of the arcuate nucleus (for review, see Simonneaux, 2020) in turn controlling the activity of gonadotropin-releasing hormone (GnRH) neurons. GnRH neurons project to the pituitary to induce gonadotropin release, which stimulates gonadal growth. The arrow connectors indicate stimulatory connections; 3V, third ventricle.

Journal of Experimental Biology (2020) 223, jeb230987. doi:10.1242/jeb.230987

as outbred colonies and provided the voles for this study. All breeding pairs were kept in climate-controlled rooms, at an ambient temperature of 21±1°C and 55±5% relative humidity and housed in transparent plastic cages (15 cm×40 cm×24 cm) provided with sawdust, dried hay, an opaque PVC tube and *ad libitum* water and food (standard rodent chow, no. 141005; Altromin International, Lage, Germany). Over the last 4 years, our captive laboratory populations are housed under long photoperiod (LP) conditions (16 h:8 h light:dark) and switched to SP (8 h:16 h light:dark) for ∼2 months at least twice a year.

The voles used in the experiments (61 males, 56 females) were both gestated and born under either LP or SP. In the center of the distribution range of *M. arvalis*, 16 h:8 h light:dark in spring occurs on 17 May, and 8 h:16 h light:dark occurs on 13 January. In the center of the distribution range of *M. oeconomus*, 16 h:8 h light:dark in spring occurs on 1 May, and 8 h:16 h light:dark occurs on 1 February. Maximum and minimum photoperiods experienced by *M. arvalis* and *M. oeconomus* at the center of their distributional ranges are 17 h:7 h and 7.5 h:16.5 h light:dark, and 19 h:5 h and 6 h:18 h light:dark, respectively. Pups were weaned and transferred to individual cages (15 cm×40 cm×24 cm) when 21 days old but remained exposed to the same photoperiod as during both gestation and birth. All voles were weighed at post-natal days 7, 15, 21, 30, 42 and 50 (Fig. 2).

Tissue collection

In order to follow development, animals were killed by decapitation, with prior sedation by CO_2, 17±1 h after lights off (*Tshβ* expression peaking in pars tuberalis) (Masumoto et al., 2010), at 15, 21, 30 and 50 days old. Brains were removed with great care to include the stalk of the pituitary containing the pars tuberalis. The hypothalamus with the pars tuberalis was dissected as described in Prendergast et al. (2013), the optic chiasm at the anterior border, and the mammillary bodies at the posterior border, and laterally at the hypothalamic sulci. The remaining hypothalamic block was cut dorsally 3–4 mm from the ventral surface. The extracted hypothalamic tissue was flash-frozen in liquid N_2 and stored at −80°C until RNA extraction. Reproductive organs were dissected and cleaned of fat, and wet masses of paired testis, paired ovary and uterus were measured (±0.0001 g).

RNA extraction, reverse transcription and real-time quantitative PCR

Total RNA was isolated from the dissected part of the hypothalamus using TRIzol reagent according to the manufacturer's protocol (Invitrogen, Carlsbad, CA, USA). In short, frozen pieces of tissue (∼0.02 g) were homogenized in 0.5 ml TRIzol reagent in a TissueLyser II (Qiagen, Hilden, Germany) (2×2 min at 30 Hz) using tubes containing a 5 mm RNase free stainless-steel bead. Subsequently, 0.1 ml chloroform was added for phase separation. Following RNA precipitation by 0.25 ml of 100% isopropanol, the obtained pellet was washed with 0.5 ml of 75% ethanol. Depending on the size, RNA pellets were diluted in an adequate volume of RNase-free H_2O (range 20–50 µl) and quantified on a Nanodrop 2000 spectrophotometer (Thermo Scientific, Waltham, MA, USA). RNA concentrations were between 109 and 3421 ng µl^{-1} and ratio of the absorbance at 260/280 nm was between 1.62 and 2.04. After DNA removal by DNase I treatment (Invitrogen), an equal quantity of RNA from each sample was used for cDNA synthesis using RevertAid H minus first-strand cDNA synthesis reagents (Thermo Scientific). Reverse transcription (RT; 40 µl) reactions were prepared using 2 µg RNA, 100 µmol l^{-1} Oligo(dT)$_{18}$, 5× reaction buffer, 20 U µl^{-1} RiboLock RNase Inhibitor, 10 mmol l^{-1} dNTP Mix and RevertAid H Minus Reverse Transcriptase (200 U µl^{-1}). Concentrations used for RT reactions can be found in the supplementary information (Table S1). RNA was reversed transcribed using a thermal cycler (S1000; Bio-Rad, Hercules, CA, USA). Incubation conditions used for RT were: 45°C for 60 min followed by 70°C for 5 min. Transcript levels were quantified by real-time qPCR using SYBR Green (KAPA SYBR FAST qPCR Master Mix, Kapa Biosystems). Twenty microliter (2 µl cDNA +18 µl Mastermix) reactions were carried out *in duplo* for each sample using 96-well plates in a Fast Real-Time PCR System (CFX96, Bio-Rad). Primers for genes of interest were designed using Primer-BLAST (NCBI) and optimized annealing temperature (T_m) and primer concentration. All primers used in this study were designed based on the annotated *Microtus ochrogaster* genome (NCBI:txid79684, GCA_000317375.1), and subsequently checked for gene specificity in the genomes of the common vole (*Microtus arvalis*) and the tundra vole (*Microtus oeconomus*), which were published by us on NCBI (NCBI:txid47230, GCA_007455615.1 and NCBI:txid64717, GCA_007455595.1) (Table S2). Thermal cycling conditions used can be found in the Table S3. Relative mRNA expression levels were calculated based on the ΔΔCT method using *Gapdh* as the reference (housekeeping) gene (Pfaffl, 2001).

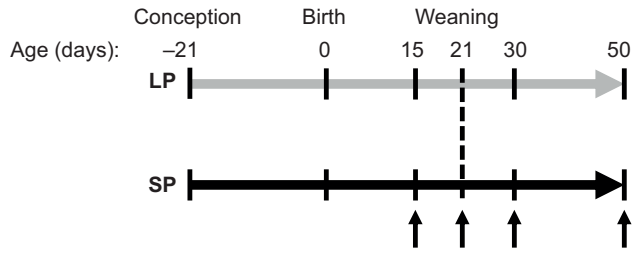

Fig. 2. Experimental design. Animals were constantly exposed to either long photoperiod (LP; 16 h:8 h light:dark) or short photoperiod (SP; 8 h:16 h light:dark) from gestation onwards. Arrows indicate sampling points for tissue collection. Age in days is depicted above the timeline. Vertical dashed line represents time of weaning (21 days old).

Statistical analysis

Sample size (N=4) was determined by a power calculation (α=0.05, power=0.80) based on the effect size (d=2.53) of an earlier study, in which gonadal mass was assessed in female voles under three different photoperiods (Król et al., 2012). Effects of age, photoperiod and species on body mass, reproductive organs and gene expression levels were determined using a type I two-way ANOVA. Tukey's honestly significant difference *post hoc* pairwise comparisons were used to compare groups at specific ages. Statistical significance was determined at P<0.05. Statistical results can be found in the Table S4. All statistical analyses were performed using RStudio (version 1.2.1335) (http://www.R-project.org/), and figures were generated using the ggplot2 package (Wickham, 2016).

RESULTS

Body mass responses for males and females

Photoperiod during gestation did not affect birth weight in either species (Fig. 3A,B). Both tundra vole males and females grow faster under LP compared with SP conditions (males, $F_{1,303}$=15.0, P<0.001; females, $F_{1,307}$=10.2, P<0.01) (Fig. 3A,B). However, no effect of photoperiod on body mass over time was observed in

Journal of Experimental Biology (2020) 223, jeb230987. doi:10.1242/jeb.230987

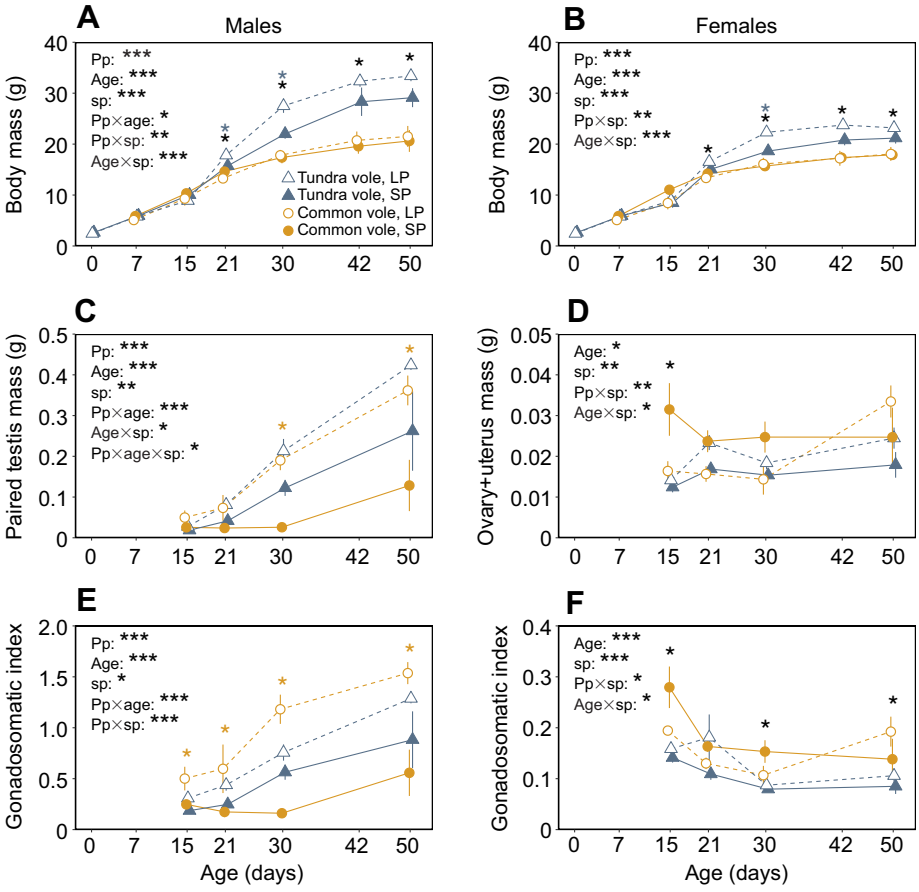

Fig. 3. Effects of constant photoperiod on growth and gonadal development. Graphs show body mass growth curves for (A) males and (B) females, (C) paired testis mass, (D) paired ovary+uterus mass, (E,F) gonadal development relative to body mass (gonadosomatic index) for common voles (orange circles) and tundra voles (blue triangles), continuously exposed to either LP (open symbols, dashed lines) or SP (filled symbols, continuous lines). Lines connect averages representing non-repeated measures. Data are means±s.e.m. Male tundra vole LP: *N*=22; male tundra vole SP: *N*=15; male common vole LP: *N*=19: male common vole SP: *N*=16; female tundra vole LP: *N*=21; female tundra vole SP: *N*=17; female common vole LP: *N*=12; female common vole SP: *N*=16. Significant effects (type I two-way ANOVA, *post hoc* Tukey's test) of photoperiod at specific ages are indicated for tundra voles (blue asterisks) and common voles (orange asterisks). Significant effects of species are indicated by black asterisks. Significant effects of photoperiod (pp), age, species (sp) and interactions are shown in each graph: **P*<0.05, ***P*<0.01, ****P*<0.001. Statistics results for ANOVAs (photoperiod, age and species) can be found in Table S4.

common vole males or females (males, $F_{1,243}$=2.1, not significant (n.s.); females, $F_{1,234}$=0.6, n.s.) (Fig. 3A,B).

Gonadal responses for males

Common vole males show faster testis growth under LP compared with SP [testis, $F_{1,33}$=17.01, P<0.001; gonoadosomatic index (GSI), $F_{1,33}$=32.2, P<0.001] (Fig. 3C,E). This photoperiodic effect on testis development is less pronounced in tundra voles (testis, $F_{1,35}$=8.3, P<0.01; GSI, $F_{1,35}$=9.3, P<0.01) (Fig. 3C,E).

Gonadal responses for females

Common vole female gonadal mass (i.e. paired ovary+uterus) is slightly higher at the beginning of development (until 30 days old) under SP compared with LP conditions ($F_{1,17}$=10.4, P<0.01) (Fig. 3D), while the opposite effect was observed in tundra voles ($F_{1,36}$=9.0, P<0.01) (Fig. 3D). For both species, these photoperiodic effects disappeared when gonadal mass was corrected for body mass (common vole, $F_{1,17}$=2.5, n.s.; tundra vole, $F_{1,36}$=2.3, n.s.) (Fig. 3F). Interestingly, gonadal mass significantly increased in 30- to 50-day-old LP common vole females ($F_{1,5}$=7.7, P<0.05) (Fig. 3D), but not in tundra voles ($F_{1,11}$=2.2, n.s.) or under SP conditions (common vole, $F_{1,7}$=0, n.s.; tundra, $F_{1,7}$=1.0, n.s.).

Photoperiod-induced changes in hypothalamic gene expression

Melatonin binds to its receptors in the pars tuberalis where it inhibits *Tshβ* expression. In males of both species, *Mtnr1a* (*Mt1*, melatonin receptor) expression in the hypothalamic block with preserved pars tuberalis was highly expressed, but unaffected by photoperiod or age (photoperiod, $F_{1,43}$=0.08, n.s.; age, $F_{3,42}$=0.94, n.s.) (Fig. 4A). In females, *Mtnr1a* expression increases approximately 2-fold with age in both species ($F_{3,40}$=9.04, P<0.001) (Fig. 4B), but no effects of photoperiod were observed ($F_{1,40}$=1.59, n.s.).

In males and females of both species, *Tshβ* expression is dramatically elevated under LP throughout development (tundra vole males, $F_{1,27}$=49.3, P<0.001; common vole males, $F_{1,27}$=21.3, P<0.001; tundra vole females, $F_{1,30}$=63.7, P<0.001; common vole females, $F_{1,22}$=60.9, P<0.001) (Fig. 4C,D). Furthermore, a clear peak in *Tshβ* expression is observed in 21-day-old LP common vole males, while such a peak is lacking in tundra vole males. However, *Tshβ* expression in tundra vole males remains similar over the course of development under LP conditions. In females, photoperiodic responses in *Tshβ* expression did not differ between species ($F_{1,40}$=0.02, n.s.).

TSHβ binds to its receptor (TSHr) in the tanycytes around the third ventricle. In tundra vole males and females, *Tshr* expression is higher under SP compared with LP (males, $F_{1,27}$=23.7, P<0.001; females, $F_{1,30}$=6.2, P<0.05) (Fig. 4E,F), while photoperiodic-induced changes in *Tshr* expression are smaller in common vole males and females (males, $F_{1,27}$=23.7, P<0.01; females, $F_{1,22}$=4.3, P<0.05) (Fig. 4E,F). Photoperiodic responses in *Tshr* expression are significantly larger in tundra vole males compared with common vole males ($F_{1,42}$=8.17, P<0.01) (Fig. 4E).

In males of both species, the largest photoperiodic effect on *Dio2*, which is increased by TSHβ, is found at weaning (day 21), with higher levels under LP compared with SP ($F_{1,42}$=14.7, P<0.001) (Fig. 4G). Interestingly, *Dio3* is lower in these animals ($F_{1,42}$=4.8, P<0.05) (Fig. 4I), leading to a high *Dio2*:*Dio3* ratio under LP at the beginning of development ($F_{1,42}$=8.5, P<0.01) (Fig. 4K). We found a similar pattern in females, with higher *Dio2* under LP compared

Journal of Experimental Biology (2020) 223, jeb230987. doi:10.1242/jeb.230987

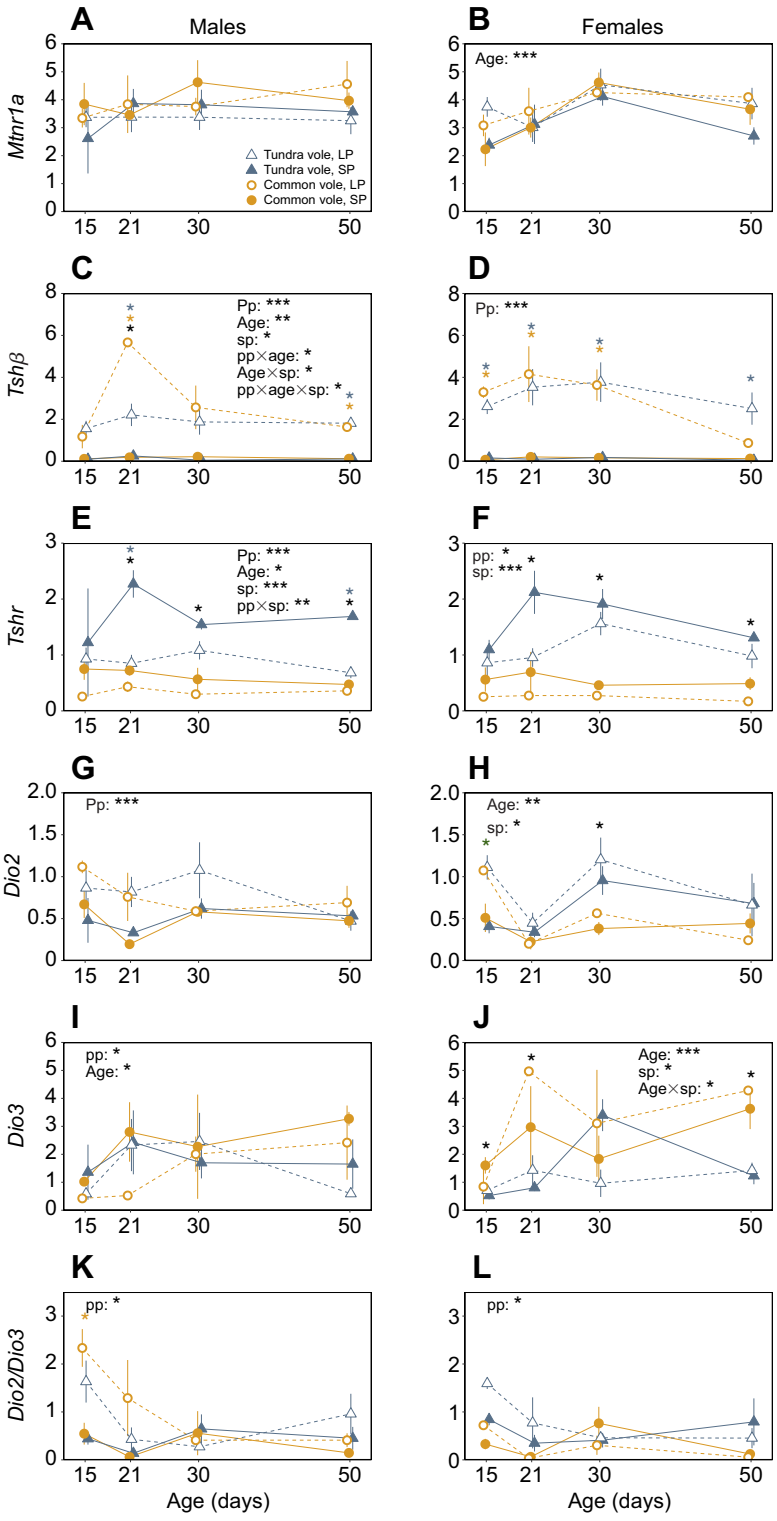

Fig. 4. Effects of constant photoperiod on gene expression levels in the developing hypothalamus. Graphs show relative gene expression levels of (A,B) *Mtnr1a*, (C,D) *Tshβ*, (E,F) *Tshr*, (G,H) *Dio2*, (I,J) *Dio3* and (K,L) *Dio2*:*Dio3* expression in the hypothalamus of developing common vole (orange circles) and tundra vole (blue triangles) males and females, respectively, under LP (open symbols, dashed lines) or SP (filled symbols, continuous lines). Lines connect averages representing non-repeated measures. Data are means±s.e.m. Male tundra vole LP: *N*=16; male tundra vole SP: *N*=13; male common vole LP: *N*=14; male common vole SP: *N*=15; female tundra vole LP: *N*=16; female tundra vole SP: *N*=16; female common vole LP: *N*=8; female common vole SP: *N*=16. Significant effects (type I two-way ANOVA, *post hoc* Tukey's test) of photoperiod at specific ages are indicate for tundra voles (blue asterisks) and common voles (orange asterisks). Significant effects of species are indicated by black asterisks. Significant effects of photoperiod (pp), age, species (sp) and interactions are shown in each graph: **P*<0.05, ***P*<0.01, ****P*<0.001. Statistics results for ANOVAs (photoperiod, age and species) can be found in Table S4.

with SP at the beginning of development (i.e. day 15) ($F_{3,10}$=8.9, P<0.01) (Fig. 4H).

In males of both species, no effects of photoperiod on Eyes Absent 3 (*Eya3*, transcription factor for the *Tshβ* promoter) ($F_{1,42}$=1.72, n.s.), Kisspeptin (*Kiss1*, hypothalamic gene involved in reproduction) ($F_{1,42}$=2.96, n.s.) and Neuropeptide VF precursor (*Npvf*, *Rfrp3*, hypothalamic gene involved in seasonal growth and reproduction) ($F_{1,42}$=0.61, n.s.) expression were found (Fig. S1A,C,E). In females, both *Kiss1* ($F_{3,40}$=4.82, P<0.01) and *Npvf* are higher under LP dependent on age ($F_{3,40}$=3.51, P<0.05) (Fig. S1D,F), but there were no effects of photoperiod on *Eya3* ($F_{1,40}$=0.30, n.s.) (Fig. S1B).

A positive correlation between the levels of *Tshβ* and *Dio2* expression was found only at the beginning of development (15 days, $F_{1,25}$=12.6, P<0.01; 21 days, $F_{1,28}$=4.0, P<0.1; 30 days, $F_{1,30}$=0.1, n.s.; 50 days, $F_{1,23}$=0.1, n.s.) (Fig. 5A–D). Moreover, no significant relationship between *Dio2* and *Dio3* expression was found (Fig. 5E–H).

Journal of Experimental Biology (2020) 223, jeb230987. doi:10.1242/jeb.230987

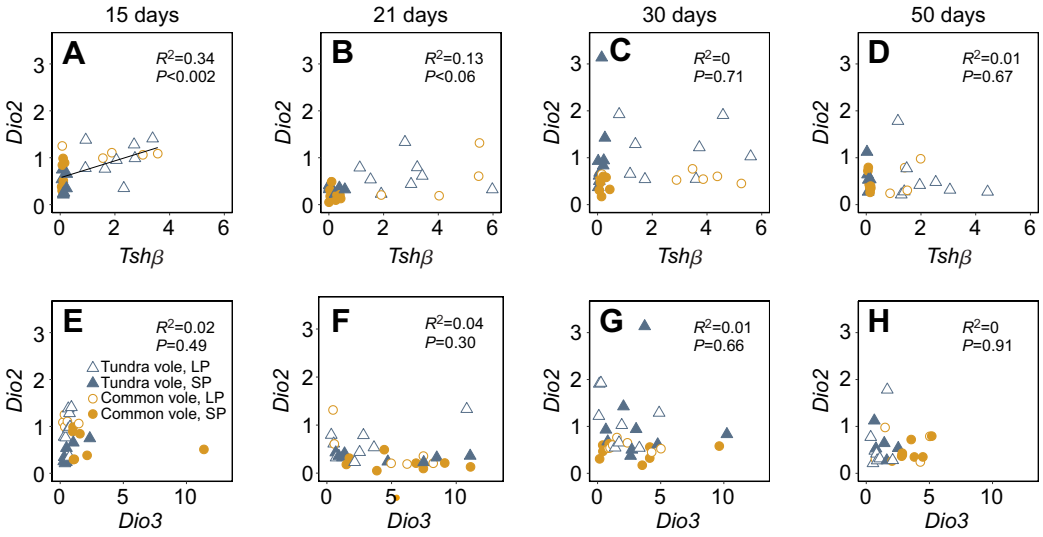

Fig. 5. Relationship between hypothalamic *Dio2*, *Dio3* and *Tshβ* expression in voles at different ages. Scatterplot of *Tshβ* versus *Dio2* gene expression at (A) 15 days old, (B) 21 days old, (C) 30 days old and (D) 50 days old. Scatterplot of *Dio3* versus *Dio2* gene expression at (E) 15 days old, (F) 21 days old, (G) 30 days old and (H) 50 days old. Open symbols indicate LP animals, filled symbols indicate SP animals. Blue triangles represent tundra voles, orange circles represent common voles. One outlier in *Dio2* expression was detected by an outlier analysis, although removing the outlier did not change the fitted linear models.

DISCUSSION

This study demonstrates different effects of constant photoperiod on the PNES in two different vole species: the common vole and the tundra vole. Overall, somatic growth is photoperiodically sensitive in the tundra vole while gonadal growth is photoperiodically sensitive in the common vole. Hypothalamic *Tshβ*, *Tshr*, *Dio2* and *Dio3* expression are highly affected by photoperiod and age, and some species differences were observed in the magnitude of these effects. Although the differences found between both vole species may provide interesting information on variation in annual timing, the data should be interpreted with caution because we cannot exclude relaxation of natural selection in our laboratory colonies.

Photoperiod-induced changes in somatic growth and gonadal development

These data demonstrate that photoperiod early in life affects pup growth in the tundra vole (Fig. 3A), and reproductive development in common vole males (Fig. 3C,E). In females, a similar photoperiodic effect on somatic growth is observed as in males. Tundra vole females grow faster under LP compared with SP, while there is no difference in growth rate between LP and SP in the common vole (Fig. 3B). In the tundra vole, somatic growth is plastic, whereas in the common vole, gonadal growth is plastic. Garden dormouse (*Eliomys quercinus*) born late in the season grow and fatten twice as fast as early born animals (Stumpfel et al., 2017), in order to partly compensate for the limited time before winter onset. This overwintering strategy might be favorable for animals with a short breeding season (i.e. at high latitude), and may also be used in tundra voles as they gain weight faster when raised under LP (i.e. late in the season) compared with SP (i.e. early in the season). Southern arvicoline species have longer breeding seasons (Tkadlec, 2000), and therefore have more time left to compensate body mass when born late in the season. Therefore, somatic growth rate may depend to a lesser extent on the timing of birth in southern species as observed in common voles raised under SP or LP.

Common vole female gonadal mass is slightly higher under SP compared with LP at the beginning of development (Fig. 3D,F). In contrast, in Siberian hamsters, uterus mass is increased after 3 weeks of constant LP exposure, which continued throughout development (Ebling, 1994; Phalen et al., 2010). In common voles, female gonadal mass increased from day 30 to day 50 in LP animals, whereas gonadal mass in SP females remained the same (Fig. 3D,F). Also, tundra vole female gonadal mass is not increased in this period of development under both LP and SP conditions. Puberty onset, based on gonadal mass, in common voles is later compared with Siberian hamsters (Phalen et al., 2010), while earlier compared with tundra voles. Therefore, LP common voles increase gonadal mass earlier in development (i.e. >30 days old) compared with LP tundra voles (i.e. >50 days old), in order to increase reproductive activity and prepare for pregnancy. An alternative hypothesis is that the tundra vole may sense 16 h:8 h light:dark not as too short for spring stimulation of reproduction, but rather as too long to switch off reproduction in autumn. These results suggest that tundra vole females have a different reproductive onset compared with common vole females under constant photoperiods. However, based on our data we cannot conclude whether the timing of the breeding season is different between those species, as we did not use naturally changing photoperiods to simulate different seasons. This can be tested by exposing voles to a broader range of different photoperiod regimes, mimicking spring and autumn photoperiod conditions in the laboratory. Our data show that the common vole invests more energy in gonadal growth, whereas the tundra vole invests more energy in body mass growth independent of gonadal growth under LP. This suggests that both body mass growth and gonadal development are plastic and can be differentially affected by photoperiod, perhaps through different mechanisms. In Siberian hamsters, the growth hormone (GH) axis is involved in photoperiodic regulation of body mass (Dumbell et al., 2015; Scherbarth et al., 2015). Our results indicate a different role for the GH axis in seasonal body mass regulation in tundra voles and common voles.

Photoperiod-induced changes in hypothalamic gene expression

Common vole males show a clear photoperiodic response in both hypothalamic gene expression and gonadal activation. Genes in the

female PNES are strongly regulated by photoperiod, which is not reflected in gonadal growth. In tundra voles, PNES gene expression profiles change accordingly with photoperiod, although the gonadal response is less sensitive to photoperiod, which is similar to the photoperiodic response observed in house mice (Masumoto et al., 2010). Because the tundra vole is more common at high latitudes, where they live in tunnels covered by snow in winter and early spring, photoperiodic information might be blocked during a large part of the year for these animals (Evernden and Fuller, 1972; Korslund, 2006). For this reason, other environmental cues, such as metabolic status, may integrate in the PNES in order to regulate the gonadal response and therefore timing of reproduction.

Photoperiod-induced changes in *Tshβ* sensitivity

In both vole species, *Tshβ* expression is higher under LP conditions during all stages of development (Fig. 4C,D), which is in agreement with previous studies in other mammals, birds and fish (for review, see Dardente et al., 2014; Nakane and Yoshimura, 2019). We sampled 17 h after lights off, when *Tshβ* expression is peaking. EYA3 is a transcription factor that binds to the *Tshβ* promoter, which promotes transcription. Perhaps we sampled too late in order to find photoperiodic-induced changes in *Eya3* expression (Fig. S1A,B), as in mice *Eya3* peaks 12 h after lights off under LP conditions (Masumoto et al., 2010).

TSH binds to its receptor in the tanycytes around the third ventricle. Although less pronounced in common voles, elevated *Tshr* expression under SP (Fig. 4E,F) may be caused by low *Tshβ* levels in the same animals (Fig. 4C,D). In a previous study, a similar relationship between *Tshr* and *Tshβ* expression in the pars tuberalis and medial basal hypothalamus of Siberian hamsters was observed (Sáenz de Miera et al., 2017). In our study, the ependymal paraventricular zone (PVZ) around the third ventricle of the brain and the pars tuberalis are both included in samples for RNA extraction and qPCR, therefore we cannot distinguish between these two brain areas. Brains were collected 17 h after lights off, when *Tshr* mRNA levels in the pars tuberalis and PVZ are predicted to be similar based on studies in sheep (Hanon et al., 2008). Similar circadian expression patterns are expected in brains of seasonal long-day breeding rodents. Therefore, the observed increase in *Tshr* expression in SP voles, of both species and sexes (Fig. 4E,F), may relate to high TSH density in the tanycytes lining the third ventricle, which might lead to increased TSH sensitivity later in life. The high *Tshr* expression in voles developing under SP (Fig. 4E,F) may favor a heightened sensitivity to increasing TSH and photoperiods later in life. This in turn would promote increased DIO2 and decreased DIO3 levels in spring. Interestingly, photoperiodic responses on *Tshr* are more pronounced in tundra voles than in common voles, suggesting that tundra voles are more sensitive to TSH protein when raised under SP. However, TSH is a dimer of gonadotropin α-subunit (αGSU) and TSHβ, and we did not measure αGSU levels in this study.

Our laboratory vole populations are originally from the same latitude in the Netherlands (53°N) where both populations overlap. This is for the common vole the center (mid-latitude) of its distribution range, while our laboratory tundra voles are from a relict population at the lower boundary of its geographical range, which is an extension for this species to operate at southern limits. For this reason, local adaptation of the PNES may have evolved differently in the two species. The elevated *Tshr* expression and therefore the possible higher sensitivity to photoperiod in tundra voles raised under SP, might favor photoperiodic induction of reproduction earlier in the spring. This might be a strategy to cope with the extremely early spring onset at the low latitude for this relict tundra vole population.

Interestingly, the large peak in *Tshβ* expression (Fig. 4C) that is only observed in 21-day-old LP common vole males may be responsible for the drastic increase in testis mass when animals are 30 days old. Faster testis growth in LP common vole males (Fig. 3C) might be induced by the 2- to 3-fold higher *Tshβ* levels compared with LP tundra vole males (Fig. 4C). However, these data have to be interpreted with caution as the current study only considered gene expression levels and did not investigate protein levels.

The reduced *Tshr* expression under LP early in life (Fig. 4E,F) may be induced by epigenetic mechanisms, such as increased levels of DNA methylation in the promoter of this gene, which will reduce its transcription. A role for epigenetic regulation of seasonal reproduction has been proposed based on studies of the adult hamster hypothalamus (Stevenson and Prendergast, 2013). In order to study the effects of photoperiodic programming in development, DNA methylation patterns of specific promoter regions of photoperiodic genes at different circadian time points need to be studied in animals exposed to different environmental conditions earlier in development.

Photoperiod-induced changes in hypothalamic *Dio2*:*Dio3* expression

The photoperiodic-induced *Tshβ* and *Tshr* expression patterns are only reflected in the downstream *Dio2*:*Dio3* expression differences at the beginning of development (Fig. 4K,L), suggesting that this part of the pathway is sensitive to TSH at a very young age. However, *Dio2* and *Dio3* are also responsive to metabolic status, which can change as a consequence of changing DIO2:DIO3 levels. Tundra and common vole females show similar photoperiodic-induced *Tshβ* patterns, while photoperiodic responses on *Tshr* are larger in tundra voles. The higher *Tshr* levels in tundra voles may be responsible for the higher *Dio2*, and lower *Dio3* levels in tundra vole females compared with common vole females. However, the photoperiodic-induced differences in gene expression levels between species are not reflected in female gonadal mass, indicating that additional signaling pathways are involved in regulating ovary and uterus growth. In males, *Dio2*:*Dio3* patterns are mainly determined by photoperiod, while different photoperiodic responses between species are lacking.

Dio2 and *Tshβ* expression correlate only at the beginning of development (i.e. at 15 days old) (Fig. 5A–D). These results are partly in agreement with the effects of constant photoperiod on hypothalamic gene expression in the Siberian hamster, showing induction of *Dio2* at birth when gestated under LP, and induction of *Dio3* at 15 days old when exposed to SP (Sáenz de Miera et al., 2017). Furthermore, it is thought that *Dio2*:*Dio3* expression profiles will shift due to both photoperiodic and metabolic changes rather than by constant conditions. Also, negative feedback on the *Dio2*:*Dio3* system might be induced by changes in metabolic status. In wild populations of Brandt's voles (*Lasiopodomys brandtii*), seasonal regulation of these genes show elevated *Dio2*:*Dio3* ratios in spring under natural photoperiods, suggesting a crucial role for those genes in determining the onset of the breeding season in wild populations (Wang et al., 2019).

Photoperiod-induced changes in hypothalamic *Kiss1* and *Npvf* expression

In females, both *Kiss1* and *Npvf* expression is higher under LP dependent on age (Fig. S1D,F), whereas in males no effects of photoperiod on these genes are found (Fig. S1C,E). Other studies

report inconsistent photoperiodic and seasonal effects on arcuate nucleus *Kiss1* expression in different species, which may be related to a negative sex steroid feedback on *Kiss1*-expressing neurons (for review, see Simonneaux, 2020). For this reason, sex- and species-dependent levels of steroid negative feedback on both *Kiss1*- and *Rfrp*-expressing neurons in the caudal hypothalamus are expected.

In conclusion, our data show that somatic growth is photoperiodic sensitive in the tundra vole while gonadal growth is photoperiodic sensitive in the common vole. Our finding that the SP-induced *Tshr* expression is more pronounced in the developing hypothalamus of the tundra vole, may lead to the expectation that programming of TSH sensitivity is an important regulator of the PNES in this species. Reproductive development seems to be more dominated by photoperiodic responses in the common vole than in the tundra vole. It is not excluded that the PNES of the tundra vole has lost its photoperiodic capacity and instead has adopted responses to other environmental variables in its post-glacial relict population at the southern edge of its distribution. This raises the possibility that the tundra vole has a stronger response to other environmental cues (e.g. temperature, food, snow cover). Both vole species develop their PNES differently, depending on photoperiod early in development, indicating that they use environmental cues differently to time reproduction.

Acknowledgements
We would like to thank Saskia Helder for her valuable help in animal care. We thank L. van de Zande for his critical comments on the paper.

Competing interests
The authors declare no competing or financial interests.

Author contributions
Conceptualization: L.v.R., D.G.H., R.A.H.; Methodology: L.v.R., D.G.H., R.A.H.; Formal analysis: L.v.R.; Investigation: L.v.R., J.v.D., R.A.H.; Data curation: L.v.R.; Writing - original draft: L.v.R., J.v.D., D.G.H., R.A.H.; Writing - review & editing: L.v.R., J.v.D., D.G.H., R.A.H.; Visualization: L.v.R.; Supervision: D.G.H., R.A.H.; Project administration: L.v.R.; Funding acquisition: D.G.H., R.A.H.

Funding
This work was funded by the Adaptive Life program of the University of Groningen (Rijksuniversiteit Groningen, B050216 to L.v.R. and R.A.H.), and by the Arctic University of Norway (Universitetet i Tromsø, to J.v.D. and D.G.H.).

Supplementary information
Supplementary information available online at
https://jeb.biologists.org/lookup/doi/10.1242/jeb.230987.supplemental

References
Baker, J. (1938). The evolution of breeding seasons. In *Evolution: Essays on Aspects of Evolutionary Biology Presented to Professor E. S. Goodrich on His 70th Birthday* (ed. G. R. DeBeer), pp. 161-177. Oxford University Press.

Caro, S. P., Schaper, S. V., Hut, R. A., Ball, G. F. and Visser, M. E. (2013). The case of the missing mechanism: how does temperature influence seasonal timing in endotherms? *PLoS Biol.* **11**, e1001517. doi:10.1371/journal.pbio.1001517

Dardente, H., Hazlerigg, D. G. and Ebling, F. J. P. (2014). Thyroid hormone and seasonal rhythmicity. *Front. Endocrinol. (Lausanne)* **5**, 19. doi:10.3389/fendo.2014.00019

Dardente, H., Wood, S., Ebling, F. and Sáenz de Miera, C. (2018). An integrative view of mammalian seasonal neuroendocrinology. *J. Neuroendocrinol.* **31**, e12729. doi:10.1111/jne.12729

Dardente, H., Wyse, C. A., Birnie, M. J., Dupré, S. M., Loudon, A. S. I., Lincoln, G. A. and Hazlerigg, D. G. (2010). A molecular switch for photoperiod responsiveness in mammals. *Curr. Biol.* **20**, 2193-2198. doi:10.1016/j.cub.2010.10.048

Dumbell, R. A., Scherbarth, F., Diedrich, V., Schmid, H. A., Steinlechner, S. and Barrett, P. (2015). Somatostatin agonist pasireotide promotes a physiological state resembling short-day acclimation in the photoperiodic male siberian hamster (*Phodopus sungorus*). *J. Neuroendocrinol.* **27**, 588-599. doi:10.1111/jne.12289

Ebling, F. J. P. (1994). Photoperiodic differences during development in the dwarf hamsters *Phodopus sungorus* and *Phodopus campbelli*. *Gen. Comp. Endocrinol.* **95**, 475-482. doi:10.1006/gcen.1994.1147

Evernden, L. N. and Fuller, W. A. (1972). Light alteration caused by snow and its importance to subnivean rodents. *Can. J. Zool.* **50**, 1023-1032. doi:10.1139/z72-137

Gerkema, M. P., Daan, S., Wilbrink, M., Hop, M. W. and Van Der Leest, F. (1993). Phase control of ultradian feeding rhythms in the common vole (*Microtus arvalis*): the roles of light and the circadian system. *J. Biol. Rhythms* **8**, 151-171. doi:10.1177/074873049300800205

Guerra, M., Blázquez, J. L., Peruzzo, B., Peláez, B., Rodríguez, S., Toranzo, D., Pastor, F. and Rodríguez, E. M. (2010). Cell organization of the rat pars tuberalis. Evidence for open communication between pars tuberalis cells, cerebrospinal fluid and tanycytes. *Cell Tissue Res.* **339**, 359-381. doi:10.1007/s00441-009-0885-8

Hanon, E. A., Lincoln, G. A., Fustin, J.-M., Dardente, H., Masson-Pévet, M., Morgan, P. J. and Hazlerigg, D. G. (2008). Ancestral TSH mechanism signals summer in a photoperiodic mammal. *Curr. Biol.* **18**, 1147-1152. doi:10.1016/j.cub.2008.06.076

Hoffmann, K. (1978). Effects of short photoperiods on puberty, growth and moult in the Djungarian hamster (*Phodopus sungorus*). *J. Reprod. Fertil.* **54**, 29-35. doi:10.1530/jrf.0.0540029

Horton, T. H. (1984). Growth and reproductive development of male *Microtus montanus* is affected by the prenatal photoperiod. *Biol. Reprod.* **31**, 499-504. doi:10.1095/biolreprod31.3.499

Horton, T. H. (1985). Cross-fostering of voles demonstrates in utero effect of photoperiod. *Biol. Reprod.* **33**, 934-939. doi:10.1095/biolreprod33.4.934

Horton, T. H. and Stetson, M. H. (1992). Maternal transfer of photoperiodic information in rodents. *Anim. Reprod. Sci.* **30**, 29-44. doi:10.1016/0378-4320(92)90004-W

Hut, R. A. (2011). Photoperiodism: shall EYA compare thee to a summer's day? *Curr. Biol.* **21**, R22-R25. doi:10.1016/j.cub.2010.11.060

Hut, R. A., Paolucci, S., Dor, R., Kyriacou, C. P. and Daan, S. (2013). Latitudinal clines: an evolutionary view on biological rhythms. *Proc. R. Soc. B Biol. Sci.* **280**, 20130433-20130433. doi:10.1098/rspb.2013.0433

Klosen, P., Lapmanee, S., Schuster, C., Guardiola, B., Hicks, D., Pevet, P. and Felder-Schmittbuhl, M. P. (2019). MT1 and MT2 melatonin receptors are expressed in nonoverlapping neuronal populations. *J. Pineal Res.* **67**, e12575. doi:10.1111/jpi.12575

Korslund, L. (2006). Activity of root voles (*Microtus oeconomus*) under snow: social encounters synchronize individual activity rhythms. *Behav. Ecol. Sociobiol.* **61**, 255-263. doi:10.1007/s00265-006-0256-3

Król, E., Douglas, A., Dardente, H., Birnie, M. J., Vinne, V. v, Eijer, W. G., Gerkema, M. P., Hazlerigg, D. G. and Hut, R. A. (2012). Strong pituitary and hypothalamic responses to photoperiod but not to 6-methoxy-2-benzoxazolinone in female common voles (*Microtus arvalis*). *Gen. Comp. Endocrinol.* **179**, 289-295. doi:10.1016/j.ygcen.2012.09.004

Lechan, R. M. and Fekete, C. (2005). Role of thyroid hormone deiodination in the hypothalamus. *Thyroid* **15**, 883-897. doi:10.1089/thy.2005.15.883

Magner, J. A. (1990). Thyroid-stimulating hormone: biosynthesis, cell biology, and bioactivity *Endocr. Rev.* **11**, 354-385. doi:10.1210/edrv-11-2-354

Malyshev, A. V., Henry, H. A. L. and Kreyling, J. (2014). Relative effects of temperature vs photoperiod on growth and cold acclimation of northern and southern ecotypes of the grass *Arrhenatherum elatius*. *Environ. Exp. Bot.* **106**, 189-196. doi:10.1016/j.envexpbot.2014.02.007

Masumoto, K. H., Ukai-Tadenuma, M., Kasukawa, T., Nagano, M., Uno, K. D., Tsujino, K., Horikawa, K., Shigeyoshi, Y. and Ueda, H. R. (2010). Acute induction of Eya3 by late-night light stimulation triggers TSHβ expression in photoperiodism. *Curr. Biol.* **20**, 2199-2206. doi:10.1016/j.cub.2010.11.038

Nakane, Y. and Yoshimura, T. (2019). Photoperiodic regulation of reproduction in vertebrates. *Annu. Rev. Anim. Biosci.* **7**, 173-194. doi:10.1146/annurev-animal-020518-115216

Nakao, N., Ono, H., Yamamura, T., Anraku, T., Takagi, T., Higashi, K., Yasuo, S., Katou, Y., Kageyama, S., Uno, Y. et al. (2008). Thyrotrophin in the pars tuberalis triggers photoperiodic response. *Nature* **452**, 317-322. doi:10.1038/nature06738

Ono, H., Hoshino, Y., Yasuo, S., Watanabe, M., Nakane, Y., Murai, A., Ebihara, S., Korf, H.-W. Yoshimura, T. (2008). Involvement of thyrotropin in photoperiodic signal transduction in mice. *Proc. Natl. Acad. Sci. USA* **105**, 18238-18242. doi:10.1073/pnas.0808952105

Peacock, J. M. (1976). Temperature and leaf growth in four grass species. *J. Appl. Ecol.* **13**, 225-232. doi:10.2307/2401942

Pfaffl, M. W. (2001). A new mathematical model for relative quantification in real-time RT-PCR. *Nucleic Acids Res.* **29**, e45. doi:10.1093/nar/29.9.e45

Phalen, A. N., Wexler, R., Cruickshank, J., Park, S. and Place, N. J. (2010). Photoperiod-induced differences in uterine growth in *Phodopus sungorus* are evident at an early age when serum estradiol and uterine estrogen receptor levels are not different. *Comp. Biochem. Physiol. A Mol. Integr. Physiol.* **155**, 115-121. doi:10.1016/j.cbpa.2009.10.024

Prendergast, B. J., Gorman, M. R. and Zucker, I. (2000). Establishment and persistence of photoperiodic memory in hamsters. *Proc. Natl. Acad. Sci. USA* **97**, 5586-5591. doi:10.1073/pnas.100098597

Prendergast, B. J., Pyter, L. M., Kampf-Lassin, A., Patel, P. N. and Stevenson, T. J. (2013). Rapid induction of hypothalamic iodothyronine deiodinase

expression by photoperiod and melatonin in juvenile Siberian hamsters (*Phodopus sungorus*). *Endocrinology* **154**, 831-841. doi:10.1210/en.2012-1990

Robson, M. J. (1967). A comparison of British and North African varieties of tall fescue (*Festuca arundinacea*). I. Leaf growth during winter and the effects on it of temperature and daylength. *J. Appl. Ecol.* **4**, 475-484. doi:10.2307/2401349

Sáenz De Miera, C. (2019). Maternal photoperiodic programming enlightens the internal regulation of thyroid-hormone deiodinases in tanycytes. *J. Neuroendocrinol.* **31**, e12679. doi:10.1111/jne.12679

Sáenz de Miera, C., Beymer, M., Routledge, K., Król, E., Selman, C., Hazlerigg, D. G. and Simonneaux, V. (2020). Photoperiodic regulation in a wild-derived mouse strain. *J. Exp. Biol.* **223**, jeb217687. doi:10.1242/jeb.217687

Sáenz de Miera, C., Bothorel, B., Jaeger, C., Simonneaux, V. and and Hazlerigg, D. (2017). Maternal photoperiod programs hypothalamic thyroid status via the fetal pituitary gland. *Proc. Natl. Acad. Sci. USA* **114**, 8408-8413. doi:10.1073/pnas.1702943114

Sáenz De Miera, C., Monecke, S., Bartzen-Sprauer, J., Laran-Chich, M. P., Pévet, P., Hazlerigg, D. G. and and Simonneaux, V. (2014). A circannual clock drives expression of genes central for seasonal reproduction. *Curr. Biol.* **24**, 1500-1506. doi:10.1016/j.cub.2014.05.024

Scherbarth, F., Diedrich, V., Dumbell, R. A., Schmid, H. A., Steinlechner, S. and Barrett, P. (2015). Somatostatin receptor activation is involved in the control of daily torpor in a seasonal mammal. *Am. J. Physiol. Regul. Integr. Comp. Physiol.* **309**, R668-R674. doi:10.1152/ajpregu.00191.2015

Simonneaux, V. (2020). A kiss to drive rhythms in reproduction. *Eur. J. Neurosci.* **51**, 509-530. doi:10.1111/ejn.14287

Stetson, M. H., Elliott, J. A. and Goldman, B. D. (1986). Maternal transfer of photoperiodic information influences the photoperiodic response of prepubertal Djungarian hamsters (*Phodopus sungorus sungorus*). *Biol. Reprod.* **34**, 664-669. doi:10.1095/biolreprod34.4.664

Stevenson, T. J. and Prendergast, B. J. (2013). Reversible DNA methylation regulates seasonal photoperiodic time measurement. *Proc. Natl. Acad. Sci. USA* **110**, 4644-4646. doi:10.1073/pnas.1310643110

Stumpfel, S., Bieber, C., Blanc, S., Ruf, T. and Giroud, S. (2017). Differences in growth rates and pre–hibernation body mass gain between early and late-born juvenile garden dormice. *J. Comp. Physiol. B* **187**, 253-263. doi:10.1007/s00360-016-1017-x

Tkadlec, E. (2000). The effects of seasonality on variation in the length of breeding season in arvicoline rodents. *Folia Zool.* **49**, 269-286.

van Dalum, J. Melum, V. J., Wood, S. H. and Hazlerigg, D. G. (2020). Maternal photoperiodic programming: melatonin and seasonal synchronization before birth. *Front. Endocrinol. (Lausanne)* **10**, 901. doi:10.3389/fendo.2019.00901

van de Zande, L., van Apeldoorn, R. C., Blijdenstein, A. F., de Jong, D., van Delden, W. and Bijlsma, R. (2000). Microsatellite analysis of population structure and genetic differentiation within and between populations of the root vole, *Microtus oeconomus* in the Netherlands. *Mol. Ecol.* **9**, 1651-1656. doi:10.1046/j.1365-294x.2000.01051.x

Von Gall, C., Stehle, J. H. and Weaver, D. R. (2002). Mammalian melatonin receptors: molecular biology and signal transduction. *Cell Tissue Res.* **309**, 151-162. doi:10.1007/s00441-002-0581-4

Von Gall, C., Weaver, D. R., Moek, J., Jilg, A., Stehle, J. H. and Korf, H.-W. (2005). Melatonin plays a crucial role in the regulation of rhythmic clock gene expression in the mouse pars tuberalis. *Ann. N.Y. Acad. Sci.* **1040**, 508-511. doi:10.1196/annals.1327.105

Wang, D., Li, N., Tian, L., Ren, F., Li, Z., Chen, Y., Liu, L., Hu, X., Zhang, X., Song, Y. et al. (2019). Dynamic expressions of hypothalamic genes regulate seasonal breeding in a natural rodent population. *Mol. Ecol.* **28**, 3508-3522. doi:10.1111/mec.15161

Wickham, H. (2016). *Ggplot2: Elegant Graphics for Data Analysis*: Springer-Verlag New York.

Williams, L. M. and Morgan, P. J. (1988). Demonstration of melatonin-binding sites on the pars tuberalis of the rat. *J. Endocrinol.* **119**, R1-R3. doi:10.1677/joe.0.119R001

Wood, S. H., Christian, H. C., Miedzinska, K., Saer, B. R. C., Johnson, M., Paton, B., Yu, L., McNeilly, J., Davis, J. R. E., McNeilly, A. S. et al. (2015). Binary switching of calendar cells in the pituitary defines the phase of the circannual cycle in mammals. *Curr. Biol.* **25**, 2651-2662. doi:10.1016/j.cub.2015.09.014

Yellon, S. M. and Goldman, B. D. (1984). Photoperiod control of reproductive development in the male Djungarian hamster (*Phodopus sungorus*). *Endocrinology* **114**, 664-670. doi:10.1210/endo-114-2-664

Supplementary information

Table S1

Preparation 40 µL Reversed-Transcription reactions concentrations of components used for RT

Component	Stock concentration	Final concentration
Oligo(dT)$_{18}$	100 µM	5 µM
5X Reaction buffer	5X	1X
RiboLock RNase Inhibitor	20 U/µL	1 U/µL
dNTP Mix	10 mM	1 mM
RevertAid H Minus Reverse Transcriptase	200 U/µL	10 U/µL
Template RNA	0.1 µg/µl	1 µg/µl

Table S2

Primers used for qPCR. Primer sequences were gene specific for M. arvalis and M. oeconomus, except for Tshβ reversed and Tshr forward for M. arvalis, and Dio3 forward and Eya3 reversed for M. oeconomus, which differ in 1 nucleotide from the used primers.

Gene	Forward primer sequence (‘5-‘3)	Reverse primer sequence (‘5-‘3)
Dio2	CAGCCAACTCCGGACTTCTT	GCCGACTTCCTGTTGGTGTA
Dio3	CAAGCATTTCCTGCGTCGTC	GATACGCAGATGGGTGGGTC
Dnmt1	TAGCCACCAAACGAAGACCC	GTTCGAGCCGCCTTTTTCTC
Dnmt3a	GAGAGGGAACTGAGACCCCA	CCCGTTTCCGTTTGCTGATG
Eya3	TGTTGGGTTCACACTCCCTG	GGGCAAAGTAAGCAGGTGTA
Gapdh	GCTGCCCAGAACATCATCCCTG	GACGACGGACACATTGGGGGTA
Kiss1	CCATGCCCACCGGTTGAGAG	GCCGAAGGAGTTCCAGTTGT
Mtnr1a	ATCGCCATTAACCGCTACTG	GAGAGTTCCGGTTTGCAGGT
Npvf	AGGCAGGGATCTTGAACCAC	TCTCTGTAGCCAGCGACTCA
Tshβ	GCTTATGGCAACAGGGTAGGA	AATACGCGCTCTCCCAGGAT
Tshr	ATCCCCAGTCTCGCGTTTTC	GCTTCTGGTGTTGCGGATTT

Table S3

Thermal cycling conditions for qPCR.

qPCR step	T (°C)	Duration (seconds)	Cycles
Enzyme activation	95	180	Hold
Denaturation	95	3	40
Annealing/ extension/ data acquisition	60	20	40
Dissociation	95	3	
	65	5	
	95	15	

	body mass (m)				**gonads (m)**				**GSI (m)**			
	Df	SS	*F*	*p*	Df	SS	*F*	*p*	Df	SS	*F*	*p*
pp	1,66		22.5261	< 0.001	1,56	0.4619	118.426	< 0.001	1,56	7.172	132.347	< 0.001
age	1,76		320.7922	< 0.001	3,56	0.9478	80.998	< 0.001	3,56	8.307	51.101	< 0.001
species	1,66		58.5611	< 0.001	1,56	0.0337	8.641	< 0.01	1,56	0.247	4.551	< 0.05
pp:age	1,76		6.8905	< 0.001	3,56	0.1169	9.994	< 0.001	3,56	1.042	6.411	< 0.001
pp:species	1,66		7.9873	< 0.05	1,56	0.0011	0.276	ns	1,56	1.033	19.060	< 0.001
age:species	1,76		44.6027	< 0.001	3,56	0.0352	3.012	< 0.05	3,56	0.028	0.171	ns
pp:age:species	1,76		0.0826	ns	3,56	0.0028	0.238	ns	3,56	0.354	2.175	ns
	***Mtnr1a* (m)**				***Tshb* (m)**				***Tshr* (m)**			
	Df	SS	*F*	*p*	Df	SS	*F*	*p*	Df	SS	*F*	*p*
pp	1,42	0.12	0.080	ns	1,42	65.07	78.822	< 0.001	1,42	4.303	33.364	< 0.001
age	3,42	4.23	0.936	ns	3,42	11.45	4.625	< 0.01	3,42	1.613	4.170	< 0.05
species	1,42	4.37	2.899	ns	1,42	4.15	5.028	< 0.05	1,42	9.763	75.709	< 0.001
pp:age	3,42	0.85	0.188	ns	3,42	9.18	3.708	< 0.05	3,42	0.690	1.783	ns
pp:species	1,42	2.53	1.676	ns	1,42	2.55	3.084	ns	1,42	1.053	8.165	< 0.01
age:species	3,42	1.17	0.258	ns	3,42	7.26	2.933	< 0.05	3,42	0.320	0.827	ns
pp:age:species	3,42	6.03	1.333	ns	3,42	8.91	3.596	< 0.05	3,42	0.953	2.464	ns
	***Dio2* (m)**				***Dio3* (m)**				***Dio2/Dio3* (m)**			
	Df	SS	*F*	*p*	Df	SS	*F*	*p*	Df	SS	*F*	*p*
pp	1,42	1.409	14.702	< 0.001	1,42	41.7	4.838	< 0.05	1,42	10.25	8.537	< 0.01
age	3,42	0.771	2.683	ns	3,42	74.6	2.885	< 0.05	3,42	7.18	1.994	ns
species	1,42	0.018	0.188	ns	1,42	7.6	0.878	ns	1,42	0.32	0.267	ns
pp:age	3,42	0.418	1.456	ns	3,42	3.3	0.129	ns	3,42	2.74	0.760	ns
pp:species	1,42	0.002	0.017	ns	1,42	10.1	1.173	ns	1,42	0.01	0.008	ns
age:species	3,42	0.540	1.877	ns	3,42	14.1	0.545	ns	3,42	5.82	1.617	ns
pp:age:species	3,42	4.025	0.897	ns	3,42	6.0	0.233	ns	3,42	3.94	1.095	ns
	***Eya3* (m)**				***Kiss1* (m)**				***Npvf* (m)**			
	Df	SS	*F*	*p*	Df	SS	*F*	*p*	Df	SS	*F*	*p*
pp	1,42	3.47	1.722	ns	1,42	237	2.956	ns	1,42	0.253	0.606	ns
age	3,42	22.49	3.716	< 0.05	3,42	5092	21.186	< 0.001	3,42	12.769	10.205	< 0.001
species	1,42	96.66	47.928	< 0.001	1,42	1252	15.621	< 0.001	1,42	0.280	0.672	ns
pp:age	3,42	2.22	0.367	ns	3,42	240	0.998	ns	3,42	0.572	0.457	ns
pp:species	1,42	3.73	1.850	ns	1,42	186	2.325	ns	1,42	0.056	0.134	ns
age:species	3,42	12.50	2.066	ns	3,42	172	0.715	ns	3,42	1.061	0.848	ns
pp:age:species	3,42	0.15	0.025	ns	3,42	80	0.331	ns	3,42	2.373	1.896	ns
	***Dnmt1* (m)**				***Dnmt3a* (m)**							
	Df	SS	*F*	*p*	Df	SS	*F*	*p*				
pp	1,42	1.19	0.676	ns	1,42	1.41	0.767	ns				
age	3,42	76.07	14.377	< 0.001	3,42	3.58	0.651	ns				
species	1,42	7.79	4.419	< 0.05	1,42	11.78	6.413	< 0.05				
pp:age	3,42	4.21	0.796	ns	3,42	1.93	0.350	ns				
pp:species	1,42	3.33	1.886	ns	1,42	0.04	0.023	ns				
age:species	3,42	4.72	0.892	ns	3,42	3.08	0.558	ns				
pp:age:species	3,42	15.91	3.008	< 0.05	3,42	7.72	1.401	ns				
	body mass (f)				**gonads (f)**				**GSI (f)**			
	Df	SS	*F*	*p*	Df	SS	*F*	*p*	Df	SS	*F*	*p*
pp	1,60		14.9452	< 0.001	1,50	0.0000919	1.575	ns	1,50	0.00002	0.0111	ns
age	1,78		169.3274	< 0.001	3,50	0.0006542	3.737	< 0.05	3,50	0.04933	8.281	< 0.001

species	1,60		17.4063	< 0.001	1,50	0.0004270	7.316	< 0.01	1,50	0.05081	25.592	< 0.001
pp:age	1,78		0.0398	ns	3,50	0.0003350	1.913	ns	3,50	0.00869	1.459	ns
pp:species	1,60		9.0244	< 0.01	1,50	0.0004222	7.235	< 0.01	1,50	0.00805	4.052	< 0.05
age:species	1,78		13.0245	< 0.001	3,50	0.0005309	3.033	< 0.05	3,50	0.01784	2.995	< 0.05
pp:age:species	1,78		0.2721	ns	3,50	0.0003238	1.850	ns	3,50	0.01251	2.101	ns
	***Mtnr1a* (f)**				***Tshβ* (f)**				***Tshr* (f)**			
	Df	SS	*F*	*p*	Df	SS	*F*	*p*	Df	SS	*F*	*p*
pp	1,40	1.59	1.593	ns	1,40	128.65	127.264	< 0.001	1,40	0.869	4.687	< 0.05
age	3,40	27.14	9.041	< 0.001	3,40	4.92	1.621	ns	3,40	1.213	2.182	ns
species	1,40	0.08	0.084	ns	1,40	0.09	0.088	ns	1,40	12.811	69.096	< 0.001
pp:age	3,40	3.90	1.300	ns	3,40	5.17	1.706	ns	3,40	0.687	1.234	ns
pp:species	1,40	0.06	0.057	ns	1,40	0.02	0.018	ns	1,40	0.193	1.043	ns
age:species	3,40	1.95	0.648	ns	3,40	1.16	0.382	ns	3,40	1.277	2.297	ns
pp:age:species	3,40	0.90	0.299	ns	3,40	2.31	0.761	ns	3,40	0.329	0.592	ns
	***Dio2* (f)**				***Dio3* (f)**				***Dio2/Dio3* (f)**			
	Df	SS	*F*	*p*	Df	SS	*F*	*p*	Df	SS	*F*	*p*
pp	1,40	0.422	2.065	ns	1,40	9.07	2.206	ns	1,40	26.29	5.976	< 0.05
age	3,40	3.262	5.318	< 0.01	3,40	81.75	6.629	< 0.001	3,40	34.84	2.640	ns
species	1,40	1.408	6.886	< 0.05	1,40	25.09	6.105	< 0.05	1,40	6.69	1.522	ns
pp:age	3,40	1.088	1.775	ns	3,40	4.39	0.356	ns	3,40	36.77	2.786	ns
pp:species	1,40	0.010	0.047	ns	1,40	14.61	3.555	ns	1,40	6.16	1.399	ns
age:species	3,40	1.674	2.730	ns	3,40	50.15	4.067	< 0.05	3,40	10.51	0.796	ns
pp:age:species	3,40	0.168	0.273	ns	3,40	16.20	1.314	ns	3,40	35.21	2.668	ns
	***Eya3* (f)**				***Kiss1* (f)**				***Npvf* (f)**			
	Df	SS	*F*	*p*	Df	SS	*F*	*p*	Df	SS	*F*	*p*
pp	1,40	0.32	0.303	ns	1,40	191	4.057	ns	1,40	3.785	14.783	< 0.001
age	3,40	10.62	3.351	< 0.05	3,40	4491	31.856	< 0.001	3,40	10.547	13.730	< 0.001
species	1,40	60.63	57.392	< 0.001	1,40	1345	28.629	< 0.001	1,40	0.796	3.108	ns
pp:age	3,40	2.99	0.943	ns	3,40	680	4.820	< 0.01	3,40	2.698	3.513	< 0.05
pp:species	1,40	0.02	0.021	ns	1,40	3	0.061	ns	1,40	1.123	4.385	< 0.05
age:species	3,40	5.07	1.601	ns	3,40	978	6.938	< 0.001	3,40	0.458	0.596	ns
pp:age:species	3,40	6.82	2.153	ns	3,40	843	5.980	< 0.01	3,40	0.876	1.140	ns

Table S4. *Statistics for type I two-way ANOVA's*

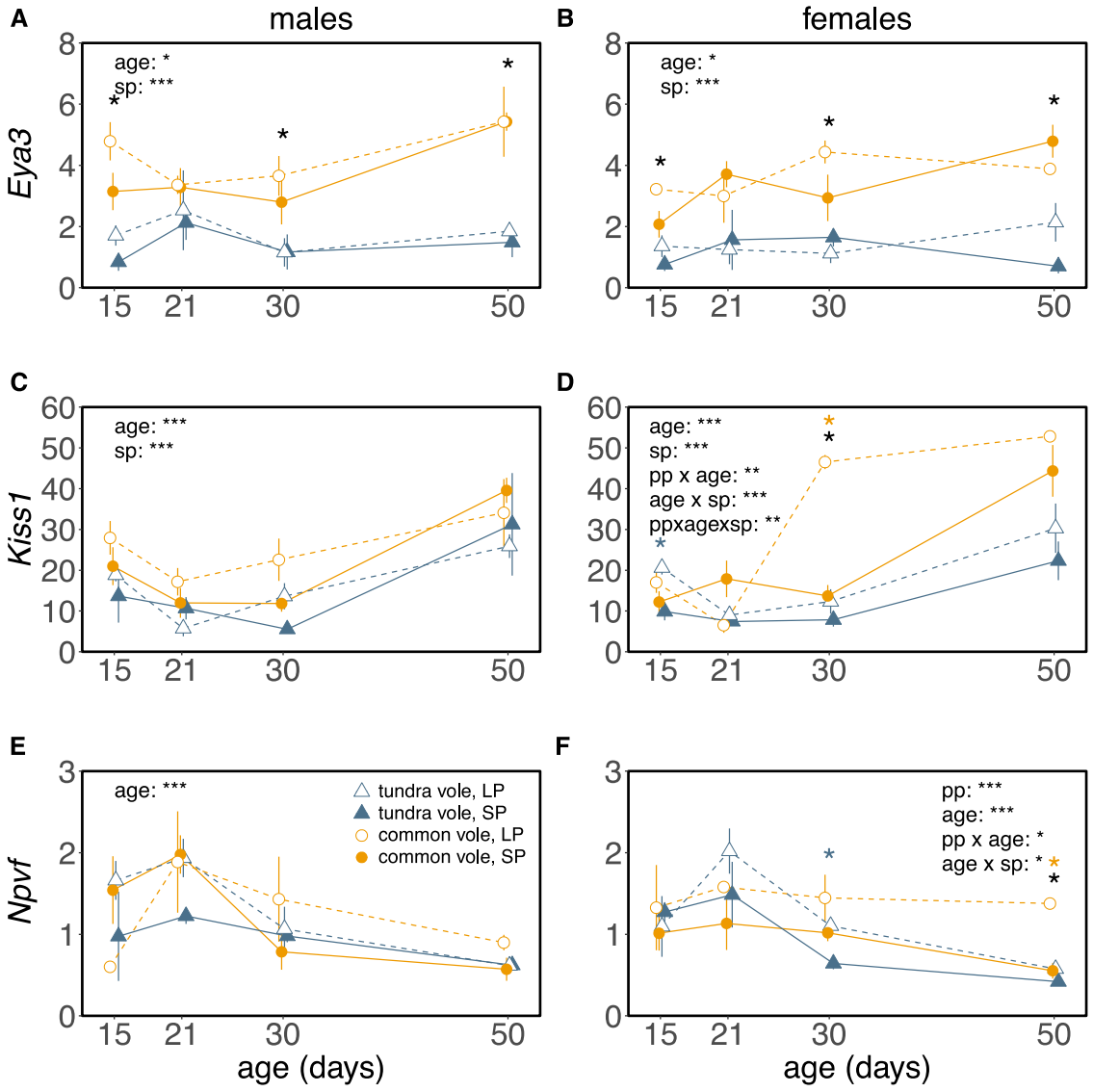

Figure S1. Effects of constant photoperiod on gene expression levels in the developing hypothalamus. Relative gene expression levels of (A, B) *Eya3*, (C, D) *Kiss1*, (E, F) *Npvf* expression in the hypothalamus of developing common (orange circles) and tundra vole (blue triangles) males and females respectively, under LP (open symbols, dashed lines) or SP (closed symbols, solid lines). Lines connect averages representing non-repeated measures. Data are mean±s.e.m.. Male tundra vole LP: n=16, male tundra vole SP: n=13, male common vole LP n=14, male common vole SP n=15. female tundra vole LP: n=16, female tundra vole SP: n=16, female common vole LP n=8, female common vole SP n=16. Significant effects (ANOVA, post-hoc Tukey) of photoperiod at specific ages are indicate for tundra voles (blue asterisks) and common voles (orange asterisks), significant effects of species are indicated by black asterisks. Significant effects of: photoperiod (pp), age (age), species (sp) and interactions are shown in each graph, $^{*}p < 0.05$, $^{**}p < 0.01$, $^{***}p < 0.001$. Statistic results for two-way ANOVA's (photoperiod, age and species) can be found in table S4.

Paper II

Received: 26 January 2021 | Revised: 25 March 2021 | Accepted: 2 April 2021

DOI: 10.1096/fj.202100162R

RESEARCH ARTICLE

THE FASEB JOURNAL

Mechanisms of temperature modulation in mammalian seasonal timing

Laura van Rosmalen[1] | **Jayme van Dalum**[2] | **Daniel Appenroth**[2] | **Renzo T. M. Roodenrijs**[1] | **Lauren de Wit**[1] | **David G. Hazlerigg**[2] | **Roelof A. Hut**[1]

[1]Chronobiology Unit, Groningen Institute for Evolutionary Life Sciences, University of Groningen, Groningen, The Netherlands

[2]Arctic Seasonal Timekeeping initiative (ASTI), Department of Arctic and Marine Biology, UiT The Arctic University of Norway, Tromsø, Norway

Correspondence
Laura van Rosmalen, Chronobiology Unit, Groningen Institute for Evolutionary Life Sciences, University of Groningen, Building 5171, Room 0344, Nijenborgh 7, 9747 AG Groningen, The Netherlands.
Email: Lauravanrosmalen@hotmail.com

Funding information
Rijksuniversiteit Groningen (University of Groningen), Grant/Award Number: B050216; Universitetet i Tromsø (UiT)

Abstract

Global warming is predicted to have major effects on the annual time windows during which species may successfully reproduce. At the organismal level, climatic shifts engage with the control mechanism for reproductive seasonality. In mammals, laboratory studies on neuroendocrine mechanism emphasize photoperiod as a predictive cue, but this is based on a restricted group of species. In contrast, field-oriented comparative analyses demonstrate that proximate bioenergetic effects on the reproductive axis are a major determinant of seasonal reproductive timing. The interaction between proximate energetic and predictive photoperiodic cues is neglected. Here, we focused on photoperiodic modulation of postnatal reproductive development in common voles (*Microtus arvalis*), a herbivorous species in which a plastic timing of breeding is well documented. We demonstrate that temperature-dependent modulation of photoperiodic responses manifest in the thyrotrophin-sensitive tanycytes of the mediobasal hypothalamus. Here, the photoperiod-dependent expression of type 2 deiodinase expression, associated with the summer phenotype was enhanced by 21°C, whereas the photoperiod-dependent expression of type 3 deiodinase expression, associated with the winter phenotype, was enhanced by 10°C in spring voles. Increased levels of testosterone were found at 21°C, whereas somatic and gonadal growth were oppositely affected by temperature. The magnitude of these temperature effects was similar in voles photoperiodical programmed for accelerated maturation (ie, born early in the breeding season) and in voles photoperiodical programmed for delayed maturation (ie, born late in the breeding season). The melatonin-sensitive pars tuberalis was relatively insensitive to temperature. These data define a mechanistic hierarchy for the integration of predictive temporal cues and proximate thermoenergetic effects in mammalian reproduction.

Abbreviations: CP, critical photoperiod; *Dio2*, iodothyronine deiodines 2; *Dio3*, iodothyronine deiodines 3; GnRH, gonadotropin-releasing hormone; LP, long photoperiod; PNES, photoperiodic neuroendocrine system; PP, photoperiod; SP, short photoperiod; T_3, triiodothyronine; *Tshβ*, thyroid-stimulating hormone β-subunit; *Tshr*, thyroid-stimulating hormone receptor.

KEYWORDS
ambient temperature, maternal photoperiodic programming, *Microtus arvalis*, photoperiodic neuroendocrine system, seasonal reproduction

1 | INTRODUCTION

Seasonal variation in environmental cues needs to be anticipated by organisms, which is essential for survival and efficient reproduction. In species occurring in temperate climatic zones, there is a high selection pressure on timing of reproduction, causing evolution of intrinsic annual timing mechanisms that accurately time physiology, morphology, and (reproductive) behavior. The reproductive potential of short-lived rodents, such as voles, often depend on rapid postnatal reproductive development leading to multiple generations of progeny within a single breeding season.[1-3] At the end of the breeding season, however, there is a necessary shift in emphasis from breeding to overwintering survival, and pups born late in summer may delay reproductive development until the following spring. Many organisms use photoperiod as a predictor of expected seasonal changes in food and climatic conditions. Studies in several species indicate that rates of reproductive development are set in utero through transplacental relay of maternal photoperiod: gestation on a short photoperiod favors accelerated postnatal reproductive development on an intermediate photoperiod, whereas gestation on a long photoperiod favors a slow rate of postnatal reproductive development on an intermediate photoperiod,[4-11] a concept named "maternal photoperiodic programming" (MPP).[12,13] Recently, we demonstrated that this phenomenon of maternal photoperiodic programming operates in species where photoperiodic cueing is the dominant mechanism for seasonal synchronization (Djungarian hamster).[11] Bronson proposed a theoretical model,[14,15] which emphasizes short life-span (ie, small mammals; short reproductive cycle) as predisposing animals to opportunistic breeding, whereas longer lifespan (ie, ungulates, hibernators; long reproductive cycle) predisposes animals to use photoperiodic cuing. This model suggests that the latter group is more vulnerable to climate change, as a shift to higher latitudes due to global warming requires a new critical photoperiod or elimination of photoperiodic responsiveness. On the other hand, short-lived mammalian species may override photoperiodic control by using an opportunistic strategy controlled by demands that compete with reproduction such as foraging conditions, temperature and food availability. Such species may therefore be less vulnerable to climate change as they may quickly adapt to temperature changes.

This led us to ask how photoperiod and temperature interact to shape postnatal reproductive development in microtine rodents noted for opportunistic breeding patterns in which nutrient supply and ambient temperature are significant modifiers of reproductive activation.[16-23] In addressing this question we aim to create a better understanding of the neurobiological basis for temperature-photoperiod interactions driving the mammalian reproductive system.[24,25]

In vertebrates, a conserved photoperiodic neuroendocrine response system measures photoperiod and subsequently drives annual rhythms in reproduction.[26,27] Light is perceived by photoreceptors located in the retina that signal to the suprachiasmatic nucleus (SCN). The SCN projects to the pineal gland, producing melatonin during darkness.[28] As a result, daylength is encoded in the duration of nocturnal melatonin secretion. Melatonin binds to its receptor (MTNR1A, MT1) in the pars tuberalis (PT) of the anterior lobe of the pituitary gland.[29-32] For that reason, the pars tuberalis is presumably the master regulator for seasonal rhythms in mammals.[33] Under long photoperiods, pineal melatonin is released for a short duration, which stimulates thyroid-stimulating hormone β-subunit (TSHβ) production in the pars tuberalis. TSHβ forms an active dimer with glycoprotein hormone alpha-subunit (α-GSU),[34] and binds to TSH receptors (TSHr) in the tanycytes around the third ventricle. Consequently, the tanycytes increase iodothyronine deiodines 2 (DIO2) production, whereas iodothyronine deiodines 3 (DIO3) is decreased, leading to higher levels of the active form of thyroid hormone (T_3) and lower levels of inactive forms (T_4 and rT_3) in the mediobasal hypothalamus (MBH). T_3 signals possibly "indirectly," through KNDy (kisspeptin/neurokinin B/Dynorphin) neurons of the arcuate nucleus (ARC) on gonadotropin-releasing hormone (GnRH) neurons in the hypothalamus.[35] GnRH neurons project to the pituitary inducing gonadotropin release, which stimulates gonadal growth and subsequently sex steroid production. The neuroanatomy, genes, and promotor elements that are crucial in this response pathway, have been identified in several mammalian and bird species,[30,36-43] including the common vole, *Microtus arvalis*.[44,45] Recently, Sáenz de Miera and colleagues demonstrated that the *Tsh-Dio2/Dio3* system is subjected to photoperiodic regulation in utero, before the fetal pineal gland starts to produce a rhythmic melatonin signal, indicating that early life maternal photoperiodic programming operates through this pathway.[11]

To explore the levels at which photoperiodic history and thermal cues are integrated in the photoperiodic neuroendocrine system (PNES), we manipulated photoperiodic history, postweaning photoperiod and ambient temperature in captive reared common voles (*M. arvalis*, Pallas 1778), a species in which flexible timing of reproduction is extensively

documented, and assessed gonadal and somatic development alongside hormone levels and hypothalamic gene expression. Here we present the results of a systematic analysis of the impact of ambient temperature on reproductive development and postnatal photoperiodic sensitivity in winter- and summer-born pups.

2 | MATERIALS AND METHODS

2.1 | Animals and experimental procedures

All experimental procedures were carried out according to the guidelines of the animal welfare body (IvD) of the University of Groningen conform to Directive 2010/63/EU and approved by the CCD (Centrale Commissie Dierproeven) of the Netherlands (CCD license number: AVD1050020171566). Common voles (*M. arvalis*) were obtained from the Lauwersmeer area, the Netherlands (53° 24′ N, 6° 16′ E).[46] The population has been kept in the laboratory as an outbred colony at the University of Groningen, which provided all animals used in this study. Adult and weaned voles were individually housed in transparent plastic cages (15 × 40 × 24 cm) provided with sawdust, dried hay, an opaque PVC tube, and ad libitum water and food (Standard rodent chow; Altromin #141005). The experiments were carried out in temperature-controlled chambers in which ambient temperature and photoperiod was manipulated as described below.

The voles used in the experiment (134 males) were gestated and born at 21°C under either a short photoperiod (SP, 8 hours of light/24 hours: born early in the breeding season) or a long photoperiod (LP, 16 hours of light/24 hours: born late in the breeding season) and weaned at 21 days. After weaning, voles were transferred to either 10°C or 21°C and a range of different photoperiods, a laboratory equivalent to different seasonal conditions (Figure 1). Postweaning photoperiods were (hours light: hours dark): 18L:6D, 16L:8D, 14L:10D, 12L:12D, 10L:14D, 8L:16D, and 6L:18D. Physiological data from 8L:16D was published elsewhere,[45] and was only applied in the winter-born group. While all postweaning photoperiods were applied at 21°C, the extreme photoperiods were omitted at 10°C for experimental efficiency (Figure 1). All voles were weighed when 7, 15, 21, 30, 42, and 50 days old.

2.2 | Tissue collections

Voles were sacrificed by decapitation, with prior CO_2 sedation, 17 ± 1 hours after lights OFF, when 50 days old. After decapitation, trunk blood was collected directly from the vole. Blood samples were left on ice until centrifugation (10 minutes, 2600G, 4°C). Plasma was transferred to a clean tube and stored at −80°C until hormonal assay. Whole brains were carefully dissected to include the proximate pituitary stalk including the pars tuberalis. Within 5 minutes after decapitation, brains were slowly frozen on a brass block surrounded by liquid N_2. Brains were stored at −80°C until proceed to in situ hybridization. Reproductive organs were dissected, cleaned of fat, and wet masses of paired testis weight were measured (±0.0001 g).

2.3 | In situ hybridization

A detailed description of the in situ hybridization protocol can be found elsewhere.[47,48] In short, 20 µm coronal brain sections were cut on a cryostat in caudal to rostral direction, starting from the mammillary bodies to the optic chiasm, to cover the area of the hypothalamus and third ventricle. Sections were mounted onto precoated Superfrost Plus slides (Thermo scientific: ref J1800AMNZ) with 6-10 sections per slide and 10 slides per individual. Antisense riboprobes of rat *Tshβ* (GenBank accession No. M10902, nucleotide position 47-412), vole *Dio2* (GenBank accession No. JF274709, position 1-775), and vole *Dio3* (GenBank accession no. JF274710, position 47-412) were

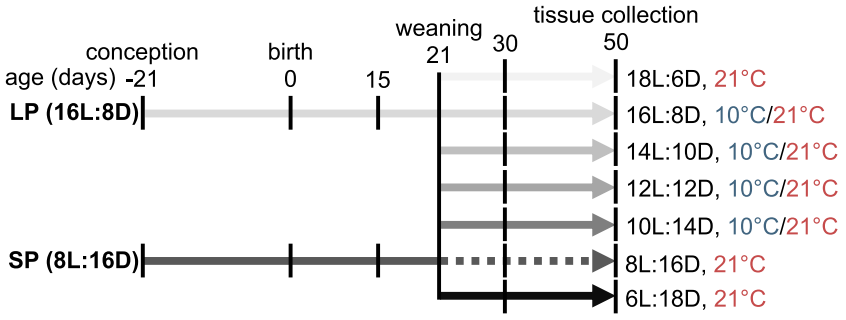

FIGURE 1 Experimental design. Conception, gestation, birth, and lactation took place under either LP (ie, summer-born) or SP (ie, winter-born) at 21°C. At the day of weaning (21 days old), animals were transferred to either 10°C or 21°C at a range of different photoperiods. 8L:16D (dashed line) was only applied in winter-born animals. Tissue collections took place when 50 days old

transcribed from linearized cDNA templates. Incorporation of 35^S-UTP (Perkin Elmer, Boston, MA, USA) was done with T7 polymerase (*Dio2* and *Dio3*) and T3 polymerase (*Tshβ*), resulting in 0.5-1.5 × 10^6 counts per minute per microliter, calculated to have 10^6 cpm/slide. All slides were fixated in paraformaldehyde, acetylated, and hybridized with radioactive probes overnight at 56°C.

Slides were washed in sodium citrate buffer the next day to remove nonspecific probe and then dehydrated in ethanol solutions, followed by air drying. The slides were exposed to an autoradiographic film (Kodak, Rochester, NY, USA) for 9 days (*Dio2* and *Dio3*) or 11 days (*Tshβ*) and developed with Carestream Kodak autoradiography GBX Developer/replenisher (P7042-1GA, Sigma) and fixer (P7167-1GA, Sigma). Films were scanned with an Epson Perfection V800 Photo scanner at 2400dpi resolution along with a calibrated optical density strip (T2115C, Stouffer Graphic Arts Equipment Co., Mishawaka, IN, USA). Analysis of integrated optical density (IOD) was done with software ImageJ, version Fuji (NIH Image, Bethesda MD, USA). The section with the highest signal was selected to represent each animal.

2.4 | Hormone analysis

Plasma testosterone levels were measured in a mouse testosterone enzyme-linked immunosorbent assay according to manufacturer's instructions (ADI-900-065; Enzo Life Sciences, New York, NY, USA). The sensitivity was 5.67 pg/mL, and the intra-assay coefficient of variation and interassay coefficient of variation were 10.8% and 9.3%, respectively.

2.5 | Calculation of critical photoperiod

Four-parameter log-logistic functions ($y = d + (c-d)/1 + (x/e)^b$) were fitted through the data using the R-package "drc,"[49] to describe the response to photoperiod as a dose-response relationship; b = slope parameter, c = minimum, d = maximum, e = 50% maximal response, where ED50 is defined as the inflexion point of the curve. Critical photoperiod was estimated by the ED50 from fitted dose-response curves. For testis mass, testosterone levels and body mass, we used a common maximum (d) within spring- and autumn experimental groups for both temperatures, but minimum (c) asymptotes were estimated for each temperature treatment. For *Tshβ*, *Dio2* and *Dio3* gene expression, the minimum (c) was set at 0. Within spring and autumn experimental groups, we set a common maximum (d) for both temperature treatments, except for *Dio3*. All fitted dose-response curve parameters can be found in Table S1. Model comparisons can be found in Table S2.

2.6 | Statistical analysis

One potential outlier for *Tshβ* were detected by boxplots, and removed from the analysis. The effects of postweaning photoperiod, ambient temperature and interactions were determined within spring and autumn experimental groups using type I two-way ANOVAs. To detect differences in growth rate between groups, we used repeated measures ANOVAs. Two-sample *t*-tests were used to determine temperature effects at specific photoperiods, and to assess changes in critical photoperiod. Statistical significance was determined at $P < .05$. All statistical analyses were performed using RStudio (version 1.2.1335),[50] and figures were generated using the R-package "ggplot2."[51] Statistic results for ANOVAs can be found in Table S3.

3 | RESULTS

3.1 | Maternal photoperiod is used to program photoperiodic gonadal responses

Exposing voles to a range of photoperiods confirms that this species shows a robust increase of testis mass, testosterone levels and body mass at long photoperiods (testis: $F_{6,70} = 39.55$, $P < .001$; testosterone: $F_{5,57} = 6.57$, $P < .001$; body mass: $F_{6,70} = 10.37$, $P < .001$; Figure 2). Fitted dose-response curves were useful to describe physiological responses to photoperiod, and allowed us to deduce ED50 (ie, critical photoperiod). In Figures 2 and 3, incomplete set of data points were available for experimental groups at 10°C. To describe dose-response curves within experimental groups, maximum response at 21°C within spring and autumn experimental groups were used, except for *Dio3*. Consequently, critical photoperiods for testosterone and Dio2 at 10°C were estimated based on extrapolated dose-response curves, and therefore have to be treated with caution.

A 1- to 2-hour shorter critical photoperiod for testis mass is observed in spring compared to autumn voles (10°C: T = 2.26, $df = 53$, $P < .03$; 21°C: T = 1.91, $df = 55$, $P < .07$; Figure 2C). Somatic growth rate is 50% higher in spring voles than in autumn voles (Figure S1 and Table S3). These findings indicate that born in winter leads to subsequent shorter critical photoperiods for reproductive activation.

3.2 | Voles at 10°C increase their gonads, but decrease testosterone levels

Lowering ambient temperature to 10°C causes an increase in testes mass (spring: $F_{1,70} = 13.18$, $P < .001$; autumn: $F_{5,50} = 12.08$, $P < .01$; Figure 2A,B). This temperature effect was primarily apparent at short photoperiods (ie, 10 and 12 hours

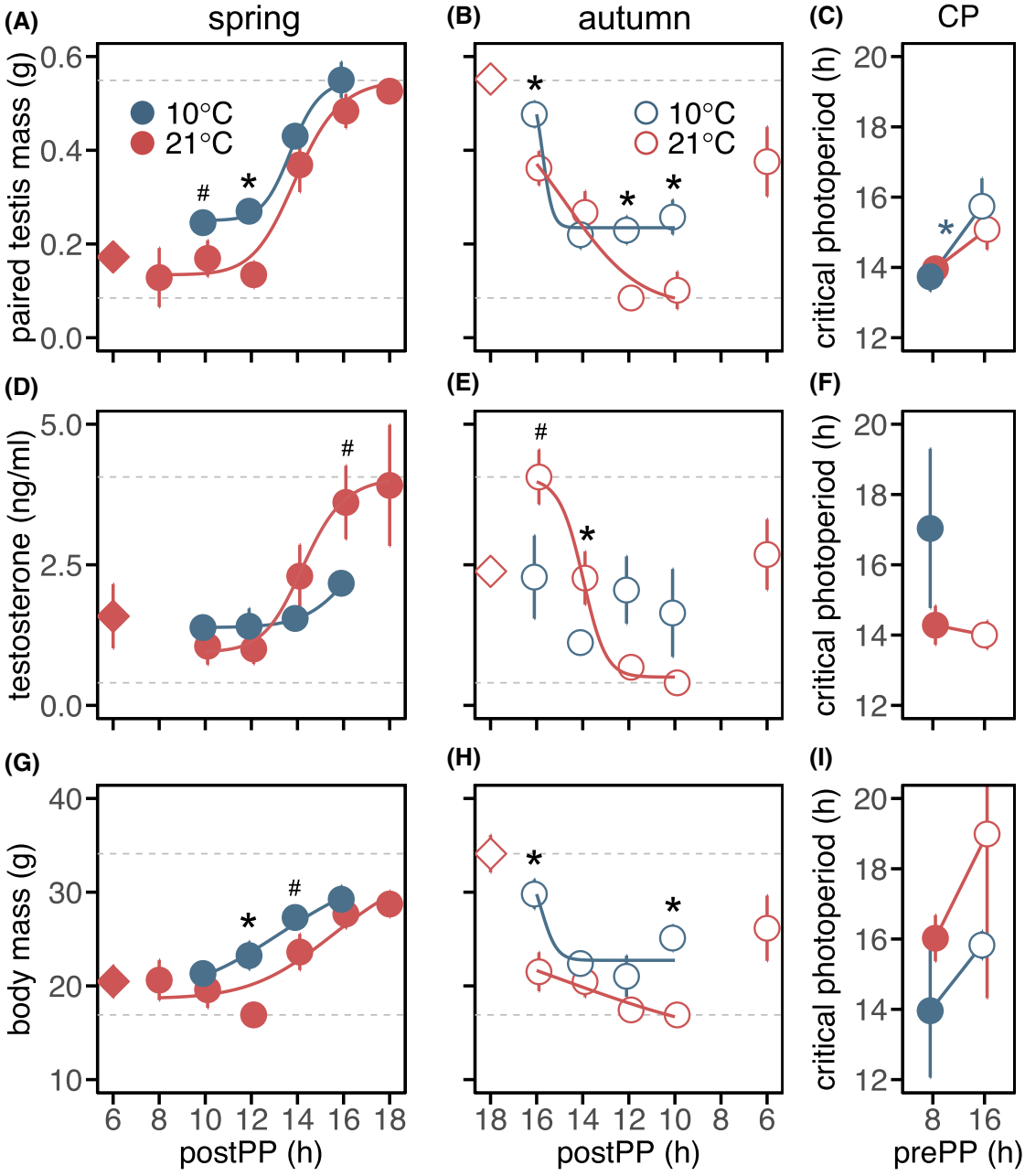

FIGURE 2 Temperature-dependent modulation of photoperiodic responses in physiological outputs. Responses to photoperiod for (A, B) paired testis mass, (D, E) plasma testosterone levels, and (G, H) body mass in 50-day-old animals for winter-born, spring (filled symbols; gestated and raised to weaning under SP) and summer-born, autumn (open symbols; gestated and raised to weaning under LP) animals, respectively, at 10°C (blue) or 21°C (red); prePP, preweaning photoperiod; postPP, postweaning photoperiod. Diamond-shaped symbols indicate photoperiodic transition in the opposite direction of round-shaped symbols. Critical photoperiods (CP) derived from fitted logistic functions are shown for (C) paired testis mass, (F) testosterone levels, and (I) body mass. Data are plotted as mean ± SEM (n = 4-8). Significant effects of contrast analyses are indicated: $^{\#}P < .1$, $^{*}P < .05$. In short, significant photoperiodic effects were found in: A, B, D, E, G, and H, significant temperature effects were found in: A, B, E, G, and H (Table S3). For dose-response curve fit parameters, we refer to Table S1; for dose-response curve model comparisons, we refer to Table S2

of light/24 hours), with twofold higher testes mass at 10°C, indicating a temperature sensitive window in early spring and late autumn (Figure S4A). Although, photoperiodic history did not change critical photoperiod for testosterone, a major lengthening of critical photoperiod was observed at 10°C (Figure 2F), resulting in a weak positive relationship between testis size and testosterone levels at 10°C (Figure S2A). Lowering temperature also accelerated somatic growth rate resulting in larger animals (spring: $F_{1,70} = 9.02$, $P < .01$; autumn: $F_{1,50} = 19.32$, $P < .001$; Figures 2G,H and S1).

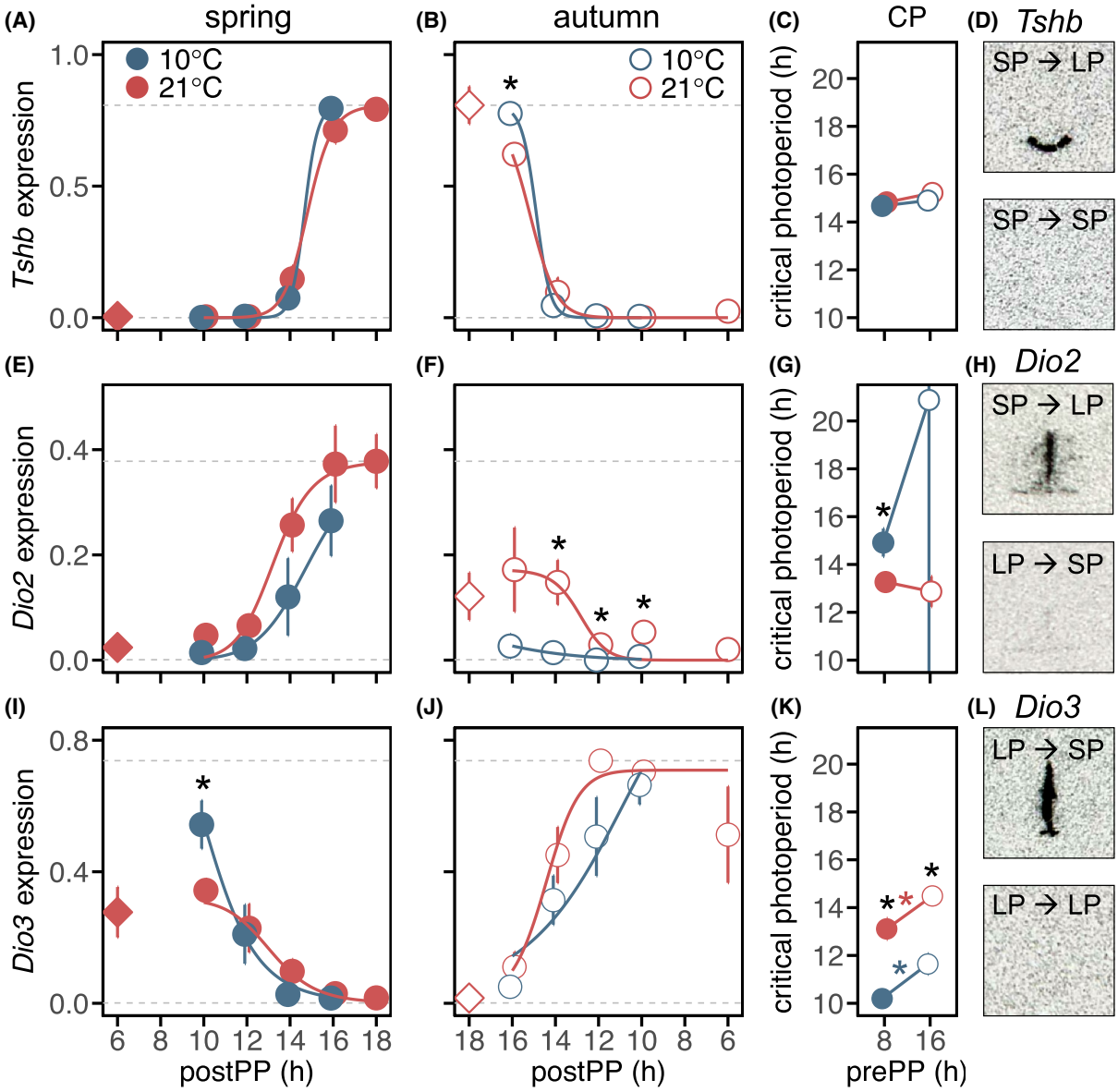

FIGURE 3 Temperature-dependent modulation of photoperiodic responses at the level of the tanycytes. Responses to photoperiod for (A, B) *Tshβ* in the pars tuberalis, (E, F) *Dio2*, and (I, J) *Dio3* in the tanycytes for winter-born, spring (filled symbols; gestated and raised to weaning under SP) and summer-born, autumn (open symbols; gestated and raised to weaning under LP) animals respectively, at 10°C (blue) or 21°C (red); prePP, preweaning photoperiod; postPP, postweaning photoperiod. Diamond-shaped symbols indicate photoperiodic transition in the opposite direction of round-shaped symbols. Images showing localization of mRNA by In situ hybridization are shown for (D) *Tshβ,* (H) *Dio2*, and (L) *Dio3* expression. Critical photoperiods (CP) derived from fitted logistic functions are shown for (C) *Tshβ*, (G) *Dio2*, and (K) *Dio3*. Data are plotted as mean ± SEM (n = 4-8). Significant effects of contrast analyses are indicated: $^{\#}P < .1$, $^{*}P < .05$. In short, significant photoperiodic effects were found in: A, B, E, I, and J, significant temperature effects were found in: E, F, and J (Table S3). For dose-response curve fit parameters we refer to Table S1; for dose-response curve model comparisons, we refer to Table S2

Overall, photoperiodic induced changes in gonadal and body mass follow and ellipse-like photoperiodic history-dependent relationship (Figure S4A,C), which is shifted upward at 10°C, indicating that temperature has an additive effect on photoperiodic-history rather than a multiplicative interaction. Photoperiodic induced changes in testosterone levels follow a temperature-dependent relationship to photoperiod, with reduced photoperiodic sensitivity at 10°C (Figure S4B).

3.3 | Photoperiodic history-dependent effects appear downstream of Tshβ in the photoperiodic axis

Melatonin binds to its receptors (MTNR1A, MT1) located in the pars tuberalis where TSHβ is produced under long photoperiods. *Tshβ* expression increases with increasing postweaning photoperiod (spring: $F_{5,39} = 233.44$, $P < .001$; autumn:

$F_{5,33} = 192.89$, $P < .001$), but is unaffected by photoperiodic-history (Figures 3A-D and S4D). TSH binds to its receptors in the tanycytes where it increases DIO2, and decreases DIO3. The observed photoperiodic responses in *Dio2* and *Dio3* expression strongly depend on photoperiodic-history: *Dio2* is enhanced in spring voles ($F_{5,81} = 3.86$, $P < .004$; Figures 3E-H and S4E), while *Dio3* is enhanced in autumn voles ($F_{5,80} = 4.30$, $P < .002$; Figures 3I-L and S4F). This results in longer critical photoperiods in autumn voles (10°C: T = 3.14, $df = 26$, $P < .005$; 21°C: T = 2.54, $df = 39$, $P < .03$; Figure 3K).

3.4 | Temperature modifies photoperiodic responses at the level of the tanycytes

Tshβ expression is unaffected by temperature (spring: $F_{1,39} = 0.01$, ns; autumn: $F_{1,33} = 1.63$, ns; Figure 3A,B), resulting in similar critical photoperiods under different conditions (Figure 3C). At 10°C, *Dio2* expression is reduced (spring: $F_{1,41} = 5.31$, $P < .05$; autumn: $F_{1,32} = 11.21$, $P < .01$; Figure 3E,F), particularly in autumn voles, where *Dio2* levels remain close to zero, even under long photoperiods. This results in longer critical photoperiods at 10°C (T = 2.40, $df = 33$, $P < .03$; Figure 3E-G). The temperature dependent change in critical photoperiod for *Dio2* is stronger in autumn than in spring voles (T = 55.52, $df = 89$, $P < .001$; Figure 3G). Temperature effects on *Dio3* expression depend on postweaning photoperiod, with slightly increased maximum expression under 10L:14D at 10°C ($F_{3,40} = 2.59$, $P < .08$; Figure 3I,J). This results in ~2 hour shorter critical photoperiods at 10°C (spring: T = 4.57, $df = 39$, $P < .001$; autumn: T = 5.17, $df = 32$, $P < .001$; Figure 3K).

Positive relationships between *Tshβ*, *Dio2* expression and testis mass, and the negative relationship between *Dio3* expression and testis mass are unaffected by temperature (Figures S2B and S3A,B,D,E). Similar positive relationships between *Tshβ* expression and testosterone, *Dio2* were observed (Figures S2C and S3C).

Overall, annual changes in *Tshβ* are primarily induced by photoperiod (Figure S4D), while photoperiodic induced changes in *Dio2* and *Dio3* follow an ellipse-like photoperiodic history-dependent relationship (Figure S4E,F), which is strongly affected by temperature for *Dio2*. The constructed annual relationship between *Tshβ* and *Dio2* confirms that *Tshβ* is either ON or OFF, and rather stable at different temperatures, while *Dio2* is completely suppressed from summer to winter at 10°C (Figure S4G). The constructed annual relationship between *Dio2* and *Dio3* shows photoperiodic-history dependence at 21°C, but not at 10°C (Figure S4I), resulting in higher *Dio3* levels at the same *Dio2* levels in warm springs.

4 | DISCUSSION

Our results confirm that ambient temperature modulates the use of photoperiod as a predictive cue for annual timing of reproduction in common voles. The melatonin-sensitive pars tuberalis was insensitive to modulation by temperature, whereas the tanycytes role in somatic and gonadal growth was sensitive to modulation by temperature. The magnitude of these temperature effects was similar in spring (ie, born early in the breeding season) and in autumn (ie, born late in the breeding season) voles. In nature, age of reproductive onset will be adjusted by the direction of photoperiodic transitions and thermal cues early in development. Although photoperiod exclusively acts as proximal predictor for seasonal metabolic preparation, temperature acts both as ultimate and proximate factor in common voles.

Physiological outputs of the photoperiodic axis (ie, testis mass, testosterone and body mass) show a positive relationship to photoperiod (Figure 2), as described in hamsters.[52,53] Gene expression patterns in the pars tuberalis (ie, *Tshβ*) and tanycytes (*Dio2*, *Dio3*) also follow a positive relationship to photoperiod (Figure 3), which supports previous findings confirming photoperiodic responsiveness of those genes in common voles.[44,45]

Here we show that photoperiodic relationships can be described by dose-response curves, from which critical photoperiods can be derived as inflexion points, ED50. Whether photoperiod can be seen as a dose is debatable, since it has been shown that it is not the photoperiodic length per se, but rather the circadian phase at which light is perceived that determines melatonin suppression leading to photoperiodic responses.[39,40] Critical photoperiods for gonadal responses have been described before in hamsters,[53-55] and at the level of the pars tuberalis and tanycytes in Soay sheep.[56,57]

The critical photoperiod for acceleration of gonadal development in voles gestated on SP is markedly shorter than for arrest of gonadal development in voles gestated on LP (Figure 2C). This difference may lead to accelerated reproductive development when born in spring, to deliver offspring in summer, when there are sufficient food resources for pregnancy, lactation and pup growth. On the other hand, long critical photoperiods in autumn voles may delay reproductive onset until next spring. In autumn animals, biphasic photoperiodic responses have been observed in physiological measures (Figure 2B,E,H), but this is not reflected in hypothalamic gene expression patterns (Figure 3B,F,J). Bimodal curves are also observed in prolactin levels and ovarian cyclicity in sheep, and suggests a limited photoperiodic window of the long day response.[58] At 53°N latitude, from which our *M. arvalis* lab population originates, civil twilight-based photoperiod varies annually between 8.92 and 18.77 hours.[59]

Therefore, the extreme photoperiods of 6:18 and 18:6 hours used in the current study are not or only briefly experienced by our voles in the field. Limited capacity of adaptive responses to these extreme photoperiods may therefore explain the high physiological responses at 6:18 and 18:6 hours and their deviation from the expected dose-response-curve relationships.

Photoperiodic history-dependent effects appear downstream of *Tshβ* in the photoperiodic-axis (Figures 2, 3 and S4), which previously has been confirmed in Siberian hamsters,[11] where increased responses to intermediate photoperiod when born under SP were described as increased sensitivity to photoperiod. This is understandable as the photoperiodic response can be described as a dose-response relationship, where the inflection point has shifted to shorter photoperiods. Hence, indicating increased sensitivity to photoperiod, and therefore increased responses to intermediate photoperiods. However, full dose-response curves are required to demonstrate changes in sensitivity. Our data describe full dose-response curves, and show that indeed the sensitivity to photoperiod has increased in animals born under SP, which explained increased responses to intermediate photoperiods. Increased *Tshr* expression in the tanycytes early in development of vole and hamsters raised under constant SP,[11,45] may lead to increased TSH sensitivity, which may therefore provide an explanation for elevated *Dio2*, and reduced *Dio3* levels in spring animals compared to autumn animals (Figure 3).

The greatest part of the dose-response curve for *Tshβ* is not affect by temperature (Figure 3A,B), but 1 outlier, with high *Tshβ* levels at short photoperiods have been removed from the data set. Interestingly, this outlier belonged to the 10°C experimental groups, indicating that photoperiodic non-responsiveness, which is observed to vary among individuals within populations,[60,61] can be triggered by low ambient temperature.

The finding that testis mass increases at 10°C, primarily under short photoperiods (Figure 2A,B), suggests that early spring and late autumn are temperature sensitive windows for gonadal development. Increasing photoperiod in combination with 10°C and ad libitum food conditions may be a predictor for nearly spring arrival. This interpretation is confirmed by annual temperature patterns at 53°N latitude (were our laboratory colony originates from), which shows that 10°C at increasing photoperiod appears in late April.[59] Our findings are inconsistent with previous studies in hamsters and other vole species, showing decreased gonadal size at 5°C under short and intermediate photoperiods.[20,54,62] This inconsistency may be explained by the fact that at 5°C ambient temperature grass growth is not initiated yet.[63-65] However, species differences in temperature sensitivity cannot be excluded. Bronson and Pryor showed that optimal temperatures for breeding in deer mice greatly varies between latitude of origin.[66] In addition, house mice reproduce in the laboratory at −6°C ambient temperature if food is available in excess throughout the day.[66] Applying a broader range of ambient temperatures under different photoperiodic transitions may reveal an optimal temperature window for reproductive onset and offset in different species.

Testis mass and testosterone levels correlate well under short photoperiods, but under longer photoperiods higher testes mass corresponds to suppressed testosterone levels at 10°C (Figures 2D,E and S2A). Testis development is a time-consuming process, but will rapidly develop in voles born in a cold spring, leading to fully developed testes later in spring when temperatures are rising and testosterone production can be quickly elevated. Increased spermatogenesis due to the presence of testosterone in the testis[68] may therefore lead to quick adaptive responses when spring arrives. Based on annual photoperiodic changes at 53°N latitude, a 14-day earlier onset of testes development (above 50% response) is predicted at 10°C, perhaps leading to a slightly longer seasonal period of large testes when temperatures are low (Figure 4A). On the other hand, testosterone production (above 50% response) may start 2 months later at 10°C, perhaps leading to a dramatic delay and shortening of the breeding season at lower ambient temperatures (Figure 4A).

To adapt annual timing of reproduction to a warming environment due to climate change, mammals need to either change critical photoperiod or eliminate photoperiodic control.[15] Previous selection experiments in short-lived rodents showed that within a single generation, the degree of photoperiodic responsiveness can be highly changed.[69-71] The finding that thermal cues can overrule photoperiodic cues along with short life expectancy and short reproductive cycles, suggests that common voles will relatively quickly ecologically adapt to climate change. Although, we experimentally assessed multiple interactions between different photoperiod and temperature conditions, we do not have data for the complete landscape of (long-term) photoperiodic transitions in relation to all different temperature combinations that occur in the field. Translating these findings to natural conditions is therefore complicated, and should be interpreted with caution. Furthermore, in our experiments, food was available ad libitum, causing voles to be able to compensate for thermoregulatory costs by increasing food intake when temperatures are low. Whether ambient temperature has similar effects on the photoperiodic axis when food is scarce, remains to be experimentally assessed. Furthermore, in this study, we assessed temperature effects on the male reproductive system, while the impact of temperature on the female reproductive system may be of greater importance, since pregnancy and lactation are energy-consuming processes.[67] In addition, spermatogenesis is a more continuous process than ovulation, and therefore the temperature effects on female reproduction may be more critical in affecting fertility. Future studies need

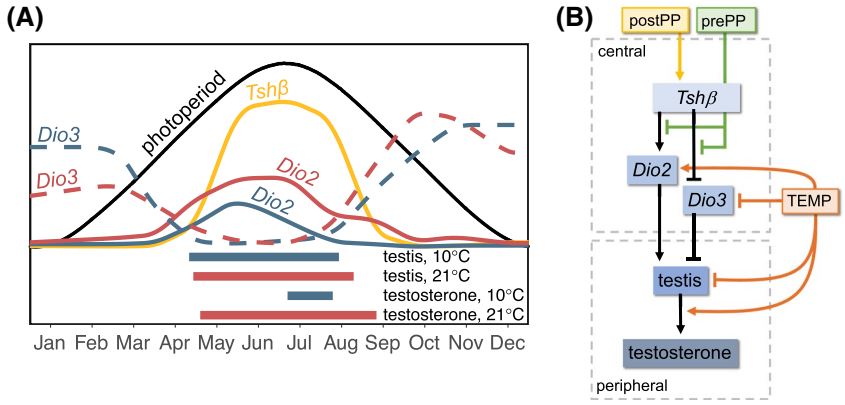

FIGURE 4 Photoperiod and temperature affect the photoperiodic neuroendocrine system. A, Photoperiodic history and temperature-dependent annual fluctuations are shown for: photoperiod (black line), *Tshβ* (yellow line), *Dio2* at 10°C (solid blue line), *Dio2* at 21°C (solid red line), *Dio3* at 10°C (dashed blue line), and *Dio3* at 21°C (dashed red line). Period when testes mass and testosterone levels are above 50% response at 10°C and 21°C is depicted below the graph. B, The scheme shows the effects of postweaning photoperiod (postPP), pre-weaning photoperiod (prePP) and ambient temperature (temp) at different levels central and peripheral in the photoperiodic neuroendocrine system

to assess whether male and female voles respond to the same environmental cues to synchronize their reproductive season.

Temperature effects at the level of the tanycytes are much more explicit, with *Dio2* being strongly downregulated and *Dio3* being slightly upregulated at 10°C in spring voles, and slightly downregulated at 10°C in autumn voles (Figures 3 and S4E,F). Although TSH generally leads to increased *Dio2* and decreased *Dio3*,[37,43,72] the absence of temperature effects in *Tshβ* is not reflected in *Dio2*/*Dio3* expression, suggesting that factors other than TSH can affect *Dio2* expression in the tanycytes. The *Dio2* ~ *Dio3* relationship has previously been shown to be mutually exclusive in common voles exposed to constant photoperiods.[44] However, this effect seems to be less strong at 21°C in relation to photoperiodic-history, where *Dio3* remains high in warm springs while *Dio2* is rising at both temperatures (Figure S4I). Higher *Dio3* levels in warm springs may result in reduced T_3 levels, which ultimately suppress gonadal development. This may provide an explanation for voles having small testes and low testosterone levels under short photoperiods at 21°C (Figures 2A,D and S4A,B).

At 21°C, *Dio2* and testosterone production are controlled by photoperiod, whereas at low temperature, photoperiodic control is limited and suppression takes place. The long critical photoperiods for *Dio2* and testosterone at low temperature, indicate that thermal cues can overrule photoperiodic signals to control seasonal reproduction, which implies opportunistic acting based on metabolic conditions. However, testis growth is under photoperiodic control under all conditions. This observation shows that different outputs of the photoperiodic system can vary in sensitivity to temperature modulation of photoperiodic responses.

Under long photoperiods, *Dio3* is close to zero at both temperatures, while *Dio2* is higher at 21°C (Figures 3E, F, I, J and S4E, F, I). This may result in high central T_3 levels, which is reflected in high testosterone levels at 21°C under LP (Figure 2D and S4B). The lack of a simple relationship between testis size and testosterone at 10°C (Figure S2A) implies that testosterone production can be regulated independent of testis size per se. One possible mechanism involves FSH which increases sertoli cell division rate,[73] and selectively restores spermatogenesis despite low testosterone levels.[74] Sustained negative steroid feedback on the hypothalamus and pituitary, regulating GnRH and FSH/LH secretion respectively might be changed by temperature.[75] This may lead to increased FSH levels, leading to accelerated testes growth and spermatogenesis, and low LH levels leading to suppressed testosterone production, when temperatures are low.

Another possible underlying mechanism involves T_3. In quail, a long-day breeding bird, low ambient temperature stimulates testicular regression, induced by T_3 induction by increased DIO2 in liver.[76] In mammals, cold exposure leads to increased DIO2 levels in brown adipose tissue (BAT), which in turn produces T_3, leading to increased circulating T_3.[77-79] Brandt's voles (*Lasiopodomys brandtii*) indeed have high serum T_3 levels when exposed to cold.[80] Although T_3 stimulates testicular regression in birds, T_3 has dual functions in promoting amphibian metamorphoses: epidermal differentiation of head and body and apoptosis of the tale.[81] Therefore, plasma T_3 may induce differential responses on Sertoli and Leydig cells,[82] leading to a lack of relationship between testis size and testosterone production under cold exposure. It would also be important to study potential mechanisms involved in temperature-induced modifications of photoperiodic central T_3 responses. One potential mechanisms is the Kiss-GnRH neuronal system located in the preoptic-area of the hypothalamus which is involved in temperature regulation.[24,25]

Altogether our findings show that photoperiodic responses in common voles are plastic, and can be modified in response to photoperiodic history and ambient temperature.

Thus, common voles show some degree of opportunism in their annual reproductive strategy. We show that photoperiodic temperature and history-dependent effects appear downstream of *Tshβ* in the photoperiodic axis (Figure 4B). Ambient temperature modifies tanycytic *Dio2*/*Dio3* relationship patterns, which is reflected in physiological responses. Our observations confirm that common voles use a photoperiodic breeding strategy, which can be modified by temperature. Because the vole is an essential herbivorous species in terrestrial ecosystems,[83] defining the mechanisms underlying temperature effects on the reproductive axis will be important for a better understanding of how annual cycling environmental cues impact reproductive function, plasticity in life-history strategies, and population cycle dynamics in vole populations in a changing climate.

ACKNOWLEDGMENTS

We thank R. Schepers for his valuable help in tissue collections and animal care, Dr. H. Dardente for providing the probes for *in situ* hybridization and Prof. Dr. M.P. Gerkema for establishing the common vole colony at the University of Groningen. This work was funded by the Adaptive Life program of the University of Groningen (B050216 to LvR, RTMR, and LdW and RAH), and by the Arctic University of Norway (Universitetet i Tromsø to JvD, DA, and DGH).

CONFLICT OF INTEREST

The authors declare no conflicting interest.

AUTHOR CONTRIBUTIONS

L. van Rosmalen, D.G. Hazlerigg, and R.A. Hut designed the experiments; L. van Rosmalen, J. van Dalum, D. Appenroth, R.T.M. Roodenrijs, L. de Wit, and R.A. Hut conducted the experiments; L. van Rosmalen and J. van Dalum analyzed the data; L. van Rosmalen, D.G. Hazlerigg, and R.A. Hut wrote the paper; all authors read and commented on the paper.

REFERENCES

1. Negus NC, Berger PJ, Forslund LG. Reproductive strategy of *Microtus montanus*. *J Mammal*. 1977;58(3):347-353.
2. Negus NC, Berger PJ, Pinter AJ. Phenotypic plasticity of the montane vole (*Microtus montanus*) in unpredictable environments. *Can J Zool*. 1992;70(11):2121-2124. https://doi.org/10.1139/z92-285
3. Negus NC, Berger PJ, Brown BW. Microtine population dynamics in a predictable environment. *Can J Zool*. 1986;64(3):785-792. https://doi.org/10.1139/z86-117
4. Hoffmann K. Effects of short photoperiods on puberty, growth and moult in the Djungarian hamster (*Phodopus sungorus*). *J Reprod Fertil*. 1973;54:29-35.
5. Horton TH. Growth and reproductive is affected development by the prenatal of male *Microtus montanus* photoperiod. *Biol Reprod*. 1984;504:499-504.
6. Stetson MH, Elliott JA, Goldman BD. Maternal transfer of photoperiodic information influences the photoperiodic response of prepubertal Djungarian hamsters (*Phodopus sungorus*). *Biol Reprod*. 1986;34(4):664-669. https://doi.org/10.1095/biolreprod34.4.664
7. Yellon SM, Goldman BD. Photoperiod control of reproductive development in the male Djungarian hamster (*Phodopus sungorus*). *Endocrinology*. 1984;114(2):664-670.
8. Horton TH. Cross-fostering of voles demonstrates in utero effect of photoperiod. *Biol Reprod*. 1985;33(4):934-939. https://doi.org/10.1095/biolreprod33.4.934
9. Horton TH, Stetson MH. Maternal transfer of photoperiodic information in rodents. *Anim Reprod Sci*. 1992;30(1-3):29-44. https://doi.org/10.1016/0378-4320(92)90004-W
10. Prendergast BJ, Gorman MR, Zucker I. Establishment and persistence of photoperiodic memory in hamsters. *Proc Natl Acad Sci*. 2000;97(10):5586-5591. https://doi.org/10.1073/pnas.100098597
11. Sáenz de Miera C, Bothorel B, Jaeger C, Simonneaux V, Hazlerigg D. Maternal photoperiod programs hypothalamic thyroid status via the fetal pituitary gland. *Proc Natl Acad Sci*. 2017;114(31):8408-8413. https://doi.org/10.1073/pnas.1702943114
12. Sáenz De Miera C. Maternal photoperiodic programming enlightens the internal regulation of thyroid-hormone deiodinases in tanycytes. *J Neuroendocrinol*. 2019;31(1):12679. https://doi.org/10.1111/jne.12679
13. Van DJ, Melum VJ, Wood SH, Hazlerigg DG. Maternal photoperiodic programming: melatonin and seasonal synchronization before birth. *Front Endocrinol (Lausanne)*. 2020;10(January):1-7. https://doi.org/10.3389/fendo.2019.00901
14. Bronson FH *Mammalian Reproductive Biology*. Chicago, IL: University of Chicago Press; 1989. https://doi.org/10.1016/0306-4530(90)90082-k
15. Bronson FH. Climate change and seasonal reproduction in mammals. *Philos Trans R Soc B Biol Sci*. 2009;364(1534):3331-3340. https://doi.org/10.1098/rstb.2009.0140
16. Negus NC, Berger PJ. Experimental triggering of reproduction in a natural population of *Microtus montanus*. *Science (80-)*. 1977;196(4295):1230-1231.
17. Sanders EH, Gardner PD, Berger PJ, Negus NC. 6-methoxybenzoxazolinone: a plant derivative that stimulates reproduction in *Microtus montanus*. *Science (80-)*. 1981;214(4216):67-69.
18. Larkin JE, Freeman DA, Zucker I. Low ambient temperature accelerates short-day responses in Siberian hamsters by altering responsiveness to melatonin. *J Biol Rhythms*. 2001;16(1):76-86. https://doi.org/10.1177/074873040101600109
19. Kriegsfeld LJ, Trasy AG, Nelson RJ. Temperature and photoperiod interact to affect reproduction and GnRH synthesis in male prairie voles. *J Neuroendocrinol*. 2000;12(6):553-558. https://doi.org/10.1046/j.1365-2826.2000.00485.x
20. Nelson RJ, Frank D, Smale L, Willoughby SB. Photoperiod and temperature affect reproductive and nonreproductive functions in male prairie voles (*Microtus ochrogaster*). *Biol Reprod*. 1989;40(3):481-485. https://doi.org/10.1095/biolreprod40.3.481
21. Steinlechner S, Puchalski W. *Mechanisms for Seasonal Control of Reproduction in Small Mammals*. Heidelberg: Springer-Verlag Berlin; 2003.
22. Nelson RJ, Dark J, Zucker I. Influence of photoperiod, nutrition and water availability on reproduction of male California voles (*Microtus californicus*). *J Reprod Fertil*. 1983;69:473-477. https://doi.org/10.1530/jrf.0.0690473
23. Simons MJP, Reimert I, van der Vinne V, et al. Ambient temperature shapes reproductive output during pregnancy and lactation

in the common vole (*Microtus arvalis*): a test of the heat dissipation limit theory. *J Exp Biol*. 2011;214(1):38-49. https://doi.org/10.1242/jeb.044230

24. Caro SP, Schaper SV, Hut RA, Ball GF, Visser ME. The case of the missing mechanism: how does temperature influence seasonal timing in endotherms? *PLoS Biol*. 2013;11(4):e1001517. https://doi.org/10.1371/journal.pbio.1001517
25. Hut RA, Dardente H, Riede SJ. Seasonal timing: how does a hibernator know when to stop hibernating? *Curr Biol*. 2014;24(13):602-605. https://doi.org/10.1016/j.cub.2014.05.061
26. Dardente H, Wood S, Ebling F, Sáenz de Miera C. An integrative view of mammalian seasonal neuroendocrinology. *J Neuroendocrinol*. 2018;31(5):e12729. https://doi.org/10.1111/jne.12729
27. Nakane Y, Yoshimura T. Photoperiodic regulation of reproduction in vertebrates. *Annu Rev Anim Biosci*. 2019;7:173-194. https://doi.org/10.1146/annurev-animal-020518-115216Copyright
28. Klein DC, Weller JL. Indole metabolism in the pineal gland: a circadian rhythm in N-acetyltransferase. *Science (80-)*. 1970;169(3950):1093-1095.
29. Williams LM, Morgan PJ. Demonstration of melatonin-binding sites on the pars tuberalis of the rat. *J Endocrinol*. 1988;119(1):1-3.
30. Dardente H, Klosen P, Pévet P, Masson-Pévet M. MT1 melatonin receptor mRNA expressing cells in the pars tuberalis of the European hamster: effect of photoperiod. *J Neuroendocrinol*. 2003;15(8):778-786. https://doi.org/10.1046/j.1365-2826.2003.01060.x
31. Morgan PJ, Barrett P, Howell HE, Helliwell R. Melatonin receptors: localization, molecular, pharmacology and physiological significance. *Neurochem Int*. 1994;24(2):101-146.
32. Yasuo S, Yoshimura T, Ebihara S, Korf HW. Melatonin transmits photoperiodic signals through the MT1 melatonin receptor. *J Neurosci*. 2009;29(9):2885-2889. https://doi.org/10.1523/JNEUROSCI.0145-09.2009
33. Hazlerigg D, Loudon A. New insights into ancient seasonal life timers. *Curr Biol*. 2008;18(17):795-804. https://doi.org/10.1016/j.cub.2008.07.040
34. Magner JA. Thyroid-stimulating hormone: biosynthesis, cell biology, and bioactivity. *Endocr Rev*. 1990;11(2):354-385.
35. Simonneaux V. A Kiss to drive rhythms in reproduction. *Eur J Neurosci*. 2020;51(1):509-530. https://doi.org/10.1111/ejn.14287
36. Hut RA. Photoperiodism: shall EYA compare thee to a summers day? *Curr Biol*. 2011;21(1):R22-R25. https://doi.org/10.1016/j.cub.2010.11.060
37. Nakao N, Ono H, Yamamura T, et al. Thyrotrophin in the pars tuberalis triggers photoperiodic response. *Nature*. 2008;452(7185):317-322. https://doi.org/10.1038/nature06738
38. Ono H, Hoshino Y, Yasuo S, et al. Involvement of thyrotropin in photoperiodic signal transduction in mice. *PNAS*. 2008;105(47):18238-18242. https://doi.org/10.1073/pnas.0808952105
39. Dardente H, Wyse CA, Birnie MJ, et al. A molecular switch for photoperiod responsiveness in mammals. *Curr Biol*. 2010;20(24):2193-2198. https://doi.org/10.1016/j.cub.2010.10.048
40. Masumoto K-H, Ukai-Tadenuma M, Kasukawa T, et al. Acute induction of Eya3 by late-night light stimulation triggers TSHβ expression in photoperiodism. *Curr Biol*. 2010;20(24):2199-2206. https://doi.org/10.1016/j.cub.2010.11.038
41. Sáenz de Miera C, Monecke S, Bartzen-Sprauer J, et al. A circannual clock drives expression of genes central for seasonal reproduction. *Curr Biol*. 2014;24(13):1500-1506. https://doi.org/10.1016/j.cub.2014.05.024
42. Wood S, Christian H, Miedzinska K, et al. Binary switching of calendar cells in the pituitary defines the phase of the circannual cycle in mammals. *Curr Biol*. 2015;25(20):2651-2662. https://doi.org/10.1016/j.cub.2015.09.014
43. Hanon EA, Lincoln GA, Fustin J-M, et al. Ancestral TSH mechanism signals summer in a photoperiodic mammal. *Curr Biol*. 2008;18(15):1147-1152. https://doi.org/10.1016/j.cub.2008.06.076
44. Król E, Douglas A, Dardente H, et al. Strong pituitary and hypothalamic responses to photoperiod but not to 6-methoxy-2-benzoxazolinone in female common voles (*Microtus arvalis*). *Gen Comp Endocrinol*. 2012;179(2):289-295. https://doi.org/10.1016/j.ygcen.2012.09.004
45. van Rosmalen L, van Dalum J, Hazlerigg DG, Hut RA. Gonads or body? differences in gonadal and somatic photoperiodic growth response in two vole species. *J Exp Biol*. 2020;223:jeb.230987. https://doi.org/10.1242/jeb.230987
46. Gerkema MP, Daan S, Wilbrink M, Hop MW, Van Der Leest F. Phase control of ultradian feeding rhythms in the common vole (*Microtus arvalis*): the roles of light and the circadian system. *J Biol Rhythms*. 1993;8(2):151-171. https://doi.org/10.1177/074873049300800205
47. Appenroth D, Melum VJ, West AC, Dardente H, Hazlerigg DG, Wagner GC. Photoperiodic induction without light-mediated circadian entrainment in a High Arctic resident bird. *J Exp Biol*. 2020;223(16):jeb220699. https://doi.org/10.1242/jeb.220699
48. Lomet D, Cognié J, Chesneau D, Dubois E, Hazlerigg D, Dardente H. The impact of thyroid hormone in seasonal breeding has a restricted transcriptional signature. *Cell Mol Life Sci*. 2018;75(5):905-919. https://doi.org/10.1007/s00018-017-2667-x
49. Ritz C, Baty F, Streibig JC, Gerhard D. Dose-response analysis using R. *PLoS One*. 2015;10(12):1-13. https://doi.org/10.1371/journal.pone.0146021
50. Team RC. *R: A Language and Environment for Statistical Computing*. Vienna, Austria: R Found Stat Comput. Published online 2013. https://doi.org/10.1108/eb003648
51. Wickham H. *Ggplot2: Elegant Graphics for Data Analysis*. New York: Springer-Verlag; 2016. https://doi.org/10.1007/978-3-319-24277-4_1
52. Elliott JA. Circadian rhythms and photoperiodic time measurement in mammals. *Fed Proc*. 1976;35(12):2339-2346.
53. Gaston S, Menaker M. Photoperiodic control of hamster testis. *Science (80-)*. 1967;158(3803):925-928.
54. Steinlechner S, Stieglitz A, Ruf T, Heldmaier G, Reiter RJ. Integration of environmental signals by the pineal gland and its significance for seasonality in small mammals. In: Fraschini F, Reiter RJ, eds. *Role of Melatonin and Pineal Peptides in Neuroimmunomodulation*. New York: Plenum Press; 1991:159-163.
55. Hoffmann K. The critical photoperiod in the Djungarian hamster *Phodopus sungorus*. In: Aschoff J, Daan S, Groos G, eds. *Vertebrate Circadian Systems*. Heidelberg: Springer-Verlag Berlin; 1982:297-304.
56. Hazlerigg D, Lomet D, Lincoln G, Dardente H. Neuroendocrine correlates of the critical day length response in the Soay sheep. *J Neuroendocrinol*. 2018;30(9):e12631. https://doi.org/10.1111/jne.12631
57. Dardente H, Lomet D, Chesneau D, Pellicer-Rubio MT, Hazlerigg D. Discontinuity in the molecular neuroendocrine response to increasing daylengths in Ile-de-France ewes: is transient Dio2

induction a key feature of circannual timing? *J Neuroendocrinol*. 2019;31(8):1-10. https://doi.org/10.1111/jne.12775
58. Wagner GC, Johnston JD, Clarke IJ, Lincoln GA, Hazlerigg DG. Redefining the limits of day length responsiveness in a seasonal mammal. *Endocrinology*. 2008;149(1):32-39. https://doi.org/10.1210/en.2007-0658
59. Hut RA, Paolucci S, Dor R, Kyriacou CP, Daan S. Latitudinal clines: an evolutionary view on biological rhythms. *Proc R Soc B Biol Sci*. 2013;280(1765):1-9. https://doi.org/10.1098/rspb.2013.0433
60. Nelson RJ. Photoperiod-nonresponsive morphs: a possible variable in *Microtine* population-density fluctuations. *Univ Chicago Press*. 1987;130(3):350-369.
61. Kliman RM, Lynch RG. Evidence for genetic variation in the occurrence of the photoresponse of the Djungarian hamster, Phodopus sungorus. *J Biol Rhythms*. 1992;7(2):161-173.
62. Baker JR, Ranson RM. Factors affecting the breeding of the field mouse (*Microtus agrestis*). Part II. temperature and food. *Proc R Soc B Biol Sci*. 1932;112(774):39-46.
63. Peacock JM. Temperature and leaf growth in four grass species. *J Appl Ecol*. 1976;13(1):225-232.
64. Peacock JM. Temperature and leaf growth in *Lolium perenne*. II. The site of temperature perception. *J Appl Ecol*. 1975;12(1):115-123.
65. Cooper JP. Climatic variation in forage grasses. I. Leaf development in climatic races of *Lolium* and *Dactylis*. *J Appl Ecol*. 1964;1(1):45-61. https://doi.org/10.2307/2401588
66. Bronson FH, Pryor S. Ambient temperature and reproductive success in rodents living at different latitudes. *Biol Reprod*. 1983;29(1):72-80.
67. Speakman JR. The physiological costs of reproduction in small mammals. *Philos Trans R Soc B Biol Sci*. 2008;363(1490):375-398. https://doi.org/10.1098/rstb.2007.2145
68. Walker WH. Testosterone signaling and the regulation of spermatogenesis. *Spermatogenesis*. 2011;1(2):116-120. https://doi.org/10.4161/spmg.1.2.16956
69. Heideman PD, Bronson FH. Characteristics of a genetic polymorphism for reproductive photoresponsiveness in the white-footed mouse (*Peromyscus leucopus*). *Biol Reprod*. 1991;44:1189-1196.
70. Goldman SL, Dhandapani K, Goldman BD. Genetic and environmental influences on short-day responsiveness in Siberian hamsters (*Phodopus sungorus*). *J Biol Rhythms*. 2000;15(5):417-428. https://doi.org/10.1177/074873000129001503
71. Spears N, Clark JR. Selection in field voles (*Microtus agrestis*) for gonadal growth under short photoperiods. *J Anim Ecol*. 1988;57(1):61-70.
72. Guerra M, Blázquez JL, Peruzzo B, et al. Cell organization of the rat pars tuberalis. Evidence for open communication between pars tuberalis cells, cerebrospinal fluid and tanycytes. *Cell Tissue Res*. 2010;339(2):359–381. https://doi.org/10.1007/s00441-009-0885-8
73. Meachem SJ, McLachlan RI, de Kretser DM, Robertson DM, Wreford NG. Neonatal exposure of rats to recombinant follicle stimulating hormone increases adult Sertoli and spermatogenic cell numbers. *Biol Reprod*. 1996;54(1):36-44. https://doi.org/10.1095/biolreprod54.1.36
74. Lerchl A, Sotiriadou S, Behre HM, et al. Restoration of spermatogenesis by follicle-stimulating hormone despite low Intratesticular testosterone in photoinhibited hypogonadotropic Djungarian hamsters (*Phodopus sungorus*). *Biol Reprod*. 1993;49(5):1108-1116.
75. Gupta D. Hypothalamic control of the mammalian sexual maturation. *Padiatr Padol*. 1977;5:83-102.
76. Ikegami K, Atsumi Y, Yorinaga E, et al. Low temperature-induced circulating triiodothyronine accelerates seasonal testicular regression. *Endocrinology*. 2015;156(2):647-659. https://doi.org/10.1210/en.2014-1741
77. Silva JE, Larsen PR. Potential of brown adipose tissue type II thyroxine 5'-deiodinase as a local and systemic source of triiodothyronine in rats. *J Clin Invest*. 1985;76(6):2296-2305. https://doi.org/10.1172/JCI112239
78. de Jesus LA, Carvalho SD, Ribeiro MO, et al. The type 2 iodothyronine deiodinase is essential for adaptive thermogenesis in brown adipose tissue. *J Clin Invest*. 2001;108(9):1379-1385. https://doi.org/10.1172/JCI200113803
79. Lowell BB, Spiegelman BM. Towards a molecular understanding of adaptive thermogenesis. *Nature*. 2000;404(6778):652-660. https://doi.org/10.1038/35007527
80. Zhang Q, Lin Y, Zhang XY, Wang DH. Cold exposure inhibits hypothalamic Kiss-1 gene expression, serum leptin concentration, and delays reproductive development in male Brandt's vole (*Lasiopodomys brandtii*). *Int J Biometeorol*. 2015;59(6):679-691. https://doi.org/10.1007/s00484-014-0879-4
81. Denver RJ. Neuroendocrinology of amphibian metamorphosis. In: Shi Y-B, ed. *Current Topics in Developmental Biology*, 1st edn, vol. 103. Burlington, VT: Elsevier Inc; 2013:195-227. https://doi.org/10.1016/B978-0-12-385979-2.00007-1
82. Wagner MS, Wajner SM, Maia AL. The role of thyroid hormone in testicular development and function. *J Endocrinol*. 2008;199(3):351-365. https://doi.org/10.1677/JOE-08-0218
83. Bakker E, Olff H, Boekhoff M, Gleighman J, Berendse F. Impact of herbivores on nitrogen cycling. *Oecologia*. 2004;138(1):91-101. https://doi.org/10.1007/s00442-003-1402-5

SUPPORTING INFORMATION

Additional Supporting Information may be found online in the Supporting Information section.

How to cite this article: van Rosmalen L, van Dalum J, Appenroth D, et al. Mechanisms of temperature modulation in mammalian seasonal timing. *The FASEB Journal*. 2021;35:e21605. https://doi.org/10.1096/fj.202100162R

Paper III

Differential effects of ambient temperature on the photoperiod-regulated spring and autumn growth programme in *Microtus oeconomus* and their relationship to the primary photoneuroendocrine response pathway.

Authors:

Mattis Jayme van Dalum[1]*, Laura van Rosmalen[2]*, Daniel Appenroth[1], Renzo T. M. Roodenrijs[2], Lauren de Wit[2], and Roelof A. Hut[2] & David G. Hazlerigg[1#]

1 Arctic Seasonal Timekeeping Initiative, Department of Arctic and Marine Biology, UiT - the Arctic University of Norway, Tromsø, 9037, Norway.

2 Chronobiology Unit, Groningen Institute for Evolutionary Life Sciences, University of Groningen, Groningen, 9747AG, The Netherlands.

#Correspondence: david.hazlerigg@uit.no

*These authors contributed equally

Keywords: Seasonality, maternal photoperiodic programming, temperature, photoperiodic neuroendocrine system, pars tuberalis, hypothalamus, Microtus oeconomus, deiodinase, thyroid signaling, testosterone somatic growth

Acknowledgements

We thank R. Schepers for his valuable help in tissue collections and animal care, Dr. H. Dardente for providing the probes for *in situ* hybridization and Prof.dr. M.P. Gerkema for establishing the common vole colony at the University of Groningen. This work was funded by the Adaptive Life program of the University of Groningen (B050216 to LvR, RTMR, LdW and RAH), and by the Arctic University of Norway (Universitetet i Tromsø, to JvD, DA and DGH).

Abstract

Seasonal mammals register photoperiodic changes through the photoneuroendocrine system (PNES) enabling them to time seasonal changes in growth, metabolism and reproduction. To a varying extent, proximate environmental factors such as ambient temperature (Ta) modulate timing of seasonal changes in physiology, conferring adaptive flexibility. While the molecular photo-neuroendocrine pathway governing the seasonal responses is well-defined, the mechanistic integration of non-photoperiodic modulatory cues is poorly understood. Here we report on a laboratory experiment which explored the interaction between Ta and photoperiod in the tundra vole, *Microtus oeconomus*, a boreal species in which the main impact of photoperiod is on post-natal somatic growth. We demonstrate that post-weaning growth potential depend on both gestational and post-weaning patterns of photoperiodic exposure, with the highest growth potential seen in animals experiencing short (8-h) gestational and long (16-h) post-weaning photoperiods – corresponding to a spring growth program. Modulation of these pre- and post-natal photoperiodic influences by Ta was asymmetric: low Ta (10C) enhanced the growth potential of animals gestated on 8-h photoperiods independent of post-weaning photoperiod exposure, whereas in animals gestated on 16-h photoperiods, showing a lower autumn programmed growth potential, the effect of Ta as highly dependent on post-weaning photoperiod – increasing potential in animals switched to a 10-h photoperiod, but decreasing it in animals switched to a 12-h photoperiod. Analysis of the primary molecular elements involved in the expression of a neuroendocrine response to photoperiod, thyrotropin beta subunit (*tshβ*) expression in the pars tuberalis, and type 2/3 deiodinase (*dio2* / *dio3*) expression in the mediobasal hypothalamus, identified *dio2* as the most Ta sensitive gene across the study as a whole, showing increased expression at higher Ta. Contrastingly *dio3* and *tshβ* were largely insensitive to Ta. Overall, these observations reveal a complex interplay between Ta and photoperiodic control of post natal growth in *M oeconomus*, and suggest that integration of Ta into the control of growth occurs downstream of the primary photoperiodic response cascade.

Introduction

In species living in the temperate and boreal zones, the scheduling of growth, development and reproduction is contingent on the annual cycle of seasonal environmental change stemming from Earth's orbit of the Sun. This has led to the evolution of seasonal synchronization mechanisms reliant on changes in the daily photoperiod as a synchronizer (Dardente, Hazlerigg and Ebling, 2014; Hazlerigg and Simonneaux, 2015; Wood and Loudon, 2018). Additionally, to a degree that varies between species, proximate factors such as nutritional status, ambient temperature (Ta) and social interactions modulate seasonal scheduling, giving phenotypic plasticity in the face of year to year variation in environmental seasonality (Bronson, 2004, 2009; Visser *et al.*, 2010).
It has been argued based on life-history considerations that modulatory effects conferring plasticity are likely to be of increased importance in smaller short lived species (e.g. non-hibernating rodents) than in larger species that survive and reproduce over multiple years (e.g. cervids) (Bronson, 2009). Accordingly, we have focused on microtine rodents as a suitable group in which to explore interactions between photoperiod and non-photic influences on seasonal physiology.

In the common vole, *M. arvalis* we recently reported that photoperiodic experience in early life shapes post-natal reproductive development, with the developmental trajectory being determined by interactive effects of photoperiod exposure experienced *in utero*, via the maternal melatonin signal, and in the juvenile period, directly through the pup's photoneuroendocrine system (van Rosmalen *et al.*, 2021). Further, we have demonstrated that temperature influences on this response are associated with changes in thyroid hormone deiodinase gene expression in the basal hypothalamus (van Rosmalen *et al.*, 2021) – establishing a point of intersection with the photoperiodic response one step removed from proximate actions of photoperiod in the pars tuberalis (PT) of the pituitary gland (Dardente, Hazlerigg and Ebling, 2014).

We have also begun to investigate photoperiodic influences in a species with a more northerly paleogeography, the tundra vole (*M. oeconomus*) (Conroy and Cook, 2000; Conway-Campbell *et al.*, 2012). In contrast to the common vole, early life photoperiod has a smaller impact on post natal reproductive development in *M. oeconomus*, while there are clear photoperiodic influences on somatic growth during the juvenile period, not seen in *M. arvalis* (van Rosmalen *et al.*, 2020). However, somatic growth in *M. arvalis* seems to be more sensitive to photoperiodic change (van Rosmalen *et al.*, 2021).

In the present study our aim was three-fold: Firstly, we wished to extend our initial characterization of early life photoperiod influences on somatic growth in *M. oeconomus* to resolve between the effects of gestational and neonatal photoperiod. Secondly, by combined manipulation of photoperiod and Ta, we sought to assess the extent to which photoperiodically programmed seasonal growth trajectories show plasticity. Finally, by analysis of gene expression in the basal

hypothalamus and PT, we sought to determine the extent to which modulatory effects of temperature on juvenile growth reflect effects on the neuroendocrine machinery of the primary photoperiodic response.

Methods

Animals and experimental procedures

All experimental procedures were carried out according to the guidelines of the animal welfare body (IvD) of the University of Groningen conform to Directive 2010/63/EU and approved by the CCD (Centrale Commissie Dierproeven) of the Netherlands (CCD license number: AVD1050020171566). Tundra or root voles (*Microtus oeconomus*) were obtained from 4 different areas in the Netherlands (Van De Zande *et al.*, 2000). The population has been kept in the laboratory as an outbred colony at the University of Groningen, which provided all animals used in this study. Adult and weaned voles were individually housed in transparent plastic cages (15 x 40 x 24 cm) provided with sawdust, dried hay, an opaque pvc tube and *ad libitum* water and food (Standard rodent chow; Altromin #141005). The experiments were carried out in temperature-controlled chambers in which ambient temperature and photoperiod was manipulated as described below.

The voles used in the experiment (93 males) were gestated and born at 21°C under either a short photoperiod (SP, 8 hours of light/ 24 hours: early breeding season, hereafter termed 'spring-programmed') or a long photoperiod (LP, 16 hours of light/24 hours: late breeding season, hereafter termed 'autumn programmed') and weaned at an age of 21-days old. After weaning, voles were transferred to either 10°C or 21°C and a range of different photoperiods, a laboratory equivalent to different seasonal conditions (Fig.1). Post-weaning photoperiods were (hours light: hours dark): 16L:8D, 14L:10D, 12L:12D, 10L:14D. Hence spring-programmed animals experienced a post-weaning increase in photoperiod, while autumn-programmed animals experienced a post-weaning decrease in photoperiod. All voles were weighed when 7, 15, 21, 30, 42 and 50 days old.

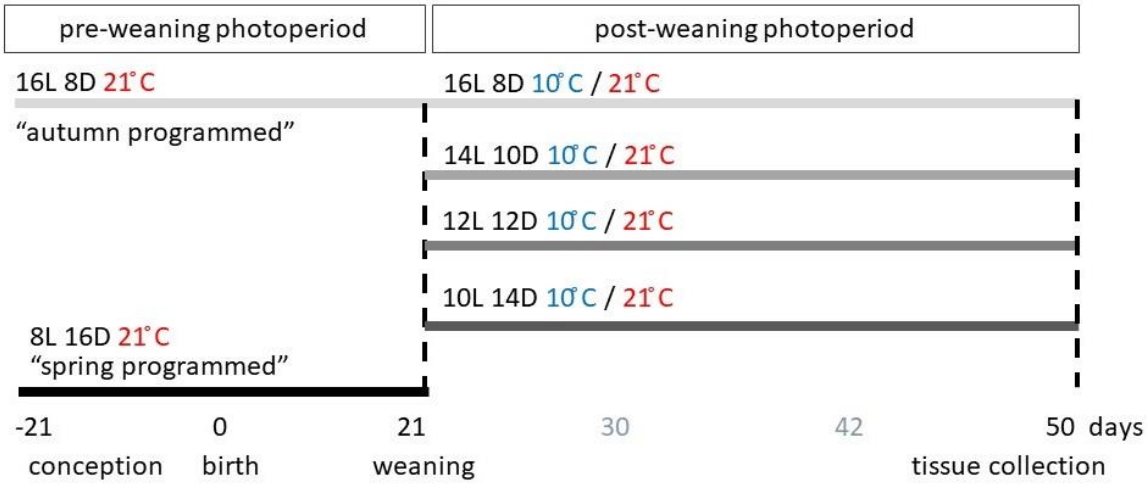

Figure 1. Experimental design. Conception, gestation, birth and lactation took place under either 16 hours of light (i.e. autumn programmed) or 8 hours of light (i.e. spring programmed) at 21°C. At the day of weaning (21 days old) voles from both pre-weaning photoperiods were transferred to four different post-weaning photoperiods at either 10°C or 21°C resulting in eight different post-weaning treatments. Tissue collections took place when 50 days old.

Tissue collection

At 50 days age, and ~ 17-h after lights-off, voles were sedated with CO_2 and then decapitated. Trunk blood was collected directly from each vole into heparinized tubes. Blood samples were left on ice until centrifugation (10 min., 2600 x g, 4°C). Plasma was transferred to a clean tube and stored at -80°C until hormonal assay. Whole brains were carefully dissected to include the proximate pituitary stalk including the pars tuberalis (PT). Within 5 minutes after decapitation, brains were slowly frozen on a brass block surrounded by liquid N_2. Brains were stored at -80°C until proceed to *in situ* hybridization. Reproductive organs were dissected, cleaned of fat, and wet masses of paired testis weight were measured (±0.0001 g).

In situ hybridization

A detailed description of the *In situ* hybridization protocol can be found elsewhere (Lomet *et al.*, 2018). Briefly, 20 µm coronal brain sections were cut on a cryostat in caudal to rostral direction, starting from the mammillary bodies to the optic chiasm, to cover the area of the hypothalamus and third ventricle. Sections were mounted onto pre-coated Superfrost Plus slides (Thermo scientific: ref J1800AMNZ) with 6-10 sections per slide and 10 slides per individual. Antisense riboprobes of rat *tshβ* (GenBank accession No. M10902, nucleotide position 47-412), *Microtus arvalis dio2* (GenBank accession No. JF274709, position 1-775) and *M. arvalis dio3* (GenBank accession no. JF274710, position 47-412) were transcribed from linearized cDNA templates. Incorporation of 35^S-UTP (Perkin Elmer, Boston, MA, USA) was done with T7 polymerase (*dio2* and *dio3*) and T3 polymerase (*tshβ*), resulting in 0,5-1,5x10^6 counts per minute per µl, calculated

to have 10^6 counts / minute /slide. All slides were fixed in paraformaldehyde, acetylated and hybridized with radioactive probes overnight at 56°C.

Slides were washed in sodium citrate buffer the next day to remove nonspecific probe and then dehydrated in ethanol solutions, followed by air drying. The slides were exposed to an autoradiographic film (Kodak, Rochester, NY, USA) for 9 days (*Dio2* and *Dio3*) or 11 days (*Tshβ*) and developed with Carestream Kodak autoradiography GBX Developer/replenisher (P7042-1GA, Sigma) and fixer (P7167-1GA, Sigma)**.** Films were scanned with an Epson Perfection V800 Photo scanner at 2400dpi resolution along with a calibrated optical density strip (T2115C, Stouffer Graphic Arts Equipment Co., Mishawaka, IN, USA). Analysis of integrated optical density (IOD) was done with software ImageJ, version Fuji (NIH Image, Bethesda MD, USA). The section with the highest signal was selected to represent each animal.

Hormone analysis

Plasma testosterone levels were measured in a mouse testosterone enzyme linked immunosorbent assay according to manufacturer's instructions (ADI-900-065; Enzo Life Sciences, New York, NY, USA). Sensitivity: 5.67 pg/ml, intra-assay coefficient of variation: 10.8%, inter-assay coefficient of variation: 9.3%.

Fitting of growth curves

Post-weaning growth in individual voles was modelled using a standard von Bertalanffy asymptotic growth function:

$$W_t = W_\infty * \left(1 - e^{-kt}\right)$$

Where W_t is the weight at time t, W_∞ is the growth potential (asymptote) and k is the rate constant for reaching the asymptotic potential. The day of weaning was set as t = 0 and mass at t = 0 was subtracted to give a zero baseline. A summary of curve fits, giving W_∞ and half-times (ln[2])/k) can be found in Table S1.

Calculation of critical photoperiod for gene expression responses

4-parameter log-logistic functions ($y = d + (c–d) / 1 + (x /e)^b$) were fitted through the data to describe the response to photoperiod as a dose-response relationship; b = slope parameter (Hill coefficient), c = minimum, d = maximum, e = 50% maximal response, where ED50 is defined as the inflexion point of the curve. Critical photoperiod (CP) was estimated by the ED50 from fitted dose-response curves. All fitted dose-response curve parameters can be found in Table S2.

Analysis of variance and post-hoc testing

The effects of post-weaning photoperiod, ambient temperature and interactions were determined within spring- and autumn-programmed experimental groups using two-way ANOVA. To detect differences in growth rate between groups, we used repeated measures ANOVAs. Where appropriate post-hoc testing was performed using Tukey's test. Statistical significance was determined at $p < 0.05$.

All curve fitting, statistical analyses and figures were generated using GraphPad Prism v9.

Results

Somatic growth

Photoperiodic conditions during gestation and prior to weaning had no significant effect on body mass recorded at weaning (G8 animals 16.5 +- 3.6 g; G16 animals 17.4 +- 3.2 g, t = 1.474, 91df, p=0.14).

The effects of Ta and post-weaning photoperiod on post-weaning somatic growth are summarized in graphically Fig 2, with curve fit parameters in Table S1. Overall, the growth potential, defined as the asymptotic weight in the von Bertalanffy function, was consistently higher in spring programmed animals (12–32g depending on post-weaning conditions) than in autumn programmed animals (5–20g depending on post-weaning conditions). Post-weaning photoperiod similarly had a strong influence on growth potential with the highest asymptotic weights on LD16:8 being some 1.5- to 2-fold greater than corresponding values under LD10:14, across all combinations of pre-weaning photoperiod and Ta. In spring programmed animals, across all post-weaning photoperiods, low Ta (10°C) in the post-weaning phase increased growth potential by up to approximately 50% compared to animals raised after weaning at 21°C (2-way ANOVA: p<0.01 for main effect of Ta, NS for Ta x post-weaning photoperiod interaction). By contrast, Ta had no effect on growth potential in autumn programmed animals. Across the study as a whole no significant variation in growth rate, i.e. the half time for the growth function, was observed.

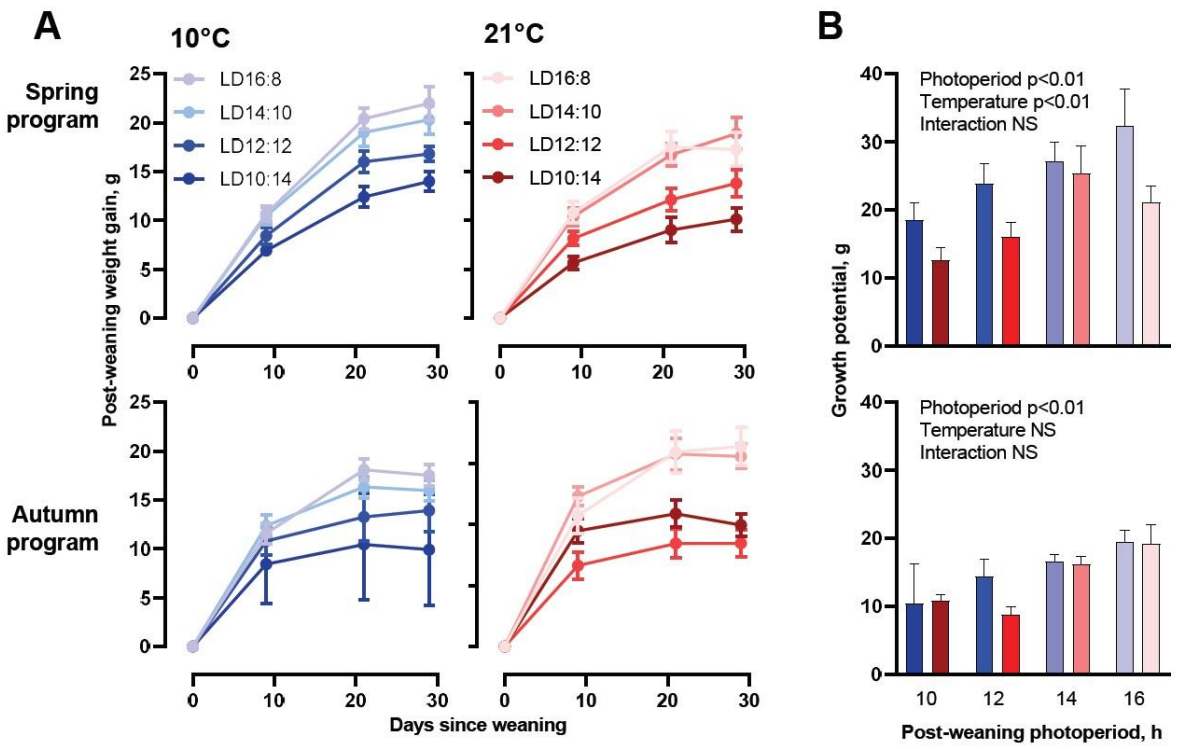

Figure 2. Post-weaning growth response in relation to photoperiod and ambient temperature. (A) Post-weaning growth curves (A) and post-weaning growth potential (B) for four different post-weaning photoperiods at 10°C (blue) or 21°C (red) in both spring (LD 8:16, top panel) and autumn (LD 16:8, bottom panel) programmed voles. Data are plotted as mean ± SEM (n = 4-8).

Photoneuroendocrine pathway gene expression

The expression of *tshβ* in the PT followed a sigmoid relationship to post-weaning photoperiod (Figure 3A, Table S2), from which critical photoperiod (CP) for the primary photoperiodic response could be estimated (N.B. in spring programmed animals this represents the CP for induction of a long day increase in *tshβ* expression, while in autumn programmed animals this represents the CP for short day suppression of *tshβ* expression). In spring programmed animals CP was not significantly affected by Ta (10°C CP_{spring}=14.73, 95CI 14.01 – 15.46; 21°C CP_{spring}=15.21, 95CI 14.93-15.49), but in autumn programmed animals low Ta significantly decreased the CP for suppression of *tshβ* expression by about 1 hour (10°C CP_{autumn}=14,38 95CI 14,09-14.96; 21°C CP_{autumn}=15.38, 95CI 15.12-15.3; $p<0.05$ for model comparison).

In contrast to *tshβ*, sigmoid model fits were poor descriptors of the patterns of *dio2* and *dio3* gene expression across the post-weaning photoperiod regimes (Fig 3B, Table S2), but clear pre- and post-weaning effects were nonetheless observed. Overall *dio2* expression was markedly higher in spring programmed animals compared to autumn programmed animals, while the inverse was observed for *dio3*.

Within spring programmed animals, *dio2* was highly sensitive to post-weaning photoperiod with the highest expression levels in LD16:8 animals being up to two orders of magnitude higher than levels in animals raised after weaning on LD10:14 ($p<0.001$ for main effect of post-weaning photoperiod by 2-way ANOVA). Across all post-weaning photoperiods, spring programmed animals raised after weaning at a higher Ta generally had higher *dio2* expression than their low Ta counterparts ($p<0.01$ for main effect of Ta, by 2-way ANOVA). Although there was no significant post-weaning photoperiod x Ta interaction under 2-way ANOVA, the effect of Ta on spring program *dio2* expression was most apparent at short post-weaning photoperiod, where expression appeared to clamped at basal / background levels at 10°C. In autumn programmed animals, *dio2* expression was uniformly low across all post-weaning photoperiods, but a positive effect of increased Ta could still be observed ($p<0.001$ for main effect by 2-way ANOVA), and as in the short post-weaning photoperiod spring program animals, this appeared to be due to a clamping down of *dio2* expression to background levels in 10°C animals.

In contrast to *dio2*, *dio3* appeared to be highly sensitive to post-weaning photoperiod ($p<0.001$for main effect under 2-way ANOVA) but insensitive to Ta. Within the spring programmed animals, *dio3* was detectable in LD10;14 and 12:12, but suppressed to background levels on the two longer post-weaning photoperiods. In autumn programmed animals, a similar *dio3* response profile was observed, with several individuals showing above baseline expression on LD14:10.

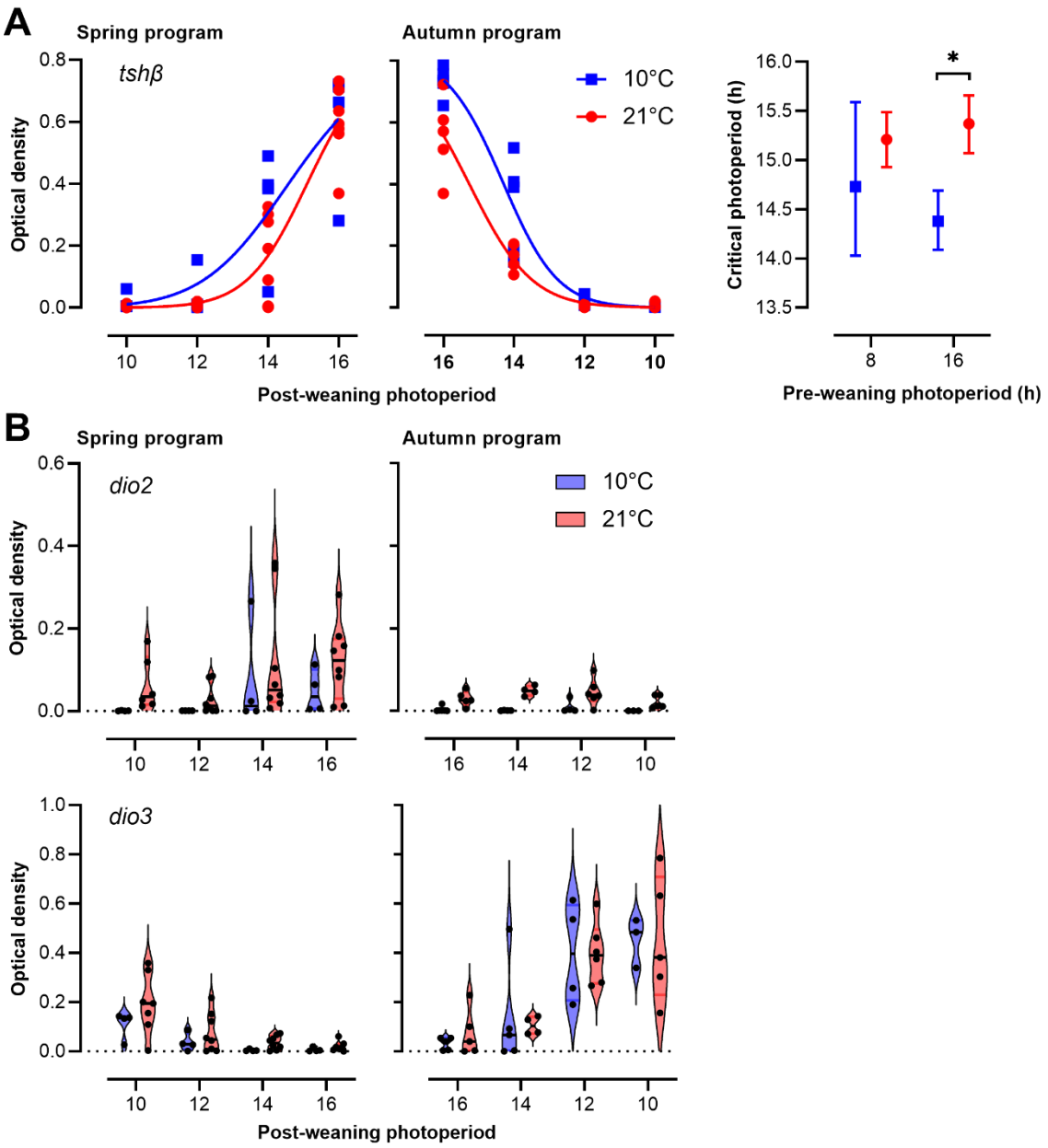

Figure 3. Tanycyte gene expression in relation to photoperiod and ambient temperature. (A) *Tshb* expression in the pars tuberalis. Each data point represents optic density measurements from individual animals. Lines are best fit curves for 4-parameter log-logistic functions, as described in the methods. Critical photoperiod derived from fitted dose-response-curves (Table S1, S2) for *Tshb*, data are mean ± 95% CL (n = 4-8), * indicates significant differences between critical photoperiod estimates (p<0,05). (B) Violin plots showing *Dio2* and *Dio3* expression in tanycytes (median=horizontal bar). In both A and B: the left panels represent spring-.programmed vole (gestated and raised to weaning under 8L) and the right panels represent autumn-programmed voles (gestated and raised to weaning under 16L) at 10°C (blue) or 21°C (red). (C) Images showing localization of mRNA by *In situ* hybridization are shown for *Tshβ, Dio2* and *Dio3* expression.. Significant effects are indicated: *$p < 0.05$.

Gonadal activation

The effects of photoperiod and Ta on gonadal weight and end point plasma testosterone levels are summarized in Fig 4. Independent of gestational photoperiod and Ta, final gonadal weights in animals held on a post-weaning photoperiod of LD16:8 were consistently about 50% higher than corresponding values in LD10:14 animals ($p<0.001$ for main effect of post-weaning photoperiod by 2-way ANOVA). Contrastingly, no significant effects of Ta on testicular growth were observed. Across the study as a whole, wide inter-individual variation in testosterone levels at time of sacrifice were observed, and no significant effects of pre- or post-weaning conditions were found.

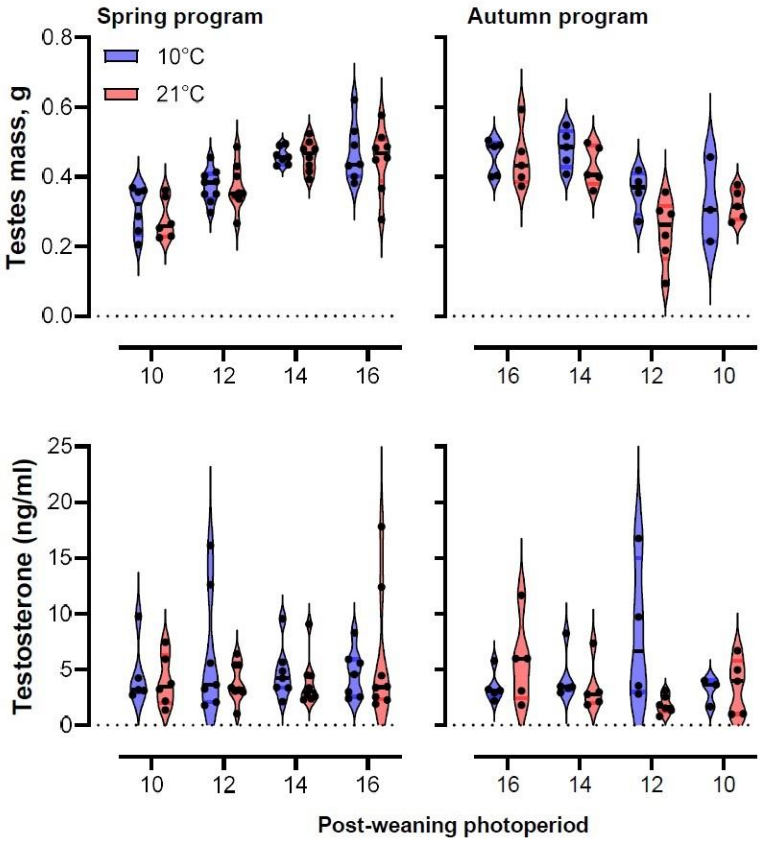

Figure 4. Activation of the gonadal axis in relation to photoperiod and ambient temperature. The violin plots show values for individual animals with the horizontal black line within each violin being the median value.

Discussion

While there is a considerable literature on the programming effects of photoperiod on post-natal reproductive development in seasonal rodent species (Sáenz de Miera, 2019; van Dalum *et al.*, 2020), few studies have focused on maternal photoperiodic programming of somatic growth (Horton, 2005). Here, we have presented a comprehensive analysis on this phenomenon in a microtine rodent in which effects on growth are at least as pronounced as those on reproductive development. Our data demonstrate that while gestational photoperiod does not affect body mass prior to weaning, it has a profound effect on post-weaning growth potential, upon which further effects of post-weaning photoperiod are superimposed. Within this framework, we also describe a complex pattern of temperature effects, with low temperature enhancing growth potential in spring- to a lesser extend in autumn-programmed voles. Analysis of corresponding effects in the photoneuroendocrine system indicates that temperature modulation of growth potential occurs downstream of the PT, and possibly involves *dio2*-mediated changes in hypothalamic thyroid hormone status.

The experiment we describe represents highly constrained artificial representation of natural environmental conditions: all animals had *ad libitum* access to food and were individually housed to avoid confounding intra-individual interactions. We therefore assume that the observed effects on growth cannot be accounted for by simple energy supply vs demand considerations – a view supported by the finding that the *highest* body masses and growth potentials were seen in voles raised after weaning at *low* Ta, when thermoregulatory energy demands will have been higher. Related to this, it is intriguing to note that while growth potential W_∞ was found to be highly labile to effects of photoperiod and Ta, we were unable to detect any effects on half times (ln[2]/k) for reaching asymptotic size. Collectively these findings support the view that early life photoperiodic experience and temperature establish a target for final body size, and that this is then achieved over an internally fixed time-window. The eco-evolutionary reasons for control of the somatic growth phase in this manner may relate to the short life spans of this species and the consequent need to complete the developmental phase and initiate reproduction before senescence takes hold.

While growth potential was sensitive to post-weaning photoperiodic experience, independent of Ta or gestational photoperiod, it was nonetheless clear that growth potential in autumn born voles was considerably lower than in spring born animals. This history-dependent aspect was also reflected in the highly asymmetric patterns of *dio2* and *dio3* expression in animals with different gestational photoperiodic history: High growth potential in spring is associated with high levels of *dio2* and low levels of *dio3*, while the converse is true in autumn programmed animals. This suggests that thyroid hormone mediated effects on hypothalamic

control (Dardente, Hazlerigg and Ebling, 2014), possibly via somatostatin signaling (Dumbell *et al.*, 2015), may account for the differing spring and autumn growth programs.

Asymmetry was also seen in the modulatory effect of Ta on post-weaning growth potential: low Ta increases potential in spring programmed animals, but is without effect in autumn born animals. We are unclear as to why this should be the case: possibly low Ta in the spring condition signals that environmental conditions suitable for reproduction are likely to occur further into the future than in a warm spring, and this in turn encourages a commitment to investing in a large mature body size for later competitiveness. Against this hypothesis, we see no corresponding disinvestment in the gonadal axis in low Ta spring animals, indeed developmental of the gonadal axis appears to entirely Ta insensitive and only mildly sensitive to photoperiodic influences (see also(van Rosmalen *et al.*, 2020, 2021)). Potentially the absence of Ta modulatory effects in autumn program voles, can be seen as a reflection of the lack of value if Ta as a predictor of forthcoming energy supply / demands in the autumn phase: nutrient supply may be largely down to plant growth that has already appeared.

Analysis of *dio2* / *dio3* gene expression provides some support for the notion that Ta, gestational and post-weaning photoperiodic influences converge at this level. This view is consistent with the concept that the tanycyte cells in which the deiodinase genes are expressed are metabolic interfaces to the hypothalamic control systems (Bolborea and Dale, 2013; Dardente, Hazlerigg and Ebling, 2014). Contrastingly, current models suggest that the regulation of *tshβ* gene expression in the PT represents the key photoperiodic switch for control of seasonal responses (Dardente *et al.*, 2010; Masumoto *et al.*, 2010), and is resistant to photoperiod-independent perturbatory effects – a resistance that might contribute to the function of the PT as a circannual calendar tissue (Lincoln, Anderson and Loudon, 2003; Wood and Loudon, 2018). In this light, we were surprised to observe a decrease in CP for suppression of *tshβ* expression in autumn programmed animals held at low Ta. Given that neither somatic growth potential nor gonadal weights show a similar pattern of response in autumn programmed animals, it is difficult to put this finding in a functional context. Nevertheless, it raises the possibility that regulation of tshb expression in the PT is more sensitive to metabolic influence than previously appreciated.

Table S1: growth curve parameters

	Prew PP (h)	T_a (˚C)	Postw PP 10 h Mean	Postw PP 10 h 95% CI	Postw PP 12 h Mean	Postw PP 12 h 95% CI	Postw PP 14 h Mean	Postw PP 14 h 95% CI	Postw PP16 h Mean	Postw PP16 h 95% CI
Post-weaning growth potential in g.	8	10	18,52	12,26- 24,79	23,85	17,29 -30,41	27,19	20,51 – 33,88	32,39	19,23- 45,55
	16	10	10,33	-14,74-35,40	14,39	6,47 – 22,31	16,53	13,46 – 19,61	19,54	15,07 – 24,02
	8	21	12,56	7,91 – 17,22	16,07	11,30 – 20,84	25,41	16,19 – 34,63	21,13	15,41 – 26,84
	16	21	10,77	8,10 – 13,44	8,83	6,04 – 11,62	16,14	12,82- 19,47	19,27	12,84 – 25,69
Post-weaning growth half-time in days (ln[2])/k)	8	10	13,15	6,30 – 19,99	15,25	6,05 – 24,45	12,90	6,32 – 19,48	15,16	6,37- 23,95
	16	10	1,39	-4,15 - 6,93	4,19	-1.21 – 9,18	4,51	3,29 – 5,72	6,76	3,20 – 10,32
	8	21	11,07	5,65 – 16,49	9,32	5,14- 13,50	13,95	1,94 – 25,96	8,68	3,35 – 14,02
	16	21	2,57	-0,99 – 6,13	4,96	1,39 – 8,53	3,95	0,95 - 6,96	8,00	2,64 – 13,36

Table S2: curve fits for gene expression

Variable	Prew PP (h)	T_a (˚C)	Hillslope (b)	95% CI	Bottom (c) 95% CI	Top (d) 95% CI	EC50 (e)	95% CI	R^2 (df)
TSHBb	8	10	11,24	4,72 to 17,77	*0*	*0,85*	14,73	14,01 to 15,46	0,76 (14)
	16	10	17,68	12,64 to 27,43	*0*	*0,85*	14,38	14,09 to 14,69	0,93 (15)
	8	21	16,92	12,74 to 22,29	*0*	*0,85*	15,21	14,93 to 15,49	0,88 (25)
	16	21	16,27	12,46 to 21,50	*0*	*0,85*	15,38	15,12 to 15,63	0,93 (18)
Dio2	8	10	5,98	-4,94 to 31,22	*0*	*0,12*	15,69	11,70 to ???	0,11(14)
	16	10	0,01	0,01 to ???	*0*	*0,12*	Unstable	(Very wide)	0,00 (15)
	8	21	0,00	0,00 to 0,00	*0*	*0,12*	Unstable	(very wide)	0,00 (29)
	16	21	0,67	-1,73 to 3,21	*0*	*0,12*	45,48	16,36 to ???	0,02 (18)
Dio3	8	10	-7,57	-21,04 to -3,93	*0*	*0,5*	8,47	6,76 to 9,43	0,68 (14)
	16	10	-14,58	??? to -5,46	*0*	*0,5*	13,09	11,94 to 14,07	0,60 (15)
	8	21	-6,48	-11,92 to -3,47	*0*	*0,5*	9,29	7,78 to 9,96	0,47 (28)
	16	21	-13,44	-46,21 to -5,18	*0*	*0,5*	13,06	12,12 to 14,19	0,58 (18)

References

Bolborea, M. and Dale, N. (2013) 'Hypothalamic tanycytes: Potential roles in the control of feeding and energy balance', *Trends in Neurosciences*. Elsevier Ltd, 36(2), pp. 91–100. doi: 10.1016/j.tins.2012.12.008.

Bronson, F. H. (2004) 'Are humans seasonally photoperiodic?', *Journal of Biological Rhythms*, 19(3), pp. 180–192. doi: 10.1177/0748730404264658.

Bronson, F. H. (2009) 'Climate change and seasonal reproduction in mammals', *Philosophical Transactions of the Royal Society B: Biological Sciences*. Royal Society, 364(1534), pp. 3331–3340. doi: 10.1098/rstb.2009.0140.

Conroy, C. J. and Cook, J. A. (2000) 'Phylogeography of a post-glacial colonizer: Microtus longicaudus (Rodentia: Muridae)', *Molecular Ecology*, 9(2), pp. 165–175. doi: 10.1046/j.1365-294X.2000.00846.x.

Conway-Campbell, B. L. *et al.* (2012) 'Molecular dynamics of ultradian glucocorticoid receptor action', *Molecular and Cellular Endocrinology*. Elsevier, pp. 383–393. doi: 10.1016/j.mce.2011.08.014.

van Dalum, J. *et al.* (2020) 'Maternal Photoperiodic Programming: Melatonin and Seasonal Synchronization Before Birth', *Frontiers in Endocrinology*, 10(January), pp. 1–7. doi: 10.3389/fendo.2019.00901.

Dardente, H. *et al.* (2010) 'A molecular switch for photoperiod responsiveness in mammals (supplemental information)', *Current Biology*. Elsevier, 20(24), pp. 2193–2198. doi: 10.1016/j.cub.2010.10.048.

Dardente, H., Hazlerigg, D. G. and Ebling, F. J. P. (2014) 'Thyroid hormone and seasonal rhythmicity', *Frontiers in Endocrinology*, 5(FEB), pp. 1–11. doi: 10.3389/fendo.2014.00019.

Dumbell, R. A. *et al.* (2015) 'Somatostatin Agonist Pasireotide Promotes a Physiological State Resembling Short-Day Acclimation in the Photoperiodic Male Siberian Hamster (Phodopus sungorus)', *Journal of Neuroendocrinology*, 27(7), pp. 588–599. doi: 10.1111/jne.12289.

Hazlerigg, D. and Simonneaux, V. (2015) *Seasonal Regulation of Reproduction in Mammals*. Fourth, *Knobil and Neill's Physiology of Reproduction*. Fourth. Elsevier. doi: 10.1016/C2011-1-07288-0.

Horton, T. H. (2005) 'Fetal origins of developmental plasticity: Animal models of induced life history variation', *American Journal of Human Biology*, 17(1), pp. 34–43. doi: 10.1002/ajhb.20092.

Lincoln, G. A., Anderson, H. and Loudon, A. (2003) 'Clock genes in calendar cells as the basis of annual timekeeping in mammals - A unifying hypothesis', *Journal of Endocrinology*, 179(1), pp. 1–13. doi: 10.1677/joe.0.1790001.

Lomet, D. *et al.* (2018) 'The impact of thyroid hormone in seasonal breeding has a restricted transcriptional signature', *Cellular and Molecular Life Sciences*. Springer International Publishing, 75(5), pp. 905–919. doi: 10.1007/s00018-017-2667-x.

Masumoto, K. H. *et al.* (2010) 'Acute induction of Eya3 by late-night light stimulation triggers TSHβ expression in photoperiodism', *Current Biology*. Elsevier Ltd, 20(24), pp. 2199–2206. doi: 10.1016/j.cub.2010.11.038.

van Rosmalen, L. *et al.* (2020) 'Gonads or body? Differences in gonadal and somatic photoperiodic growth response in two vole species', *The Journal of Experimental Biology*, 223, p. jeb.230987. doi: 10.1242/jeb.230987.

van Rosmalen, L. *et al.* (2021) 'Mechanisms of temperature modulation in mammalian seasonal timing', *FASEB Journal*, 35(5), pp. 1–12. doi: 10.1096/fj.202100162R.

Sáenz de Miera, C. (2019) 'Maternal photoperiodic programming enlightens the internal regulation of thyroid-hormone deiodinases in tanycytes', *Journal of Neuroendocrinology*, 31(1), pp. 1–11. doi: 10.1111/jne.12679.

Visser, M. E. *et al.* (2010) 'Phenology, seasonal timing and circannual rhythms: towards a unified framework', *Philosophical Transactions of the Royal Society B: Biological Sciences*, 365(1555), pp. 3113–3127. doi: 10.1098/rstb.2010.0111.

Wood, S. and Loudon, A. (2018) 'The pars tuberalis: The site of the circannual clock in mammals?', *General and Comparative Endocrinology*. The Authors, 258, pp. 222–235. doi: 10.1016/j.ygcen.2017.06.029.
Van De Zande, L. *et al.* (2000) 'Microsatellite analysis of population structure and genetic differentiation within and between populations of the root vole, Microtus oeconomus in the Netherlands', *Molecular Ecology*, 9(10), pp. 1651–1656. doi: 10.1046/j.1365-294X.2000.01051.x.

Paper IV

Evidence for repeated local gene duplication at the *Aldh1a1* locus in an herbivorous rodent *(Microtus oeconomus)*.

Authors:

Mattis J. van Dalum[1], Simen R. Sandve[2], Patrik R. Mörch[3], Roelof. A. Hut[4], David G. Hazlerigg[1]

[1] Arctic Chronobiology and Physiology, Arctic and Marine Biology, UiT – the Arctic University of Norway, 9019 Tromsø, Norway

[2] Centre of Integrative Genetics, Department of Animal and Aquaculture Sciences, Norwegian University of Life Sciences, Ås NO-1432

[3] Evolutionsbiologisk centrum (EBC), Department of Ecology and Genetics, Animal Ecology. Uppsala University, 752 36 Uppsala, Sweden.

[4] Chronobiology Unit, Groningen Institute for Evolutionary Life Sciences, University of Groningen, Groningen, 9747AG, the Netherlands.

Author contributions:

Mattis J. van Dalum: writing, figures, and data analysis.

Simen R. Sandve: assembly of the reference genome and construction of phylogenetic trees

Patrik R. Mörch: bioinformatics assistance

David G. Hazlerigg: supervision and editing of manuscript

Roelof.A.Hut (University of Groningen): editing of manuscript and provision of *Microtus arvalis* genome.

Acknowledgements

Karol Zub (Polish Academy of Sciences) – provision of *M.oeconomus* samples from Poland

Siw Turid Killengreen (University of Tromsø- The Arctic University of Norway) – provision of M.oeconomus samples from Northern Norway

Jakob Högland (Uppsala University) – provision computational resources

Abstract

Environmental seasonality varies greatly across latitudes, and mammals have evolved mechanisms to synchronize physiology and reproduction to the seasons. The predictable latitude dependent annual day length cycle is the cue used by internal timing mechanisms to predict temperature changes. The mammalian photoneuroendocrine system (PNES) is well characterized, yet little is known about sources of variation and local adaptation. Therefore, we searched for signatures of selection between a Northern- and Southern European population of the rapidly evolving and widely distributed tundra vole (*Microtus oeconomus).* We performed pooled whole genome sequencing and calculated the fixation index (F_{ST}) and heterozygosity with 20 kbp non-overlapping sliding windows. Genes located in high F_{ST} windows and the nearest upstream and downstream genes were reported. One of the strongest F_{ST} signals was found in a genomic region that harbored a cluster of *Aldh1a1* paralogs. Additional comparative genomics analyses revealed that the signal peak overlapped an *Aldh1a1* duplicate not present in mouse or rat. This cluster contained three additional *Aldh1a1* paralogues in the tundra vole, reed vole (*M.fortis*) and prairie vole (*M.ochrogaster*) and two in the common vole (*M.arvalis*) and field vole (*M.agrestis*). The *Aldh1a7* could not be located in the prairie vole but was present in the mouse, rat and other *Microtus* species. Since *Aldh1* family members are implicated both in seasonal PNES function and in processing of the herbivorous diet, further studies are required to determine the functional significance of these findings

Introduction

Environmental seasonality varies greatly with latitude, and higher latitudes are associated with lower winter temperatures, large annual changes in day length and strong seasonality in food supply. Organisms native to these environments have evolved physiological mechanisms to adapt to the cold and synchronize life history events with the seasons. The predictable annual day length cycle is the cue used by an internal timing mechanism to predict seasonal temperature changes (Hazlerigg and Simonneaux 2015). This predictable photoperiod-temperature relationship serves as a calendar for seasonal organisms to prepare behavior and physiology in time (Hut et al. 2013). The latitude dependent photoperiod-temperature relation is expected to drive local adaptations in seasonal time keeping mechanisms in a cline-like fashion. Observable output is the shortening of the breeding season with increasing latitude as documented in deer mice (*Peromyscus),* lagomorphs and cervids (Bronson 1985). Northern versus southern meadow voles (*Microtus pennsylvanicus*) also showed a differential immune response in relation to short photoperiods (Pyter, Weil, and Nelson 2005). Yet evidence for a latitudinal cline in genetic components associated with timekeeping is scarce and mostly comes from insects (Hut et al. 2013).

In vertebrates, photoperiodic information is received through the photoneuroendocrine system (PNES). In mammals, the nocturnal secretion of melatonin internalizes day length information and controls the seasonal secretion of thyroid-stimulating hormone (TSH) from *pars tuberalis* into the hypothalamus (Nakao, Ono, and Yoshimura 2008; Dardente et al. 2010; Hanon et al. 2008). Photoperiod driven TSH signaling translates in downstream, species-specific adaptations such as seasonal reproduction, hibernation and molt (Dardente, Hazlerigg, and Ebling 2014; Dardente et al. 2010). The mammalian PNES is well characterized (Hazlerigg and Simonneaux 2015; Wood and Loudon 2014; Yoshimura 2006; Prendergast 2005), yet it is unclear how selection operates in adaptations to local photoperiod-temperature relations. Pittendrigh & Takamura (1989) first discussed an expected latitudinal cline in the circadian timekeeping system and clock gene polymorphisms found in birds (Johnsen et al. 2007)and fish (O'Malley and Banks 2008; O'Malley, Ford, and Hard 2010) suggest the potential to find signatures of selection in PNES related genes.

Genome-wide screenings for signatures of selection potential provide an unbiased approach to assess the evolution of seasonal timekeeping mechanisms in mammals. Signatures of selection are defined as a reduction or a change in genetic variation in certain genomic regions because of natural selection pressures, leading to functional differences between populations (Bertolini et al. 2018; Messer and Petrov 2013). Positive selection on a favoured allele tends to drive it to

fixation, leading to an overall reduction in heterozygosity in a given region (Messer and Petrov 2013; Vitti, Grossman, and Sabeti 2013). This is detectable in high local fixation index (F_{ST}) scores. Genome-wide selection studies have mostly been done on domestic species and have revealed selection on the thyroid stimulating hormone receptor (*TSHr*) and the associated lack of seasonal breeding in chickens (Rubin et al. 2010).

Voles (*Microtus sp.)* are seasonally breeding, non-hibernating, herbivorous rodents with a wide distribution range reaching from equatorial zones to the arctic, occurring both in Eurasia as in North America. The *Microtus* genus one of the most speciose among mammals (Jaarola et al. 2004), and is rapidly evolving, which is reflected in the high mutation rate and frequent occurrence of chromosomal restructuring (Triant and DeWoody 2006; Sitnikova et al. 2007). Voles mostly feed on grass and a seasonal shift in diet has been observed in *M.pennsylvanicus* (Lindroth and Batzli 1984), *M.agrestis* (Evans 1973; Ecke et al. 2018) and *M.oeconomus* (Bergman and Krebs 1993). At higher latitudes, voles breed from spring to autumn with overwintering individuals coming to reproduction first in spring (Gliwicz 1996; Lambin, Krebs, and Scott 1992). Photoperiod affects vole reproduction mostly in growth rate and maturation of pups. The increasing photoperiods in spring accelerates reproductive maturation of newborn pups whereas the decreasing photoperiod after the summer solstice decelerates growth and delays maturation until the next spring, preparing the pups to overwinter (Horton 1985, Gliwicz 1996). Voles are phenotypically plastic regarding the timing of breeding and opportunistic winter breeding has been observed in various species, also at higher latitudes (Tast and Kaikusalo 1976; Kerbeshian, Bronson, and Bellis 1994).

The tundra vole (*Microtus oeconomus)* is the most wide spread vole species in both longitude (from Western Europe to Alaska) and latitude (45-72°N). In Lithuania (55-56°N) the breeding seasons lasts from April to October and starts already under the snow (Balčiauskas, Balčiauskiene, and Janonyte 2012). Occasional winter breeding has been observed as far north as 69°N in Finland (Tast 1966; Tast and Kaikusalo 1976). Tundra voles thus encounter a wide range of photoperiod-temperature relations, which makes this species an excellent model to study genetic adaptation to different seasonal environments in mammals. Tundra voles and Common voles (*Microtus arvalis)* from similar locations responded differently to a range of photoperiods and temperatures in the lab (Van Rosmalen et al. 2020), which could reflect genetic variation in the PNES that may have been affected by latitudinal selection. Therefore, our aim was to screen for signatures of selection across the whole genome of the tundra vole through comparing a Northern (70°N) and Southern European (53°N) population. We have

chosen an unbiased, genome wide approach to screen for selected genes associated seasonal time keeping, cold adaptation, immune response, energy expenditure and seasonal diet changes.

Materials and Methods

Tundra vole reference genome

Liver from a male tundra vole (*Microtus oeconomus)* housed in an outbred lab colony at the University of Groningen was dissected out and stored at -80. High molecular weight DNA was isolated from 25mg frozen liver using Nanobind Tissue Big DNA Kit from Circulomics. Extracted DNA was needle shared using a 27G blunt end needle, then size selection was performed by using the Short Read Elimination Kit from Circulomics. Two sequencing libraries were prepared by using the LSK-109 kit, following the Genomic DNA by Ligation Nanopore Protocol. Both libraries from the same individual were combined and divided into three batches. Sequencing on one Promethion flow cell (FLO-PRO002) was performed by sequentially loading the three library pools.

Reads were first filtered using fastp v0.19.5 (10.1093/bioinformatics/bty560), with the parameters '--disable_trim_poly_g --disable_adapter_trimming -q 7 -l 4000 -f 50'. The resulting filtered reads were assembled with Flye v2.8 with the parameters '--nano-raw $INPUT --min-overlap 15000 --genome-size 3g' (Kolmogorov et al. 2019) and polished with Pepper v0.0.6 ('--model_path pepper_r941_guppy305_human.pkl') (Shafin et al. 2021) after mapping with Minimap2 v2.17 with the parameter '-ax map-ont' (doi:10.1093/bioinformatics/bty191). A final step of error correction was done by mapping Illumina reads to the genome using the Burrows-Wheeler Aligner (BWA) (Li and Durbin 2009) with bwa-mem v0.7.17 (arXiv:1303.3997v2), before using Pilon v0.0.6 with the default parameters (Walker et al. 2014) using a dataset with 77-fold coverage of Illumina sequencing reads (Short read archive project accession: PRJEB33458).

Tissue collection of two tundra vole populations

Tissue samples from wild tundra voles were obtained from Northern Norway representing the Northern population (n=12, with 5 males, 7 females) and Poland representing the Southern population (n=13, with 5 males, 8 females). The northern population was sampled on September 1st 2015 in the Troms & Finnmark county, Ifjordfjellet region between the towns Lakselv and Tana (70°24'N 27°16'E) at an altitude of about 400 m above sea level (Fig. 1). The Southern

population is sampled in Białowieża (52°42'N 23°51'E) at an altitude of 160 m over the period from June to October in the years from 2010 to 2014.

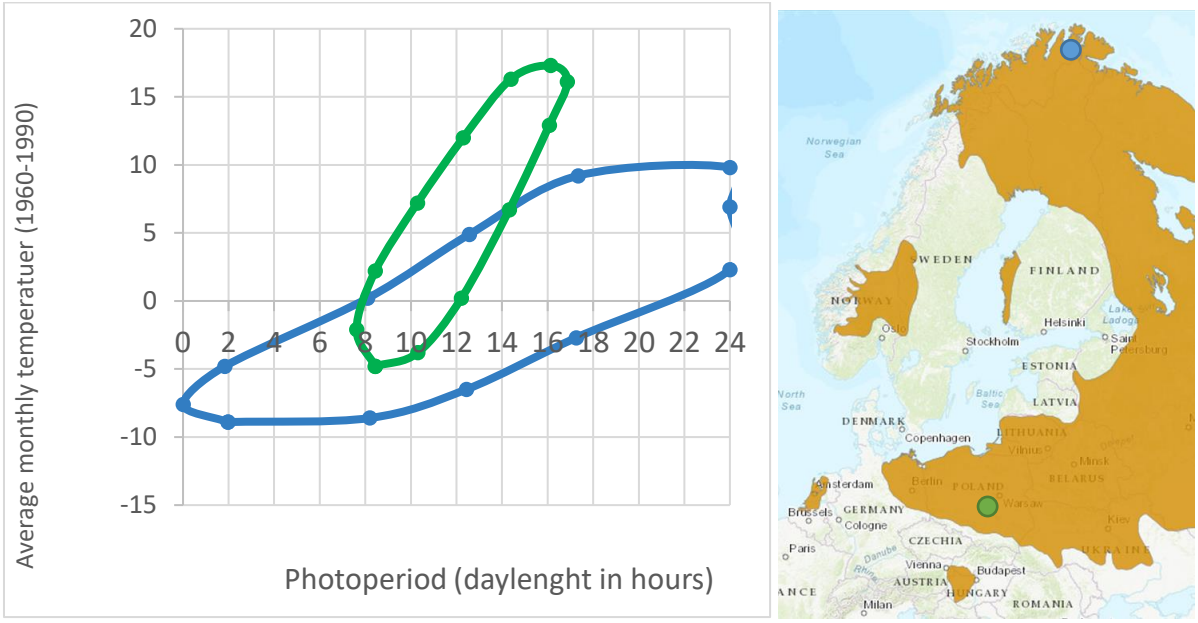

Figure 1. Trapping areas and photoperiod-temperature ellipses. Finnmark, Northern Norway (blue) and Białowieża, Poland (green).

DNA extraction and sequencing

From the Norwegian population, a 25mg muscle sample was dissected directly from each individual. From the Poland population, a ~2cm tail sample was sent dry. Total genomic DNA was extracted using the DNeasy Blood & Tissue kit (Qiagen, Hilden, Germany) following the instructions of the manufacturer. Prior to DNA isolation the samples were ruptured with a TissueLyser II (Qiagen, Hilden Germany) by placing a 5 mm stainless steel bead in standard 2ml Eppendorf tubes containing the samples. The machine was run on 25 Hz for five minutes. In the last step of the kit, the samples were eluded twice with 200µl AE buffer (10mM Tris-Cl 0.5mM EDTA; PH 9.0), to achieve a total volume of 400µl. The sample quality and concentration was measured with Nanodrop 2000 (Thermoscientific TM, Waltham, Massachusetts, United States).

Sanger sequencing (by Eurofins Genomics, Ebersberg, Germany) of a 136 bp fragment of the Cytochrome B gene (position 666 – 801) was used to confirm the samples as *Microtus oeconomus* by aligning the sequences against the NCBI database (Sayers et al. 2021) using BLAST (Altschul et al. 1990) . Cytochrome B primers and PCR amplification conditions were taken from the paper by Galan, Pagès, & Cosson (2012): L15411F 5'-GAY AAA RTY CCV TTY CAY CC-3' and H15546R 5'-AAR TAY CAY TCD GGY TTR AT-3' and PCR instructions described there.

In preparation for Illumina sequencing, 1 µl Rnase A (10mg/ml stock; VWR E866-1ML) was added to 400µl of DNA samples and incubated them at 37 degrees Celsius for 20 minutes. The samples were cleaned through ethanol precipitation and purity was checked with Nanodrop followed by Qubit (Invitrogen Qubit 2.0) analysis for a more precise concentration estimation. DNA quality was checked on a 0.8% agarose gel ran for 30 min on 100 volt. Genomic DNA of the individuals within a population was pooled with each individual contributing equally in amount of DNA. Truseq PCR free libraries were created for each population pool. Pools were sequenced on an Illumina Hiseq 3000 machine with 150 bp paired end reads on 8 lanes in total, resulting in an average coverage of ~191 fold per site and ~15 fold per individual.

Trimming and alignment of reads

The quality of both forward and reverse reads was checked for each lane with FastQC (S. Andrews 2010) software. The forward reads were better in quality than the reverse reads. Raw reads were trimmed with Trimmomatic version 0.39 (Bolger, Lohse, and Usadel 2014) on paired end mode and adaptors (Truseq3-PE-2.fa) were clipped off with the ILLUMINACLIP setting on default (seedmismatches 3, palindrone clip threshold on 30 and simple clip threshold on 10). Reads were trimmed by cropping 7 base pairs from the beginning and 20 base pairs off the ending of each read, resulting in a trimmed read length of 123 bp. FastQC quality check was run again after trimming.

The trimmed reads of each lane were mapped onto the *M.oeconomus* reference genome (NCBI:txid64717) with BWA using bwa mem on default setting. Alignment quality checks for each lane were performed with Samtools (Li et al. 2009) flagstat. Ambiguous read mappings with a quality score below 20 were removed and files were further sorted with Samtools sort and converted into bam.files. The aligned lanes were then merged into one .bam file for each population and further merged into one pileup file with Samtools mpileup with option –B to reduce false SNPs (single nucleotide polymorphisms) caused by misalignments.

Fst analysis with PoPoolation 2

The pileup file was converted into a sync file by using the scripts of the PoPoolation 2 software (Kofler, Pandey, and Schlötterer 2011). Minimum base quality score for base calling was set on 20. SNP calling and pairwise allele frequency calculations were done with PoPoolation2 (snp-frequency-diff-pl). Only regions with a minimum average coverage per population of 50- 400 fold were included. The minimum read count for a SNP was 15, which represents about one individual per population given the estimated average 15x coverage per individual. One individual represents 7,7% (Poland) and 8,3% (Norway) of the population which is higher than

the 5% threshold for minor alleles used by most genome wide population studies (Chheda et al. 2017)

Signatures of selection were screened through calculating the mean fixation index (F_{ST}) for non-overlapping sliding windows of 20.000 bp across the entire genome in regions where the minimum average coverage per population was between 50-400 fold. In addition, F_{ST} values were calculated for each individual SNP. F_{ST} values were calculated from the allele-frequencies using the standard equation as shown in Hartl & Clark (2007). Heterozygosity (H_p) were calculated scores for both populations separately in R (R Core Team 2019), using the tidyverse package (Wickham, Averick, et al. 2019) for the 20kbp windows and per SNP. In addition, we took the average between H_p scores per population and calculated the total heterozygosity score of both populations taken together.

Before further analysis and drawing of plots, 4464 windows with fewer than 10 SNPs were removed and contigs smaller than 4 Mbp were cut off as the average coverage dropped from ~150 to ~100, leaving 105157 windows for analysis. Then all F_{st} and H_p scores for both the 20kbp windows and per SNP were Z-transformed by subtracting the mean of all observations from each single observation and divide this by the standard deviation of all observations. Frequency distributions were made in R to determine the one-tailed 95% significance percentiles for ZF_{ST} (positive side) and ZH_p (negative side).

Gene annotation and identification of paralogues and orthologues

To be able to identify candidate genes under divergent selection we first produced a lightweight gene annotation using the Liftoff software (Shumate and Salzberg 2021) based on most recent ensembl mouse annotation (CL57BL6) (Howe et al. 2021). In-depth comparative genomics to other voles (*Microtus arvalis* NCBI:txid47230, genome provided by R.A. Hut, Groningen University), *Microtus ochrogaster* NCBI:txid79684, *Microtus agrestis* NCBI:txid29092, *Microtus fortis* NCBI:txid100897) rodents (*Mus musculus* NCBI:txid10090 , *Rattus norvegicus* NCBI:txid10116) and rabbit (*Oryctolagus caniculus* NCBI:txid9986) were done using the BLAST+ suite (Camacho et al. 2009). Genomes and F_{ST} values were visualised in the Interactive Genome Viewer (Robinson et al. 2011). Comparative genomics figures were drawn and statistics were performed in R, using the packages dplyr (Wickham, François, et al. 2019), ggplot2 (Wickham 2009) GridExtra, Grid, GridText (Murrell 1999) and viridis (Garnier et al. 2021).

Construction of a phylogenetic tree

The multiple sequence alignment program MAFFT (Katoh and Standley 2013) was used to align coding sequences of the *Aldh1a1* and *Aldh1a1*-like genes of the species mentioned above. Mega X (Kumar et al. 2018) was used to construct a phylogenetic tree using the maximum likelihood (ML) algorithm and the substitution model GTR+G+I. We included gap sequences and estimated topology uncertainty using 100 bootstrap replicates. The rabbit (*Oryctolagus caniculus*, NCBI:txid9986) *Aldh1a1* sequence was used as an outgroup to root the tree. The resulting nexus tree file was imported into R using seqinr (Charif and Lobry 2007) and the tree was visualized in R using the ape package (Paradis and Schliep 2019).

Results

Microtus oeconomus de novo *assembly*

De novo sequencing of the tundra vole using Promethion resulted in 990.948 high quality reads with a mean size of 37.000 bp. The final genome assembly, following the error correction steps, contained 269 fragments (scaffolds and contigs), covering 2.19 Gbp. The maximum fragment length was 131.34 Mbp and the fragment N50 was 60.75 Mbp (Statistics table S1).

Genome wide selection signatures between a Northern and Southern tundra vole population

After mapping the pooled genomes of the two populations onto the reference genome, we found a total of 69,522,739 SNPS and an average of 643 SNPs per 20 kbp sequence length. On average, 31.5% of the base pairs were polymorphic between the two populations and the average heterozygosity (H_p) for the Northern (Finnmark) population was higher than for the Southern (Poland) population. Manhattan plots summarise the results in Figure 2 and table S2.

After Z-transforming the F_{ST} scores we found 216 windows below the 0,5% percentile of the Fst frequency distribution (Fig. 2), and of these, 61 windows contained one or several known genes as indicated by the lift-off software that used mouse sequence homology. The other windows fell in intergenic regions and for these windows, we have looked for the nearest upstream and downstream gene. The results of this survey are summarised in table S6. Genes that fell within F_{ST}-windows were mostly vomeronasal- and olfactory receptors, as well as genes involved in the immune system, such as *CD1d1* antigen and *CD1d2*, immunoglobulin kappa chain variable 9-124, variable 13-85 and variable 8-18, immunoglobulin heavy variable V12-3 (*Ighv 12-3*) and *Ighv 4-2*. Olfactory receptor 1537 and 1111, vomeronasal 1 receptor 15, vomeronasal 2, receptor 116, taste receptors type 2 members 125, 142 and 113 but also serotonin receptor 5B (*Htr5b*) fell within an high F_{ST}-window ($p<0.005$).

Three genes known to be involved in the photoneuroendocrine system were found neighbouring high F_{ST} windows that fell in an intergenic region. The melatonin receptor 1b (*Mtnr1b*) lies 1.9 Mbp upstream of a window with an F_{ST} of 0.20; the iodothyronine deiodinase 2 (*Dio2*) lies 240 kbp upstream of a window with an F_{ST} 0.48, and aldehyde dehydrogenase 1 family member a1 (*Aldh1a1)* lies 80kbp upstream of two successive windows with F_{ST} of 0.68 and 0.66. Additionally, the *Aldh1a7* lies 160kb downstream of the second of these two high F_{ST} windows. We therefore decided to focus further analysis on the *Aldh1a1* region.

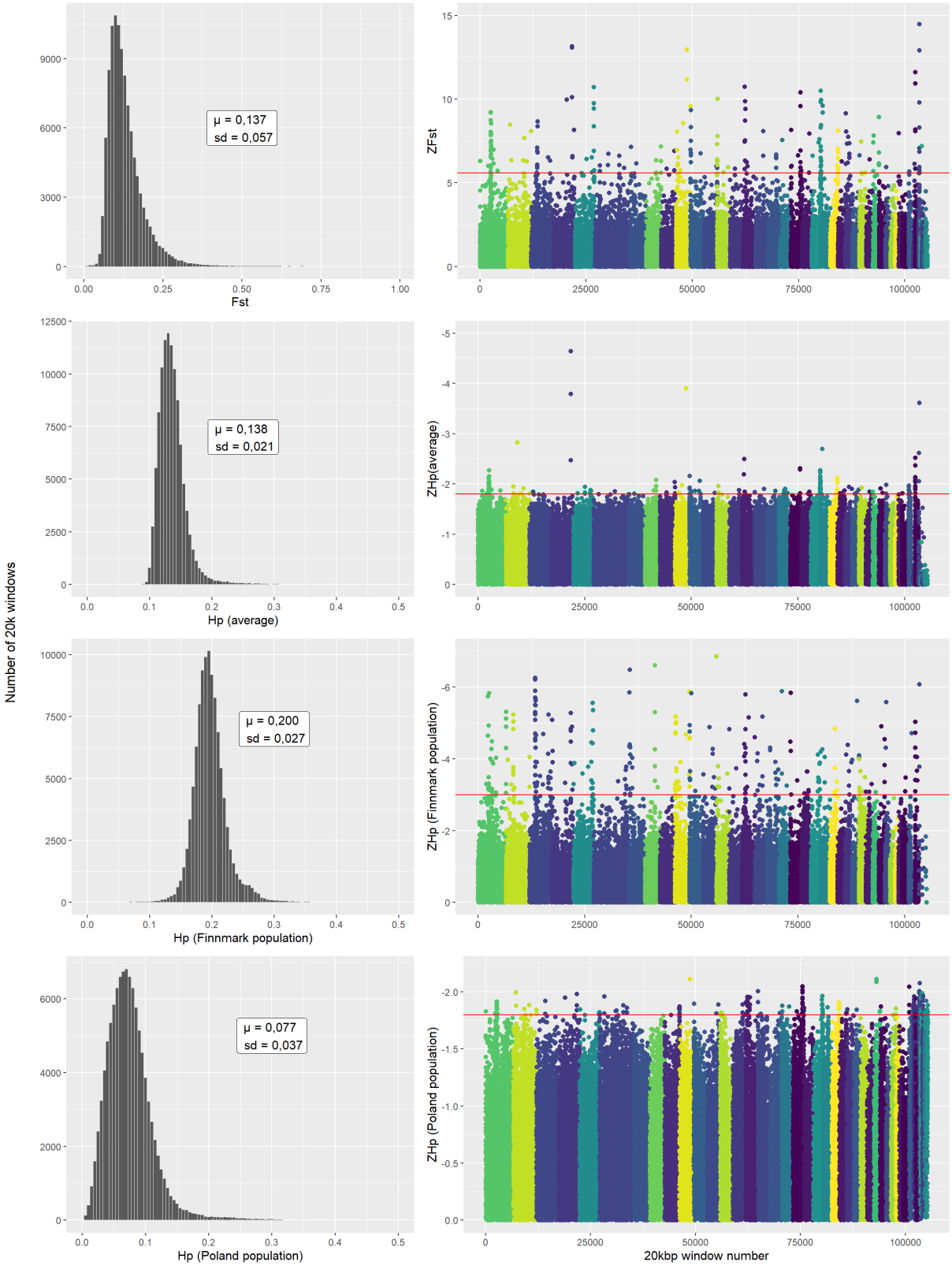

Figure 2. Signatures of selection between a Northern and Southern European tundra vole population. Frequency distribution of F_{ST} and average heterozygosity between the two vole populations (H_p). Genome wide Manhattan plots of ZF_{ST} (>0) and Z-transformed average heterozygosity (ZH_p <0). F_{ST} and H_p were calculated for 20kbp non-overlapping sliding windows. ZF_{ST} and ZH_p were calculated for the same windows after removal of windows with fewer than 10 SNPs and contigs <4mbp. The horizontal line indicates the one-tailed 99.95 percentile of all ZF_{ST} (>0) and ZH_p (<0) values. Contigs and scaffolds are given different colours and are arranged after size.

Selection on an Aldh1a- *paralogue*

In the 238 kbp intergenic region between *Aldh1a1* and *Aldh1a7*, we found additional BLAST matches of prairie vole *(Microtus ochrogaster) Aldh1a1* mRNA sequences and mouse *(Mus musculus) Aldh1a7* mRNA. Mapping revealed three almost complete *Aldh1a* paralogues falling in this region (Fig. 4, Fig. 5A,). These three paralogues had a translated amino acid sequence similarity of 82.1-98.4% with prairie vole ALDH1A1 and a 76.4-96.2% similarity with mouse ALDH1A7. The tundra vole *Aldh1a1* and *Aldh1a7* genes both contain 13 exons and all 13 exons were also present in the third paralogue (hereafter *Aldh1aX3*). However, BLAST could not map exon 7 in *Aldh1aX1* and *Aldh1aX2* (table S4, Figure 5A). ALDH1A1 and ALDH1A7 are closely related to one another with an amino acid similarity of 91% in the tundra vole. The translated paralogue amino acid sequences shared also 87.6 – 89.9% similarity with tundra vole ALDH1A1 and 93.0 – 95.0% with tundra vole ALDH1A7. Variable- and conserved regions in the amino acid alignments are presented in figure 4. Positions at key sites determining the size of the substrate entry channel as described by Sobreira et al. (2011) are more variable than other regions.

Figure 3 shows the ZF_{ST} and heterozygosity scores per SNP on the *Aldh1a1* locus with the genes and paralogues coloured (colours are based on CDS sequences, from the first to the last translated exon). The first paralogue (*Aldh1aX1*) carried the strongest signature of selection with a mean F_{ST} per SNP of 0.448 (ZF_{ST} 3.46) on a total of 536 SNPs of which 216 were above the 0.5% percentile, as is marked by the horizontal line. *Aldh1aX3* had the most SNPs (1736), two of which were non-synonymous and 14 were significant. These were all clustered in one narrow band. Heterozygosity (H_p) scores for both *Aldh1a1* and *Aldh1a7* and the paralogues were higher for the Northern versus the Southern population. The lowest ZH_p in the Northern population was on the first paralogue *Aldh1aX1* (H_p 0.21, ZH_p -0.1) whereas this was on *Aldh1a1* (H_p 0.02, ZH_p -0.55) in the Southern population. The highest heterozygosity scores were on *Aldh1a7* in both populations (See Fig.3 and table S3).

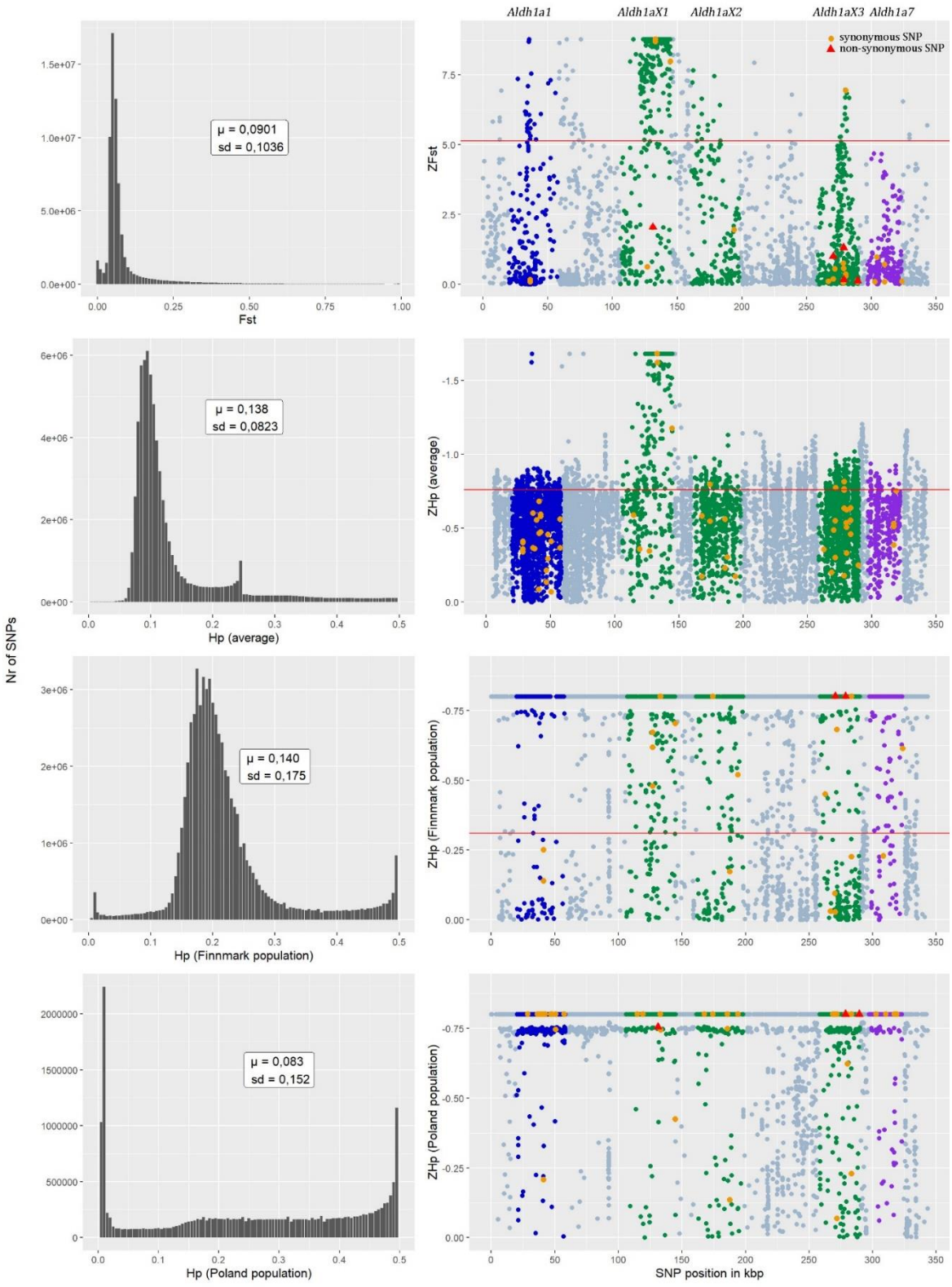

Figure 3. Signatures of selection on the *Aldh1a1 – Aldh1a7* locus between a Northern and Southern European tundra vole population. Genome-wide frequency distribution of F_{st} and average heterozygosity between populations (H_p) were calculated for each individual SNP. Manhattan plots of Z-transformed F_{ST} (>0) and H_p (<0) per SNP (>0). The horizontal line indicates the one-tailed 99.5 percentile of all ZF_{ST} (>0) and ZH_p (<0) per SNP values. Blue: *Aldh1a1*, Green: *Aldh1* paralogues, purple: *Aldh1a7*, orange: SNPs in exons, red: non-synonymous SNPs. Genes are marked based on CDS sequences from the first to the last translated exon.


Exon1
Exon2
Exon3
Moeconomus_ALDH1A1_F MSSPAQPEIPAPLANLKIQYTKIFINNEWHDSVSGKKFPVINPATEEVICHVEEGDKADV 60
Moeconomus_ALDH1AX1_R MSSPAQPEIPAPLSDLKIQYTKIFINNEWHDSVSGKKFPVFNPATEEIMCHVEEGDKADV 60
Moeconomus_ALDH1AX2_R MSSPAQPEIPAPLSDLKIQYTKIFINNEWHDSVSGKKFPVFNPATEEVICHVEEGDKADV 60
Moeconomus_ALDH1AX3_F MSSPAQPEIPAPLGNLKIQYTKIFINNEWHDSVSGKKFPVINPATEEVICHVEEGDKADV 60
Moeconomus_ALDH1A7_R MSSPAQPEIPAPLNDLKIQYTKIFINNEWHDSVSGKKFPVFNPATEEIICHVEEGDKADV 60
Exon4
Moeconomus_ALDH1A1_F DKAVKAARQAFQIGSTWRTMDASERGRLLNKLADLMERDRLLLATMEALNGGKVFANAYL 120
Moeconomus_ALDH1AX1_R DKAVKAARQAFQIGSPWRTMDASERGRLLNKLADLMERDRLLLTTMESMNGGKVFSHTYM 120
Moeconomus_ALDH1AX2_R DKAVKAARQAFQIGSPWRTMDASERGRLLNKLADLMERDRLLLATMESMNAGKVFPQAYM 120
Moeconomus_ALDH1AX3_F DKAVKAARQAFQIGSPWRTMDASERGRLLNKLADLMERDHLLLATMESMNAGKIFRHAYM 120
Moeconomus_ALDH1A7_R DKAVKAARQAFQIGSTWRTMDASERGRLLNKLADLMERDRLLLTTMESMNAGKVFPHAYT 120
Exon5
Exon6
Moeconomus_ALDH1A1_F ADLGGCIKALKYCAGWADKIHGQTIPSDGDIFTYTRREPIGVCGQIIPWNFPLLMFIWKI 180
Moeconomus_ALDH1AX1_R LDLDVSIKTLKYCAGWADKIHGQTIPSDGDIFTYTRREPIGMCGQIIPWNGPLVMFTWKI 180
Moeconomus_ALDH1AX2_R MDLDISIKALKYCAGWADKIHGQTIPSDGDIFTYTRREPIGVCGQIIPWNGPLIMLTWKI 180
Moeconomus_ALDH1AX3_F TAVGISIKTLKYCAGWADKIHGQTIPSDGDIFTYTRREPIGVCGQIIPWNGPLVMFAWKI 180
Moeconomus_ALDH1A7_R MDLEVSIKILKYCAGWADKIHGQTIPSDGDIFTYTRREPIGVCGQIIPWNGPLFVFTGKL 180
Exon7
Moeconomus_ALDH1A1_F GPALACGNTVIVKPAEQTPLTALHMASLVKEAGIPPGVVNIVPGYGPTAGAAISSHMDID 240
Moeconomus_ALDH1AX1_R GPALACGNTVIVKPAEQTPLTALHMASLIKE---------- 211
Moeconomus_ALDH1AX2_R GPALACGNTVIVKPAEQTPLTALHMASLVIE---------- 211
Moeconomus_ALDH1AX3_F GPALACGNTVIVKPAEQTPLTALHMASLVKEAGFPPGVVNVVPGYGPTAGAAISSHMDID 240
Moeconomus_ALDH1A7_R APALACGNTVIVKPAEQTPLTALHMASLVKEAGFPAGVVNVVPGYGPTAGAAISSHMDID 240
Exon8
Exon9
Moeconomus_ALDH1A1_F KVAFTGSTEVGKLIKEAAGKSNLKRVTLELGGKSPCIVFADADCNMAVEFAHHGVFYHQG 300
Moeconomus_ALDH1AX1_R ---------VGKLVKEAAGKSNLKRVTLELGGKSPCIVFADADCDSAVEFAHQGVFFNQG 262
Moeconomus_ALDH1AX2_R ---------VGKLIKEAAGKSNLKRVTLELGGKSPCIVFADADCDNAVEFAHQGVFFHQG 262
Moeconomus_ALDH1AX3_F KVAFTGSTEVGKLIKEAAGKSNLKRVTLELGGKSPCIVFADADCDSAVEFAHQGVFFHQG 300
Moeconomus_ALDH1A7_R KVSFTGSTEVGKLIKEAAGKSNLKRVTLELGGKSPCIVFADADCDSAVEFAHQGVFCHQG 300

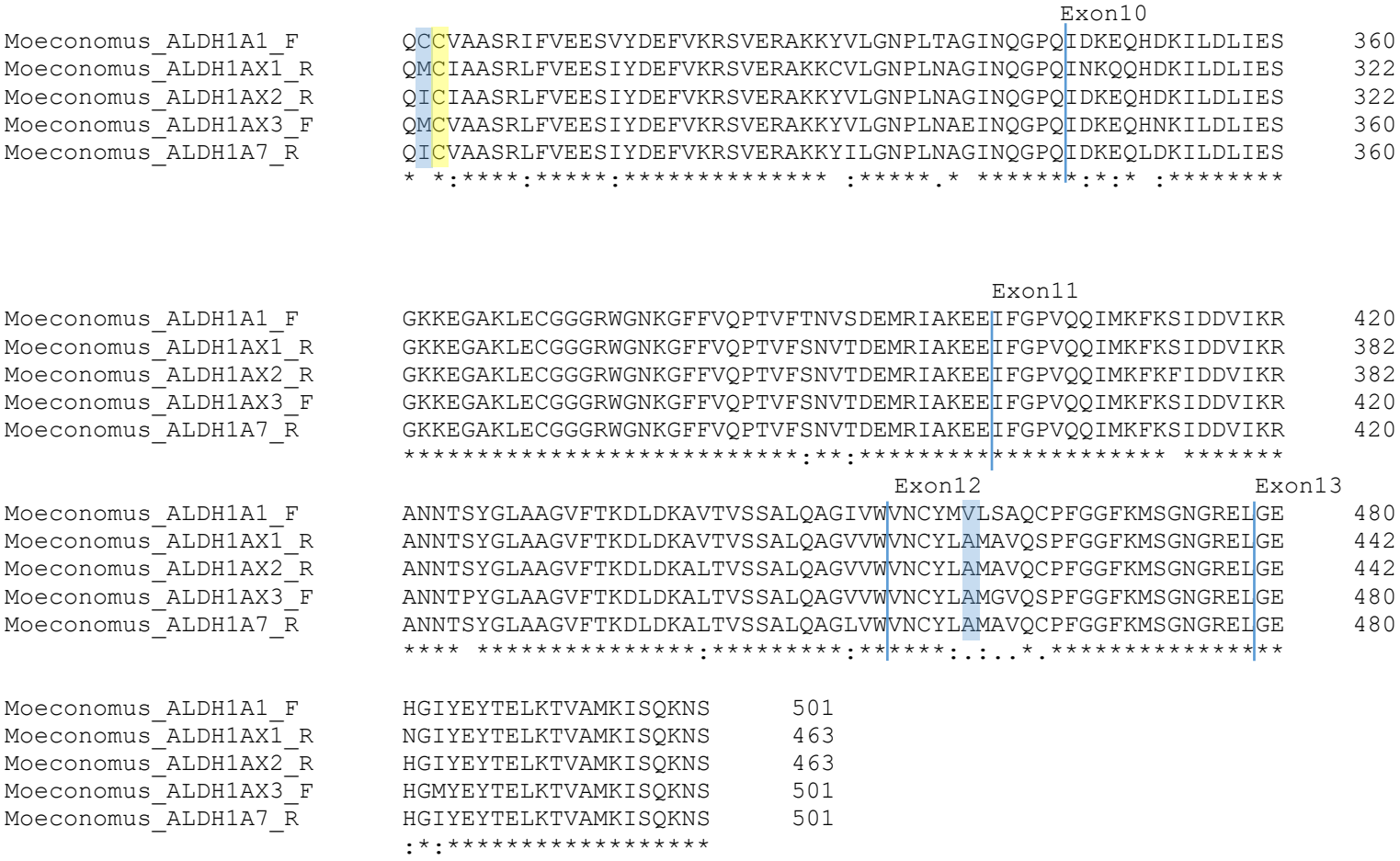

Figure 4. A**lignment of predicted protein sequences of *Microtus oeconomus Aldh1a1*, the three paralogues and *Aldh1a7***. Blue: substrate entry channel locations marked based on (Sobreira et al. 2011) with 124: mouth of the channel, 459: neck of the channel, 302: bottom of the channel, close to the catalytic site (303). Yellow: active sites based on SWISS-model Repository P24549 (Bienert et al. 2017) 170: transition site stabilizer, 303: nucleophile, 269: proton acceptor.

Aldh1a *paralogues in other* Microtus *species.*

We also searched in other *Microtus* genomes for *Aldh1a* paralogues and found a similar pattern in the reed vole (*M.fortis),* prairie vole (*M.ochrogaster),* field vole (*M.agrestis),* and common vole (*M.arvalis)* as in the tundra vole (Fig.5B). *Aldh1a* paralogues in other voles all had higher similarity scores with the *Aldh1a7* protein sequence for a given species (84.2-95.46%) compared to *Aldh1a1* (81.37-92.44%).

Most exons could be mapped with BLAST, although exon 7 could not be found in most paralogues (table S5). Only the tundra vole, field vole and common vole had one complete 13-exons containing paralogue. Despite this, all sequences were translatable without any premature stop-codons or frame-shift mutations. Like in the tundra vole, paralogues were located between the *Aldh1a1* and *Aldh1a7* gene in all species investigated, except in the common vole (*Microtus arvalis)* in which the third paralogue was located 37,59 Mbp of *Aldh1a1,* on the same contig.

The prairie vole (*M.ochrogaster*) *Aldh1a7* could not be found. The genome is fully annotated and three *Aldh1a1*-like genes (NCBI gene ID: 101983531, NCBI gene ID: 113456534, NCBI gene ID: 101997257) were mapped directly downstream of *Aldh1a1.* The predicted exon structure was different from *Aldh1a1* and different compared to other voles, with the first paralogue containing 11 exons, the second 8 and the third 11. These paralogues also had the lowest protein sequence similarity scores (80.2 -86.7%) with *M.ochrogaster Aldh1a1* compared to paralogues in the other *Microtus* species investigated. Interestingly, the similarity scores with *M.agrestis Aldh1a7* were higher (84.4-91.95%).

The phylogenetic tree (Fig.6) based on CDS shows a cluster of vole *Aldh1a1* mirroring the species tree phylogeny (Barbosa et al. 2018; Jaarola et al. 2004). Mouse *Aldh1a1* and *Aldh1a7* formed a separate cluster from *Microtus Aldh1a1* and the paralogues. The other paralogues form three clusters, and the clustering of *M.oeconomus* and *M.fortis* indicates either a specific duplication in these two species or gene loss in the *M.arvalis* and *M.agrestis* lineage.

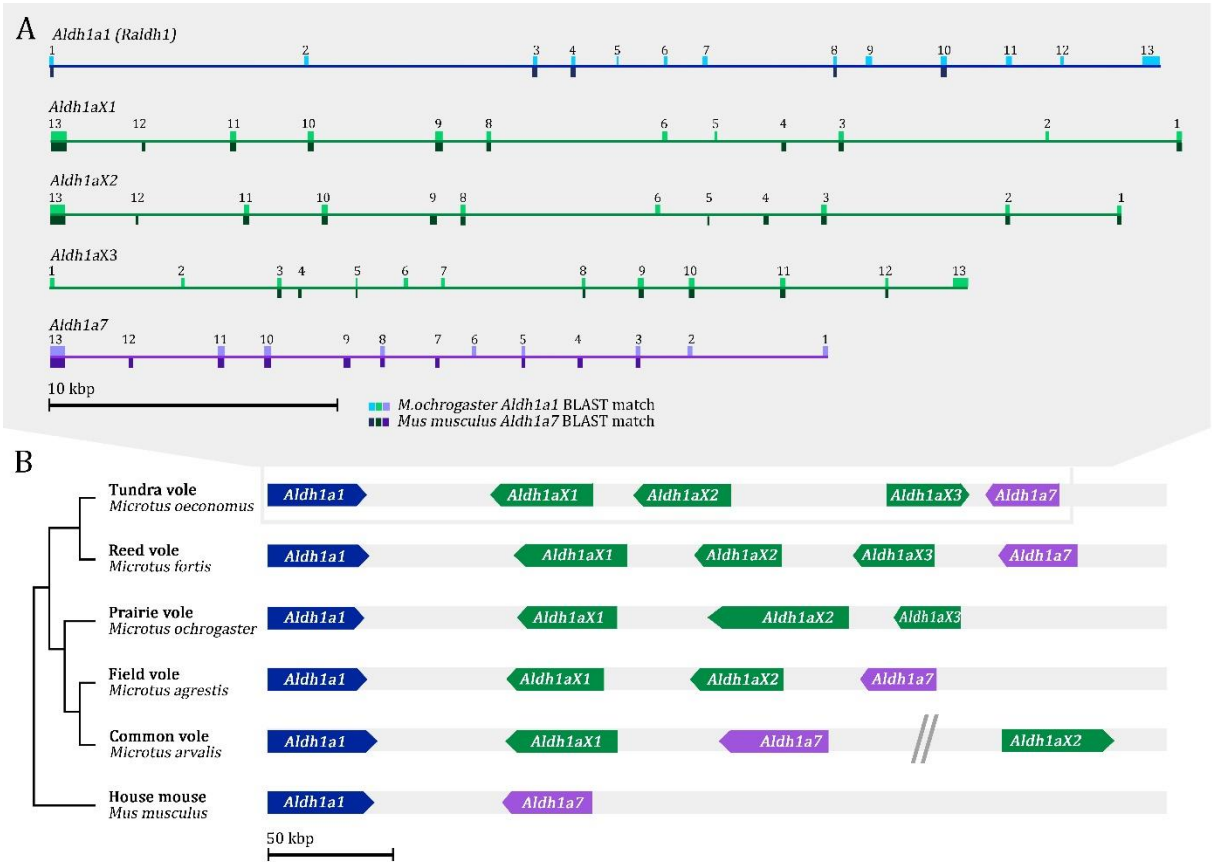

Figure 5: The *Aldh1a1-Aldh1a7* locus in various *Microtus* species compared to the mouse. A) BLAST matches with *M.ochrogaster Aldh1a1* (light colours above the lines) mRNA sequences and mouse *Aldh1a7* (dark colours below the lines) sequences onto the *M.oeconomus* reference genome, showing three *Aldh1a* gene paralogues. B) Schematic overview of *Aldh1a* paralogues in other *Microtus* species.

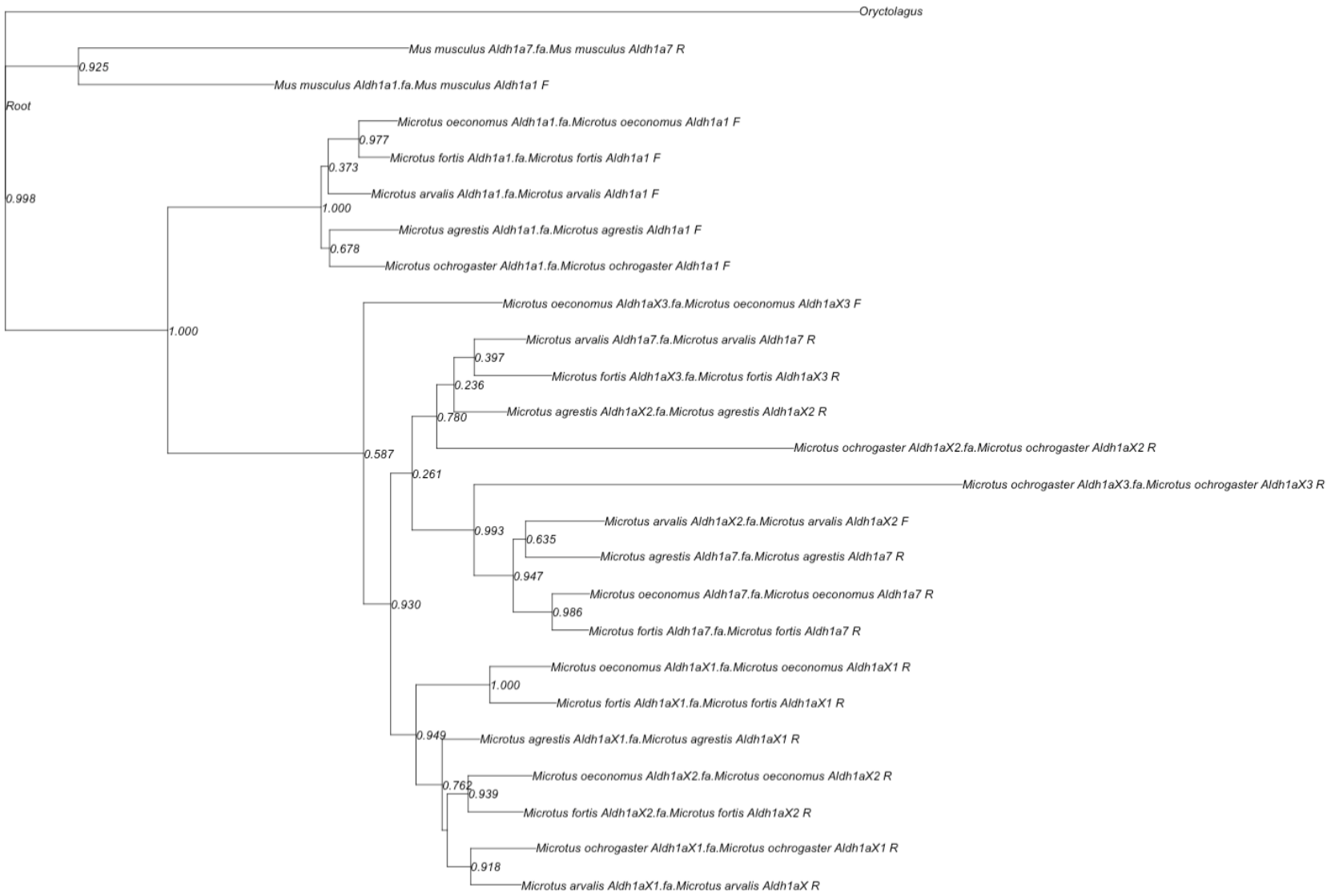

Figure 6: phylogenetic tree based on Aldh1a1 and Aldh1a1-like paralogue CDS sequences. Numbers indicate bootstrapping (100 replicates) values.

Discussion

We have found a strong signature of positive selection on an *Aldh1a* paralogue on the *Aldh1a1* – *Aldh1a7* locus between a Northern- and Southern European population of tundra voles (*Microtus oeconomus*). In addition, we found signatures of selection downstream of the PNES related genes *Dio2* and *Mtnr1b*.

Population differences and Microtus evolution

The average heterozygosity was higher in the northern population from Finnmark than in the southern population from Poland. One feature of positive selection is a reduction in genetic diversity, which could indicate a higher evolution rate in the Poland population. Molecular evolution rates in mammals tend to be slower at high latitudes and altitudes, possibly due to the lower ambient temperature (Gillman et al. 2009), resulting in more positive selection at lower latitudes (Yiming et al. 2021). However, mammals are endothermic and low ambient temperature may not affect mutation rate directly. Alternatively, competition with ectotherms at lower latitudes could increase the evolution rate in endotherms through the 'Red Queen' effect (Gillman et al. 2009). Another possible reason for this differentiation is paleogeographic history since the northern and southern populations belong to different phylogeographical groups that re-colonized Europe via distinct routes after the last glaciation (Brunhoff et al. 2003).

The number of SNPs in tundra voles was relatively high compared to other mammals with 321.6 SNPs per 10 kbp compared to 10.5-12.7 between dog breeds (Karlsson et al. 2007), and 5.28-8.44 in human SNP databases (Zhao et al. 2003). This is in line with the 60-100 times faster speciation rate in *Microtus* compared to other mammals (Sitnikova et al. 2007) and the high chromosomal instability observed in *Microtus* (Lemskaya et al. 2010; Triant and DeWoody 2006). The genus has evolved in less than two million years and currently consists of more than 60 species, which translates in a speciation rate of 30 every million years (Triant and DeWoody 2006).

With our current study, we cannot distinguish selective forces operating on these two populations. This could be improved with data from more populations and with correlations between phenotypical features (e.g. breeding season onset and offset, behavioural data, body mass, pelage quality, social structures), ecological parameters (predation, food availability) and environmental variables (e.g. snow cover, precipitation).

Potential latitudinal selection signatures

We have assessed genes in- and surrounding 20kbp windows with high fixation rates. Most of these windows fell in non-coding regions, which may have a regulatory function. Adaptation happens mostly in areas regulating gene expression (Bird, Stranger, and Dermitzakis 2006) or in regions facilitating phenotypic plasticity (Nussey et al. 2005). Further investigation of regulatory regions could be a new avenue to assess evolutionary differences between these populations, but methodology to assess this in a genome wide fashion is still developing. In order to get an impression of potentially selected genes, we assessed the nearest upstream- and downstream genes, neighboring high F_{ST} regions. However, this should be taken with caution as regulatory areas can be up to 900 kbp away from the actual gene (Schoenfelder and Fraser 2019). Furthermore, we have investigated only clear, hard selective sweeps, which are characterized by a reduction in genetic variation around the adaptive site and neighboring regions affected by linkage disequilibrium. However, Messer & Petrov, (2013) argue that the dominant mode of adaptation is through soft selective sweeps, which are more difficult to distinguish from neutral polymorphisms, as genetic diversity is not necessarily reduced in selected regions. This could hide many more cryptic selection signatures, but this also emphasizes the significance of the genes found in our current analysis. In these hard selective sweeps, we have observed several genes associated with immune function. Immune function fluctuates with the seasons (Pyter, Weil, and Nelson 2005; Dopico et al. 2015; Walton, Weil, and Nelson 2011) which could be stronger at higher latitudes. Meadow voles (*Microtus pennsylvanicus)* from a northern (62°N) and southern population and (53°N) had a differential delayed type hypersensitivity response under various photoperiods (Pyter, Weil, and Nelson 2005). We also found a selection signature on two vomeronasal receptors. These receptors detect pheromones and which could play a role in social- and sexual behaviour. In addition, we found two olfactory receptors and three taste receptors, which could indicate diet related differences between the two populations (Connor, Zhou, and Liu 2018) requiring altered chemoreception. Our dataset featured many more genes and further exploration and gene ontology analysis could provide more insight in metabolic pathways and relationships between genes under selection between these two populations.

PNES related genes

We have found selection signatures downstream of three genes involved in the photo neuroendocrine system, namely iodothyronine deiodinase 2 (*Dio2*), the melatonin receptor 1b (*Mtnr1b*) and aldehyde dehydrogenase 1 family member A1 (*Aldh1a1*). The latter is also known as retinalaldehyde dehydrogenase 1 (*Raldh1*). *Dio2* expression in the median eminence (ME) of the hypothalamus is strongly affected by photoperiod in voles (van Rosmalen et al. 2021; Król et

al. 2012) and coordinates a summer phenotype. Its magnitude of expression was lower in tundra voles compared to common voles (*M.arvalis*) which are native to lower latitudes. The first component of the PNES is melatonin secreted by the pineal gland, which tightly follows the onset and offset of the dark phase and thereby internalizes daylight information. Melatonin is received by melatonin 1a receptors (MT1) in the *pars tuberalis* (PT) of the pituitary from where the seasonal phenotype is further orchestrated (H. Dardente et al. 2003; Klosen et al. 2019; Johnston et al. 2003). However, we found a signature of selection just downstream of the melatonin 1b receptor (MT2) which is not present in the *pars tuberalis* but knockout studies suggest that MT2 is present on different immune tissues and may play a role in photoperiod-enhanced immunity (Drazen and Nelson 2001).

The most well-studied central seasonal timekeeping mechanism is through the thyroid hormone axis in the PT and ME (Nakao, Ono, and Yoshimura 2008; E. A. Hanon et al. 2010; Hugues Dardente, Hazlerigg, and Ebling 2014). However, there is strong evidence for a second seasonal pathway in the same region, involving retinoic acid (RA) signaling (Shearer et al. 2010; Helfer et al. 2012; Stoney et al. 2016). RA is synthesized in the ME by ALDH1A1 (RALDH1, retinaldehyde dehydrogenase) which is highly expressed under long photoperiods and induced by thyroid hormones (Stoney et al. 2016). RA in the ME regulates transcription via nuclear receptors and it is potentially involved in appetite regulation, body weight control and energy metabolism (Helfer, Barrett, and Morgan 2019; Ebling and Barrett 2008). Tundra voles respond stronger to photoperiod in regulating growth and body mass compared to common voles (*M.arvalis*) while the common vole is more photoperiodic in regulating gonadal growth (van Rosmalen et al. 2021). Genetic differentiation in the hypothalamic RA signaling pathway is a potential basis for this observed difference on photosensitivity. Hypothalamic *Aldh1a1* expression studies between different species under a variety of photoperiods could provide more insight in the potential involvement of RA signaling in seasonal phenotype regulation.

Selection on an Aldh1a- *paralogue*

Interestingly, we detected a strong selection signature downstream of the *Aldh1a1* gene and upstream of the *Aldh1a7* gene where we found three *Aldh1a1*-like paralogues (*Aldh1aX1, Aldh1aX2, Aldh1aX3)*. The strongest evidence for selection was on the *Aldh1aX1* and this gene had the highest sequence homology with *Aldh1a7. Aldh1aX1* and *Aldh1aX2* lacked exon 7 but other *Aldh1a1* exons, functional domains and active sites as mentioned by (Sobreira et al. 2011) were present in all paralogues. However, without RNAseq data, we cannot confirm whether these are pseudogenes or completely functional genes. Pseudogenes are characterized by premature stop codons and frameshift mutations (Tutar 2012), which were not detected in any

of the three paralogues found in tundra voles. Yet pseudogenes could be involved in regulating their parent genes (Tutar 2012), which would suggests that the *Aldh1a1*-like paralogues may regulate expression of *Aldh1a1* or *Aldh1a7*.
Aldh1a7 has so far only been found in rodents (Touloupi et al. 2019) and it has a 90,62 % protein sequence similarity with *Aldh1a1* in mice . In most mammals, *Aldh1a1* (*Raldh1*) has only two sister genes, namely *Aldh1a2* (*Raldh2*) and *Aldh1a3* (*Raldh3*)(Holmes 2015; Cañestro et al. 2009). All three gene products are capable of RA synthesis and have retinaldehyde is their main substrate (Cañestro et al. 2009; Koppaka et al. 2012). Rodent ALDH1A7, however, does not seem to synthesize RA, despite its high sequence similarity with ALDH1A1 (Hsu et al. 1999; Alnouti and Klaassen 2008). Therefore, it may not be involved in seasonal RA signaling in the hypothalamus. Yet, its expression pattern is similar to *Aldh1a1*, except for high expression in the kidneys where ALDH1A1 is low or absent (Hsu et al. 1999). Little is known about the specific function of ALDH1A7 and further expression studies could give more clarification.

More generally, aldehyde dehydrogenases are present in all life forms and are involved in detoxification of aldehydes produced under oxidative stress (Singh et al. 2013) and in alcohol metabolism (Vasiliou and Nebert 2005; Koppaka et al. 2012; Cañestro et al. 2009). Throughout metazoan evolution, there have been several ALDH gene duplications, resulting in a large family of genes (20 in the mouse, 19 in humans) which are specialized in metabolizing aldehydes of different molecular weighs (Sobreira et al. 2011; Koppaka et al. 2012). This requires structural variation in substrate entry channels suitable for large or small molecules. The ALDH1A (RALDH) family deviated from the ancestral small-channeled ALDHs in having a large channel, capable of metabolizing larger aldehydes such as retinaldehyde. However, the closely related ALDH2 has a smaller channel and is mainly involved in alcohol metabolism (Sobreira et al. 2011; Vasiliou and Nebert 2005). Investigation of amino acids present at key positions in these entry channels as done by Sobreira et al., (2011), indicated that ALDH1A7 and the three ALDH1AX paralogues in tundra voles may have a narrower substrate entry channel than ALDH1A1. This could mean a novel function different from the RALDH sister genes. So far, no placental mammals other than rodents were found to possess *Aldh1a7* but neither the mouse (*Mus musculus)* nor the rat (*Rattus norvegicus)* had additional *Aldh1a1* copies. Two to four *Aldh1a1-like* paralogues near the *Aldh1a1* locus were also present in other rodents such as the bank vole (*Myodes glareolus* NCBI:txid447135), Eastern Deer mouse (*Peromyscus maniculatus* NCBI:txid10042*)* golden hamster (*Mesocricetus auratus* NCBI:txid10036 *)*, guinea pig (*Cavia porcellus* NCBI:txid10141*),* and naked mole rat (*Heterocephalus glaber* NCBI:txid10181). Lagomorphs, the closet sister clade of the rodents, had no *Aldh1a1*-like paralogues. Further

phylogenetic research across a wider range of mammals and rodents could resolve the origin of these *Aldh1a1*-like paralogues.

Interestingly, marsupial opossums *(Monodelphis domestica),* and Tasmanian devils (*Sarcophilus harrisii*) also have three *Aldh1a1*-like paralogues (*Aldh1a4, Aldh1a5* and *Aldh1a6)*, located directly downstream of *Aldh1a1,* but do not possess *Aldh1a7,* and it is suggested that these *Aldh1a1*-like genes are involved in detoxification (Holmes 2009, 2015). Additionally, ALDH1A1 mediates an alternative pathway of GABA synthesis by dopamine neurons in the brain. GABA co-release was modulated by alcohol and reduced *Aldh1a1* expression enhanced alcohol consumption and preference (Kim et al. 2015). The wide functional range of ALDH1A1 and other ALDHs complicates the speculation about the function of the *Aldh1a1-like* gene under selection between the two tundra vole populations and the additional *Aldh1a1*-like copies in general. High physical activity levels of rodents such as *Myodes rutilus* and carbohydrate food fermentation could contribute to relatively high ethanol- and acetaldehyde levels in the blood and the requirement of increased ALDH activity (Kolosova and Kershengol'ts 2017). Seasonal changes in diet and food quality from grass and sedges to more moss and lichens (Bergman and Krebs 1993) may also affect ADH-ALDH activity. Acetaldehyde is small molecule which is most effectively metabolized by the small-channeled ALDH2 and less effectively by ALDH1A1 (Sobreira et al. 2011). Given our suggested small substrate entry channel of ALDH1A7 and the ALDH1AX paralogues, these could assume a similar function as ALDH2. Yet this remains open for further investigation.

A study on northern cold-adapted red-backed voles (*Myodes rutilus)* revealed higher endogenous ethanol and acetaldehyde levels in blood and higher associated aldehyde dehydrogenase activity compared to non-cold adapted laboratory rats (Kolosova and Kershengol'ts 2017). This effect was particularly pronounced in winter and the authors suggested that oxidative stress and mild hypoxia under the snow could cause the need for higher ADH-ALDH activity. Snow- and ice cover can also increase ethanol production (Andrews 1996) in partially fermented vegetation ingested by voles. In Białowieża, Poland (53°N), voles experienced 78 days of snow cover with a mean depth of 13 cm (Zub et al. 2012). Tundra voles studied in Finse (Norway, 60°N) live under a snow cover with a maximum depth of 2m that lasts from October to early June (Korslund 2006). The duration of snow cover is comparable in Ifjordfjellet, Northern Norway (70°N), where our vole samples were obtained. This long period of thick snow cover in Northern Norway, which could require increased ADH-ALDH activity in the tundra voles living under the snow.

Conclusion

We performed pooled whole genome sequencing on a northern (70°N) and southern (53°N) European population of tundra voles (*Microtus oeconomus*) and found several genes under selection. Among these were vomeronasal receptors, olfactory receptors and several immune system related genes. Our main finding was strong positive selection on a seemingly complete *Aldh1a* paralogue, located downstream of *Aldh1a1* and upstream of *Aldh1a7*. We found three *Aldh1a1*- like paralogues between *Aldh1a1* and *Aldh1a7* in tundra voles and similar paralogues in other rodents at the same locus. *Aldh1a1* is associated with seasonal time keeping and is potentially involved in seasonal body mass regulation through RA signaling in the hypothalamus. Aldehyde dehydrogenases have a wide range of functions, including detoxification and alcohol metabolism. The exact function of *Aldh1a7* and these paralogues is unclear but our results support a significant role for these genes in microtine voles. Further sequencing of other tundra vole populations from various longitudes and latitudes could clarify whether selection on this *Aldh1a* paralogue is associated with latitude.

Supplementary material

Table S1: *M.oeconomus de novo* assembly statistics generated from both short Illumina sequence reads and long nanopore reads.

Number of scaffolds	269
Total size of scaffolds	2,189,948,392 bp
Longest scaffold	131,328,197 bp
Shortest scaffold	2,143 bp
Number of scaffolds > 500 bp	269 (100.0%)
Number of scaffolds > 1K bp	269 (100.0%)
Number of scaffolds > 10K bp	230 (86.1%)
Number of scaffolds > 100K bp	129 (48.3%)
Number of scaffolds > 1M bp	71 (26.6%)
Mean scaffold size	8,202,054 bp
Median scaffold size	90,999 bp
N50 scaffold length	60,754,688
L50 scaffold count	13
scaffold %A	28.87
scaffold %C	21.15
scaffold %G	21.15
scaffold %T	28.87
scaffold %N	0.00

Table S2: overall statistics of the genomic data.

	Mean	**SD**	**range**
SNPs per 20kbp window	643.2	175.30	0-3634
Average minimum coverage	152.5	13.96	52.2-324.2
Heterozygosity both populations	0.138	0.021	0.04 – 0.41
Heterozygosity Northern population	0.200	0.027	0.01-0.48
Heterozygosity Southern population	0.077	0.037	0 – 0.045
F_{ST}	0.137	0.067	0.01 to 0.96

Table S3: Statistics for *Aldh1a1, Aldh1a7* and *Aldh1a* paralogues (X1-3) between the Finnmark (70N) and Poland (53N) population of *M.oeconomus*

	Nr SNPs	**F_{ST} (ZF_{ST})**	**H^p (ZH_p) - Finnmark**	**H^p (ZH_p) - Poland**
Aldh1a1	1700	0.086 (-0.004)	0.21 (0.28)	0.02 (-0.55)
Aldh1aX1	536	0.448 (3.46)	0.21 (-0.10)	0.02 (-0.29)
Aldh1aX2	776	0.10 (0.16)	0.16 (0.10)	0.08 (-0.32)
Aldh1aX3	1736	0.10 (0.11)	0.21 (0.42)	0.06 (-0.47)
Aldh1a7	645	0.09 (0.02)	0.272 (0.44)	0.169 (0.2)

Table S4: Percent similarity between *Aldh1a* paralogues and *Aldh1a1* and *Aldh1a7* translated amino acid sequences within *Microtus* species.

M.oeconomus	***Aldh1a1***	***Aldh1a7***	***Exons not mapped***
Aldh1aX1	89.57	92.99	7
Aldh1aX2	91.99	95.03	7
Aldh1aX3	91.60	93.01	
M.arvalis	***Aldh1a1***	***Aldh1a7***	
Aldh1aX1	92.44	95.46	7
Aldh1aX2	89.62	93.61	
M.ochrogaster	***Aldh1a1***	***M.agrestis Aldh1a7***	
Aldh1aX1	81.37	84.20	7,1
Aldh1aX2	83.33	89.47	1,5,6,7,8,13
Aldh1aX3	87.13	91.95	6,12,13
M.agrestis	***Aldh1a1***	***Aldh1a7***	
Aldh1aX1	92.22	95.46	7
Aldh1aX2	91.42	95.81	
M.fortis	***Aldh1a1***	***Aldh1a7***	
Aldh1aX1	90.93	92.66	7
Aldh1aX2	92.01	94.82	7
Aldh1aX3	91.61	94.82	1,7

Table S5: Genes located in- and around 20 kbp windows with a significantly high ZF_{ST} value (p<0,005). The window with the high mean F_{ST} value is given, along with the nearest upstream and downstream gene. Neighbouring high F_{ST} regions were considered as belonging to one and the same peak when there were no further genes located between the nearest downstream gene and the nearest upstream gene of two neighbouring high F_{ST} windows.

peak	Window nr	Nr SNPs	Average minimum coverage	F_{ST}	ZF_{ST}	*Gene symbol*	Full name
1	1	137	93	0.49	**6.31****	***Cd1d1, Cd1d2***	CD1d1 antigen, CD1d2 antigen
	4	260	150	0.22	1.43	*Dclk2*	doublecortin like kinase2
2	1943	505	166.7	0.08	-1.02	*Fxr1*	fragile x mental retardation gene1
	1950	250	133.6	0.48	**6.02****		intergenic
	2073	705	153.2	0.11	-0.47	*Atp11b*	AtPase phospholipid transporting 11B
3	2406	524	162	0.08	-1.05	*Tb11xr1*	transducin(beta)like 1X-linked receptor 1
	2468	146	151.9	0.58	**7.86****		intergenic
	2475	87	148.1	0.66	**9.24****		intergenic
	2483	125	153.1	0.46	**5.69****		intergenic
	2484	63	139.2	0.63	**8.75****		intergenic
	2489	248	155.7	0.44	5.28*	*Agtr1b*	Angiotensin II receptor, type 1b
4	2510	490	163.1	0.19	1.01	*Hsp3*	Heat shock protein 3
	2511	525	154.1	0.13	-0.05	*Cp*	Ceruloplasmin
	2516	69	135.4	0.48	**6.01****		intergenic
	2521	54	159.2	0.51	**6.56****		intergenic
	2524	115	134.2	0.45	**5.63****		intergenic
	2528	159	139.8	0.35	3.79*	*Tubgcp5*	tubulin gamma complex associated protein 5
	2532	584	152.4	0.21	1.22	*Siglech*	sialic acid binding Ig-like lectin H
	2535	132	141.5	0.53	**6.94****		intergenic
	2536	105	138.4	0.66	**9.22****		intergenic
	2537	157	140.2	0.59	**8.06****		intergenic
	2538	99	114.1	0.56	**7.41****		intergenic
	2558	91	126.3	0.48	**6.05****		intergenic
	2561	244	147	0.47	**5.92****		intergenic
	2562	192	176.4	0.55	**7.26****		intergenic
	2563	269	154.5	0.56	**7.52****		intergenic
	2564	186	150.1	0.52	**6.73****		intergenic
	2567	627	168.2	0.22	1.42	*Aasdhppt*	aminoadipate-semialdehyde dehydrogenase-phosphopantetheinyl transferase
	2569	547	161.8	0.22	1.46	*Kbtbd3*	kelch repeat and BTB domain containing 3
	2571	155	140.9	0.58	**7.90****		intergenic
	2572	138	143.6	0.62	**8.56****		intergenic
	2573	253	149.3	0.54	**7.12****		intergenic
	2574	500	165.3	0.21	1.34	*Msantd4*	Myb/SANT DNA binding domain containing 4 with coiled-coils
	2575	636	162.9	0.22	1.39	*Gria4*	glutamate ionotropic receptor AMPA type subunit 4
5	2864	812	161.3	0.08	-0.98	*Cntn5*	contactin 5
	2905	592	156.3	0.50	**6.46****	*Gm47037*	predicted protein 47037
	2956	494	164.1	0.08	-0.94	*Jrkl*	Jrk-like

6	3086	587	147.5	0.20	1.12	*Mtnr1b*	Melatonin receptor 1b
	3118	916	157.9	0.07	-1.14	*Fat3*	FAT atypical cadherin 3
	3181	399	153.7	0.49	**6.17****		intergenic
	3182	845	161.2	0.53	**6.99****		intergenic
	3199	500	160.6	0.09	-0.75	*Chordc1*	cysteine and histidine rich domain containing 1
7	4165	518	164.3	0.21	1.27	*Olfr945*	olfactory receptor 945
	4166	320	156.7	0.46	**5.73****	***Olfr1537***	olfactory receptor 1537
	4167	587	158.2	0.29	2.67	*Olfr947*	olfactory receptor 947
8	7038	1208	162.3	0.10	-0.60	*Cntnap5*	contactin associated protein-like 5B
	7108	34	58.9	0.62	**8.49****		intergenic
	7185	495	138.8	0.23	1.63	*Tsn*	Translin
9	7346	809	147.8	0.24	1.81	*Ccdc93*	coiled-coil domain containing 93
	7347	336	140.2	0.50	**6.36****	***Htr5b***	5-hydroxytryptamine (serotonin) receptor 5B
	7349	563	140.1	0.16	0.33	*Ddx18*	DEAD-box helicase 18
10	10049	605	151.1	0.09	-0.77	*Ube2e2*	ubiquitin conjugating enzyme E2 E2
	10163	761	164.7	0.50	**6.35****		intergenic
	10166	724	153	0.10	-0.74	*Capza1*	capping actin protein of muscle Z-line subunit alpha 1
11	10331	676	171.7	0.08	-1.04	*Ccser2*	coiled-coil serine rich protein 2
	10381	528	155.6	0.57	**7.70****		intergenic
	10384	746	153.1	0.10	-0.56	*Grid1*	glutamate ionotropic receptor delta type subunit 1
12	10953	605	142.3	0.11	-0.39	*Olfml2b*	olfactomedin like 2B
	10956	352	150.1	0.49	**6.28****	***Atf6***	activating transcription factor 6
	10963	665	148	0.14	0.06	*Dusp12*	dual specificity phosphatase 12
13	12065	1747	188.8	0.20	1.08	*Cr2*	complement receptor 2
	12068	246	149.6	0.59	**8.10****		intergenic
14	13376	201	149.9	0.38	4.35*	*Vmn1r12*	vomeronasal 1 receptor 12
	13378	358	137.5	0.45	**5.61****	*Vmn1r15*	vomeronasal 1 receptor 15
	13380	333	153.8	0.38	4.27*	*Vmn1r8*	vomeronasal 1 receptor 8
15	13423	1091	143.7	0.25	2.08	*Igkv10-94*	immunoglobulin kappa variable 10-94
	13424	198	82.5	0.54	**7.12****		intergenic
	13425	154	105.9	0.48	**6.08****	***Gm49508***	Predicted protein 49508
	13426	1037	156.8	0.19	0.98	*Igkv12-125*	immunoglobulin kappa variable 12-125
	13436	895	205.5	0.04	-1.79	*igkv1-110*	immunoglobulin kappa variable 1-110
	13439	230	109.3	0.48	**6.00****	***Igkv9-124***	immunoglobulin kappa chain variable 9-124
	13442	456	148.4	0.27	2.36	*Igkv14*	immunoglobulin kappa chain variable 14
	13477	941	152.7	0.21	1.28	*Igkv12-46*	immunoglobulin kappa variable 12-46
	13478	569	150.1	0.53	**6.92****		intergenic
	13480	1789	142.6	0.47	**5.90****	***Igkv13-85***	immunoglobulin kappa chain variable 13-85
	13481	1546	141	0.37	4.17*	*Igkv4-58*	immunoglobulin kappa variable 4-58
	13559	94	139.6	0.15	0.18	*Igkv-6-25*	immunoglobulin kappa chain variable
	13566	562	134.4	0.63	**8.67****		intergenic
	13567	910	150.2	0.61	**8.39****	***Igkv8-18***	Immunoglobulin kappa variable 8-18

	13569	177	155.1	0.52	**6.82****		intergenic
	13570	717	160.6	0.24	1.88	*Igkv3-2*	immunoglobulin kappa variable 3-2
16	16004	497	156.6	0.26	2.25	*Erc1*	ELKS/RAB6-interacting/CAST family member 1
	16006	343	148.8	0.51	**6.54****		intergenic
	16007	538	145.6	0.20	1.20	*Rad52*	RAD52 homolog, DNA repair protein
	16008	527	164.1	0.15	0.19	*Wnk1*	WNK lysine deficient protein kinase 1
17	16547	874	167.4	0.31	3.01*	*Tpt1-ps3, Tas2r146*	tumor protein, translationally-controlled, pseudogene 3 / taste receptor, type 2, member 146, pseudogene 1
	16548	824	168	0.50	**6.34****	***Tas2r125, Tas2r142, Tas2r113***	taste receptor, type 2, member 125, 142,113
	16552	505	143.7	0.18	0.74	*Tas2r116*	taste receptor, type 2, member 116
18	20441	593	140.8	0.13	-0.21	*Galnt9*	polypeptide N-acetylgalactosaminyltransferase 9
	20442	512	143.7	0.19	0.96	*Oas1g*	2'-5' oligoadenylate synthetase
	20443	496	122.2	0.70	**9.98*****	***Oas1g, Oas1d, Oas1c***	2'-5' oligoadenylate synthetase
	20444	406	138.6	0.24	1.88	*Oas1f*	2'-5' oligoadenylate synthetase
	20445	1029	145.6	0.18	0.84	*Rph3a*	rabphilin 3A
19	21690	458	151.8	0.24	1.88	*Cks1brt*	cyclin-dependent kinases regulatory subunit
	21691	242	139.7	0.88	**13.10*****		intergenic
	21692	98	86.9	0.88	**13.17*****		intergenic
	21693	609	151.1	0.71	**10.13*****	***Cyp3a44***	cytochrome P450, family 3, subfamily a, polypeptide 44
	21694	644	173.8	0.37	4.19*	*Cyp3a44*	cytochrome P450, family 3, subfamily a, polypeptide 44
	21695	851	219.1	0.40	4.67*	*Cyp3a44*	cytochrome P450, family 3, subfamily a, polypeptide 44
	21696	421	118.3	0.51	**6.53****		rgenic
	21698	230	147.8	0.51	**6.60****	***Cyp3a41b***	cytochrome P450, family 3, subfamily a, polypeptide 41B
	21703	789	160	0.12	-0.30	*cyp3a16*	cytochrome P450, family 3, subfamily a, polypeptide 16
20	22129	556	145.7	0.18	0.75	*Cers4*	ceramide synthase 4
	22133	196	136.8	0.60	**8.16****		intergenic
	22134	351	135.7	0.40	4.60*	*Vmn2r-ps89*	vomeronasal 2, receptor, pseudogene 89
21	25034	472	168.3	0.31	3.11*	*Rab28*	RAB28, member RAS oncogene family
	25036	544	156.6	0.50	**6.43****		intergenic
	25048	662	161	0.16	0.35	*4930519EQ7 Rik*	
	25119	740	158.2	0.19	0.95	*Hs3st1*	heparan sulfate-glucosamine 3-sulfotransferase 1
22	26308	656	150.8	0.19	0.98	*B3gnt2*	UDP-GlcNAc:betaGal beta-1,3-N-acetylglucosaminyltransferase 2
	26315	550	142.1	0.51	**6.53****	***Commd1***	copper metabolism domain containing 1
	26316	498	151.3	0.45	**5.63****	***Commd1***	
	26317	372	146.6	0.26	2.24	*Zrsr1*	zinc finger (CCCH type), RNA binding motif and serine/arginine rich 1

23	26801	253	152.2	0.14	-0.02	*Rpl26-ps6*	ribosomal protein L26, pseudogene 6
	26802	513	166.4	0.11	-0.52	*Zfp119a*	zinc finger protein 119a
	26810	43	58.4	0.74	**10.73*** **	***Gm44215***	predicted gene, 44215
	26811	30	53.8	0.53	**6.92****		intergenic
	26813	51	67.2	0.69	**9.75*** **	***Gm6627***	predicted gene 6627
	26814	108	69.6	0.61	**8.40****		intergenic
	26815	31	63.5	0.67	**9.46****		intergenic
	26842	144	126.7	0.46	**5.76****		intergenic
	26915	381	158.4	0.29	2.66	*Zfp959*	zinc finger protein 959
24	26923	468	128.5	0.24	1.90	*Tle2*	transducin-like enhancer of split 2
	26924	355	122.8	0.46	**5.76****	***Tle5***	TLE family member 5, transcriptional modulator
	26925	317	128.3	0.27	2.34	*Gna11*	guanine nucleotide binding protein, alpha 11
25	28240	398	139.5	0.17	0.60	*Snta1*	syntrophin, acidic 1
	28243	573	136.2	0.48	**6.04****	***Cdk5rap1, Bpifb9a***	CDK5 regulatory subunit associated protein 1
	28244	524	143.8	0.20	1.15	*Bpifb9a*	BPI fold containing family B, member 9A
	28245	558	143	0.17	0.62	*Bpifb9b*	BPI fold containing family B, member 9B
	28248	570	143	0.26	2.16	*Bpifb1*	BPI fold containing family B, member 1
	28249	524	148.4	0.46	**5.71****	***Bpifa5***	BPI fold containing family A, member 5
	28250	637	147.5	0.37	4.11*	*Bpifa1*	BPI fold containing family A, member 1
26	30134	611	183.2	0.12	-0.36	*Olfr1306*	olfactory receptor 1306
	30136	181	130.6	0.48	**6.07****		intergenic
	30137	752	161.6	0.17	0.65	*Olfr1316*	olfactory receptor 1316
	30195	967	168.5	0.10	-0.58	*Slc5a12*	solute carrier family 5 (sodium/glucose cotransporter), member 12
	30204	463	153.5	0.52	**6.75****		intergenic
	30207	676	161.3	0.10	-0.66	*Fibin*	fin bud initiation factor homolog
27	32790	476	132.6	0.16	0.33	*Slc6a9*	solute carrier family 6 (neurotransmitter transporter, glycine), member 9
	32794	263	137.5	0.48	**6.07****	***Klf17***	Kruppel-like factor 17
	32795	11	133.8	0.51	**6.64****	***Gm48297***	predicted protein 48297
	32801	455	141.7	0.33	3.38	*Dmap1*	DNA methyltransferase 1 associated protein 1
	32802	464	145.6	0.15	0.19	*Eri3*	exoribonuclease 3
28	33895	769	162.2	0.13	-0.07	*Elalv2*	ELAV like RNA binding protein 1
	33921	611	161.9	0.47	**5.91****		intergenic
	33961	761	161.2	0.09	-0.89	*Dmrta1*	doublesex and mab-3 related transcription factor like family A1
29	35559	881	186.5	0.07	-1.16	*Ighv12-3*	immunoglobulin heavy variable V12-3
	35563	28	59.1	0.54	**7.16****		intergenic
	35574	483	141.7	0.09	-0.79	*Ighv4-2*	immunoglobulin heavy variable V4-2
30	36747	699	164.5	0.19	0.99	*Dio2*	iodothyronine deiodinase 2
	36759	434	156	0.48	**6.16****		intergenic
	36763	539	164.2	0.14	0.13	*Nrxn3*	neurexin 3
31	41453	703	169.8	0.13	-0.03	*Akr1c20*	aldo-keto reductase family 1, member C20

	41457	290	150.6	0.50	**6.36****		intergenic
	41461	1210	178.7	0.14	0.05	*Akr1c12*	aldo-keto reductase family 1, member C12
	41471	246	159.6	0.45	**5.62****	***Akr1cl***	aldo-keto reductase family 1, member C-like
	41472	822	166	0.15	0.29	*Akr1c14*	aldo-keto reductase family 1, member C14
	41480	396	154.9	0.13	-0.10	*Akr1c6*	aldo-keto reductase family 1, member C6
32	42616	397	153.6	0.24	1.80	*Wac*	WW domain containing adaptor with coiled-coil
	42618	64	135.3	0.45	**5.61****		intergenic
	42619	134	151.7	0.49	**6.32****		intergenic
	42622	132	133.5	0.54	**7.17****		intergenic
	42623	152	132.2	0.54	**7.19****		intergenic
33	43857	384	161.1	0.22	1.45	*Iigp1*	interferon inducible GTPase 1
	43885	789	158.7	0.47	**5.85****	***Chsy3***	chondroitin sulfate synthase 3
	43900	796	151.1	0.22	1.44	*Minar2*	membrane integral NOTCH2 associated receptor 2
	45648	744	158.5	0.10	-0.69	*Dsc3*	desmocollin
34	45686	804	141	0.46	**5.77****		intergenic
	45720	680	156.5	0.53	**6.92****	***Gm6070***	predicted gene 6070
	45786	811	158.1	0.13	-0.18	*Cdh2*	cadherin 2
35	46425	232	132.9	0.18	0.82	*Vmn2r49*	vomeronasal 2, receptor 49
	46427	253	127.9	0.59	**8.07****	***Rps19-ps6***	ribosomal protein S19, pseudogene 6
	46428	190	162.9	0.53	**6.96****	***Vmn2r116***	vomeronasal 2, receptor 116
	46430	608	164.5	0.11	-0.40	*Zfp40*	zinc finger protein 40
36	46512	225	156.1	0.22	1.42	*Zfp825*	zinc finger protein 825
	46525	375	154.8	0.48	**6.05****		intergenic
	46537	718	168.3	0.10	-0.66	*Sim1*	single-minded family bHLH transcription factor 1
37	46612	934	177.9	0.17	0.57	*Grik2*	glutamate receptor, ionotropic, kainate 2 (beta 2)
	46616	554	153.9	0.49	**6.18****		intergenic
	46693	594	163.3	0.51	**6.53****		intergenic
	46700	583	166.1	0.12	-0.36	*Pgk1*	phosphoglycerate kinase 1
	46736	455	159.5	0.22	1.42	*Hace1*	HECT domain and ankyrin repeat containing, E3 ubiquitin protein ligase 1
38	46884	520	149.9	0.21	1.32	*Bnip3l*	BCL2/adenovirus E1B interacting protein 3-like [Mus musculus
	46887	476	152.6	0.45	**5.63****	***Ostm1***	osteopetrosis associated transmembrane protein 1
	46892	614	141.7	0.10	-0.61	*Nr2e*	nuclear receptor subfamily 2, group F, member 2
39	47147	693	159.3	0.09	-0.77	*Hs3st5*	heparan sulfate (glucosamine) 3-O-sulfotransferase 5
	47196	844	164.5	0.46	**5.77****		intergenic
	47214	811	164.1	0.14	-0.02	*Frk*	fyn-related Src family tyrosine kinase
40	47821	549	162.2	0.31	3.11	*Lama2*	laminin subunit alpha 2
	47823	500	156.6	0.62	**8.57****		intergenic
	47825	815	162.3	0.19	0.95	*Arhgap18*	Rho GTPase activating protein 18
41	48677	636	149.4	0.09	-0.88	*Lrp11*	LDL receptor related protein 11
	48680	884	153.1	0.12	-0.30	*H60b*	histocompatibility 60b

	48684	16	69.5	0.77	**11.19*** **	***H60c***	histocompatibility 60c
	48685	63	77.2	0.87	**12.97*** **		intergenic
	48688	541	127.6	0.29	2.75*	*Reat1d*	retinoic acid early transcript delta
	48706	678	150.3	0.10	-0.65	*Ppp1r14c*	protein phosphatase 1 regulatory inhibitor subunit 14C
42	49512	973	156.6	0.15	0.18	*Olfr1107*	olfactory receptor 1107
	49513	17	71.5	0.68	**9.60*** **	***Olfr1111***	olfactory receptor 1111
	49517	821	166.8	0.25	2.03	*Olfr1112*	olfactory receptor 1112
43	49570	79	148.1	0.32	3.32	*Araf*	Araf proto-oncogene, serine/threonine kinase
	49573	47	151.7	0.53	**7.00** **		intergenic
	49599	650	161.3	0.09	-0.75	*Car2*	carbonic anhydrase 2
44	49614	642	167.9	0.15	0.30	*Lrrcc1*	leucine rich repeat and coiled-coil centrosomal protein 1
	49616	101	154.6	0.49	**6.25** **		intergenic
	49618	159	141	0.56	**7.51** **		intergenic
	49619	135	134.9	0.67	**9.36** **		intergenic
	49621	87	159.5	0.61	**8.35** **		intergenic
	49629	470	161.4	0.32	3.31*	*Slc7a12*	solute carrier family 7 (cationic amino acid transporter, y+ system), member 12
	49631	186	111.8	0.52	**6.78** **		intergenic
	49632	167	137.9	0.51	**6.64** **		intergenic
	49636	326	157.8	0.18	0.84	*Ralyl*	RALY RNA binding protein like
45	51939	607	149.1	0.19	0.95	*Zfp-462*	zinc finger protein 462
	51951	465	150.1	0.52	**6.77** **	***Rad23b***	RAD23 homolog B, nucleotide excision repair protein
	51963	536	136.9	0.16	0.46	*Klf4*	Kruppel-like factor 4 (
46	55608	347	149.9	0.25	2.05	*Sprr2k*	small proline-rich protein 2K
	55609	245	142	0.48	**6.02** **		intergenic
	55611	358	154.7	0.38	4.33*	*Sprr2j*	small proline-rich protein 2J, pseudogene
47	55817	649	154.6	0.09	-0.91	*Kirrel*	kirre like nephrin family adhesion molecule 1
	55821	43	129.9	0.47	**5.90** **		intergenic
	55827	159	73.1	0.47	**5.89** **		intergenic
48	55846	187	106.7	0.55	**7.33** **		intergenic
	55847	193	116.1	0.49	**6.29** **		intergenic
	55860	63	108.4	0.48	**6.06** **		intergenic
	55861	35	91.4	0.50	**6.42** **		intergenic
	55880	76	71.7	0.70	**10.03*** **		intergenic
	55883	67	72.6	0.58	**7.81** **		intergenic
	55884	66	109.8	0.50	**6.34** **		intergenic
	55891	653	166.4	0.11	-0.40	*Mucl2*	mucin-like 2
	55902	343	133.2	0.12	-0.22	*Ppp1r1a*	protein phosphatase 1 regulatory inhibitor subunit 1A
49	57340	658	145.8	0.09	-0.89	*Dennd3*	DENN/MADD domain containing 3
	57345	691	158.6	0.46	**5.64** **	***Ptk2***	protein tyrosine kinase 2
	57355	327	135.7	0.19	0.87	*Ago2*	argonaute RISC catalytic subunit 2
50	58366	382	167.1	0.13	-0.08	*Csmd3*	CUB and Sushi multiple domains 3

	58389	514	156.8	0.47	**5.96****	***Ptma-ps2***	prothymosin alpha, pseudogene 2
	58423	617	163.5	0.18	0.75	*Kcnv1*	potassium channel, subfamily V, member 1
51	60027	478	147.2	0.15	0.17	*Nf1*	neurofibromin 1
	60031	422	140.7	0.47	**5.87****		intergenic
	60033	386	153.1	0.08	-1.06	*Wsb1*	WD repeat and SOCS box-containing 1
52	62316	431	160.1	0.08	-0.99	*Zfp709*	zinc finger protein 709
	62322	143	136.5	0.74	**10.74*****	***Gm13862***	predicted gene 13862
	62324	109	151	0.56	**7.46****		intergenic
	62325	558	170.6	0.19	0.92	*Gng10*	guanine nucleotide binding protein (G protein), gamma 10
	62331	171	152.4	0.47	**5.82****		intergenic
	62341	359	144.2	0.56	**7.53****	***Gm3325, Gm49049***	Predicted gene 3325, 40909
	62342	199	149.6	0.70	**9.89*****		intergenic
	62345	706	165.3	0.07	-1.13	*BC024063*	cDNA sequence BC024063
	62352	668	151	0.20	1.05	*Lzts1*	leucine zipper tumor suppressor 1
53	62393	579	159.1	0.12	-0.36	*Sh2d4a*	SH2 domain containing 4A
	62396	62	154.4	0.63	**8.72****	***Gm4903, Gm19764***	Predicted gene 4903, 19764
	62401	301	175.4	0.49	**6.33****		intergenic
	62403	436	161.6	0.18	0.83	*Psd3-215*	pleckstrin and Sec7 domain containing 3
	62520	791	162.9	0.16	0.44	*Marchf1*	membrane associated ring-CH-type finger 1
	62522	842	146.8	0.67	9.42**		intergenic
	62539	741	146.5	0.07	-1.19	*Smim31*	small integral membrane protein 31
	62542	695	151.1	0.13	-0.05	*Apela*	apelin receptor early endogenous ligand
54	62765	1355	163.8	0.10	-0.64	*Aadat*	aminoadipate aminotransferase
	62806	622	159.2	0.49	**6.25****		intergenic
	62829	820	160.9	0.11	-0.55	*Galntl6*	UDP-N-acetyl-alpha-D-galactosamine:polypeptide N-acetylgalactosaminyltransferase-like 6
55	62960	682	165.8	0.18	0.75	*Adam29*	ADAM metallopeptidase domain 29
	62976	14	86.7	0.48	**6.00****		intergenic
	62980	545	161.1	0.14	0.05	*Gpm6a*	glycoprotein m6a
56	66611	766	169.7	0.11	-0.55	*Slc5a7*	solute carrier family 5 (choline transporter), member 7
	66624	35	101.1	0.59	**8.09****		intergenic
	66625	188	129	0.51	**6.62****		intergenic
	66633	537	147	0.12	-0.26	*Zfp345*	zinc finger protein 345
57	69666	342	160.5	0.33	3.39*	*Gzmc*	granzyme C
	69667	687	136.2	0.50	**6.48****	***Gzme***	granzyme E
	69668	736	156	0.24	1.78	*Gzmn*	granzyme N
	69671	635	172.4	0.30	2.98*	*Ctsg*	cathepsin G
	69672	738	146	0.52	**6.70****	***Mcpt8***	mast cell protease 8
	69674	529	156.1	0.24	1.77	*Mcpt-ps1*	mast cell protease, pseudogene 1
	69675	519	157.7	0.16	0.37	*Mcpt1*	mast cell protease 1
58	69717	468	139	0.11	-0.39	*Trac*	T cell receptor alpha constant

	69720	499	160.8	0.47	**5.91****	***Eif1ad14***	eukaryotic translation initiation factor 1A domain containing 14
	69721	511	144.1	0.51	**6.60****		intergenic
	69729	1049	157.8	0.12	-0.25	*Trav13n*	T cell receptor alpha variable 13N-4
59	71158	502	160	0.13	-0.06	*Abo*	ABO blood group (transferase A, alpha 1-3-N-acetylgalactosaminyltransferase, transferase B, alpha 1-3-galactosyltransferase)
	71165	33	80.6	0.56	**7.56****		intergenic
	71175	507	150.4	0.10	-0.67	*Dipk1b*	divergent protein kinase domain 1B
60	73271	655	149.9	0.16	0.43	*Incenp*	inner centromere protein
	73279	154	136.5	0.60	**8.17****	***Gm12583***	predicted protein 12583
	73281	351	123.1	0.47	**5.98****		intergenic
	73289	316	145.6	0.48	**6.01****	***Gm48269***	predicted protein 48269
	73291	428	155.1	0.28	2.57	*Snrpert*	mall nuclear ribonucleoprotein E, pseudogene
61	74824	814	155.7	0.06	-1.38	*Gde1*	glycerophosphodiester phosphodiesterase 1
	74828	865	136.3	0.51	**6.66****	***Tmc5***	transmembrane channel-like gene family 5
	74830	671	143.2	0.10	-0.65	*Tmc7*	transmembrane channel-like gene family 7
62	75415	665	161.1	0.13	-0.05	*Olfr700, Olfr701*	Olfractory receptor 700 and 701
	75422	404	138.7	0.47	**5.93****	***Gvin3***	GTPase, very large interferon inducible, family member 3
	75425	938	162.4	0.53	**6.94****	***Gvin-ps6***	GTPase, very large interferon inducible, pseudogene 6
	75426	824	145.1	0.68	**9.60*****		intergenic
	75427	1005	158.6	0.73	**10.41*****		intergenic
	75428	488	158.1	0.46	**5.64****	***Gm5383***	predicted gene 5383
	75429	855	159.7	0.49	**6.25****		intergenic
	75430	893	227	0.30	2.91*	*Gvin2*	GTPase, very large interferon inducible, family member 2
	75433	1020	184.8	0.18	0.81	*Gvin-ps5*	GTPase, very large interferon inducible, pseudogene 5
	75436	240	122.3	0.47	**5.90****		intergenic
	75453	42	57.2	0.29	2.65	*Gvin-ps2, Gvin-ps3*	GTPase, very large interferon inducible, pseudogene 2 and 3
63	75583	328	152.3	0.20	1.13	*Olfr564*	Olfactory receptor 564
	75585	140	111.4	0.46	**5.74****		intergenic
	75586	498	160.2	0.18	0.84	*Olfr562-ps1*	Olfactory receptor 562, pseudogene 1
64	77416	698	162.3	0.08	-0.97	*Nsun3*	NOL1/NOP2/Sun domain family member 3
	77446	719	167.3	0.45	**5.61****		intergenic
	77476	775	168.2	0.59	**7.95****		intergenic
	77496	728	169.1	0.16	0.42	*Epha6*	Eph receptor A6
65	78220	457	143.3	0.22	1.46	*Tenm4*	teneurin transmembrane protein 4
	78306	1096	159.3	0.51	**6.63****		intergenic
	78327	577	153.2	0.14	0.11	*Prss23*	protease, serine 23
	78337	597	148.3	0.12	-0.30	*Me3*	malic enzyme 3, NADP(+)-dependent, mitochondrial
66	79713	633	169.1	0.11	-0.51	*Mkrn3*	makorin, ring finger protein,

	79721	399	156.2	0.56	**7.42****	***Gm8145***	predicted gene 8145
	79722	732	163	0.37	4.20*	*Mrgprb2*	MAS-related GPR, member B2
67	79884	812	158.5	0.07	-1.26	*Gas2*	growth arrest specific 2
	79885	634	158.5	0.11	-0.46	*Svip*	small VCP/p97-interacting protein
	79892	201	132	0.57	7.62*		intergenic
	79899	540	135.5	0.28	2.51	*Mrgprb11-ps*	MAS-related GPR, member B11, pseudogene
68	80122	547	155.2	0.11	-0.46	*Zfp715*	zinc finger protein 715
	80133	1502	195.3	0.22	1.44	*A26c2*	ANKRD26-like family C, member 2
	80137	212	131.6	0.53	6.92*		intergenic
	80151	87	143.5	0.73	**10.50*****		intergenic
	80156	204	158.2	0.50	**6.50****		intergenic
	80158	473	167.3	0.45	**5.61****		intergenic
	80159	247	153.5	0.69	**9.83*****		intergenic
	80160	421	162.9	0.50	**6.50****		intergenic
	80161	283	150.3	0.61	**8.32****		intergenic
	80163	295	148.4	0.54	**7.18****		intergenic
	80167	187	161.4	0.53	**6.94****		intergenic
	80169	430	158	0.50	**6.51****		intergenic
	80174	352	156.5	0.47	**5.97****		intergenic
	80230	513	162.9	0.19	1.03	*Luzp2*	leucine zipper protein 2
	80235	145	156.8	0.61	**8.46****	***Luzp2***	leucine zipper protein 2
	80242	451	155.1	0.49	**6.33****	***Luzp2***	leucine zipper protein 2
	80243	325	161.2	0.49	**6.29****	***Luzp2***	leucine zipper protein 2
	80254	44	115.6	0.23	1.59	*Rpl19.ps11*	ribosomal protein L19, pseudogene 11
	80257	11	103.1	0.70	**9.96*****	***Gm15566***	Predicted gene 15566
	80262	247	146.4	0.46	**5.72****		intergenic
	80271	125	160.6	0.53	**6.94****		intergenic
	80272	227	136.5	0.48	**6.06****		intergenic
69	80627	837	169.6	0.17	0.59	*Aldh1a1*	aldehyde dehydrogenase 1 family member A1
	80631	268	151	0.68	**9.62*****	***Aldh1aX1***	*Aldh1a* paralogue
	80632	312	149.7	0.66	**9.20****	***Aldh1aX1***	*Aldh1a* paralogue
	80640	548	162.7	0.09	-0.74	*Aldah1a7*	aldehyde dehydrogenase 1 family member A7
70	84108	498	165.3	0.12	-0.21	*Slf1*	SMC5-SMC6 complex localization factor 1
	84122	63	135.3	0.48	**6.04****	***Mctp1***	multiple C2 domains, transmembrane 1
	84145	642	165.5	0.09	-0.75	*Fam81b*	family with sequence similarity 81, member B
71	84171	505	158.9	0.15	0.17	*Ell2*	elongation factor for RNA polymerase II 2
	84179	291	139.2	0.53	**7.04****	***Gm37158***	predicted gene 37158
	84198	592	166.7	0.13	-0.18	*Pcsk1*	proprotein convertase subtilisin/kexin type 1
72	84225	362	138	0.13	-0.19	*Erap1*	endoplasmic reticulum aminopeptidase 1
	84237	170	153.1	0.46	**5.80****		intergenic
	84238	86	134.2	0.52	**6.81****		intergenic
	84242	69	132.4	0.50	**6.50****		intergenic
	84243	108	141.3	0.50	**6.43****		intergenic
	84244	144	147.8	0.47	**5.98****		intergenic

	84245	157	135.6	0.46	**5.64****		intergenic
	84248	163	70.6	0.60	**8.12****		intergenic
	84249	116	77.7	0.47	**5.87****		intergenic
	84250	156	96.3	0.45	**5.63****		intergenic
73	85121	623	164.7	0.10	-0.72	*Mettl25*	methyltransferase like 25
	85150	660	170.3	0.49	**6.28****	***Ppfia2***	protein tyrosine phosphatase, receptor type, f polypeptide (PTPRF), interacting protein (liprin), alpha 2
	85153	582	165.6	0.10	-0.58	*Acss3*	acyl-CoA synthetase short-chain family member 3
74	86122	1380	150.9	0.22	1.51	*Ceacam1*	carcinoembryonic antigen-related cell adhesion molecule 2
	86124	580	136.8	0.48	**6.14****		intergenic
	86125	428	142.5	0.65	**9.16****		intergenic
	86128	582	151	0.13	-0.11	*Ceacam10*	carcinoembryonic antigen-related cell adhesion molecule 10
	86132	880	113.2	0.20	1.14	*Ceacam2*	carcinoembryonic antigen-related cell adhesion molecule 2
	86143	144	78.8	0.59	**8.07****		intergenic
	86148	513	139.4	0.20	1.15	*Dmac2, B3gnt8*	distal membrane arm assembly component 2 and UDP-GlcNAc:betaGal beta-1,3-N-acetylglucosaminyltransferase 8
75	86344	521	130.2	0.13	-0.04	*Ffar2*	free fatty acid receptor 2
	86350	405	136.5	0.55	**7.35****	***Ffar1***	free fatty acid receptor 1
	86352	525	139.4	0.18	0.69	*Ffar3*	free fatty acid receptor 3
76	86585	986	154.6	0.15	0.17	*Pop4*	processing of precursor 4, ribonuclease P/MRP family
	86590	208	139.2	0.49	**6.23****	***Gm5592***	predicted protein 5592
	86591	234	167.6	0.29	2.75	*Aw146154*	expressed sequence AW146154
	86599	631	157.1	0.13	-0.07	*Zfp619*	zinc finger protein 619
	86669	681	150.1	0.15	0.31	*Vstm2b*	V-set and transmembrane domain containing 2B
	86678	172	126.1	0.57	**7.75****		intergenic
	86679	477	141.6	0.16	0.34	*Ddx11*	DEAD/H box helicase 11
77	86860	583	149.7	0.14	0.11	*Efna5*	ephrin A5
	86960	698	169.2	0.51	**6.55****		intergenic
	86970	590	162.8	0.55	**7.37****		intergenic
	86972	834	167.5	0.52	**6.74****		intergenic
	86973	387	161.4	0.50	**6.50****		intergenic
	87027	786	157.2	0.13	-0.11	*Nudt12*	nudix (nucleoside diphosphate linked moiety X)-type motif 12
	87028	740	163.4	0.14	0.15	*Pdzph1*	PDZ and pleckstrin homology domains 1
78	89280	738	159.7	0.16	0.38	*Mthfs*	5, 10-methenyltetrahydrofolate synthetase
	89281	512	165.9	0.29	2.72*	*Bcl2a1a, Bcl2a1c*	B cell leukemia/lymphoma 2 related protein A1a and A1c
	89285	23	107.9	0.51	**6.65****		intergenic
79	89725	351	150.2	0.31	3.11*	*Luc7l2*	LUC7-like 2 pre-mRNA splicing factor
	89726	321	140.9	0.56	**7.46****	***Fmc1***	formation of mitochondrial complex V assembly factor 1 homolog
	89727	559	151.6	0.39	4.46*	*Ubn2*	ubinuclein 2

80	90565	895	171.8	0.14	0.13	*Kcnd2*	potassium voltage-gated channel, Shal-related family, member 2
	90630	514	162.1	0.45	5.62**	*intergenic*	
	90665	904	167.8	0.08	-0.96	*Lsm8*	LSM8 homolog, U6 small nuclear RNA associated
81	91725	709	174.6	0.09	-0.76	*Cdh9*	cadherin 9
	91729	720	169	0.50	**6.42****		intergenic
	91846	828	162.2	0.19	0.94	*Cdh6*	cadherin 6
82	92558	708	158.6	0.20	1.20	*Nectin3*	nectin cell adhesion molecule 3
	92570	695	163.1	0.56	**7.41****		intergenic
	92593	722	161.7	0.46	**5.72****		intergenic
	92628	523	143	0.14	0.00	*Dppa4*	developmental pluripotency associated 4
	92630	467	149	0.58	**7.82****		intergenic
	92636	904	158.9	0.09	-0.75	*Morc1*	microrchidia 1
83	93918	363	162.9	0.19	0.91	*Iglv3*	immunoglobulin lambda variable 3
	93923	177	146.7	0.52	**6.82****		intergenic
	93924	148	152.7	0.64	**8.95****		intergenic
	93927	153	153.4	0.48	**6.06****		intergenic
	93929	238	142.6	0.49	**6.18****		intergenic
	93932	565	94.1	0.18	0.83	*Iglv1*	immunoglobulin lambda variable 1
84	95624	583	156.5	0.13	-0.10	*Rpl10a-ps1*	ribosomal protein L10A, pseudogene 1
	95626	641	147.4	0.47	**5.94****	***Pth2r***	parathyroid hormone 2 receptor
	95649	358	146.5	0.21	1.22	*Sp110*	Sp110 nuclear body protein
85	98584	195	140.3	0.59	7.97**		intergenic
	98586	304	158.7	0.16	0.50	*Olfr1191-ps1*	olfactory receptor 1191, pseudogene 1
86	100986	760	164.3	0.26	2.19	*Hepacam2*	HEPACAM family member 2
	100990	646	165	0.46	5.69**	*Vps50*	VPS50 EARP/GARPII complex subunit
	100996	710	165.4	0.16	0.44	*Calcr*	calcitonin receptor
87	102233	517	105.4	0.11	-0.45	*Chst7*	carbohydrate (N-acetylglucosamino) sulfotransferase 7
	102251	572	105.5	0.15	0.17	*Selenok-ps4*	selenoprotein K, pseudogene 4
	102267	36	98.9	0.48	**6.14****		intergenic
	102278	550	106.4	0.12	-0.29	*Dipk2b*	divergent protein kinase domain 2B
88	102442	338	82.9	0.47	**5.86****		intergenic
	102450	45	136.4	0.79	**11.63*****		intergenic
	102452	119	155.1	0.60	**8.20****		intergenic
	102459	76	140.2	0.76	**10.94*****	***Gucy1a2***	guanylate cyclase 1 soluble subunit alpha 2
	102460	62	153.7	0.59	**8.09****	***Gucy1a2***	guanylate cyclase 1 soluble subunit alpha 2
	102478	464	157.8	0.16	0.35	*Cwf19l2*	CWF19 like cell cycle control factor 2
89	103341	599	111.1	0.19	0.86	*Slitrk2*	SLIT and NTRK like family member 2
	103352	386	103.3	0.26	2.15	*4930447F04 Rik*	RIKEN cDNA 4930447F04 gene
	103359	193	97.6	0.54	**7.09****		intergenic
	103360	142	93.3	0.61	**8.33****		intergenic
	103361	212	97.8	0.52	**6.86****		intergenic

	103363	636	103.1	0.23	1.65	*Gm6760*	Predicted gene 6760
	103367	248	100.3	0.46	**5.79****		intergenic
	103369	163	99.1	0.47	**5.94****		intergenic
	103372	209	100.2	0.47	**5.95****		intergenic
	103373	53	105.1	0.96	**14.49*****		intergenic
	103378	212	103.9	0.46	**5.64****		intergenic
	103380	82	97.7	0.69	**9.81*****		intergenic
	103383	320	105.6	0.19	0.88	*Ctag2*	cancer/testis antigen 2
	103391	71	95.6	0.87	**12.93*****		intergenic
	103402	624	114.5	0.14	0.13	*Slitrk4*	SLIT and NTRK like family member 4
90	103945	587	107.8	0.10	-0.57	*Pgr15l*	G protein-coupled receptor 15-like
	103955	230	90.5	0.54	**7.20****		intergenic
	103961	716	110.9	0.14	0.06	*Gpr165*	G protein-coupled receptor 165
	103967	605	108.8	0.11	-0.41	*Heph*	hephaestin

References

Alnouti, Yazen, and Curtis D. Klaassen. 2008. "Tissue Distribution, Ontogeny, and Regulation of Aldehyde Dehydrogenase (Aldh) Enzymes MRNA by Prototypical Microsomal Enzyme Inducers in Mice." *Toxicological Sciences* 101 (1): 51–64. https://doi.org/10.1093/toxsci/kfm280.

Altschul, S., W. Gish, W. Miller, E.W. Meyers, and D.J. Lipman. 1990. "Basic Local Alignment Search Tool." *Journal of Molecular Biology* 215: 403–10. https://doi.org/10.1006/jmbi.1990.9999.

Andrews, C. J. 1996. "How Do Plants Survive Ice?" *Annals of Botany* 78 (5): 529–36. https://doi.org/10.1006/anbo.1996.0157.

Andrews, Simon. 2010. "FastQC - A Quality Control Tool for High Throughput Sequence Data." *Babraham Bioinformatics*. http://www.bioinformatics.babraham.ac.uk/projects/fastqc/.

Balčiauskas, Linas, Laima Balčiauskiene, and Agne Janonyte. 2012. "Reproduction of the Root Vole (Microtus Oeconomus) at the Edge of Its Distribution Range." *Turkish Journal of Zoology* 36 (5): 668–75. https://doi.org/10.3906/zoo-1111-20.

Barbosa, Soraia, Joana Paupério, Svetlana V. Pavlova, Paulo C. Alves, and Jeremy B. Searle. 2018. "The Microtus Voles: Resolving the Phylogeny of One of the Most Speciose Mammalian Genera Using Genomics." *Molecular Phylogenetics and Evolution* 125 (January): 85–92. https://doi.org/10.1016/j.ympev.2018.03.017.

Bergman, C. M., and C. J. Krebs. 1993. "Diet Overlap of Collared Lemmings and Tundra Voles at Pearce Point, Northwest Territories." *Canadian Journal of Zoology* 71 (9): 1703–9. https://doi.org/10.1139/z93-241.

Bertolini, Francesca, Bertrand Servin, Andrea Talenti, Estelle Rochat, Eui Soo Kim, Claire Oget, Isabelle Palhière, et al. 2018. "Signatures of Selection and Environmental Adaptation across the Goat Genome Post-Domestication 06 Biological Sciences 0604 Genetics." *Genetics Selection Evolution* 50 (1): 1–24. https://doi.org/10.1186/s12711-018-0421-y.

Bienert, Stefan, Andrew Waterhouse, Tjaart A.P. De Beer, Gerardo Tauriello, Gabriel Studer, Lorenza Bordoli, and Torsten Schwede. 2017. "The SWISS-MODEL Repository-New Features and Functionality." *Nucleic Acids Research* 45: D313–19. https://doi.org/10.1093/nar/gkw1132.

Bird, Christine P., Barbara E. Stranger, and Emmanouil T. Dermitzakis. 2006. "Functional Variation and Evolution of Non-Coding DNA." *Current Opinion in Genetics and Development* 16: 559–64. https://doi.org/10.1016/j.gde.2006.10.003.

Bolger, Anthony M., Marc Lohse, and Bjoern Usadel. 2014. "Trimmomatic: A Flexible Trimmer for Illumina Sequence Data." *Bioinformatics* 30 (15): 2114–20. https://doi.org/10.1093/bioinformatics/btu170.

Bronson, Franklin H. 1985. "Mammalian Reproduction: An Ecological Perspective." *Biology of Reproduction* 32 (1): 1–26. https://doi.org/10.1095/biolreprod32.1.1.

Brunhoff, Cecilia, K. E. Galbreath, V. B. Fedorov, J. A. Cook, and M. Jaarola. 2003. "Holarctic Phylogeography of the Root Vole (Microtus Oeconomus): Implications for Late Quaternary Biogeography of High Latitudes." *Molecular Ecology* 12 (4): 957–68. https://doi.org/10.1046/j.1365-294X.2003.01796.x.

Camacho, Christiam, George Coulouris, Vahram Avagyan, Ning Ma, Jason Papadopoulos, Kevin Bealer, and Thomas L. Madden. 2009. "BLAST+: Architecture and Applications." *BMC Bioinformatics*. https://doi.org/10.1186/1471-2105-10-421.

Cañestro, Cristian, Julian M. Catchen, Adriana Rodríguez-Marí, Hayato Yokoi, and John H. Postlethwait. 2009. "Consequences of Lineage-Specific Gene Loss on Functional Evolution of Surviving Paralogs: ALDH1A and Retinoic Acid Signaling in Vertebrate Genomes." *PLoS Genetics* 5 (5). https://doi.org/10.1371/journal.pgen.1000496.

Charif, Delphine, and Jean R. Lobry. 2007. "SeqinR 1.0-2: A Contributed Package to the R Project for Statistical Computing Devoted to Biological Sequences Retrieval and Analysis." In *Structural Approaches to Sequence Evolution: Molecules, Networks, Populations*, edited by U. Bastolla, M. Porto, H Roman, and M Vendrusolo, 207–32. Springer Verlag, New York. https://doi.org/10.1007/978-3-540-35306-5_10.

Chheda, Himanshu, Priit Palta, Matti Pirinen, Shane McCarthy, Klaudia Walter, Seppo Koskinen, Veikko Salomaa, et al. 2017. "Whole-Genome View of the Consequences of a Population Bottleneck Using 2926 Genome Sequences from Finland and United Kingdom." *European Journal of Human Genetics* 25 (4): 477–84. https://doi.org/10.1038/ejhg.2016.205.

Connor, Erin E., Yang Zhou, and George E. Liu. 2018. "The Essence of Appetite: Does Olfactory Receptor Variation Play a Role?" *Journal of Animal Science* 96 (4): 1551–58. https://doi.org/10.1093/jas/sky068.

Dardente, H., P. Klosen, P. Pévet, and M. Masson-Pévet. 2003. "MT1 Melatonin Receptor MRNA Expressing Cells in the Pars Tuberalis of the European Hamster: Effect of Photoperiod." *Journal of Neuroendocrinology* 15 (8): 778–86. https://doi.org/10.1046/j.1365-2826.2003.01060.x.

Dardente, Hugues, David G. Hazlerigg, and Francis J.P. Ebling. 2014. "Thyroid Hormone and Seasonal Rhythmicity." *Frontiers in Endocrinology* 5 (FEB): 1–11. https://doi.org/10.3389/fendo.2014.00019.

Dardente, Hugues, Cathy A. Wyse, Mike J. Birnie, Sandrine M. Dupré, Andrew S.I. Loudon, Gerald A. Lincoln, and David G. Hazlerigg. 2010. "A Molecular Switch for Photoperiod Responsiveness in Mammals." *Current Biology* 20 (24): 2193–98. https://doi.org/10.1016/j.cub.2010.10.048.

Dopico, Xaquin Castro, Marina Evangelou, Ricardo C. Ferreira, Hui Guo, Marcin L. Pekalski, Deborah J. Smyth, Nicholas Cooper, et al. 2015. "Widespread Seasonal Gene Expression Reveals Annual Differences in Human Immunity and Physiology." *Nature Communications* 6 (May): 1–13. https://doi.org/10.1038/ncomms8000.

Drazen, Deborah L., and Randy J. Nelson. 2001. "Melatonin Receptor Subtype MT2 (Mel 1b) and Not Mt1 (Mel 1a) Is Associated with Melatonin-Induced Enhancement of Cell-Mediated and Humoral Immunity." *Neuroendocrinology* 74

(3): 178–84. https://doi.org/10.1159/000054684.
Ebling, Francis J.P., and P. Barrett. 2008. “The Regulation of Seasonal Changes in Food Intake and Body Weight.” *Journal of Neuroendocrinology* 20 (6): 827–33. https://doi.org/10.1111/j.1365-2826.2008.01721.x.
Ecke, Frauke, Åsa M.M. Berglund, Ilia Rodushkin, Emma Engström, Nicola Pallavicini, Dieke Sörlin, Erik Nyholm, and Birger Hörnfeldt. 2018. “Seasonal Shift of Diet in Bank Voles Explains Trophic Fate of Anthropogenic Osmium?” *Science of the Total Environment* 624: 1634–39. https://doi.org/10.1016/j.scitotenv.2017.10.056.
Evans, Dianne M. 1973. “Seasonal Variations in the Body Composition and Nutrition of the Vole Microtus Agrestis.” *Journal of Animal Ecology* 42 (1): 1–18.
Galan, Maxime, Marie Pagès, and Jean François Cosson. 2012. “Next-Generation Sequencing for Rodent Barcoding: Species Identification from Fresh, Degraded and Environmental Samples.” *PLoS ONE* 7 (11). https://doi.org/10.1371/journal.pone.0048374.
Garnier, Simon, Noam Ross, Robert Rudis, Pedro A. Camargo, Marco Sciaini, and Cédric Scherer. 2021. “Viridis - Colorblind-Friendly Color Maps for R.” 2021. https://doi.org/doi: 10.5281/zenodo.4679424.
Gillman, Len N., D. Jeanette Keeling, Howard A. Ross, and Shane D. Wright. 2009. “Latitude, Elevation and the Tempo of Molecular Evolution in Mammals.” *Proceedings of the Royal Society B: Biological Sciences* 276 (1671): 3353–59. https://doi.org/10.1098/rspb.2009.0674.
Gliwicz, Joanna. 1996. “Life History of Voles: Growth and Maturation in Seasonal Cohorts of the Root Vole.” *Miscellania Zoologica* 19 (1): 1–12.
Hanon, E. A., K. Routledge, H. Dardente, M. Masson-Pévet, P. J. Morgan, and D. G. Hazlerigg. 2010. “Effect of Photoperiod on the Thyroid-Stimulating Hormone Neuroendocrine System in the European Hamster (Cricetus Cricetus).” *Journal of Neuroendocrinology* 22 (1): 51–55. https://doi.org/10.1111/j.1365-2826.2009.01937.x.
Hanon, Elodie A., Gerald A. Lincoln, Jean Michel Fustin, Hugues Dardente, Mireille Masson-Pévet, Peter J. Morgan, and David G. Hazlerigg. 2008. “Ancestral TSH Mechanism Signals Summer in a Photoperiodic Mammal.” *Current Biology* 18 (15): 1147–52. https://doi.org/10.1016/j.cub.2008.06.076.
Hartl, Daniel L., and Andrew G. Clark. 2007. *Principles of Population Genetics*. Fourth Edi. Sunderland, Mass. : Sinauer Associates.
Hazlerigg, David, and Valerie Simonneaux. 2015. *Seasonal Regulation of Reproduction in Mammals*. *Knobil and Neill’s Physiology of Reproduction*. Fourth. Elsevier. https://doi.org/10.1016/C2011-1-07288-0.
Helfer, Gisela, Perry Barrett, and Peter J. Morgan. 2019. “A Unifying Hypothesis for Control of Body Weight and Reproduction in Seasonally Breeding Mammals.” *Journal of Neuroendocrinology* 31 (3): 1–12. https://doi.org/10.1111/jne.12680.
Helfer, Gisela, Alexander W. Ross, Laura Russell, Lynn M. Thomson, Kirsty D. Shearer, Timothy H. Goodman, Peter J. McCaffery, and Peter J. Morgan. 2012. “Photoperiod Regulates Vitamin A and Wnt/β-Catenin Signaling in F344 Rats.” *Endocrinology* 153 (2): 815–24. https://doi.org/10.1210/en.2011-1792.
Holmes, Roger S. 2009. “Opossum Aldehyde Dehydrogenases: Evidence for Four ALDH1A1-like Genes on Chromosome 6 and ALDH1A2 and ALDH1A3 Genes on Chromosome 1.” *Biochemical Genetics* 47 (9–10): 609–24. https://doi.org/10.1007/s10528-009-9245-3.
———. 2015. “Comparative and Evolutionary Studies of Vertebrate ALDH1A-like Genes and Proteins.” *Chemico-Biological Interactions* 234: 4–11. https://doi.org/10.1016/j.cbi.2014.11.002.
Howe, Kevin L., Premanand Achuthan, James Allen, Jamie Allen, Jorge Alvarez-Jarreta, M. Ridwan Amode, Irina M. Armean, et al. 2021. “Ensembl 2021.” *Nucleic Acids Research* 49 (D1): D884–91. https://doi.org/10.1093/nar/gkaa942.
Hsu, Lily C., Wen Chung Chang, Ines Hoffmann, and Gregg Duester. 1999. “Molecular Analysis of Two Closely Related Mouse Aldehyde Dehydrogenase Genes: Identification of a Role for Aldh1, but Not Aldh-Pb, in the Biosynthesis of Retinoic Acid.” *Biochemical Journal*. https://doi.org/10.1042/0264-6021:3390387.
Hut, Roelof A., Silvia Paolucci, Roi Dor, Charalambos P. Kyriacou, and Serge Daan. 2013. “Latitudinal Clines: An Evolutionary View on Biological Rhythms.” *Proceedings of the Royal Society B: Biological Sciences*. https://doi.org/10.1098/rspb.2013.0433.
Jaarola, Maarit, Natália Martínková, Islam Gündüz, Cecilia Brunhoff, Jan Zima, Adam Nadachowski, Giovanni Amori, et al. 2004. “Molecular Phylogeny of the Speciose Vole Genus Microtus (Arvicolinae, Rodentia) Inferred from Mitochondrial DNA Sequences.” *Molecular Phylogenetics and Evolution* 33 (3): 647–63. https://doi.org/10.1016/j.ympev.2004.07.015.
Johnsen, A., A. E. Fidler, S. Kuhn, K. L. Carter, A. Hoffmann, I. R. Barr, C. Biard, et al. 2007. “Avian Clock Gene Polymorphism: Evidence for a Latitudinal Cline in Allele Frequencies.” *Molecular Ecology* 16 (22): 4867–80. https://doi.org/10.1111/j.1365-294X.2007.03552.x.
Johnston, J. D., S. Messager, P. Barrett, and David G. Hazlerigg. 2003. “Melatonin Action in the Pituitary: Neuroendocrine Synchronizer and Developmental Modulator?” *Journal of Neuroendocrinology* 15 (4): 405–8. https://doi.org/10.1046/j.1365-2826.2003.00972.x.
Karlsson, Elinor K., Izabella Baranowska, Claire M. Wade, Nicolette H.C. Salmon Hillbertz, Michael C. Zody, Nathan Anderson, Tara M. Biagi, et al. 2007. “Efficient Mapping of Mendelian Traits in Dogs through Genome-Wide Association.” *Nature Genetics* 39 (11): 1321–28. https://doi.org/10.1038/ng.2007.10.
Katoh, Kazutaka, and Daron M. Standley. 2013. “MAFFT Multiple Sequence Alignment Software Version 7: Improvements in Performance and Usability.” *Molecular Biology and Evolution* 30 (4): 772–80. https://doi.org/10.1093/molbev/mst010.

Kerbeshian, M. C., F. H. Bronson, and E. D. Bellis. 1994. “Variation in Reproductive Photoresponsiveness in a Wild Population of Meadow Voles.” *Biology of Reproduction* 50 (4): 745–50. https://doi.org/10.1095/biolreprod50.4.745.

Kim, Jae Ick, Subhashree Ganesan, Sarah X. Luo, Yu Wei Wu, Esther Park, Eric J. Huang, Lu Chen, and Jun B. Ding. 2015. “Aldehyde Dehydrogenase 1a1 Mediates a GABA Synthesis Pathway in Midbrain Dopaminergic Neurons.” *Science* 350 (6256): 102–6. https://doi.org/10.1126/science.aac4690.

Klosen, Paul, Sarawut Lapmanee, Carole Schuster, Beatrice Guardiola, David Hicks, Paul Pevet, and Marie Paule Felder-Schmittbuhl. 2019. “MT1 and MT2 Melatonin Receptors Are Expressed in Nonoverlapping Neuronal Populations.” *Journal of Pineal Research* 67 (1): 1–19. https://doi.org/10.1111/jpi.12575.

Kofler, Robert, Ram Vinay Pandey, and Christian Schlötterer. 2011. “PoPoolation2: Identifying Differentiation between Populations Using Sequencing of Pooled DNA Samples (Pool-Seq).” *Bioinformatics* 27 (24): 3435–36. https://doi.org/10.1093/bioinformatics/btr589.

Kolmogorov, Mikhail, Jeffrey Yuan, Yu Lin, and Pavel A. Pevzner. 2019. “Assembly of Long, Error-Prone Reads Using Repeat Graphs.” *Nature Biotechnology* 37: 540–46. https://doi.org/10.1038/s41587-019-0072-8.

Kolosova, O. N., and B. M. Kershengol’ts. 2017. “Endogenous Ethanol and Acetaldehyde in the Mechanisms of Adaptation of Small Mammals to Northern Conditions.” *Russian Journal of Ecology* 48 (1): 68–72. https://doi.org/10.1134/S1067413617010088.

Koppaka, Vindhya, David C. Thompson, Ying Chen, Manuel Ellermann, Kyriacos C. Nicolaou, Risto O. Juvonen, Dennis Petersen, Richard A. Deitrich, Thomas D. Hurley, and Vasilis Vasiliou Dr. 2012. “Aldehyde Dehydrogenase Inhibitors: A Comprehensive Review of the Pharmacology, Mechanism of Action, Substrate Specificity, and Clinical Application.” *Pharmacological Reviews* 64 (3): 520–39. https://doi.org/10.1124/pr.111.005538.

Korslund, Lars. 2006. “Activity of Root Voles (Microtus Oeconomus) under Snow: Social Encounters Synchronize Individual Activity Rhythms.” *Behavioral Ecology and Sociobiology* 61 (2): 255–63. https://doi.org/10.1007/s00265-006-0256-3.

Król, Elzbieta, Alex Douglas, Hugues Dardente, Mike J. Birnie, Vincent van der Vinne, Willem G. Eijer, Menno P. Gerkema, David G. Hazlerigg, and Roelof A. Hut. 2012. “Strong Pituitary and Hypothalamic Responses to Photoperiod but Not to 6-Methoxy-2-Benzoxazolinone in Female Common Voles (Microtus Arvalis).” *General and Comparative Endocrinology* 179 (2): 289–95. https://doi.org/10.1016/j.ygcen.2012.09.004.

Kumar, Sudhir, Glen Stecher, Michael Li, Christina Knyaz, and Koichiro Tamura. 2018. “MEGA X: Molecular Evolutionary Genetics Analysis across Computing Platforms.” *Molecular Biology and Evolution* 35: 1547–49. https://doi.org/10.1093/molbev/msy096.

Lambin, Xavier, Charles J. Krebs, and Beth Scott. 1992. “Spacing System of the Tundra Vole (Microtus Oeconomus) during the Breeding Season in Canada’s Western Arctic.” *Canadian Journal of Zoology* 70: 2068–72.

Lemskaya, Natalia A., Svetlana A. Romanenko, Feodor N. Golenishchev, Nadezhda V. Rubtsova, Olga V. Sablina, Natalya A. Serdukova, Patricia C.M. O’Brien, et al. 2010. “Chromosomal Evolution of Arvicolinae (Cricetidae, Rodentia). III. Karyotype Relationships of Ten Microtus Species.” *Chromosome Research* 18 (4): 459–71. https://doi.org/10.1007/s10577-010-9124-0.

Li, Heng, and Richard Durbin. 2009. “Fast and Accurate Short Read Alignment with Burrows-Wheeler Transform.” *Bioinformatics* 25 (14): 1754–60. https://doi.org/10.1093/bioinformatics/btp324.

Li, Heng, Bob Handsaker, Alec Wysoker, Tim Fennell, Jue Ruan, Nils Homer, Gabor Marth, Goncalo Abecasis, Richard Durbin, and 1000 Genome Project Data Processing Subgroup. 2009. “The Sequence Alignment / Map Format and SAMtools.” *Bioinformatics* 25 (16): 2078–79.

Lindroth, R. L., and G. O. Batzli. 1984. “Food Habits of the Meadow Vole (Microtus Pennsylvanicus) in Bluegrass and Prairie Habitats.” *Journal of Mammalogy* 65 (4): 600–606. https://doi.org/10.2307/1380843.

Messer, Philipp W., and Dmitri A. Petrov. 2013. “Population Genomics of Rapid Adaptation by Soft Selective Sweeps.” *Trends in Ecology and Evolution* 28 (11): 659–69. https://doi.org/10.1016/j.tree.2013.08.003.

Murrell, Paul R. 1999. “Layouts: A Mechanism for Arranging Plots on a Page.” *Journal of Computational and Graphical Statistics* 8: 121–34. https://doi.org/10.2307/1390924.

Nakao, Nobuhiro, Hiroko Ono, and Takashi Yoshimura. 2008. “Thyroid Hormones and Seasonal Reproductive Neuroendocrine Interactions.” *Reproduction* 136 (1): 1–8. https://doi.org/10.1530/REP-08-0041.

Nussey, Daniel H., Erik Postma, Phillip Gienapp, and Marcel E. Visser. 2005. “Evolution: Selection on Heritable Phenotypic Plasticity in a Wild Bird Population.” *Science* 310 (5746): 304–6. https://doi.org/10.1126/science.1117004.

O’Malley, Kathleen G., and Michael A. Banks. 2008. “A Latitudinal Cline in the Chinook Salmon (Oncorhynchus Tshawytscha) Clock Gene: Evidence for Selection on PolyQ Length Variants.” *Proceedings of the Royal Society B: Biological Sciences* 275 (1653): 2813–21. https://doi.org/10.1098/rspb.2008.0524.

O’Malley, Kathleen G., Michael J. Ford, and Jeffrey J. Hard. 2010. “Clock Polymorphism in Pacific Salmon: Evidence for Variable Selection along a Latitudinal Gradient.” *Proceedings of the Royal Society B: Biological Sciences* 277 (1701): 3703–14. https://doi.org/10.1098/rspb.2010.0762.

Paradis, Emmanuel, and Klaus Schliep. 2019. “Ape 5.0: An Environment for Modern Phylogenetics and Evolutionary Analyses in R.” *Bioinformatics* 35: 526–28. https://doi.org/10.1093/bioinformatics/bty633.

Pittendrigh, Colin S, and Tsuguhiko Takamura. 1989. “Latitudinal Clines in the Properties of a Circadian Pacemaker.” *Journal of Biological Rhythms* 4 (2): 217–35. https://doi.org/10.1007/978-3-642-16483-5_1176.

Prendergast, Brian J. 2005. “Internalization of Seasonal Time.” *Hormones and Behavior* 48 (5): 503–11. https://doi.org/10.1016/j.yhbeh.2005.05.013.

Pyter, L. M., Z. M. Weil, and R. J. Nelson. 2005. “Latitude Affects Photoperiod-Induced Changes in Immune Response in Meadow Voles (Microtus Pennsylvanicus).” *Canadian Journal of Zoology* 83 (10): 1271–78. https://doi.org/10.1139/z05-121.

R Core Team. 2019. “R: A Language and Environment for Statistical Computing.” *R Foundation for Statistical Computing*. Vienna, Austria. https://doi.org/ISBN 3-900051-07-0.

Robinson, James T., Helga Thorvaldsdóttir, Wendy Winckler, Mitchell Guttman, Eric S. Lander, Gad Getz, and Jill P. Mesirov. 2011. “Integrative Genomics Viewer.” *Nature Biotechnology* 29: 24–26. https://doi.org/10.1038/nbt.1754.

Rosmalen, Laura van, Jayme van Dalum, Daniel Appenroth, Renzo T.M. Roodenrijs, Lauren de Wit, David G. Hazlerigg, and Roelof A. Hut. 2021. “Mechanisms of Temperature Modulation in Mammalian Seasonal Timing.” *FASEB Journal* 35 (5): 1–12. https://doi.org/10.1096/fj.202100162R.

Rosmalen, Laura Van, Jayme Van Dalum, David G. Hazlerigg, and Roelof A. Hut. 2020. “Gonads or Body? Differences in Gonadal and Somatic Photoperiodic Growth Response in Two Vole Species.” *Journal of Experimental Biology*. https://doi.org/10.1242/jeb.230987.

Rubin, Carl Johan, Michael C. Zody, Jonas Eriksson, Jennifer R.S. Meadows, Ellen Sherwood, Matthew T. Webster, Lin Jiang, et al. 2010. “Whole-Genome Resequencing Reveals Loci under Selection during Chicken Domestication.” *Nature* 464 (7288): 587–91. https://doi.org/10.1038/nature08832.

Sayers, Eric W., Jeffrey Beck, Evan E. Bolton, Devon Bourexis, James R. Brister, Kathi Canese, Donald C. Comeau, et al. 2021. “Database Resources of the National Center for Biotechnology Information.” *Nucleic Acids Research* 49 (D1): D10–17. https://doi.org/10.1093/nar/gkaa892.

Schoenfelder, Stefan, and Peter Fraser. 2019. “Long-Range Enhancer–Promoter Contacts in Gene Expression Control.” *Nature Reviews Genetics* 20 (8): 437–55. https://doi.org/10.1038/s41576-019-0128-0.

Shafin, Kishwar, Trevor Pesout, Pi-Chuan Chang, Maria Nattestad, Alexey Kolesnikov, Sidharth Goel, Gunjan Baid, et al. 2021. “Haplotype-Aware Variant Calling Enables High Accuracy in Nanopore Long-Reads Using Deep Neural Networks.” *BioRxiv*.

Shearer, Kirsty D., Timothy H. Goodman, Alexander W. Ross, Laura Reilly, Peter J. Morgan, and Peter J. McCaffery. 2010. “Photoperiodic Regulation of Retinoic Acid Signaling in the Hypothalamus.” *Journal of Neurochemistry* 112 (1): 246–57. https://doi.org/10.1111/j.1471-4159.2009.06455.x.

Shumate, Alaina, and Steven L Salzberg. 2021. “Liftoff: Accurate Mapping of Gene Annotations.” *Bioinformatics*. https://doi.org/10.1093/bioinformatics/btaa1016.

Singh, Surendra, Chad Brocker, Vindhya Koppaka, Ying Chen, Brian C. Jackson, Akiko Matsumoto, David C. Thompson, and Vasilis Vasiliou. 2013. “Aldehyde Dehydrogenases in Cellular Responses to Oxidative/ Electrophilicstress.” *Free Radical Biology and Medicine* 56: 89–101. https://doi.org/10.1016/j.freeradbiomed.2012.11.010.

Sitnikova, Natalia A., Svetlana A. Romanenko, Patricia C.M. O’Brien, Polina L. Perelman, Beiyuan Fu, Nadezhda V. Rubtsova, Natalya A. Serdukova, et al. 2007. “Chromosomal Evolution of Arvicolinae (Cricetidae, Rodentia). I. The Genome Homology of Tundra Vole, Field Vole, Mouse and Golden Hamster Revealed by Comparative Chromosome Painting.” *Chromosome Research* 15 (4): 447–56. https://doi.org/10.1007/s10577-007-1137-y.

Sobreira, Tiago J.P., Ferdinand Marlétaz, Marcos Simões-Costa, Deborah Schechtman, Alexandre C. Pereira, Frédéric Brunet, Sarah Sweeney, et al. 2011. “Structural Shifts of Aldehyde Dehydrogenase Enzymes Were Instrumental for the Early Evolution of Retinoid-Dependent Axial Patterning in Metazoans.” *Proceedings of the National Academy of Sciences of the United States of America* 108 (1): 226–31. https://doi.org/10.1073/pnas.1011223108.

Stoney, Patrick N., Gisela Helfer, Diana Rodrigues, Peter J. Morgan, and Peter Mccaffery. 2016. “Thyroid Hormone Activation of Retinoic Acid Synthesis in Hypothalamic Tanycytes.” *Glia* 64 (3): 425–39. https://doi.org/10.1002/glia.22938.

Tast, Johan. 1966. “The Root Vole, Microtus Oeconomus (Pallas) as an Inhabitant of Seasonally Flooded Land.” *Annales Zoologici Fennici* 3 (3): I27-I7I.

Tast, Johan, and Asko Kaikusalo. 1976. “Winter Breeding of the Root Vole , Microtus Oeconomus , in 1972 / 1973 at Kilpisjärvi , Finnish Lapland” 13 (3): 174–78.

Touloupi, Katerina, Jenni Küblbeck, Angeliki Magklara, Ferdinand Molnár, Mika Reinisalo, Maria Konstandi, Paavo Honkakoski, and Periklis Pappas. 2019. “The Basis for Strain-Dependent Rat Aldehyde Dehydrogenase 1A7 (ALDH1A7) Gene Expression.” *Molecular Pharmacology* 96 (5): 655–63. https://doi.org/10.1124/mol.119.117424.

Triant, Deborah A., and J. Andrew DeWoody. 2006. “Accelerated Molecular Evolution in Microtus (Rodentia) as Assessed via Complete Mitochondrial Genome Sequences.” *Genetica* 128 (1–3): 95–108. https://doi.org/10.1007/s10709-005-5538-6.

Tutar, Yusuf. 2012. “Pseudogenes.” *Comparative and Functional Genomics* 2012: 6–9. https://doi.org/10.1155/2012/424526.

Vasiliou, Vasilis, and Daniel W. Nebert. 2005. “Analysis and Update of the Human Aldehyde Dehydrogenase (ALDH) Gene Family.” *Human Genomics* 2 (2): 138–43. https://doi.org/10.1186/1479-7364-2-2-138.

Vitti, Joseph J., Sharon R. Grossman, and Pardis C. Sabeti. 2013. “Detecting Natural Selection in Genomic Data.” *Annual Review of Genetics* 47: 97–120. https://doi.org/10.1146/annurev-genet-111212-133526.

Walton, James C., Zachary M. Weil, and Randy J. Nelson. 2011. “Influence of Photoperiod on Hormones, Behavior, and Immune Function.” *Frontiers in Neuroendocrinology* 32 (3): 303–19. https://doi.org/10.1016/j.yfrne.2010.12.003.

Wickham, Hadley. 2009. *Ggplot2*. *Journal of Statistical Software*. New York, NY: Springer. https://doi.org/10.1007/978-0-387-98141-3.

Wickham, Hadley, Mara Averick, Jennifer Bryan, Winston Chang, Lucy McGowan, Romain François, Garrett Grolemund, et al. 2019. “Welcome to the Tidyverse.” *Journal of Open Source Software*. https://doi.org/10.21105/joss.01686.

Wickham, Hadley, Romain François, Lionel Henry, and Kirill Müller. 2019. “Dplyr: A Grammar of Data Manipulation. R Package Version.” *Media*.

Wood, Shona, and Andrew Loudon. 2014. “Clocks for All Seasons: Unwinding the Roles and Mechanisms of Circadian and Interval Timers in the Hypothalamus and Pituitary.” *Journal of Endocrinology* 222 (2). https://doi.org/10.1530/JOE-14-0141.

Yiming, Li, Wang Siqi, Cheng Chaoyuan, Zhang Jiaqi, Wang Supen, Hou Xianglei, Liu Xuan, Yang Xuejiao, and Li Xianping. 2021. “Latitudinal Gradients in Genetic Diversity and Natural Selection at a Highly Adaptive Gene in Terrestrial Mammals.” *Ecography* 44 (2): 206–18. https://doi.org/10.1111/ecog.05082.

Yoshimura, Takashi. 2006. “Molecular Mechanism of the Photoperiodic Response of Gonads in Birds and Mammals.” *Comparative Biochemistry and Physiology - A Molecular and Integrative Physiology* 144 (3): 345–50. https://doi.org/10.1016/j.cbpa.2005.09.009.

Zhao, Zhongming, Yun Xin Fu, David Hewett-Emmett, and Eric Boerwinkle. 2003. “Investigating Single Nucleotide Polymorphism (SNP) Density in the Human Genome and Its Implications for Molecular Evolution.” *Gene* 312: 207–13. https://doi.org/10.1016/S0378-1119(03)00670-X.

Zub, K., B. Jędrzejewska, W. Jędrzejewski, and K. A. Bartoń. 2012. “Cyclic Voles and Shrews and Non-Cyclic Mice in a Marginal Grassland within European Temperate Forest.” *Acta Theriologica* 57 (3): 205–16. https://doi.org/10.1007/s13364-012-0072-2.